Limit Analysis of Structures: Novel Computational Techniques

by

Husham Ahmed
B.Sc. (Eng.), M.Sc. (Eng.)

A thesis submitted to the Department of Civil and Structural Engineering, the University of Sheffield in partial fulfilment of the requirements for the Degree of Doctor of Philosophy

April 2005

Abstract

Compared with elastic deformation analysis techniques, limit analysis methods that are amenable to computerization have yet to reach the same level of development. Yet such work has important practical value. The present work is primarily concerned with the development of a general model for the limit analysis of reinforced concrete (RC) and masonry structures. A novel limit analysis method for RC slabs and bridge decks that overcomes the problems encountered by previous workers in this field has been developed. Ultimate load analyses have been carried out by discretizing the slab deck into a large number of rigid elements. Novel mathematical rules to describe how adjacent elements should interact with each other have been used in the formation of the requisite Linear Programming (LP) tableau. Appropriate state-of-the-art algorithms have been employed to solve the underlying linear programming problem. The results obtained agree quite well with known exact solutions for various different slab configurations, boundary conditions and loading arrangements. An attempt to obtain a rigorous upper-bound solution (i.e. satisfying kinematical admissibility criteria) using the method ability to identify sensible failure patterns has also been made, and rigorous upper-bound solutions have been obtained for a number of problems.

In the context of masonry structures, a new computational limit analysis procedure for rigid block assemblages comprising non-associative frictional interfaces has been developed in this thesis. The procedure involves the successive solution of simple LP sub-problems. Behaviour of a contact in each sub-problem is governed by a Mohr-Coulomb failure surface with an effective cohesion intercept and an initially negative angle of friction. Both these parameters are updated at each iteration by referring to the real problem, with the angle of friction also being successively relaxed towards zero (thereby implying zero dilatancy). The procedure has been applied to a wide variety of example problems, including benchmark problems from the literature and also to much larger problems. For one such problem contained in

the literature, it has been found that the load factor computed using the proposed procedure was virtually identical to that computed previously but this has been obtained two orders of magnitude more quickly.

Recent developments to the RING computational limit analysis software for masonry arch bridges are also described (non-associative friction, gross-displacement analysis features). A number of examples of local authority bridge problems are re-assessed in the light of the new features. The new version of RING (version 1.5) has been found to be much faster with execution speeds up to 200 times faster than the previous version.

Acknowledgements

The author wishes to express his sincere gratitude to Dr Matthew Gilbert for his excellent supervision, guidance and many constructive discussions which have been a source of simulating ideas during the course of this study.

The financial support provided by the Engineering and Physical Sciences Research Council (EPSRC), the Gordon Memorial College Trust and the John Carr Memorial Fund is fully acknowledged.

Finally, the author would like to express his deepest appreciation to his family for their support and encouragement and understanding throughout the course of his work. In particular, the author's parents have been a continued source of moral and financial support for his many years in academia. The endless support and patience of his wife is affectionally acknowledged.

Declaration

Except where specific reference has been made to the work of others, this thesis is the result of my own work. No part of it has been submitted to any university or other educational establishment for a degree, diploma, or other qualification.

Husham Ahmed

Contents

List of Tables

List of Figures

Chapter 1

Introduction

1.1 Background

Reinforced concrete (RC) and masonry structures need to be regularly checked, particularly as the design variables under which these structures were originally designed are continuously changing such that the capability of these structures to survive into the future becomes questionable.

One ancient type of structures is the bridge. Masonry arch bridges and RC bridges together represent the majority of the bridge stock in the UK. There are over 40,000 masonry arch bridges ranging from small remote bridges over mountain streams to major viaducts carrying arterial mainline railways. Whilst masonry arch bridges were mostly designed using 'rules of thumb', RC bridges (the majority of which were built in the last century) were often designed using conservative design methods based on linear elastic theory.

When these bridges were built, the nature and volume of modern traffic could not have been envisaged by their designers. The continuous increase in vehicle weights means these bridges need to be regularly assessed. Uncertainties regarding the

capability of existing bridges to carry increasing vehicle weights may well lead to weight restrictions being imposed on these bridges. To avoid the need for such measures to be taken, either (i) costly strengthening works must be carried out or (ii) more sophisticated structural analysis must be undertaken to demonstrate that a given bridge has the adequate load carrying capacity.

Structural analysis offers many options to address the problem in hand. Two methods are often referred to: finite element methods and plastic analysis methods. Elastic finite element methods can now be employed to carry out a linear elastic analysis of bridges. One of the weaknesses of linear elastic analysis is its inability to reflect the real behaviour of structures under abnormal or ultimate loading conditions. Almost all structures behave nonlinearly before attaining their limit of resistance. Therefore, if a finite element approach is chosen for ultimate load analysis, non-linear finite element methods should be applied. However, non-linear finite element methods are more suited to in-depth, specialized assessments of major structures or for laboratory research, and this is not presently considered to be a practical option for use in assessing large numbers of existing bridges. Although this situation may change in the future, as computing developments continuously result in decreasing costs and increasing speed execution, the comprehensive mechanical characterization of the materials that is required, the need for calibration and the requirement of adequate knowledge of sophisticated non-linear solution techniques by the practitioner are still likely to limit their application.

In contrast to non-linear finite element methods, plastic analysis methods are conceptually simple, easy to apply and allow quick estimates of the ultimate load to be made. Despite this, plastic methods have not been adopted widely for use in practice, partly because of the misconception amongst engineers that such methods are difficult to apply and are not amenable to automation. This has limited their development and the extent to which they are currently applied in practice. How-

ever, if it is possible to develop user friendly computer programs capable of treating a wide variety of problems with minimal computational effort, then plastic analysis methods could find many applications in everyday civil engineering practice. Bearing this in mind, here the aim is to demonstrate that plastic methods can be computerized and that the computerized forms of these methods can be efficient in comparison with other methods, such as non-linear finite element methods.

1.2 Objectives and methodology

The fundamental objective of the research described in this thesis is to develop a general model for the limit analysis of RC and masonry structures, and to apply this model to a variety of practical problems. This will be achieved through the following:

1. Developing novel limit analysis methods for RC slabs and bridge decks, overcoming the problems encountered by previous workers in this field. Ultimate load carrying capacity analyses will be carried out by discretizing the slab deck into a large number of rigid elements. Novel mathematical rules to describe how adjacent elements should interact with each other will then be used in the formulation of the requisite LP tableau. These rules will differ in important respects from the over-restrictive rules adopted by previous workers in this field, to ensure that safe estimates of structural strength are obtained. Appropriate state-of-the-art algorithms will be employed to solve the underlying LP sub-problem.

2. Developing a novel method for the limit analysis of rigid block assemblages comprising non-associative frictional interfaces based on a computationally efficient rigid block analysis formulation. The method will involve solving a series of LP problems with successively modified failure surfaces (rather than

working directly with the full Mixed Complementarity Problem (MCP) as others have done). The proposed method will be capable of quickly ascertaining whether associative and non-associative solutions differ and identifying 'good' estimates of the load factor for a wide range of problems.

3. Applying the above methods to a variety of practical case study problems in the field of RC slabs and masonry gravity structures.

1.3 Summary of the thesis

The thesis is arranged in seven core chapters. Three of these (chapters 4, 5 and 6) are presented as self-contained manuscripts suitable for submission as journal/conference papers. The fourth chapter, which currently comprises a single paper, will be split into two and submitted to academic journals. The first of these will introduce the Sheffield method and its application to problems with known exact solutions. The second will cover the application of the Sheffield method to selected study cases from literature and the possibility of obtaining upper-bound solutions from the method. The paper which is presented in the fifth chapter has already been submitted to Computers & Structures. Results appeared in the six chapter intended to be published in journals accessible to practising engineers. As a result of using the three-paper format, some overlap in the content may occur.

In addition, two computer programs were also developed by the author. The first program concerns the limit analysis of RC slabs based on an automated form of the yield line method and the second program is for the limit analysis of masonry structures based on the rigid block method of analysis. These programs are intended to be the basis for the development of analysis tools which will be useful in the assessment/design of RC and masonry structures.

Apart from the fifth chapter which was a result of collaborative efforts, and Ap-

pendix A which contains a joint conference paper, all work presented in this thesis is the author's own work. The author contribution to the paper presented in the fifth chapter is that he developed the original algorithm and implemented this in a computer program. He then investigated a number of case study problems from the literature and showed that the method performed well. This evolved into a conference paper. Other authors have contributed to this work in the form of additional examples and a literature review.

In chapter 2, a summary of basic limit analysis concepts is provided. Application of mathematical programming to limit analysis is also reviewed. The kinematic and static approaches to limit analysis are discussed and presented in a general vector-matrix form.

Chapter 3 reviews the background to the yield line method of analysis. The usefulness of the yield line method as a design tool is examined. Yield line theory is then presented and theoretical considerations are discussed.

Chapter 4 presents a novel limit analysis method for RC slabs and bridge decks that overcomes the problems encountered by earlier workers in this field. Previous work in the field of automated yield line analysis is reviewed and shortcomings of this work are identified. The Munro and Da Fonseca yield line analysis formulation for RC slabs is presented and its performance characteristics are discussed. A new LP formulation for yield line analysis of RC slabs is presented and a computer program based on this formulation is developed. The computer program is tested with benchmark problems and case study problems from the literature. A new algorithm to obtain rigorous upper-bound solutions using the proposed method is developed and implemented.

Chapter 5 presents a new computational limit analysis procedure for rigid block assemblages comprising non-associative frictional interfaces. The development of computational models for masonry structure is discussed. A discrete block model

with frictional constraints is presented. The associative friction problem formulation is discussed and presented in vector-matrix form. An algorithm for non-associative friction problems is developed and incorporated into a computer program. A number of example problems are then investigated using the proposed method.

Chapter 6 is devoted to practical application of computational limit analysis to masonry arch bridges using the RING software which has been greatly enhanced following the work undertaken by the author. Some of the practical requirements that a bridge analysis program has to fulfil in order to be useful to practitioners and the position of the current version of RING (version 1.5) with respect to these requirements are discussed. Recent developments to the software are described. A number of typical local authority bridges are re-assessed in the light of the new features.

In chapter 7, issues which have arisen during the development of the different methods of analysis are discussed and observations are made. In chapter 8, conclusions are drawn and recommendations for further research are given.

Additionally, three appendices are also included:

Appendix A is a paper presented at "The Ninth International Conference on Civil and Structural Engineering Computing", Egmond-aan-Zee, the Netherlands, September 2003. Here the computational efficiency of two rigid block analysis formulations for application to masonry structures is discussed. An alternative 'joint equilibrium' formulation developed by the author is presented. The new formulation is then compared with the 'redundant forces' formulation already in use in RING 1.1.

Appendix B reviews the basics of mathematical programming with the main focus on linear programming. The Simplex method and the interior-point methods as solution techniques are examined. The concept of duality is discussed and the dual of a linear program in standard form is presented. The Lagrangian function and

Karush-Kuhn-Tucker conditions are reviewed.

Appendix C is devoted to computer code for SLAB. The basic features of object oriented programming are discussed. The different classes used in SLAB are reviewed and computer flow chart is presented.

Chapter 2

Structural Mechanics and Mathematical Programming

2.1 Background

Structural mechanics is concerned with the study of the structural response to an action or loading applied upon a structure. The structural response is described by defining the relations between external forces, internal forces and deformations of structural materials in the form of relationships which involve variables such as the structural loading, the structural material properties, the stress and the strains developed in the structure and the displacement undergone by the structure.

Within the field of structural mechanics, plastic analysis methods stand as an integral part of the structural engineer's toolbox, having for many decades served to estimate the collapse load of structures. Plastic analysis is concerned with the determination of the maximum load amplification (or load safety factor) which can be sustained by a perfectly-plastic structure subjected to given loads. Information on the stress-state at collapse and the collapse mechanism may be obtained as a

by-product. Plastic collapse takes place when a suitable number and disposition of plastic zones are formed, converting the structure into a mechanism. For perfectly-plastic materials, a further small change in configuration of the structure can be induced without any change in the applied loads, and the mechanism motion that follows is that of a set of adjacent rigid bodies with deformations concentrated exclusively in the plastic zones.

In recent years, plastic analysis methods have received increased interest. Perfect plasticity models were extensively used in the new Eurocode for concrete structures [1]. Many of the plastic analysis methods are based on hand calculation methods, and numerous methods such as the strip method and the yield line method for RC slabs were developed. However, the scope of limit state calculation is wider and other applications include the limit analysis of masonry arches. The success of plastic analysis methods lies largely on the ability of these methods to provide relatively accurate results (with minimal computational effort) for problems that may have complicated geometries and loading conditions.

Limit analysis has a simple mathematical basis yet describes a reasonably realistic non-linear behaviour. When an exact solution is obtainable by the analysis, it gives the ultimate load limit of a structure. Approximate solutions provide bounds on the limit loads.

Connections between limit analysis and mathematical programming theory were recognized as soon as the fundamental theorems of limit analysis were established, and the limit analysis/design problem for trusses, beams and frames was rather straightforwardly cast in linear programming form [2, 3, 4]. Since then, the application of mathematical programming to limit analysis has been extensively researched.

In this chapter a summary of basic limit analysis concepts is made. The application of mathematical programming to limit analysis is reviewed. The kinematic and static

approaches to limit analysis are discussed and presented in a general vector-matrix form, to be used in later chapters.

2.2 Limit analysis basics

Limit analysis relies on the use of a rigid-perfectly plastic material model. A perfectly plastic material may be defined as a material which undergoes unlimited plastic deformations under constant stress when it is subjected to a homogeneous state of stress. Although rigid-perfectly plastic materials do not exist in reality, it is still a valid assumption when the plastic strains are much higher than elastic strains.

The basic assumptions for limit analysis theory are that brittle failures due to shear, bond loss, and sudden flexural compression are prevented. That is, it is assumed implicitly that no section in the structure might lose its strength before all the hinges have formed. For example, in the case of a RC slab this means that all yield lines must be capable of reaching the boundaries of the slab before any portion loses its moment-carrying capacity due to excessive rotation.

2.2.1 Static, kinematic and constitutive relations

The two essential theories underlying limit analysis had been developed in full generality and rigour by the early 1950s in the form of the static (or 'safe' or 'lower-bound') theorem and the kinematic (or 'unsafe' or 'upper-bound') theorem. Static relations express the equilibrium of forces and kinematic relations express the compatibility of deformations. Static relations and kinematic relations can be better explained in the light of the mechanics of deformable structures as discussed by Smith [5]. In basic terms, three types of mechanical laws represent the basis of the mechanics of deformable structures:

1. The laws of kinetics which define the relationship between the internal forces in a structural member and the applied loads by the changes in moments of the masses involved in the motion. These laws arise from the balance of momenta of a system of mass particles in motion as defined by Newton's law. The laws of statics or of equilibrium replace the laws of kinetics when the path of motion of the structure is changed in such a way that the changes in moments are approaching zero. Equilibrium equations, which are based on the original un-displaced structure, can be used to define the relationship between the applied loads and the internal forces within the structural system when the current total displacement is small.

2. The laws of kinematics which link the deformation in each of the structural members to the current total displacements of the whole structure. Kinematic relations implicitly define the concept of compatibility. The compatibility of any structural system implies that the structural elements all remain properly connected within the whole system during the entire process of system deformation.

3. The constitutive relations which relate the strain rates produced in the material to imposed stress rates.

Within the context of perfectly-plastic materials, the constitutive equations consist of two parts: the yield condition and the flow rule. The yield condition describes the combinations of stresses or internal forces that can produce yielding, and the flow rule describes the relationship between these and the resulting plastic strains during yielding.

2.2.2 Upper-bound methods

Upper-bound methods postulate a collapse mechanism and ensure that:

1. The equilibrium condition is satisfied throughout the structure.

2. The collapse mechanism is compatible with the boundary conditions.

Since there is no consideration given for elements lying between the postulated failure zones to examine whether the yield conditions there have been violated, the collapse load factor obtained using this method will be greater than or equal to the true load factor. However, if all possible collapse mechanisms are examined, the one giving the lowest collapse load factor will be the correct mechanism.

2.2.3 Lower-bound methods

Generally, lower-bound methods involve finding a distribution of internal actions (forces and moments) at collapse to ensure that:

1. The yield conditions are not violated anywhere in the structure[†].

2. The equilibrium equations are satisfied at all positions.

As the name indicates, the collapse load factor given by this method will always be lower than the actual one unless the most critical distribution of internal actions is identified.

2.3 Mathematical programming application to limit analysis

Mathematical programming techniques and their application to structural mechanics have been through a period of intense research development. A vast body of

[†] This implies that in the case of a RC slab the moment is less than the plastic moment of resistance; in the case of an arch the thrust-line lies wholly within the arch barrel.

information on the subject has been built up by a number of researchers working in the field of structural mechanics and it has now reached the stage where it can be applied to real world problems. In itself, mathematical programming is the science and art of the optimization of functions under constraints which are generally inequalities but for special cases where the constraints are exclusively equations, the mathematical programming problem reduces to a classical (i.e. Lagrangian) optimization problem (for further information on the subject, the reader is referred to Appendix B).

Over the past few centuries, great efforts have been made towards obtaining exact analytical solutions for problems in the field of structural mechanics. However, even when the assumption of linear behaviour for the material and geometrically linear deformations are assumed to hold true, the need to turn to numerical techniques to obtain solutions has been recognized if general problems are to be successfully considered. Whilst analytical solutions began to lose their appeal with the advent of fast and powerful computing machines, numerical techniques became more popular and matrix-based methods for structural mechanics were regarded as powerful techniques to automate the process of finding numerical solutions.

On the face of an almost impossible task of generating analytical solutions with some degree of generality for two and three dimensional structures, the development of numerical solution schemes became the logical response. This prompted the idea of discretizing the structure into finite elements which has been seen as leading to a most versatile formulation that fits perfectly with the available matrix methods previously developed for framed structures. As soon as finite element methods were developed, the connection between the limit analysis methods and mathematical programming was established. This has been seen as a perfect way to encode the structural behaviour.

Historically, mathematical programming has been motivated and fostered by the

presence of real-life problems in fields such as strategy, economics and management rather than structural mechanics problems. Structural mechanics and linear programming were anticipated simultaneously in an 1823 memoire to the French Academy of Sciences by Fourier [6], but it was over a century later before these ideas were fully developed [7].

Linear programming and limit analysis re-emerged almost simultaneously, but separately, in the work of Kantorovich and Gdovzev, respectively, just before the second world war (for example see [8]). The subsequent contributions of Dantzig's and Prager's schools soon after that time gave linear programming significant recognition and positioned it in an important place within the field of mathematics and mechanics. The introduction of mathematical programming techniques first to problems of plastic collapse and then to a much broader range of elasto-plastic problem was then recognized as leading to a convenient framework for the formulation of a wide variety of structural mechanics problems.

In the early 1950s, limit analysis of frames was treated as a problem in linear programming and debated as such, sometimes jointly by research workers in the fields of structural mechanics (Greenberg, Zienkiewicz) and applied mathematics (Charnes, Lemke) [9]. This paved the way for much work to be done on the application of mathematical programming techniques to the formulation and solution of structural analysis problems [10, 11, 12, 13, 14]. The significant trend displayed there concerned the establishment of a unified and comprehensive formalism through which all problems can be conveniently described and in which a central role is played by the Karush-Kuhn-Tucker theory of mathematical programming[†] [15, 16].

Naturally, plastic analysis problems take the form of vectorial relations involving

[†] Kuhn and Tucker generalized the theory of optimization to the case of inequality constraints in 1951. However, Karush had already described the optimality conditions in his dissertation in 1939. For this reason, the conditions arising from the Kuhn-Tucker theorem are usually referred to as the Karush-Kuhn-Tucker conditions.

equilibrium, compatibility, and constitutive laws. If it is possible to cast these equations in the form of Karush-Kuhn-Tucker conditions and with certain conditions of convexity also being satisfied, dual mathematical programs can be derived.

Generally in limit analysis problems static and kinematic constraints occur in a naturally uncoupled form, and by applying the Karush-Kuhn-Tucker theorem, a pair of primal-dual linear programs is obtained [17]. These programs encode the limit analysis theorems and the uniqueness theorem is obtained directly from the duality theorem of linear programming. Static and kinematic relations for limit analysis are usually linear equations. If there is no stress-resultant interaction, the yield equations also take the form of linear equations. In some situations, piece-wise linearization may be adopted to substitute non-linear relationships with an increased number of linear relationships.

The discrete nature of mathematical programming implies the discretization of continuum structures. For two dimensional structures, some early work used a finite difference representation or a series expansion of the independent variables. One of the drawbacks of the finite difference formulation was its inability to guarantee true bounds but only approximations to the actual collapse load [18]. The versatility of the finite element method led to its general preference in subsequent work. One important advantage of the finite element approach is that the static and kinematic admissibility of stress (displacement) fields can be rigorously guaranteed, thus preserving the bounding nature of the solution. The first finite element formulation was for a compatible model in plane stress [19]. Finite element formulations for planar limit analysis have since been developed extensively and applied to a wide range of problems in structural engineering [20, 21, 22, 23, 24]. The static theorem was used to formulate the problem as a mathematical program for use in finite element models which are expressed in terms of stress functions [25, 26, 27, 28]. In a similar fashion, the kinematic theorem is invoked to formulate the corresponding

mathematical program for compatible models which are expressed in terms of nodal displacements [29, 30, 31, 32].

Initially, not much attention was paid to limit analysis/finite element formulations of plate bending problems. Hodge and Belytschko's [33] work appeared to be the first of its kind in this area, soon followed by a number of other workers [34, 35, 36, 37], developing similar techniques.

The special case of Johansens' yield line method for RC slabs has been given particular attention and Munro and Da Fonseca's yield line analysis method, which used finite elements and linear programming [17], was a break-through in the area of the application of mathematical programming to limit analysis of RC slabs. It opened the door for much work to be subsequently done in this area. A number of researchers attempted to improve the performance of the method by applying different techniques such as sequential linear programming [38, 39, 40] and/or geometrical optimization [41, 42, 43, 44].

Mathematical programming techniques have not only been restricted to the analysis of steel and concrete structures. The analysis of masonry structures is another area where mathematical programming techniques have been successfully applied. The application of limit analysis to the study of masonry structures was pioneered in modern times by Heyman [45] who placed masonry arch analysis securely within the bounds of the plastic theory. Livesley [46] made the link with mathematical programming and presented a general method for the analysis of masonry arches based on an 'equilibrium' formulation. Following Livesley's work, a number of researchers have developed procedures to model masonry structures. Most notable contributions in recent years include the work of Boothby and Brown [47, 23, 48], Melbourne and Gilbert [49, 50, 51, 52, 53], Fishwick [54], Baggio and Trovalusci [55], Livesley [56], Ferris and Tin-Loi [57].

The significant outcome of the research undertaken in the area of the application of mathematical programming to limit analysis of structures is that the importance of mathematical programming is not confined to its computational aspects, but it has also a theoretical role to play. The way that mathematical programming unifies discrete problems of structural plasticity and continues formalism through which primal-dual external principles may be generated means that mathematical programming yields not only a unified formalism for discretized structural mechanics problems but also algorithms for their automatic numerical solution [58]. The refined mathematical foundation and the richness of theorems of mathematical programming present interesting and useful structural interpretations. The integration of these distinct features of mathematical programming with well-constructed algorithms through which numerical solutions may be obtained for such formulation sets practical problem-solving in structural plasticity within a strong scientific discipline [5].

Despite the fact that the possibility of obtaining minimum weight designs automatically using plastic theory and linear programming has now been appreciated for a long time, such techniques have not been used much in practice until recently. Limited computing power, coupled with the relatively primitive algorithms available in the past meant that other solution methods at that time found favour. The vast improvement in computing power and the dramatic enhancements in the optimization algorithms available has the potential to change this.

2.4 Limit analysis formulations

Whilst the use of plastic theory as a means of predicting the collapse load of steel frames has been extensively investigated, in parallel, a considerable effort was devoted to hand computational methods. Two methods emerged: the upper-bound

method and the lower-bound method. The upper-bound method involves identifying all the possible collapse mechanisms and then, using virtual work considerations, establishing the lowest load at which any of these will be activated. This has been described as the 'upper-bound' or 'unsafe' method because, if all the possible collapse mechanisms have not been identified, the predicted collapse load may be above the theoretical value and hence unsafe to use in an analysis or design context. On the other hand, 'lower-bound' or 'safe' procedures involve examining force systems in equilibrium with the applied loads and which do not violate the yield conditions. The correct theoretical collapse load is the minimum of all possible 'unsafe' solutions or the maximum of all the possible 'safe' solutions. The advancement of powerful computers made it possible to reformulate the hand calculation methods in terms of methods suited for large numerical computations. As with the hand calculation methods, the numerical computations can be based on either the upper-bound (kinematic approach) or the lower-bound (static approach) theorem of plasticity, and are carried out as optimizations.

2.4.1 The kinematic approach

Generally, if structural rotations and displacements correspond to a possible collapse mechanism that satisfies the conditions of geometric compatibility, then the work done at all sections in the structure will be positive (in the case of skeletal structures the value of moments at hinge points are equal to the fully plastic resistance moments). According to the upper-bound theorem of limit analysis, the load factor is obtained by minimizing the kinematically admissible load multiplier. This can be stated as a problem of linear programming. Thus, the kinematic formulation in general terms for a structure discretized to n elements with m interfaces between these elements may be presented as follows:

$$\text{Minimize} \quad \lambda \mathbf{f}_L^{\mathrm{T}}\mathbf{d}=\mathbf{f}_D^{\mathrm{T}}\mathbf{d} + \mathbf{g}^{\mathrm{T}}\mathbf{u} \tag{2.1}$$

where λ is the collapse load factor and where the whole structure live load, dead load, element displacement rates, interface forces and displacement rates vectors are denoted respectively $\mathbf{f}_L^{\mathrm{T}}=[\mathbf{f}_{L_1},\mathbf{f}_{L_2},...,\mathbf{f}_{L_n}]$, $\mathbf{f}_D^{\mathrm{T}}=[\mathbf{f}_{D_1},\mathbf{f}_{D_2},...,\mathbf{f}_{D_n}]$, $\mathbf{d}^{\mathrm{T}}=[\mathbf{d}_1,\mathbf{d}_2,...,\mathbf{d}_n]$, $\mathbf{g}^{\mathrm{T}}=[\mathbf{g}_1,\mathbf{g}_2,...,\mathbf{g}_m]$ and $\mathbf{u}^{\mathrm{T}}=[\mathbf{u}_1,\mathbf{u}_2,...,\mathbf{u}_m]$ and where the element live load, dead load and displacement rates vectors are denoted respectively $\mathbf{f}_{L_j}^{\mathrm{T}}=[f_{L_{x_j}}, f_{L_{y_j}}, f_{L_{z_j}}, m_{L_{x_j}}, m_{L_{y_j}}, m_{L_{z_j}}]$, $\mathbf{f}_{D_j}^{\mathrm{T}}=[f_{D_{x_j}}, f_{D_{y_j}}, f_{D_{z_j}}, m_{D_{x_j}}, m_{D_{y_j}}, m_{D_{z_j}}]$, $\mathbf{d}_j^{\mathrm{T}} = [\delta_{x_j}, \delta_{y_j}, \delta_{z_j}, \phi_{x_j}, \phi_{y_j}, \phi_{z_j}]$ where $\delta_{x_j}, \delta_{y_j}, \delta_{z_j}, \phi_{x_j}, \phi_{y_j}$ and ϕ_{z_j} represent, respectively, the element translations in x, y and z directions and the element rotations about the x, y and z axes and where the interface displacement rates and forces vectors are denoted respectively $\mathbf{u}_i^{\mathrm{T}} = [u_{x_i}, u_{y_i}, u_{z_i}, \theta_{x_i}, \theta_{y_i}, \theta_{z_i}]$ where $u_{x_i}, u_{y_i}, u_{z_i}, \theta_{x_i}, \theta_{y_i}$ and θ_{z_i} are respectively the local x, y and z-translational displacement of interface i, and the local rotation about the x, y and z axes, $\mathbf{g}_i^{\mathrm{T}}=[f_{l_{x_i}}, f_{l_{y_i}}, f_{l_{z_i}}, m_{l_{x_i}}, m_{l_{y_i}}, m_{l_{z_i}}]$ where $f_{l_{x_i}}, f_{l_{y_i}}, f_{l_{z_i}}, m_{l_{x_i}}, m_{l_{y_i}}$ and $m_{l_{z_i}}$ are respectively the force and the bending moment limits at interface i in the x, y and z directions.

Subject to constraints which impose:

1. Geometric compatibility:

$$\mathbf{u} = \mathbf{B}^{\mathrm{T}}\mathbf{d} \tag{2.2}$$

   where $\mathbf{B}^{\mathrm{T}}$ is a suitable $(6m \times 6n)$ geometric compatibility matrix derived from the geometry of the structure.

2. A unit work:

   Displace the structure according to the live load such that:

$$\mathbf{f}_L^{\mathrm{T}}\mathbf{d} = 1 \tag{2.3}$$

2.4.2 The static (equilibrium) approach

In the static (equilibrium) approach the aim is to find a set of internal forces which maximizes the intensity of an external load. These are in equilibrium with a certain multiple of the applied loading and should not violate the yield conditions at plastic failure zones within the structure. According to the lower-bound theorem of limit analysis, the load factor is obtained by maximizing the load multiplier. This can be stated as a problem of linear programming. For a discrete structure, this can be written in matrix notation as :

$$\text{Maximize } \lambda \tag{2.4}$$

Subject to constraints which:

1. Equilibrium:

$$\lambda \mathbf{f}_L = \mathbf{f}_D + \mathbf{B}\mathbf{q} \tag{2.5}$$

where λ is the collapse load factor and where the whole structure live load, dead load and resulting forces at interfaces are denoted respectively $\mathbf{f}_L^{\mathrm{T}}=[\mathbf{f}_{L_1},\mathbf{f}_{L_2},\ldots,\mathbf{f}_{L_n}]$, $\mathbf{f}_D^{\mathrm{T}}=[\mathbf{f}_{D_1},\mathbf{f}_{D_2},\ldots,\mathbf{f}_{D_n}]$ and $\mathbf{q}^{\mathrm{T}}=[\mathbf{q}_1,\mathbf{q}_2,\ldots,\mathbf{q}_m]$. And where the element live load, dead load and the interface forces and moments are denoted respectively $\mathbf{f}_{L_j}^{\mathrm{T}}=[f_{L_{x_j}}, f_{L_{y_j}}, f_{L_{z_j}}, m_{L_{x_j}}, m_{L_{y_j}}, m_{L_{z_j}}]$, $\mathbf{f}_{D_j}^{\mathrm{T}}=[f_{D_{x_j}}, f_{D_{y_j}}, f_{D_{z_j}}, m_{D_{x_j}}, m_{D_{y_j}}, m_{D_{z_j}}]$ and $\mathbf{q}_i^{\mathrm{T}}=[f_{x_i}, f_{y_i}, f_{z_i}, m_{x_i}, m_{y_i}, m_{z_i}]$ where $f_{x_i}, f_{y_i}, f_{z_i}, m_{x_i}, m_{y_i}$ and m_{z_i} are respectively the forces and the bending moments at interface i.

2. Yield conditions:

$$-\mathbf{g} \leq \mathbf{q} \leq \mathbf{g} \tag{2.6}$$

Considering both formulations; Charnes *et al.* [9] showed that when 'mechanism' and 'equilibrium' formulations of the limit analysis are linearized they give rise to dual linear programming problems. These concepts are shown in Fig. 2.1 together with the static-kinematic analogy. It worth mentioning here that static formulations obtained as dual to the kinematic formulations (as has been done here) do not necessarily lead to true 'lower-bound' solutions.

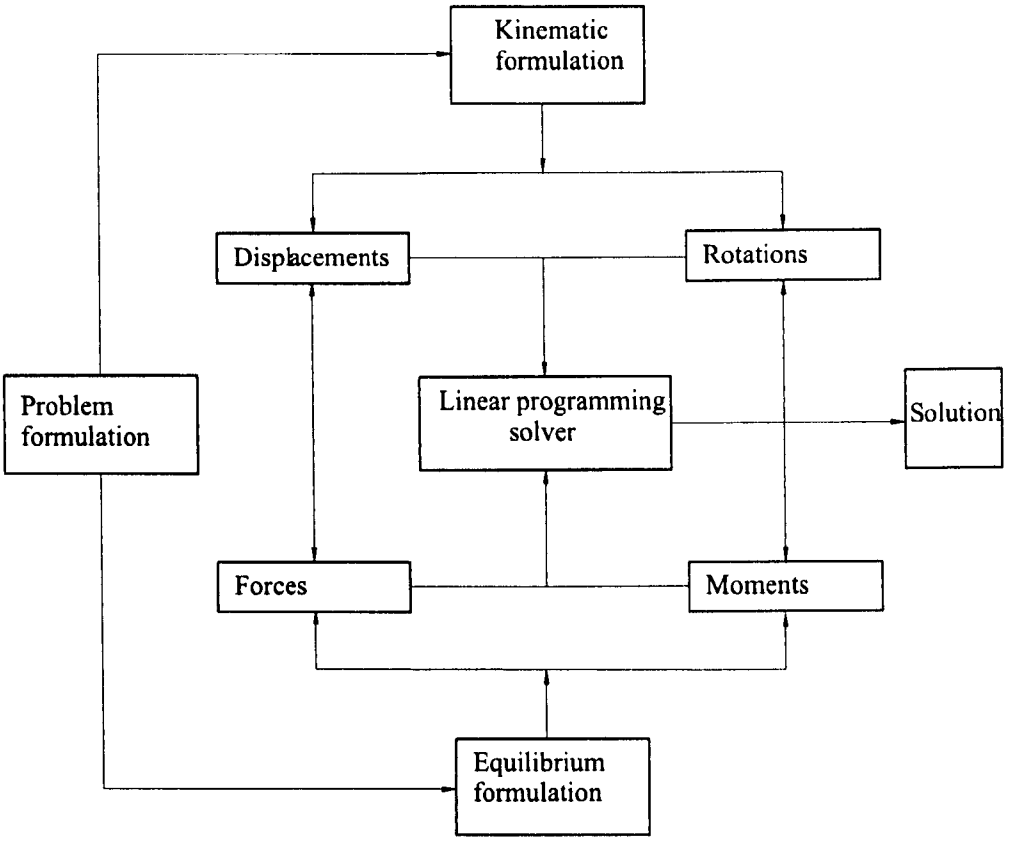

Figure 2.1: Static-kinematic analogy

The above representation presents plastic analysis in forms amenable for computerization. Making use of this, a variety of plastic analysis problems may be addressed. In this context, the yield line analysis of RC slabs is investigated in the fourth chapter. The problem of analyzing masonry structures can also be tackled using this approach; this is carried out in the fifth chapter of this thesis.

References

[1] European Standard. Eurocode 2: Design of concrete structures, part 1: General rules and rules for buildings, December 1991. ENV 1992-1-1.

[2] Greenberg, H. J. and Prager, W. Limit design of beams and frames. *Proc. ASCE*, 77:1–12, 1951.

[3] Foulkes, J. The minimum weight design. *Quarterly Applied Mathematics*, 10:347–358, 1953.

[4] Heyman, J. Plastic design of beams and plane frames for minimum weight. *The Structural Engineer*, 31:1–12, 1953.

[5] Smith, D. L. (editor). Mathematical programming methods in structural plasticity. *International Centre for Mechanical Sciences. Courses and lectures*, (229):1–20, 1998.

[6] Maier, G. Mathematical programming methods in structural analysis. *Proceedings of the International Symposium on Variational Methods in Engineering, University of Southampton*, 2:A1/22–A1/54, 1972.

[7] Maier, G. and Munro, J. Mathematical programming applications to engineering plastic analysis. *Applied Mechanics Reviews*, 35(12):1631–1643, 1982.

[8] Maier, G. Mathematical programming applications to structural mechanics: some introductory thoughts. *Engineering Structures*, 6(1):2–6, 1984.

[9] Charnes, A., Lemke, C. E. and Zienkiewicz, O. C. Virtual work, linear programming and plastic limit analysis. *Proceedings of the Royal Society*, 251(1264):110–116, 1959.

[10] Prager, W. Linear programming and limit analysis, Rand Corporation, Report p-1122, June 1957.

[11] Livesley, R. K. A. A compact fortran sequence for limit analysis. *International Journal for Numerical Methods in Engineering*, 5:446–449, 1973.

[12] Smith, D. L. and Munro J. Plastic analysis and synthesis of frames subjected to multiple loadings. *Engineering Optimization*, 2:145–157, 1976.

[13] Maier, G. and Nappi, A. A theory of no-tension discretized structural systems. *Engineering Structures*, 12(4):227–234, 1990.

[14] Tam, T. and Jennings, A. Computing alternative optimal collapse mechanisms. *International Journal for Numerical Methods in Engineering*, 33(6):1197–1216, 1992.

[15] Karush, W. *Minima of Functions of Several Variables with Inequalities as Side Constraints.* MSc Thesis, Department of Mathematics, University of Chicago, 1939.

[16] Kuhn, H. W. and Tucker, A. W. Nonlinear programming. *Proceedings of the 2nd Berkeley Symposium on Mathematical Statistics and Probability*, 481–492, Brekeley, University of California Press., 1951.

[17] Munro, J. and Da Fonseca, A. M. A. Yield line method by finite elements and linear programming. *The Structural Engineer*, 56B:37–44, 1978.

[18] Faccioli, E. and Vitiello, E. A finite element, linear programming method for the limit analysis of thin plates. *International Journal for Numerical Methods in Engineering*, 5:311–325, 1973.

[19] Hayes, D. J. and Marcel, P. V. Determination of upper bounds for problems in plane stress using finite element techniques. *International Journal of Mechanical Sciences*, 9:245–251, 1967.

[20] Anderheggen, A. and Knopfel, H. Finite element limit analysis using linear programming. *International Journal of Solids and Structures*, 8:1413–1431, 1972.

[21] Christiansen, E. and Andersen, K. D. Computation of collapse states with von mises type yield condition. *International Journal for Numerical Methods in Engineering*, 46(8):1185–1202, 1999.

[22] Christiansen, E. Computation of limit loads. *International Journal for Numerical Methods in Engineering*, 17(10):1547–1570, 1981.

[23] Boothby, T. E. and Brown, C. B. A general lower and upper bound theorem of static stability. *Engineering Structures*, 15(15):189–196, 1993.

[24] Avdelas, AV. Determination of the collapse load of plastic structures by the use of an upper bounding algorithm. *Computers & Structures*, 40(4):1003–1008, 1991.

[25] Krabbenhoft, K. and Damkilde, L. Lower bound limit analysis of slabs with non-linear yield criteria. *Computers & Structures*, 80:2043–2057, 2002.

[26] Poulsen, P. N. and Damkilde, L. Limit state analysis of reinforced concrete plates subjected to in-plane forces. *International Journal of Solids and Structures*, 37(42):6011–6029, 2000.

[27] Andersen, K. D. and Christiansen, E. Limit analysis with the dual affine scaling algorithm. *Journal of Computational and Applied Mathematics*, 59(2):233–243, 1995.

[28] Krenk, S., Damkilde, L. and Hoyer, O. Limit analysis and optimal-design of plates with equilibrium elements. *Journal of Engineering Mechanics-ASCE*, 120(6):1237–1254, 1994.

[29] Andersen, K. D., Christiansen, E. and Overton, M. L. Computing limit loads by minimizing a sum of norms. *SIAM Journal on Scientific Computing*, 19(3):1046–1062, 1998.

[30] Capsoni, A. and Corradi, L. A finite element formulation of the rigid-plastic limit analysis problem. *International Journal for Numerical Methods in Engineering*, 40(11):2063–2068, 1997.

[31] Jiang, G. L. Non-linear finite-element formulation of kinematic limit analysis. *International Journal for Numerical Methods in Engineering*, 38(16):2775–2807, 1995.

[32] Liu, Y. H., Cen, Z. Z. and Xu, B. Y. A numerical-method for plastic limit analysis of 3-d structures. *International Journal of Solids and Structures*, 32(12):1645–1658, 1995.

[33] Hodge, P.G. and Belytschko, T. Numerical methods for the limit analysis of plates. *Journal of Applied Mechanics*, 35:796–802, 1968.

[34] Casciaro, R. and Cascini, L. A mixed formulation and mixed finite-elements for limit analysis. *International Journal for Numerical Methods in Engineering*, 18(2):211–243, 1982.

[35] Christiansen, E. and Larsen, S. Computations in limit analysis for plastic plates. *International Journal for Numerical Methods in Engineering*, 19(2):169–184, 1983.

[36] Capsoni, A. and Corradi, L. Limit analysis of plates-a finite element formulation. *Structural Engineering and Mechanics*, 8(4):325–341, 1999.

[37] Allen, J. D., Collins, I. F. and Lowe, P. G. Limit analysis of plates and isoperimetric-inequalities. *Philosophical Transactions of The Royal Society of London Series A-Mathematical Physical and Engineering Sciences*, 347(1682):113–137, 1994.

[38] Johnson, D. Yield line analysis by sequential linear programming. *International Journal of Solids Structures*, 32(10):1395–1404, 1995.

[39] Johnson, D. Automated yield-line analysis of orthotropic slabs. *International Journal of Solids and Structures*, 33(1):1–10, 1996.

[40] Thavalingam, A., Jennings, A., McKeown, J. J. and Sloan, D. Computer-assisted generation of yield-line patterns for uniformly loaded isotropic slabs using an optimisation strategy. *Engineering Structures*, 21(6):488–496, 1999.

[41] Johnson, D. Mechanism determination by automated yield-line analysis. *The Structural Engineer*, 72:323–327, 1994.

[42] Thavalingam, A., Jennings, A., McKeown, J. J. and Sloan, D. A computerised method for rigid-plastic yield-line analysis of slabs. *Computers & Structures*, 68(6):601–612, 1998.

[43] Ramsay, A. C. A. and Johnson, D. Analysis of practical slab configurations using automated yield-line analysis and geometric optimization of fracture patterns. *Engineering Structures*, 20(8):647–654, 1998.

[44] Dickens, J. and Jones, L. A general computer program for the yield-line solution of edge supported slabs. *Computers & Structures*, 30(3):465–476, 88.

[45] Heyman, J. *The masonry arch.* Ellis Horwood, Chichester, UK, 1982.

[46] Livesley, R. K. A. Limit analysis of structures formed from rigid blocks. *International Journal for Numerical Methods in Engineering*, 12:1853–1871, 1978.

[47] Boothby, T. E. and Brown, C. B. Stability of masonry piers and arches. *Journal of Engineering Mechanics, ASCE*, 83:118–367, 1992.

[48] Boothby, T. E. and Brown, C. B. Stability of masonry piers and arches including sliding. *Journal of Engineering Mechanics, ASCE*, 120:304–319, 1994.

[49] Gilbert M. *The behaviour of masonry arch bridges containing defects.* PhD Thesis, University of Manchester, 1993.

[50] Gilbert, M. and Melbourne, C. Rigid-block analysis of masonry structures. *The Structural Engineer*, 72:356–360, 1994.

[51] Melbourne, C. and Gilbert, M. The behaviour of multiring brickwork arch bridges. *The Structural Engineer*, 73:39–47, 1995.

[52] Melbourne, C. and Gilbert, M. Modelling masonry arch bridges. *Computational Modelling of Masonry, Brickwork and Blockwork Structures*, 197–220, Saxe-Coburg, 2001.

[53] Gilbert, M. Gross displacement mechanism analysis of masonry bridges and tunnels. *Proceedings of the 11th International Brick/Block masonry conference*, Shanghai, 1997.

[54] Fishwick, R. J. *Limit analysis of rigid block structures.* PhD Thesis, University of Portsmouth, Department of Civil Engineering, 1996.

[55] Baggio, C. and Trovalusci, P. Limit analysis for no-tension and frictional three-dimensional discrete systems. *Mechanics of Structures and Machines*, 26:287–304, 1998.

[56] Livesley, R. K. A. A computational model for the limit analysis of three-dimensional masonary structures. *Meccanica*, 27(1):61–72, 1992.

[57] Ferris, M. C. and Tin-Loi, F. Limit analysis of frictional block assemblies as a mathematical program with complementarity constraints. *International Journal of Mechanical Sciences*, 43(1):209–224, 2001.

[58] Da Fonseca, A. M. A. *Plastic analysis and synthesis of plates and shells by mathematical programming.* PhD Thesis, Imperial College London, Department of Civil Engineering, 1979.

Chapter 3

Yield Line Analysis of RC Slabs: Background

3.1 Introduction

Structural engineers are most often concerned with designing a new structure or assessing an existing one. The main task of the structural design engineer is to decide the materials to be used in the structure to be designed and the disposition and the nature of the elements of the structure. All elements need to work together so that the structure can withstand efficiently the expected conditions during its life-time, whilst bearing in mind the criteria of economy and safety.

The design procedure involves selecting of the initial sizes for the structural members, performing analysis using these sections and properties and iterative modification of the member sizes accordingly. The design criteria are often selected to suit the theory employed in the analysis and design of the structure.

Based on the analysis result, structural engineers can judge whether the members

meet the requirements and provide an adequate resistance to the loading combination under consideration.

On the other hand, the main task of an assessment engineer is to check whether the structure to be assessed has an adequate load carrying capacity.

The philosophy behind the structural assessment process differs from the philosophy adopted for the structural design process. Whilst the main interest of assessment engineers is generally to check whether the structure is adequate at the ultimate limit state, design engineers have also to check whether the structure is adequate at the serviceability limit state.

Despite this difference, it can be seen that in both cases a major aspect is structural analysis; that is the determination of stresses, strains, internal forces and displacements of a given structure under given loading conditions.

Linear elastic analysis is mostly used as the results obtained from such analysis have been used primarily as the input for the calculation of actions and displacements and for sizing the structural members. However, in some situations when designing/assessing RC slabs, complex shapes, support conditions and/or the presence of openings or unusual loading conditions may be encountered. Consequently, simplified design/analysis using linear elastic approaches may not be useful.

The available plastic approaches for the problem are the yield line method and the strip method. The yield line method is particularly suitable for slabs with considerable complexity of geometry or loading patterns. On the other hand, the strip method is valuable when the slab contains openings. One distinct advantage of the yield line method is that solutions are possible for any shape of a slab, where as most other approaches are applicable to rectangular shapes, with rigorous computations for boundary effects for other shapes. The engineer can, with ease, find the required moment capacity for a triangular, trapezoidal, rectangular, circular and any other

conceivable shape provided that the failure mechanism is known or predictable.

There has been a recent revival in interest in the yield line method. One of the outcomes from the European Concrete Building Project at Cardington is that yield line design of concrete flat slabs was found to be '*easily the best opportunity identifiable to the concrete frame industry*' [1]. In the same context, the British Cement Association, on behalf of the industry sponsors of the Reinforced Concrete Council, has recently published a document covering practical yield line design [1] to promote better knowledge and understanding of RC analysis and design by using more efficient and effective analysis tools such as the yield line analysis method.

Structural design of RC slabs based on the yield line method appears to be economic, simple and versatile. The majority of RC slabs designed using the yield line method are quick and easy to construct [1]. These slabs are usually thin and possess very low amounts of reinforcement distributed regularly across the slab. This regular reinforcement simplifies detailing and makes reinforcement easy to fix on site, speeding-up the construction process. Furthermore, yield line design further produces very economic RC slabs as it exploits the full capacity of the steel at the ultimate limit state.

Among the many possible methods for RC slabs design, yield line design appears to yield the minimum weight of reinforcement combined with least complication. This argument was exemplified on the in-situ building of the European Concrete Building Project at Cardington. In the Cardington project, three different methods of design and detailing were used. The floor slabs were designed in accordance with EC23 (DD ENV 1992-1-1) by various designers using:

1. The equivalent frame method as described in BS 8110

2. Elastic finite element analysis

3. Yield line analysis

Each floor was uniquely designed, detailed and constructed. The resulting output in terms of reinforcement weight and arrangement was then compared. Each of these methods has advantages and disadvantages with respect to the rest. For example, the sub-frame method with BS 8110 is best suited to be used in the design when tackling irregular frames. However there is no guarantee that the method will produce the most efficient design. A resort to a computerized version of the method may also be necessary.

For floors with irregular supports or geometry, large openings or carry concentrated heavy loads the finite element method is the most suitable for the job. However, experience and an extra care is needed when modelling geometry, material properties and loads on the structure. An additional advantage of the method is that it will facilitate the performance of a cracked section analysis to predict deflections and crack widths.

Using the yield line method in design will produce the most economic and uniform distribution of reinforcement. The method will enable efficient use of uniform loose bar in one or two way spanning slabs attractive particularly for sagging moment reinforcement.

In the Cardington project, the yield line method was used to design the 4th floor and it was found to give rise to the least amount of reinforcement. As shown in Table 3.1, for a complete floor, 14.5 tonnes of reinforcement would have been used using yield line theory compared to 16.9 tonnes using conventional elastic design methods.

Apart from the heavy blanket cover solution, the design based on the yield line method at Cardington [1] also led to the least bar marks being required.

Figure 3.1 shows the 4th floor at Cardington [1] during the construction phase. The half in the foreground was designed using yield line design and needed T12@200mm (565mm^2/m) for reinforcing. The other half towards the top of the picture was elastically designed and required a reinforcement of T16@175mm (1148mm^2/m). Thus the comparative economy of yield line design is clearly evident.

Floor No.	Flexural reinforcement	Tonnes /floor*	No. of bar marks/floor
1	Traditional loose bar - Elastic Design	16.9	75
2	Traditional loose bar	17.1	76
3	Rationalised loose bar	15.3**	54
4	Blanket cover loose bar - 1/2 **Yield Line Design** 1/2 Elastic Design	14.5* 23.2*	22 33
5	One-way mats - Elastic Design	19.9	42
6	Blanket cover two-way mats - FE Design	25.5	20
7	Not part of the particular research project		

* Rates given are for a whole floor. ** 1.6 tonnes additional reinforcement would have been required to meet normal deflection criteria.

Table 3.1: Configurations of flexural reinforcement in the in-situ building at Cardington

Figure 3.1: European Concrete Building Project at Cardington

3.1.1 Yield line design and serviceability limit states

One concerning issue with the yield line method, when used in the design of RC slabs, is that as a limit analysis method, it does not provide any information about the serviceability limit state behavior of the structure. In order to produce a reliable design using the method, the designer has to ensure that the relevant serviceability requirements, in particular, the limit state of deflection and cracking are satisfied. These may require a separate elastic analysis of deflection and cracking.

3.1.1.1 Deflection

Span/(effective depth) in conjunction with yield moments may be used to ensure that the actual span/(effective depth) ratio is less than the allowable span/(effective depth) ratio as specified in design codes. In the case where the actual deflection is required, simplified analysis methods or finite element methods may be employed.

3.1.1.2 Cracking

The yield line method offers the freedom of choosing arrangements of reinforcement that lead to simple detailing. However, it has to be taken into account that such arrangements should not result in a distribution of ultimate moments of resistance at the various sections throughout the slab which differ significantly from the distribution of moments given by the elastic theory. This is necessary to avoid excessive cracking at the service load, which takes place when low steel ratios at highly stressed sections are used. To limit cracking, bar spacing should be chosen to comply with the design code.

3.1.1.3 Ductility

The yield line method assumes that the slab has sufficient ductility to allow the full mechanism to be developed before crushing or any other failure modes is occur. The requirements of section ductility should be considered when determining the maximum amount of steel that can be placed in the slab. To ensure that the reinforcement will yield before the concrete fails, design codes usually provide provisions for the allowable ratios and also restrict the type of reinforcement can be used.

Ensuring that the slab has a sufficient ductility is also important from a safety point of view. Slabs with sufficient ductility will show warning signs before collapse. Adequate ductility is also economically feasible as it enables better load distribution through out the structure (load sharing).

3.2 Yield line theory

Yield line theory was originated by Ingerslev [2] who in 1922 presented a paper to the Institution of Structural Engineers in London on the collapse modes of rectangular slabs. The theory was substantially developed by Johansen [3], who published his PhD thesis on the subject in 1943. Researchers such as Kemp [4], Jones [5],[6], Wood [7],[6], Park [8], Morley [9] and many others have extended Johansen's ideas, perhaps further than he envisaged. Their intention has been to place yield line theory within the domain of classical and rigorous plastic theory. Their collective efforts led the validity of the theory being well established and made it a formidable international design tool. During the second half of the last century, the method and its application to slabs and slab-beam structures has been exposed to an intensive period of research all over the world. The results of this research have been widely reported.

Yield line method applications have not just been restricted to RC slabs; it has also been used to assess the structural performance of bolted and welded joints in steel plates [10]. However, its main application is to RC slabs (in particular 'under-reinforced' concrete slabs) where the yielding of the steel reinforcement is dominant.

3.2.1 Basic assumptions of the yield line method

The yield line method has traditionally relied on a number of assumptions. The basic assumptions are:

1. The slab is under-reinforced and collapsing because the moment capacity is met; not by other failure modes such as shear or loss of bond

   In order to apply the yield line method, the slab has to behave as a perfectly-plastic structural element. This requires the idealization of the moment-curvature relationship as the elastic perfectly-plastic curve with a long horizontal portion. This implies that the percentage of reinforcement in the slab has to be small enough for the slab not to fail by crushing of the compressed concrete before the collapse mechanism is formed. Consequently, the use of other material apart from the mild steel in concrete structures such as the use of high tensile steel may result in slabs which are not compatible with the basic assumptions.

2. The span/depth ratio is high enough such that the slab will fail in bending

   The failure mode is strongly dependent on the span/depth ratio. The higher the ratio, the more likely the slab will fail in bending.

3. Elastic deflections are negligible compared with plastic ones

   If the elastic deflections can be ignored in comparison with the plastic ones, the individual parts of the slab can be considered as plane (rigid regions) and

their intersections, the yield lines, as straight lines. That is, all rotations take place in the yield lines only. The assumed collapse mechanism is defined by a pattern of yield lines along which the reinforcement has yielded. Along these straight lines, the bending moment is the principal moment and the torsional moment is zero. Accordingly, all the shear forces at the yield line become zero.

4. The reinforcement is isotropic and orthogonal

   The yield line method applies to slabs with orthogonal isotropic reinforcements. However, the difference in the effective depth due to the fact that bars in any side of the slab cannot be placed at the same level is neglected. Orthotropic slabs may be transformed to equivalent isotropic slabs, for which analysis is usually easier, by invoking the affinity theory.

   The assumption of isotropy/orthogonality reinforcement means twisting moments are zero, in other cases where the moment in one direction does not equal the moment in a direction which is perpendicular to this, it is assumed that the twisting moment is zero.

5. Columns are considered to act as simple supports

   This is valid for long slender columns where a considerable rotation of the slab at the column is allowed [3]. Usually, the column will meet the slab rotation with a moment of some value, which should be incorporated into the equilibrium equation. However, column failures are not plastic; they may be due either to crushing or cracking. With long slender columns, column moments have negligible values compared to slab moments and can be safely disregarded completely from the calculations.

6. The effect of strain hardening of the reinforcement is negligible

   When calculating the moments of resistance of RC slabs, strain hardening in the reinforcement is not accounted for. This strain hardening can be responsi-

ble for increasing the moment of resistance of a section up to 10% [11] above the calculated value due to its increased effect when the percentage of steel is low, as in slabs.

7. The effect of changes in geometry due to deflection is negligible

   The yield line method is based on the assumption that the mid-plane remains unstrained subsequent to bending. This assumption is valid provided that there are no relatively large deflections compared with the slab thickness induced by loading.

   For relatively large deflections, appreciable deformations of the middle surface will occur and membrane or arching action will take place. The more a slab deflects, the more significant is the membrane action.

   Membrane action enhances the strength of a RC slab because of the in-plane forces developed at the supports or mid span. A typical load-deflection curve of a rectangular slab uniformly loaded and fixed along all the edges is shown in Fig. 3.2.

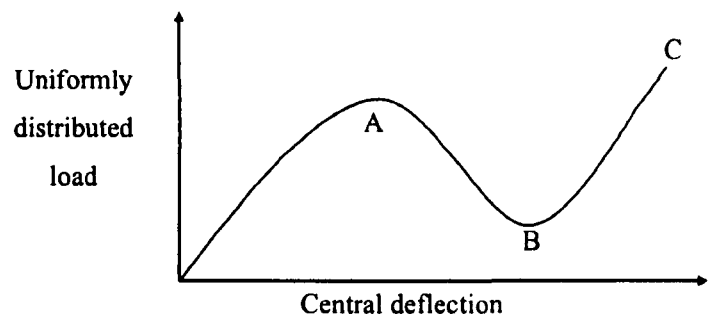

Figure 3.2: Typical load-deflection response of a restrained concrete slab

Referring to Fig. 3.2, crushing of the concrete in the central zone and the instability of the dome formed within the slab results in the peak at (A). The maximum compressive force induced in the supports occurs at/or after this peak. As deflection increases, the supported load decreases rapidly due

to the reduction in compressive membrane forces, and a stage is eventually reached near (B) where the membrane forces in the central region change from compression to tension. Beyond (B), the load is carried almost entirely by the reinforcement acting as a tensile membrane until fracture of the steel finally occurs at (C).

Based on the load-deflection response described above, two types of membrane action in RC slabs have been identified: tensile membrane action and compressive membrane action.

Tensile membrane action occurs after the slab has exceeded its compressive membrane capacity and has begun to undergo large deflections. For simply supported edges where the edges provide little or no restraint, horizontal tensile and compressive stresses have to form in the slab to ensure horizontal equilibrium. The effect of the tensile stresses is to reduce the moment of resistance of the slab, whereas the compressive stresses increase the moment of resistance. The increase in moment of resistance in the compression zone outweighs the reduction in the tension zone, with a consequent increase in the load-carrying capacity above the yield line load. If sufficient lateral restraint is provided, the tensile strength of the steel sections can provide additional capacity that will delay the progressive collapse of the slab. Full-depth cracking, inward support movement, and large deflections usually accompany the tensile membrane action.

Compressive membrane action takes place in slabs that have effective horizontal edge restraint (as is often the case with fixed supported edges). It occurs as a result of the great difference between the tensile and compressive strengths of concrete. The opening of cracks cause the slab to become lodged between the restraining edges and instigate a migration of the neutral axis, accompanied by in-plane expansion of the slab at its main boundaries. If this natural tendency to expand is restrained, very large compressive stresses in the slab

will be induced and across the slab the moment of resistance becomes very large. This may increase the load carrying capacity by 200% or more above the yield load. An idealized illustration of the arching effect in a slab strip is shown in Fig. 3.3.

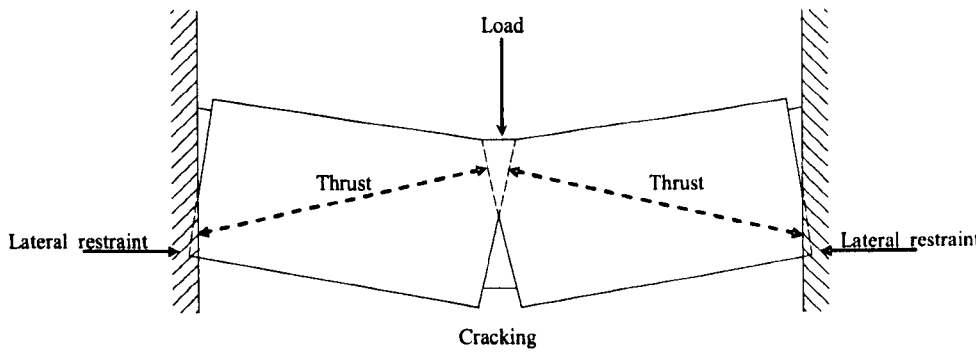

Figure 3.3: Arching action in a RC slab strip

It is worth mentioning in this regard Ockleston's observations [12]. From his monitoring of the demolition of an old hospital, he observed that it was virtually impossible to collapse a slab surrounded by other slabs (providing horizontal restraint) by vertical loading. Tests carried out on slabs through to failure have shown that the actual mode of failure is often a form of buckling. Recently, a number of small scale tests have been carried out in the Department of Civil and Structural Engineering, at the University of Sheffield [13]. In all tests, higher load factors than predicted using the yield line method have been obtained. However, in the majority of these tests, the mechanism of collapse load does not appear to be significantly affected by the membrane action, and corresponded closely to that predicted by the yield line method.

3.2.2 Yield line analysis of slabs

As an analysis tool for RC slabs, the yield line method looks at the condition of a slab just prior to collapse, when the slab can take no more increments of loading without failing. At this stage, cracks have occurred in the slab at positions where the ultimate moment of resistance of the section has been reached and where the reinforcement has yielded, owing to the fact that the slab is under-reinforced. These cracks form lines, along which the ultimate moment of resistance perpendicular to it have also been reached. These are known as yield lines. Initially, only the areas of highest moment will crack, causing a localized loss of stiffness in the section and leading to redistribution of moments within the slab. The areas adjacent to the cracked sections then have to take an increased moment, which causes them to crack also. This crack propagation continues until the yield line reaches a boundary or a free edge. At this point there can be no more increase in loading as the slab is at incipient collapse. This is shown for a square sided slab in Fig. 3.4.

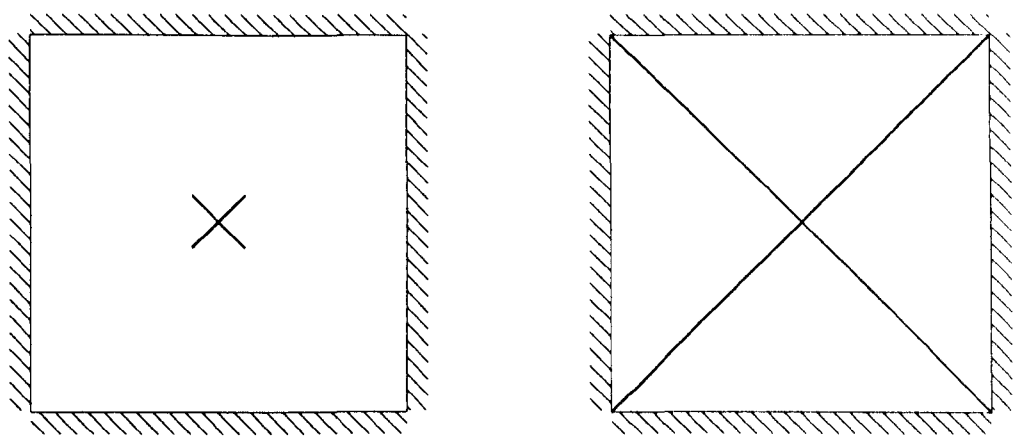

Figure 3.4: A simply supported square sided slab subject to UDL: (a) initial cracking; (b) final yield line pattern

The formation of yield lines must obey the square yield criterion. According to

the square yield criterion shown on Fig. 3.5, a yield line will form along the axis of a bending moment that has reached the moment of resistance of the slab. The square yield criterion imposes certain restrictions on how the yield lines can form. For example, a positive yield line and two negative yield lines cannot meet at the corners of a fixed edged slab. This is attributable to the fact that the intersection of true yield lines having different signs is only possible when there are only two and these cross each other at a right angle (a condition which is impossible to satisfy at corners). It is known that, at true yield lines, only the greatest principle moment acts and accordingly, torsional moments vanish. However, if there exist one sagging and two hogging yield lines, torsional moments will exist. This can be explained with the help of Mohr's circle, as shown in Fig. 3.6 for the case where one sagging and two hogging yield lines intersect. Here it is clear that there are generally torsional moments in the yield lines.

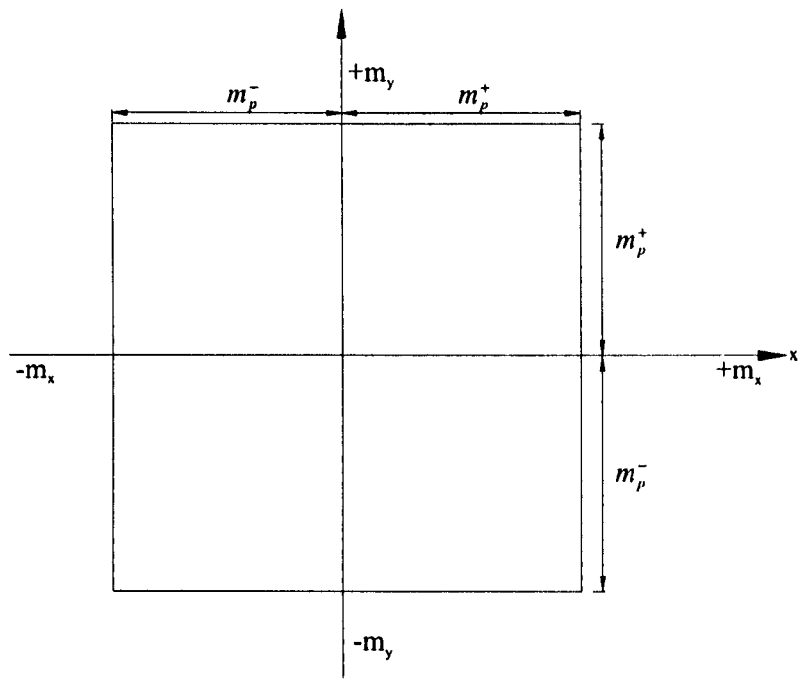

Figure 3.5: The square yield criterion

The method enables prediction of the load required to activate a pre-specified yield

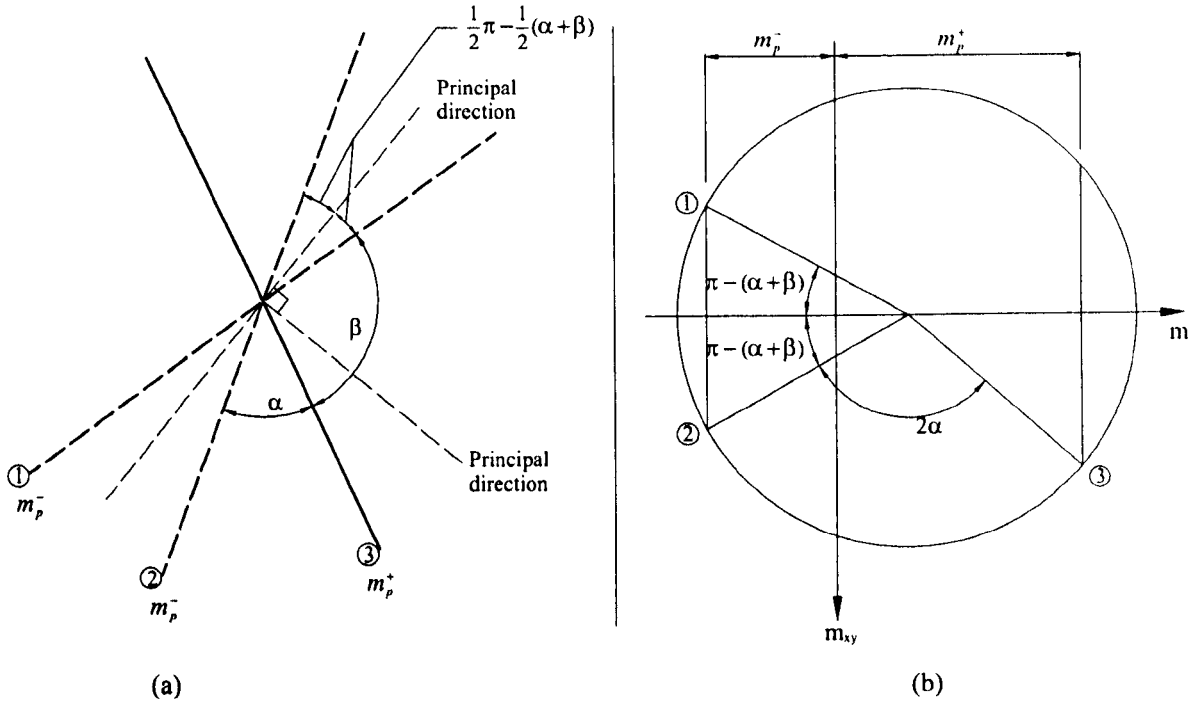

Figure 3.6: (a) Intersection of two sagging and one hogging yield lines; (b) corresponding Mohr's circle

line mechanism. This may be achieved either by the method of virtual work or by the equilibrium method. Both methods are related to each other and lead to an upper-bound solution to the collapse load for the slab. In the virtual work method, the load which activates the pre-specified yield line mechanism is determined by equating the work done by the external loads to the internal energy dissipated at the yield lines during a small motion of the mechanism.

Using the equilibrium method, the equilibrium of each segment of the yield line pattern under the action of its bending and torsional moments and shear forces is considered. A number of equilibrium equations are written by taking the moment about a suitable axis. These are then solved simultaneously to obtain the unknown dimensions of the yield line pattern under investigation.

3.3 Yield line method basics

3.3.1 Notation

The convention used throughout the thesis to illustrate types of supports, axes of rotations and yield lines is shown in Fig. 3.7.

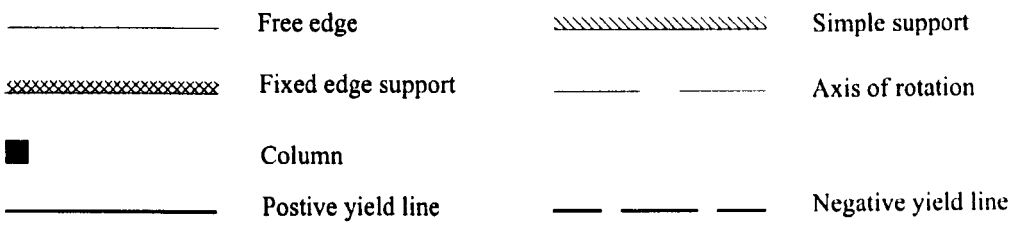

Figure 3.7: Convention for illustrating slab boundary conditions, axes of rotation, and yield lines

3.3.2 Moment of resistance

To perform a yield line analysis it is crucial to know the moment of resistance along a yield line. A yield line will not normally coincide with the line of reinforcement, but will usually make some angle θ to the line as shown in Fig. 3.8. Johansen's stepped yield criteria is used to solve the problem of having the yield line at an arbitrary angle to the reinforcement by dividing the line into a number of steps orthogonal to the reinforcement, as shown in Fig. 3.8 (b).

The moment per unit length normal to the yield line, m_{p_n}, is made up of two components, as shown in Fig. 3.8 (c).

$$m_{p_n} l = m_{p_1} l_1 \cos\theta + m_{p_2} l_2 \sin\theta \tag{3.1}$$

where l_1=$l\cos\theta$ and l_2=$l\sin\theta$

Hence

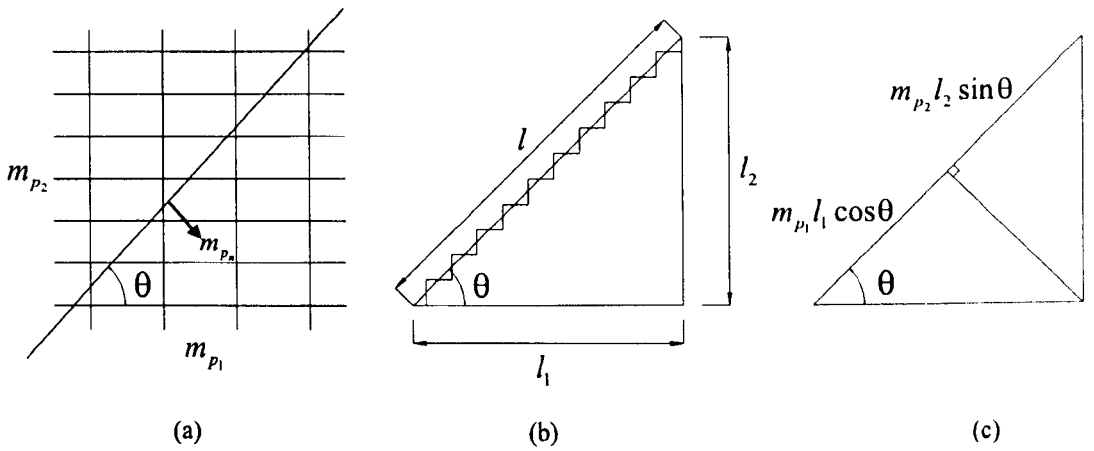

Figure 3.8: (a) Yield line inclined at angle θ to the reinforcement; (b) Johansen's stepped yield line; (c) moment of resistance

$$m_{p_n} = m_{p_1} \cos^2\theta + m_{p_2} \sin^2\theta \tag{3.2}$$

For cases when $\theta = 0$, the transverse reinforcement is not needed and $m_{p_n} = m_{p_1}$. When $m_{p_1} = m_{p_2} = m_p$ the value of m_{p_n} is also m_p, i.e. the moment of resistance of the slab is uniform in whichever direction is chosen, i.e. whatever value θ takes. When a slab has equal moments of resistance in two mutually perpendicular directions it is said to be isotropically reinforced. For simple slab geometries it is not too difficult to find the rotations of the yield lines, but when the geometry of the slab is more complex, this may not possible. In this situation, it is convenient to split the slab vectorially into components in the x and y directions and use the following equation:

$$\text{Internal work} = m_{p_x} l_x \theta_x + m_{p_y} l_y \theta_y \tag{3.3}$$

where m_{p_x} and m_{p_y} are the yield (plastic) moments in the x and y directions, l_x and l_y are the projection of the yield line onto each axis and θ_x and θ_y are the rotations about each axis.

3.3.3 Pattern rules

The patterns that yield lines make are easily identified for simple shapes such as the simply supported square slab shown in Fig. 3.9, but are not so apparent for more complex shapes. For this reason rules or guidelines have been set-out for pattern determination.

When choosing a pattern of yield lines for the analysis of a slab, it must be done so that the rigid regions bounded by the yield lines are allowed to remain rigid and uncracked. As the rigid regions that rotate are plane sections, then the intersection of two rigid regions, i.e. a yield line, must be straight. Therefore, all yield lines are straight.

If a rigid region rotates, it must do so about an axis. In Fig. 3.9, a rigid region 'a' rotates about line AB, region 'b' rotates about BC, 'c' about CD and 'd' about DA. From this example, it is clear that when a and b rotate, their line of intersection, yield line EB, also intersect with the axis of rotation of a and b, lines AB and BC respectively. This is a condition that must always be fulfilled.

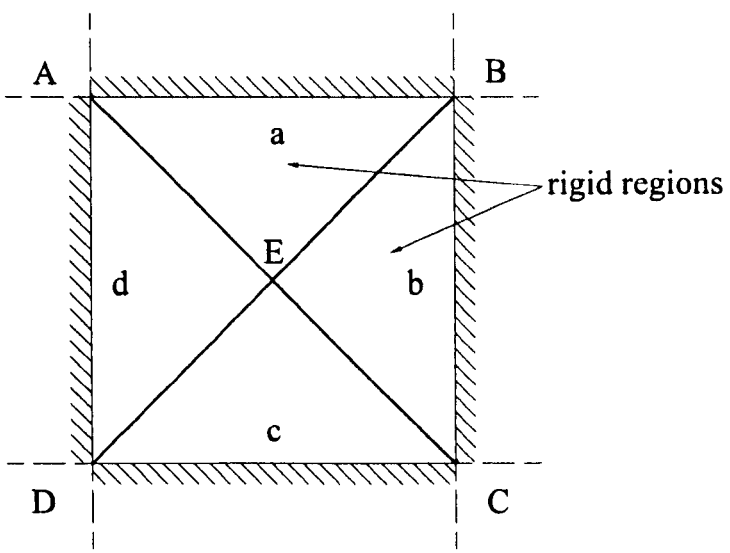

Figure 3.9: Axis of rotations of rigid region

A yield line itself does not have to intersect directly with another axis of rotation, it can intersect on an extension of one, as shown in Fig. 3.10. The intersection of the three yield lines is not constrained to be exactly at point A on the diagram, it could be at point B, but in this case, the yield line extension must still pass through point C. The actual point where the yield lines meet depends on the reinforcement and the loading present.

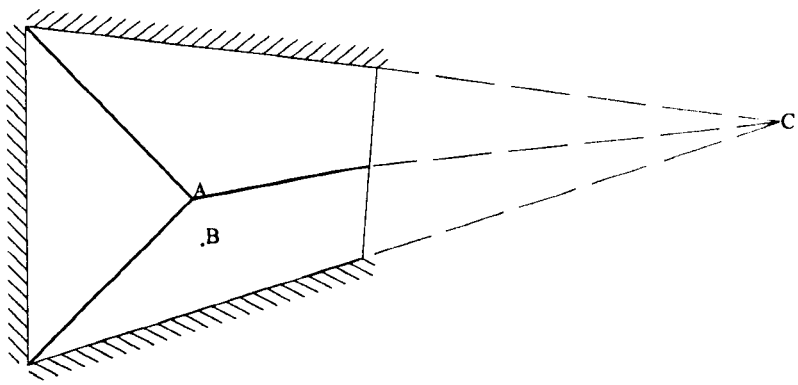

Figure 3.10: Axes of rotation and extension of yield line intersecting at a point

In some cases, such as where a slab is simply supported at two ends only, as shown in Fig. 3.11, the axis of rotation intersects with the yield lines at infinity.

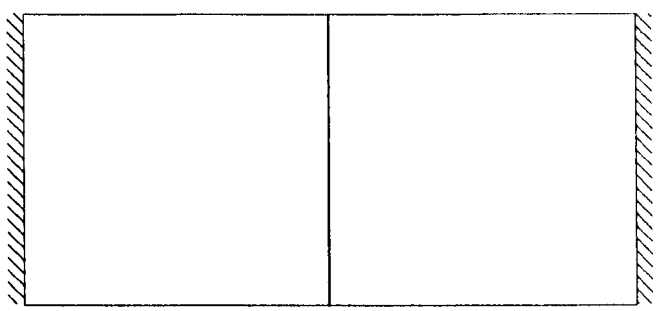

Figure 3.11: Axes of rotation and yield line intersecting at infinity

As well as line supports, simple and fixed, columns can also act as an axis of rotation i.e. an axis of rotation passes over the column, as shown in Fig. 3.12.

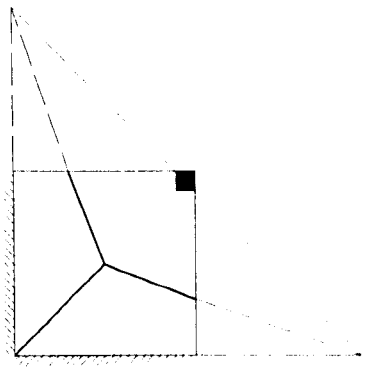

Figure 3.12: An axis of rotation at a column

Any symmetry in a slab is also present in the yield line pattern, as in the square-sided slab of Fig. 3.9.

The rules covered here can be explicitly stated as follows:

- Yield lines are straight.
- Yield lines terminate at slab boundaries.
- Yield lines (or their extensions) pass through the intersection of the axes of rotation of the rigid regions which the yield line lies at the intersection of.
- Axes of rotation lie along lines of support, on columns or along the yield lines themselves.
- Symmetry of the slab is maintained in the yield line pattern.

3.3.4 Fan mechanisms

A special form of mechanism is produced when concentrated (point loads) are introduced or when a slab rests on a column, as shown in Fig. 3.13. This is called a

fan mechanism, for obvious reasons. Here cracks propagate radially from the point of loading and may extend as far as they can until it is not possible to do so, for instance up to a free edge as shown in Fig. 3.14.

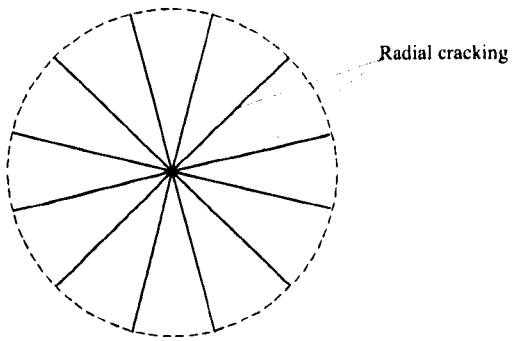

Figure 3.13: A fan mechanism

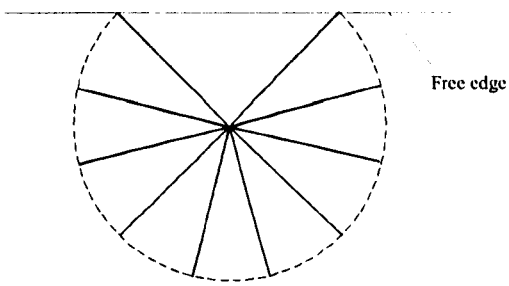

Figure 3.14: A fan mechanism near a free edge

The negative (hogging) yield line, which occurs around the perimeter of a fan mechanism, may seem to be an arc although it is in fact a number of straight lines.

3.3.5 Corner levers

Corner levers are another special case which result from the square yield criterion (Fig. 3.5). The square yield criterion forbids one positive and two negative yield lines meeting at a corner in a slab, meaning that diagonal patterns such as those for a square slab with fixed supports cannot occur as this criterion is contravened and an alternative mechanism must therefore occur. One mechanism involving corner

levers is shown in Fig. 3.15, where corner levers form instead of the diagonal yield line intersecting the corner of the slab.

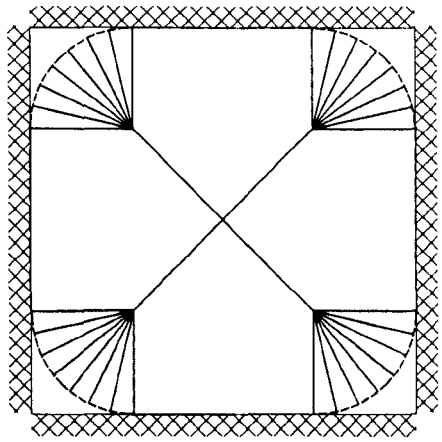

Figure 3.15: Corner levers set up so as to prevent violation of square yield criterion at corners

3.4 Example

The slab shown in Fig. 3.16 is simply supported on all four sides with equal reinforcement in both the x and y directions (therefore also having equal plastic moments m_p per unit length). There is only bottom reinforcement. The slab is subject to a uniform pressure of intensity p per unit area. The problem is to find the load factor which if applied to the live load will lead to collapse. For this example the yield line pattern is assumed to be as in Fig. 3.16(a). Using a modified version of equation 2.1 and assuming that each segment between the yield lines is an "element" and each yield line between the segments is an "interface", m will be 4 and n will also be 4. As the pattern and its dimension is known in advance, there is no need for the minimization process.

Applying the principle of virtual work and assuming that the self weight of the slab is negligible compared to the live load, equation 2.1 can be re-written as:

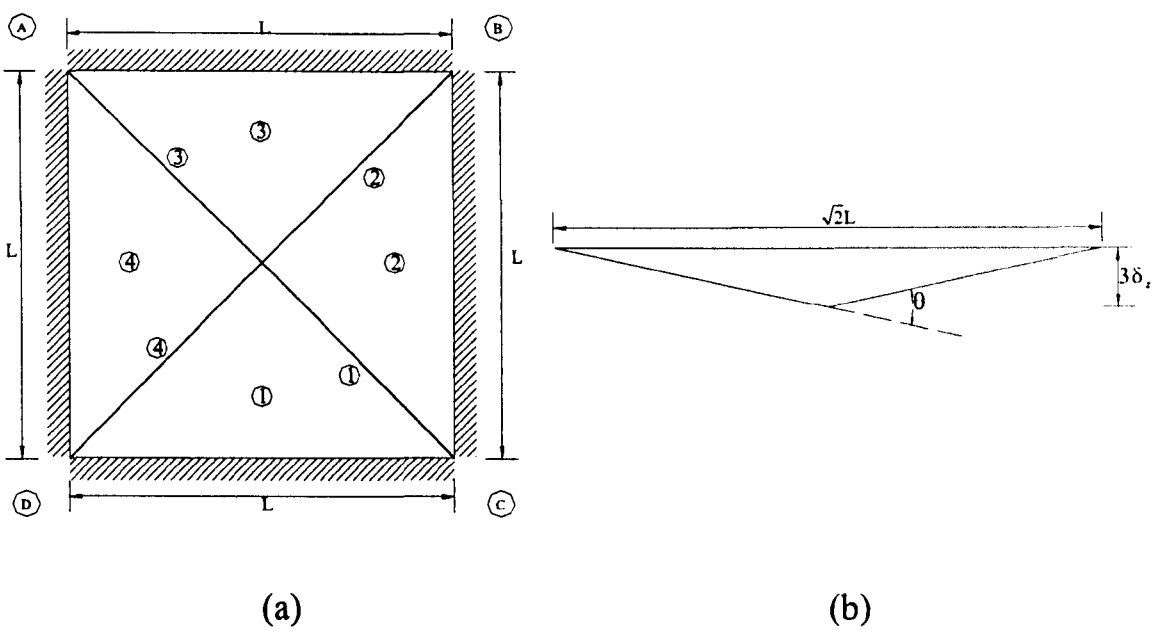

Figure 3.16: Example 1: (a) yield line pattern for a simply supported slab; (b) section normal to AC or BD

$$\lambda \mathbf{f}_L^{\mathrm{T}} \mathbf{d} = \mathbf{g}^{\mathrm{T}} \mathbf{u} \tag{3.4}$$

where $\lambda \mathbf{f}_L^{\mathrm{T}} \mathbf{d}$ represents the internal work and $\mathbf{g}^{\mathrm{T}} \mathbf{u}$ the external work.

The internal work and the external work can be evaluated as follows:

1. Internal work

   For a slab element, moments are limited to the slab plastic moments. This means:

$$\left.\begin{aligned} m_{l_{x_i}} &= m_{p_{x_i}} \\ m_{l_{y_i}} &= m_{p_{y_i}} \\ m_{l_{z_i}} &= 0 \\ f_{l_{x_i}} &= f_{l_{y_i}} = f_{l_{z_i}} = 0 \end{aligned}\right\} \text{for each interface, } i = 1,...,4 \tag{3.5}$$

$$\Rightarrow \quad \mathbf{g}^{\mathrm{T}} = [m_{p_{x_1}}\ m_{p_{y_1}}\ m_{p_{x_2}}\ m_{p_{y_2}}\ m_{p_{x_3}}\ m_{p_{y_3}}\ m_{p_{x_4}}\ m_{p_{y_4}}] \tag{3.6}$$

   and as there are no translational movements between elements at this interface

   $\Rightarrow$

$$\left.\begin{aligned} u_{x_i} = u_{y_i} = u_{z_i} &= 0 \\ \theta_{z_i} &= 0 \end{aligned}\right\} \text{for each interface, } i = 1,...,4 \tag{3.7}$$

$$\Rightarrow \quad \mathbf{u}^{\mathrm{T}} = [\theta_{x_1}\ \theta_{y_1}\ \theta_{x_2}\ \theta_{y_2}\ \theta_{x_3}\ \theta_{y_3}\ \theta_{x_4}\ \theta_{y_4}] \tag{3.8}$$

   Equation 3.6, 3.8 can be compactly rewritten by combining the rotations at each interface as follows:

$$\mathbf{g}^{\mathrm{T}} = [m_{p_1}\ m_{p_2}\ m_{p_3}\ m_{p_4}] \tag{3.9}$$

$$\mathbf{u}^{\mathrm{T}} = [\theta_1 \ \theta_2 \ \theta_3 \ \theta_4] \tag{3.10}$$

where m_{p_i} is the ultimate moment of resistance at yield line i and θ_i is the same yield line rotation. As the slab is isotropically reinforced, $m_{p_1} = m_{p_2} = m_{p_3} = m_{p_4} = m_p$ and $m_{p_i} = m_p l_i$ where l_i is the length of yield line i, $l_1 = l_2 = l_3 = l_4 = \frac{L}{\sqrt{2}}$. Also from symmetry $\theta_1 = \theta_2 = \theta_3 = \theta_4$.

From basic trigonometry, $\theta_1 = \frac{2(3\sqrt{2}\delta_{z_1})}{L} = \frac{6\sqrt{2}\delta_{z_1}}{L}$.

Re-arranging all equations:

$$\text{Internal work} = \begin{bmatrix} \frac{m_p L}{\sqrt{2}} & \frac{m_p L}{\sqrt{2}} & \frac{m_p L}{\sqrt{2}} & \frac{m_p L}{\sqrt{2}} \end{bmatrix} \begin{bmatrix} \frac{6\sqrt{2}\delta_{z_1}}{L} \\ \frac{6\sqrt{2}\delta_{z_1}}{L} \\ \frac{6\sqrt{2}\delta_{z_1}}{L} \\ \frac{6\sqrt{2}\delta_{z_1}}{L} \end{bmatrix} \tag{3.11}$$

$$\Rightarrow \quad \text{Internal work} = 24 m_p \delta_{z_1} \tag{3.12}$$

2. External work

The uniformly distributed load is assumed to act at the center of each of the four elements. Accordingly, the vertical load P_j at the center of element j can be calculated as $p_j A_j$, where A_j is the total area of element j.

Considering that only the vertical loads are applied, this implies:

$$\left.\begin{aligned} & f_{L_{x_j}} = f_{L_{y_j}} = 0 \\ & m_{L_{x_j}} = m_{L_{y_j}} = m_{L_{z_j}} = 0 \\ & f_{L_{z_j}} = p_j A_j \end{aligned}\right\} \text{for each element, } j = 1,...,4 \quad (3.13)$$

$$\Rightarrow \quad \mathbf{f}_L^{\mathrm{T}} = [P_1 \; P_2 \; P_3 \; P_4] \quad (3.14)$$

Supposing that the slab surface lies in the x-y plane, this entails:

$$\left.\begin{aligned} & \delta_{x_j} = \delta_{y_j} = 0 \\ & \phi_{z_j} = 0 \end{aligned}\right\} \text{for each element, } j = 1,...,4 \quad (3.15)$$

And as there are no applied moments in the live load, $\phi_{x_j}, \phi_{y_j}, \phi_{z_j}$ can be omitted from the element displacements vector.

$$\Rightarrow \quad \mathbf{d}^{\mathrm{T}} = [\delta_{z_1} \; \delta_{z_2} \; \delta_{z_3} \; \delta_{z_4}] \quad (3.16)$$

Because of symmetry, $P_1 = P_2 = P_3 = P_4$ and $\delta_{z_1} = \delta_{z_2} = \delta_{z_3} = \delta_{z_4}$. Also $P_1 = p_1 A_1 = 0.25 p_1 L^2$

$$\Rightarrow \quad \text{External work} = \lambda \begin{bmatrix} 0.25p_1L^2 & 0.25p_1L^2 & 0.25p_1L^2 & 0.25p_1L^2 \end{bmatrix} \begin{bmatrix} \delta_{z_1} \\ \delta_{z_1} \\ \delta_{z_1} \\ \delta_{z_1} \end{bmatrix} \quad (3.17)$$

$$\Rightarrow \quad \text{External work} = \lambda p_1 L^2 \delta_{z_1} \quad (3.18)$$

Equating internal work to external work gives:

$$\lambda p_1 L^2 \delta_{z_1} = 24 m_p \delta_{z_1} \Rightarrow \lambda = \frac{24 m_p}{p_1 L^2}$$

If m_p is taken as 1 and $p_1 L^2$ as 1 $\Rightarrow \lambda = 24$.

The static approach can also be used to find λ. Consider the equilibrium of element 1. Taking the moment about DC gives:

$$\lambda p_1 (0.25 L^2) \left(\frac{L}{6}\right) = m_p \left(\frac{L}{2} + \frac{L}{2}\right) \text{ or } \lambda = \frac{24 m_p}{p_1 L^2}$$

3.5 Closing remarks

Having reviewed yield line analysis basics, the next chapter is devoted to automated yield line analysis methods. Previous and on-going research into yield line optimization will be reviewed. The static and kinematic approaches for yield line analysis formulations will be discussed and presented. A computer program based on the modified static and kinematic formulations will be developed and implemented. Samples of the program output will be presented and discussed.

References

[1] Kennedy, G. and Goodchild, C. *Practical Yield Line Design.* British Cement Association, Crowthorne, UK, 1990.

[2] Ingerslev, A. The strength of rectangular slabs. *The Structural Engineer*, 1(1):3–14, 1923.

[3] Johansen, K. W. *Yield Line Theory.* Cement and Concrete Association, London, UK, 1962.

[4] Kemp, K. O. The yield criterion for orthotropically reinforced concrete slabs. *International Journal of Mechanical Sciences*, 7:737–746, 1965.

[5] Jones, L. L. *Ultimate Load Analysis of Reinforced and Pre-stressed Concrete Structures.* Chatto & Windus, London, UK, 1962.

[6] Jones, L. L. and Wood, R. H. *Yield Line Analysis of Slabs.* Thames and Hudson, London, UK, 1967.

[7] Wood, R. H. *Plastic and Elastic Design of Slabs and Plates with Particular Reference to Reinforced Concrete Floor Slabs.* Thames and Hudson, London, UK, 1961.

[8] Park, R. and Gamble, W. L. *Reinforced Concrete Slabs.* Wiley & Sons, New York, U.S.A, 2000.

[9] Morley, C. T. On the yield criterion of an orthogonally reinforced concrete slab element. *International Journal of Mechanics and Physics*, 14:33–47, 1966.

[10] Sumner, E. A. *Unified Design of Extended End-Plate Moment Connections Subject to Cyclic Loading.* PhD Thesis, Virginia Polytechnic Institute and State University, 2003.

[11] Stuart, S. J. *Plastic Methods for Steel and Concrete Structures.* Macmillan Press Ltd, London, UK, 2002.

[12] Moy, S. S. J. *Plastic Methods for Steel and Concrete Structures.* Macmillan Education, London, UK, 1996.

[13] Foster, S. G., Bailey, C. G., Burgess, I. W. and Plank, R. J. Experimental behaviour of concrete floor slabs at large displacements. *Engineering Structures*, 26(26):1231–1247, 2004.

Chapter 4

Automated Yield Line Analysis of RC Slabs

4.1 Abstract

A novel limit analysis method for RC slabs and bridge decks that overcomes the problems encountered by previous workers in this field is developed. An ultimate load carrying capacity analysis is carried out by discretizing the slab deck into a large number of rigid elements. A kinematic approach is adopted and novel mathematical rules to describe how adjacent elements should interact with each other are used in the formation of the requisite linear programming tableau. These rules differ in important respects from the over restrictive rules adopted by previous workers in this field. This ensures that safe estimates of structural strength are obtained. Once a work equation has been set up, a solution is then sought using a linear programming algorithm. Appropriate state-of-the-art algorithms have been employed to solve the underlying LP problem. The results obtained agree quite well with known exact solutions for various different slab configurations, boundary conditions and loading arrangements. An attempt to obtain rigorous upper-bound solutions (i.e.

satisfying kinematical admissibility criteria) using the method has also been made, and rigorous upper-bound solutions have been obtained for a number of problems.

Keywords: Automated yield line analysis; Shear forces; Linear programming

4.2 Introduction

Although yield line theory is long established, it is still not that widely used in practice. This may partly be due to engineers being concerned that they have failed to identify the critical failure mechanism and partly because of the unfamiliar nature and possible complexity of the calculations for all but the simplest cases. In this respect, the method would therefore appear to be well-suited to computerization. If it were possible to develop an automated yield line analysis/design software, it is likely that the method will be regularly used by practicing engineers.

4.3 Literature review: research into yield line optimization

In order for the exact solution to the problem of finding the critical load factor for RC slabs to be found, the correct mechanism must first be identified. For simple slabs, the choice will be limited to only a few possibilities and the solution may easily be obtained using hand calculation by setting out the problem in terms of the geometry of a particular pattern with unknown variables (such as ratios or angles) and then differentiating the load factor with respect to the unknowns. This form of analysis requires the selection of possible mechanisms and then refinement of them, which is done here by finding the turning point of the load factor parameter.

For more complex slab layouts it becomes increasingly difficult to identify potential mechanisms and thus the refinement may lead to the optimum for the mechanism selected, but the critical mechanism may have been neglected entirely. It is this area, the identification of critical yield line patterns, that is the major problem when yield line analysis is implemented into computer programs. For the program to be effective, a general approach should be considered whereby all possible mechanisms are considered and the overall optimum values of all potential mechanisms are analysed. This can be achieved by automating the process of mechanism selection.

Before discussing in detail the computerization of upper-bound limit analysis of RC slabs using the yield line method, it is worthwhile to review previous work undertaken on the computerization using lower-bound formulations. Procedures combining lower-bound methods and linear programming were initially proposed to automate RC slabs analysis. Hodge and Blelytschko's [1] work on numerical methods for limit analysis of plates appeared to be the first of its kind in this area. With particular consideration of RC slabs, Anderheggen and Knopfel's work [2] was the first attempt to computerize the limit analysis of RC slabs. Linear equilibrium or kinematic compatibility equations were formulated and parametric stress fields and displacements fields had to be assumed prior to the analysis. There were approximated by means of finite elements. Two plate-bending models were proposed: (i) a linear-linear model where linear deflections and linear bending moments was assumed, and (ii) a linear-constant model where linear deflections and a constant moment distribution was assumed. One of the drawbacks of this method was the slow convergence of the load factor, which is attributed to the model's poor representation of the internal forces.

Krenk *et al.* [3] presented a finite element formulation for the limit analysis of perfectly-plastic plates using triangular equilibrium elements. Elements were formulated using three moment components at each corner. Equivalent corner forces

including shear and torsion moment contributions were derived in a simple vector format. A static formulation was adopted and the problem was linearized by approximating the non-linear yield surface with eight planes. As a linear programming problem, duality theory [4] was invoked to obtain displacements and rotations. From the examples they presented it appears that the method produces lower-bound solutions. However, nothing is mentioned about the outcomes of the method if the number of elements is increased above 8 per side. However, in a subsequent paper [5] the same authors acknowledged that, in the case of fixed edged slabs, the load factor obtained with this method actually converged to a value which was higher than the exact solution. This clearly means this method is not a rigorous lower-bound method; indeed this was acknowledged in their conclusions. They concluded that a lower-bound can not be guaranteed because of the assumptions made about the load distribution and the corresponding restrictions on the moment field.

Recently, Krabbenhoft and Damkilde [5], presented a finite element formulation for the limit analysis of perfectly-plastic slabs. An element with linear moment fields, for which equilibrium is satisfied, was proposed. Equilibrium equations for the triangular plate bending element were derived using area coordinates. Both load and material optimization problems were formulated and by means of the duality theory of linear programming, the displacements were extracted from the dual variables. From the examples they presented, the method may seem promising, however there are a few concerns. Firstly, special solvers had to be employed. For a method to be practically usable, ordinary linear programming solvers, preferably, should be used. Also, nothing is mentioned about the method performance when the number of divisions per side is higher than 14 .

For upper-bound methods, automated techniques for the yield line method have focused on the evaluation of the collapse load factors for specified trial mechanisms by computerizing traditional hand techniques. However this tends to be of lim-

ited applicability. A more general automated approach is to apply mathematical programming techniques.

Early work on an automated method was carried out by Munro and Da Fonseca [6]. In the Munro and Da Fonseca method, the slab to be analysed is discretized as a mesh of rigid triangular elements and yield lines are constrained to develop only along inter-element boundaries and boundary edges. The displacements of the nodes at the corners of the triangles are used to describe the slab deformations due to external loading. Since the finite elements are assumed to act as flat plates, the angle of rotation across any interface between any two elements, or an element and an edge, is constant along this interface. Depending on which formulation is adopted, geometric compatibility or equilibrium conditions, yield constraints and an optimization function based on virtual work are developed and assembled using Karush-Kuhn-Tucker conditions giving a mathematical model in the form of a linear programming problem.

The yield line analysis automation procedure developed by Munro and Da Fonseca enables simultaneous investigation of a number of potential yield line mechanisms. Thus with this method, many potential mechanisms, each having a different collapse load factor are defined by a single mesh. The yield line mechanism which gives the lowest load factor is likely to be the critical collapse mechanism. The identification of the critical yield line pattern is carried out automatically as part of the linear programming solution process. The collapse mechanism does not need to be specified or known initially since the procedure will identify the critical yield pattern.

Whereas the automation of the yield line analysis method by Munro and Da Fonseca represented a considerable advance, the stipulated mesh size and orientation does affect results and remains a matter of judgment of the user. For the examples they presented, the critical mechanism was already known in advance so they selected the mesh to coincide with the yield line pattern and as such no attempt for

selecting the correct topography of the problem was necessary. Balasubramanyam and Kalyanaraman [7] developed a similar method to Munro and Da Fonseca and examined ways of defining the mesh geometry in order to avoid particularly poor predictions. Depending heavily on previous work in the field of plastic theory and on the work carried out by Cohn *et al.* [8], they assumed that a failure mechanism of a slab can be considered to consist of a number independent mechanisms, with linear programming being used to find the optimum combination of these.

Bauer and Redwood [9] proposed a computerized numerical method based on the virtual work technique. In order to find the critical yield line pattern, the method generates a series of yield line patterns and the pattern giving the minimum yield load is retained as the solution. Around the same time, Dickens and Jones [10] developed a method to automate the traditional hand approach; however this is restricted to a limited range of boundary conditions.

Shoemaker [11] developed a computer program to analyse RC rectangular slabs under different combinations of edge conditions. Here the geometric and strength data have to be supplied by the user. Once the data are provided, the program will iterate through a number of pre-defined yield line patterns evaluating the nominal load for each one by equating the internal work and the external virtual work. The smallest nominal load is assumed to be the upper-bound solution for the collapse load. The program was applied to the case of a balcony rectangular floor with free and simple supports. The program identified the fourth yield line pattern as being critical and the slab capacity as 222.31psf (10.7kN/m^2). However this value was incorrect and led to grossly underestimate the quantity of reinforcement needed for the slab as demonstrated by Hillerborg [12]. Using a simple calculation, he demonstrated that for the same yield line pattern, the slab capacity is actually 194psf (9.33kN/m^2). This value is 13% less than the answer given by Shoemaker's program. He went further and showed that another yield line pattern will produce a 177psf

(8.47kN/m^2). A complicated version of this pattern will reduce the slab capacity to 117psf (5.6kN/m^2) which is 47% lower than the value given by Shoemaker. This clearly demonstrates the importance of identifying the most critical yield line pattern when designing slabs, as the identification of wrong failure patterns may result in unsafe designs. It also highlights the importance of calibrating computer programs against known solutions, or performing simple checks to ensure that the program is producing reliable results.

Islam *et al.* [13] presented a computer-oriented procedure for the yield line analysis of slabs. Here they employed the procedure described by Dickens and Jones [10] with the modification of replacing the arbitrary method of deciding the new yield line pattern in successive iterations by a search direction determined on the basis of a non-linear Simplex algorithm. They based their procedure on the concept of calculating the ratio of the slab moment m and the uniformly distributed load p, i.e. m/p, for the yield line pattern by virtual work and equilibrium methods and by making the m/p values obtained by the two methods converge. The non-linear Simplex algorithm was employed for this reason.

All of these methods generally make prior assumptions about the yield line pattern or require the user to define the likely yield line pattern. This restricts their range of application and does not produce general, versatile, analysis tools.

Although the automated yield line method proposed by Munro and Da Fonseca is generally able to identify the critical yield line pattern, provided that a suitable mesh is chosen, in many cases optimizing the geometry of this pattern can lead to further reductions in the load factor. The geometric optimization of yield line patterns has been tackled Johnson [14, 15, 16] and Jennings *et al.* [17, 18].

Johnson [14] attempted to tackle the problem by using a sequential linear programming procedure. After having postulated a conventional Munro and Da Fonseca analysis he then considered geometric variation of the chosen yield line patterns by

using linear geometric sensitivities or so called 'move limits', which are variables that control how far the portions of yield lines can move. The drawbacks associated with this method are:

- Direct generation of critical collapse modes is not generally possible.
- The geometric variables are only likely to have a significant effect on collapse load in the case of yield line systems which are geometrically variable in, or close to, region of hogging bending.

In a similar vein, Johnson [15] addressed the problem of identifying the critical geometry of yield line patterns and he presented a two-phase solution. The first phase was to set up a "fine" mesh using the triangulation of the Munro and Da Fonseca method. Once the program produced a viable solution, the second phase was to optimize the phase 1 pattern by adjusting the geometry of the yield line pattern previously identified to obtain a lower load factor. Although it may seem that this approach will lead to an optimal solution for the problem, there are many doubts about this. The postulated yield line pattern is restricted to the assumed mesh and consequently it is not capable of modelling yield line patterns that do not coincide with the presumed mesh. For example, the mesh shown in Fig. 4.1 cannot model a yield pattern involving a hogging yield line AB[†]; instead it would probably model the yield line as the dashed lines in the figure, where this mechanism is critical. Alternatively, the mechanism may involve a yield line from A through C to B. In both cases, the resulting load factor will likely be higher than the critical one. Additionally, the mesh used means it is virtually impossible to model fan type mechanisms no matter what the level of refinement.

Sloan *et al.* [17] presented a semi-automatic method to predict the mechanisms which are most likely to cause collapse. Here they adopted a computational tech-

[†] Of course other yield lines are needed in positions where the hogging yield changes direction. However these are omitted here for clarity.

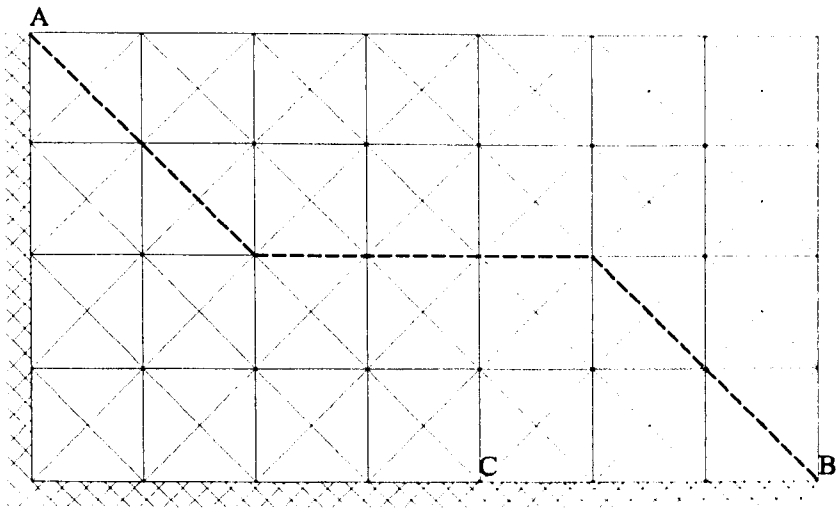

Figure 4.1: Example of inaccurate size/orientation

nique employing linear programming to evaluate the Munro and Da Fonseca solution for any given trial element geometry. Non-linear optimization techniques, based on a modified conjugate gradient method, were used to control the optimization of the nodal geometry. Analytically linearized constraint equations were developed to be used with the conjugate gradient method, in order to overcome problems caused by the existence of discontinuities in the slope of the objective function. Constraints were applied to ensure that no node could cross an edge, no triangular element could disappear and no element could be created during the mesh adjustment process, i.e. restricting the search area to regions having the same yield line topology. The method however suffers from severe disadvantages. Firstly: the procedure is 'semi-automatic'; only configurations having the same topology are considered in the optimization process. Secondly: the method lacks generality, it is restricted only to isotropic slabs subjected to uniformly distributed loading and therefore it cannot be used in situations where line loads are present. Thirdly: the user is required to input triangular element meshes having different topologies where it is envisaged that these could yield more critical mechanisms. This leads to a situation where the decision of choosing the mesh remains one of user-judgment.

The same authors later presented a similar approach but this time the computer was used to generate the starting triangular mesh [18]. Although it may seem like one of the shortcomings of their previous work had been overcome, the modified approach effectively depends on the basic assumption that local minima do not exist. This is known not to hold true.

Recently, Liu [19] developed another automatic computational method for yield line analysis. The basic procedure is based on considering the three dimensional geometric compatibility of the slab elements at collapse. He adopted a radical approach which recognizes that all yield lines inside the slab must be common to pairs of rigid slab elements and each of these elements must have rotated plastically about a common axis. These axes of rotations may be determined using basic rules, which govern the prediction of yield lines patterns; meanwhile the whole system must satisfy geometric compatibility criteria.

The overall work equation is expressed in terms of yield line pattern parameters, the loading arrangement and the moment capacity due to reinforcement arrangement. Once the work equation is set up, the required flexural resistance can then be determined by the maximization of the virtual work equation using an iterative conjugate gradient method. The iterative procedure starts with an initial guess automatically generated by the program assuming that the relative rotations in all slab elements are unity.

Although the procedure can be applied to variety of slab configurations and loading combinations, two shortcomings can easily be identified: (i) the proposed method is not suitable for slabs which have reflex internal angles at any corners (ii) the proposed method cannot identify fan-type yield line patterns.

4.4 Linear programming and yield line analysis of RC slabs: A new approach.

4.4.1 Introduction

From the previous review of work undertaken in the field of yield line analysis automation, the shortcomings of existing methods can be classified into two main groups:

1. Methods which cannot identify some yield line patterns such as the fan mechanism or patterns involving corner levers. This is primarily because the yield lines are restricted to develop only along the element boundaries. This includes the methods of: Munro and Da Fonseca [6], Balasubramanyam and Kalyanaraman [7], Johnson [14], Johnson [15], Liu [19].

2. Methods which place some restrictions on the geometrical configuration, reinforcement arrangement and loading patterns that can be handled. This applied to the methods proposed by Sloan *et al.* [18], Liu [19].

Having identified the drawbacks associated with previous approaches, the objective here is to develop a new automatic computational method to perform yield line analysis. The proposed method will be applicable to a variety of geometrical configurations, reinforcement arrangements and loading patterns. Furthermore, the proposed method will be capable of identifying failure mechanisms which involve fan mechanisms or corner levers. These two characteristics represent a major advance in the field of yield line analysis and overcome the previously identified shortcomings.

Since the new method builds on the method originally proposed by Munro and Da Fonseca, the latter will be first studied in some details.

4.4.2 Yield line analysis of RC slabs: the Munro and Da Fonseca method

As previously mentioned, in the method proposed by Munro and Da Fonseca [6], the slab to be analysed is divided into triangular elements with yield lines being restricted to develop only along the edges of the triangular mesh and/or at supporting edges. Out-of-plane deformations are governed by element nodal displacement variables. The angle of rotation between adjacent elements is constant based on the assumption that triangular elements behave as flat plates. A typical element is shown in Fig. 4.2.

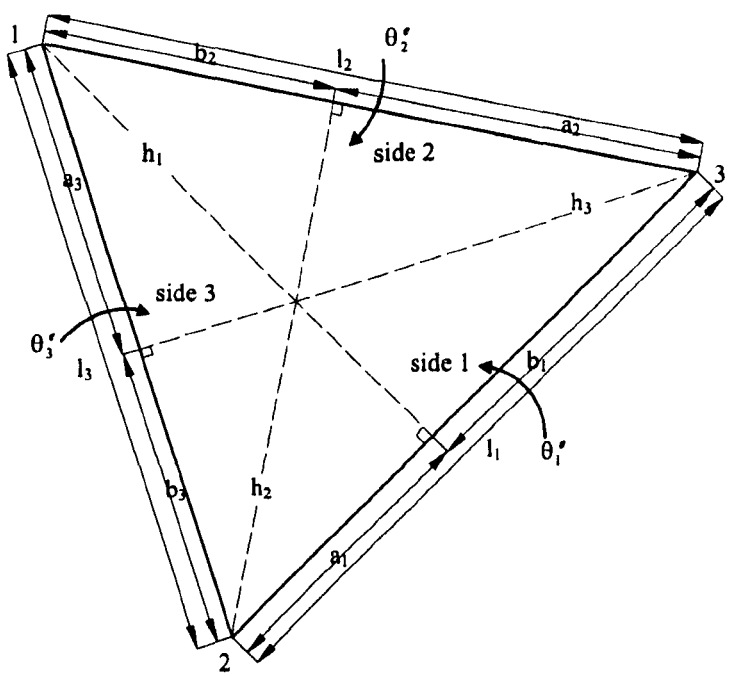

Figure 4.2: Geometry of a triangular element

The kinematic equation defining the rotation θ_i^e based on the geometry shown in Fig. 4.2 can be written as:

$$\begin{bmatrix} \theta_1^e \\ \theta_2^e \\ \theta_3^e \end{bmatrix} = \begin{bmatrix} \frac{-1}{h_1} & \frac{b_1}{l_1 h_1} & \frac{-a_1}{l_1 h_1} \\ \frac{-a_2}{l_2 h_2} & \frac{-1}{h_2} & \frac{b_2}{l_2 h_2} \\ \frac{b_3}{l_3 h_3} & \frac{-a_3}{l_3 h_3} & \frac{-1}{h_3} \end{bmatrix} \begin{bmatrix} w_1 \\ w_2 \\ w_3 \end{bmatrix} \tag{4.1}$$

where θ_1^e represents the rotation at edge 1, w_1 represents the displacement at node 1. Edge rotations and nodal displacements for a slab discretized to n elements with m interfaces between these elements can be presented in vector-matrix form as follows:

$$\boldsymbol{\Theta}^{\mathbf{e}} = \mathbf{E}\mathbf{w} \tag{4.2}$$

where $\boldsymbol{\Theta}^{\mathbf{e}}$ is a $3n$-vector of edge rotations, $\mathbf{E}$ is a suitable $(3n \times 3n)$ transformation matrix and $\mathbf{w}$ is a $3n$-vector of nodal displacements . To differentiate between positive (sagging) and negative (hogging) edge rotations, it is convenient to replace θ_i^e with θ_i^{e+}- θ_i^{e-} where θ_i^{e+} , $\theta_i^{e-} \geq 0$.

Thus, the kinematic formulation for the Munro and Da Fonseca method can be stated as follows:

$$\text{minimize} \quad \lambda \mathbf{p}_L^{\mathrm{T}} \mathbf{w} = \mathbf{m}_p^{\mathrm{T}} \boldsymbol{\Theta} \tag{4.3}$$

where λ is the collapse load factor and where $\mathbf{p}_L$ is a $3n$-vector of the applied nodal forces, $\mathbf{m}_p^{\mathrm{T}} = [m_{p_1}^+, m_{p_1}^-, m_{p_2}^+, m_{p_2}^-, ..., m_{p_m}^+, m_{p_m}^-]$, $\boldsymbol{\Theta}^{\mathrm{T}} = [\theta_1^+, \theta_1^-, \theta_2^+, \theta_2^-, ..., \theta_m^+, \theta_m^-]$ and $\boldsymbol{\Theta} = \mathbf{N}\boldsymbol{\Theta}^{\mathbf{e}}$ where $\mathbf{N}$ is a suitable $(2m \times 6n)$ transformation matrix.

Subject to geometric compatibility and unit work constraints. These constraints can be defined as follows:

$$\boldsymbol{\Theta}^{\mathbf{e}} - \mathbf{E}\mathbf{w} = \mathbf{0} \tag{4.4}$$

$$\mathbf{p}_L^T \mathbf{w} = 1 \tag{4.5}$$

The above formulation has been incorporated into a computer program. In order to validate the program output, two examples are presented in the next section.

4.4.2.1 Simply supported square slabs

Consider a simply supported square slab with unit side length, unit moment of resistance per unit length and subject to a uniformly distributed pressure of unit intensity. The critical load factor for this problem is known to be 24. The program successfully identified this load factor and the corresponding failure pattern as shown in Fig. 4.3.

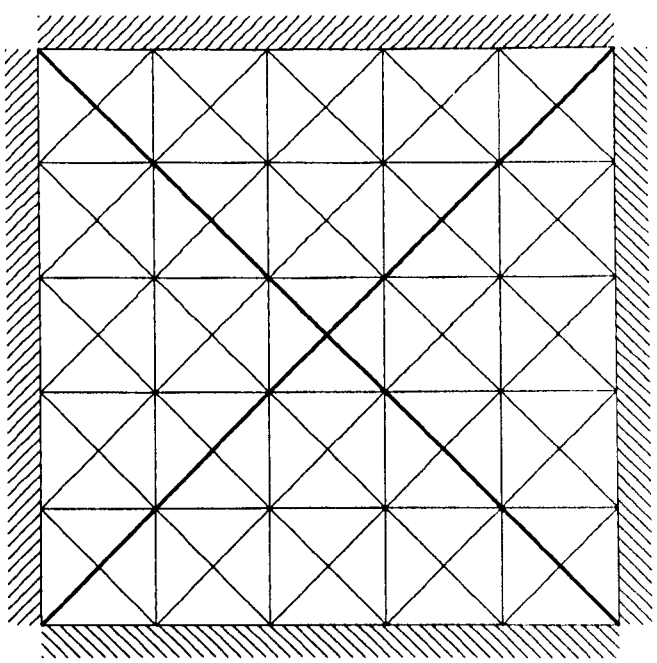

Figure 4.3: Yield line pattern for a simply supported square slab

4.4.2.2 One-way simply supported slab

The one-way simply supported slab shown in Fig. 4.4 which is subject to uniformly distributed pressure of unit intensity and it has a unit moment of resistance per m, has been analysed using the same computer program. The known load factor for this slab is 2. The program gives the exact load factor as well as the correct failure pattern as shown in Fig. 4.4(b).

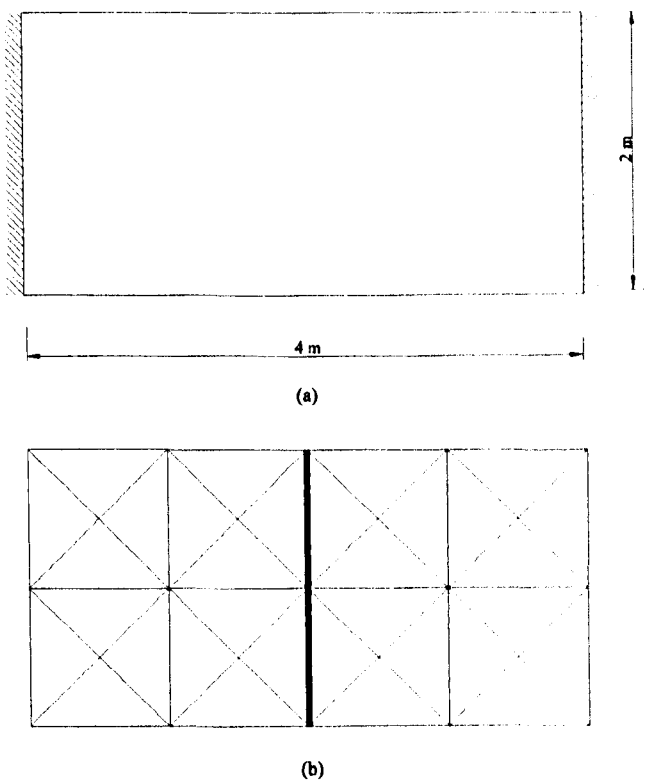

Figure 4.4: (a) One-way simply supported slab; (b) yield line pattern

4.4.3 Yield line analysis of RC slabs: A new linear programming formulation

To illustrate the performance characteristics of the classical procedure based on the Munro and Da Fonseca approach, and in particular the strong influence of the mesh orientation on the computed load factor, consider the case of the simply supported slab which has been dealt with in section 4.4.2.1. Depending on the number and the orientation of elements; different results and failure patterns are obtained as shown in Fig. 4.5:

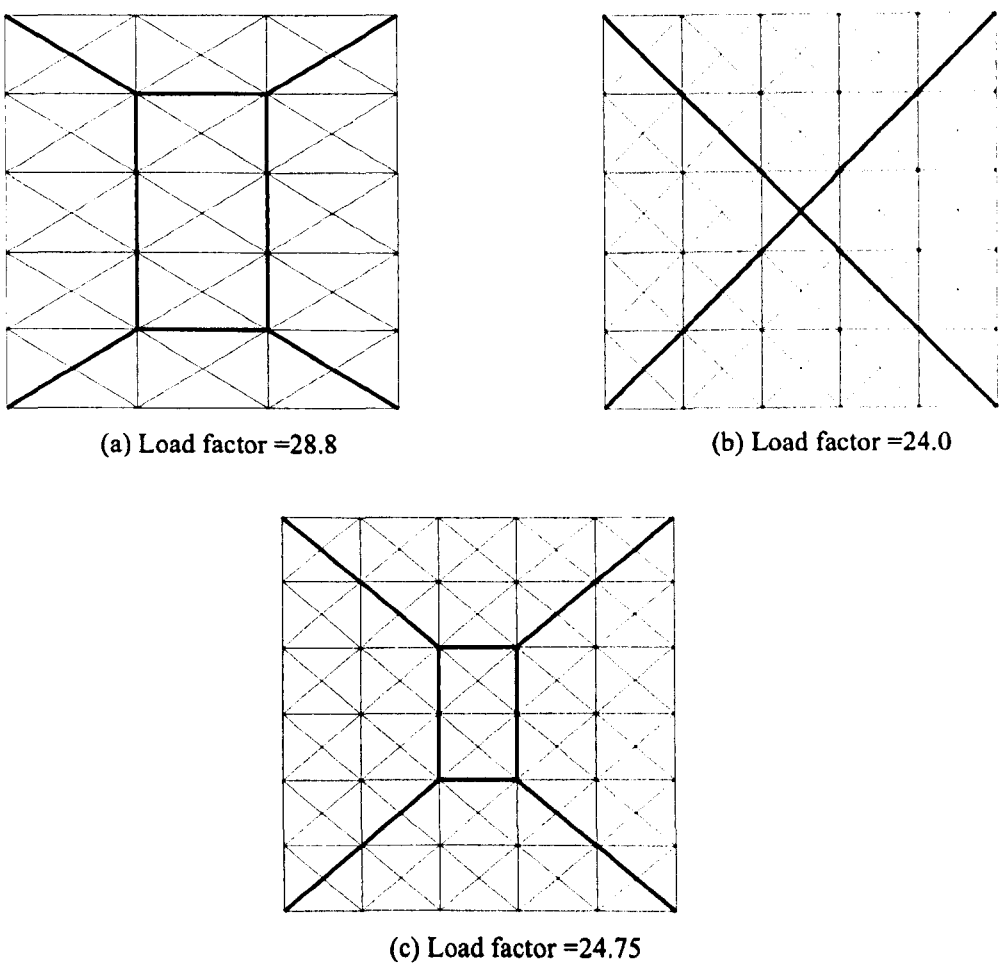

(a) Load factor =28.8

(b) Load factor =24.0

(c) Load factor =24.75

Figure 4.5: The effect of mesh size/orientation: (a) 3:5 ratio; (b) 1:1 ratio; (c) 5:6 ratio

The reason that the load factors obtained in the case of Fig. 4.5(a) and Fig. 4.5(c) are higher than the exact solution may be attributed to the fact that, in these two cases, the boundaries of the finite elements in the mesh do not coincide with the actual critical yield line pattern. Consequently, in these cases the maximum moment resides inside the elements rather than on the element boundaries. As the bending moment at these lines is less than the maximum moment, shear forces will exist in practice. If shear forces at yield lines are incorporated into the formulation, this will potentially enable the formulation to predict the correct load factor regardless of mesh orientation, as demonstrated by the following simple example.

Suppose the beam/one-way slab shown in Fig. 4.6(a) is discretized into 3 elements, each having a length of 2m, and subjected to a uniformly distributed load p =1.0kN/m^2 and the yield moment of the slab m_p = 4.5kN.m/m. At collapse, the bending moment at the interface between elements 1 and 2 can easily be shown to be = 4.0kN.m.

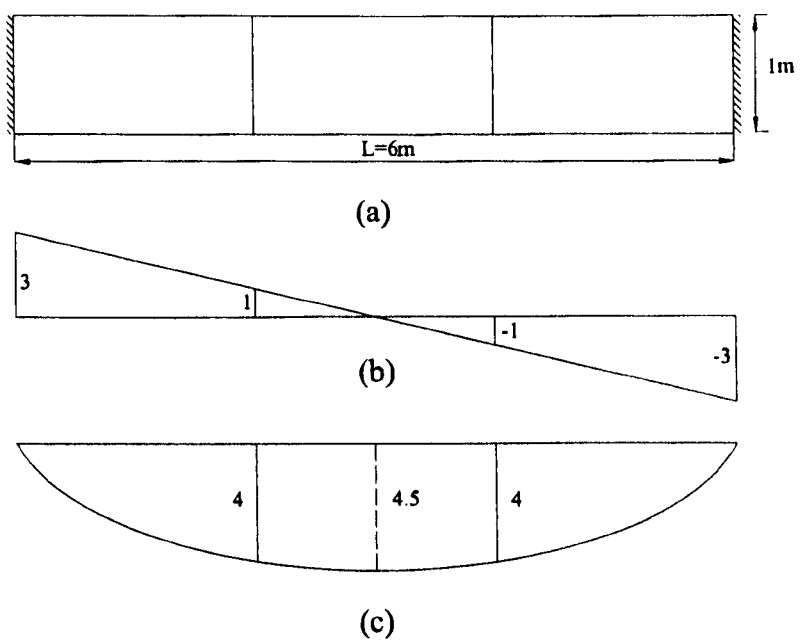

Figure 4.6: (a) One-way simply supported slab; (b) shear force diagram; (c) bending moment diagram

If this is now modelled using three elements, an optimization procedure will identify the collapse mechanism shown in Fig. 4.7(a) as being critical. Accordingly, the load factor will be calculated as $9m/(pL^2)$. As $m = m_p$ at these sections, the load factor will be equal to $(9)(4.5)/(1 \times 6^2) = 1.125$. However, the correct failure mechanism, which is shown in Fig. 4.7, will produce a lower load factor, equal to $8m_p/(1 \times 6^2) = 1$.

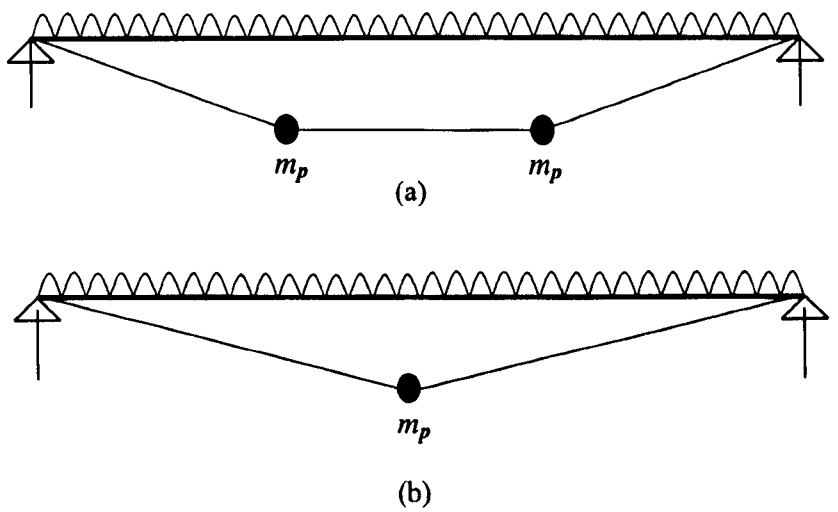

Figure 4.7: (a) Predicted failure mechanism associated with the 3-element idealization of Fig. 4.6; (b) correct failure mechanism

Now suppose the yield conditions at the interface boundary between adjacent elements are modified so that :

$$m + s.d \leq m_p^+ \text{ or } m \leq m_p^+ - s.d \tag{4.6}$$

where s is the shear force and d is some distance from the interface where the shear force exists. Suppose this distance is taken as half the distance between the element centroid and the interface under consideration:

$$m \leq 4.5 - (3-2) \times (1.0 \times 0.5) \Rightarrow m \leq 4.0$$

Now, the load factor will be $9 \times 4/(1 \times 6^2) = 1$ as it should be. Here the exact solution

is obtained despite the fact the element boundaries do not coincide with points of maximum moment.

Thus this simple example illustrates the possibility of correcting solutions obtained using the Munro and Da Fonseca method. From this point forward, the new method will be referred to as the "Sheffield method".

The basic principle behind the Sheffield method, from a kinematic prospective, is to discretize the slab to be analysed as a mesh of triangular or quadrilateral elements with inter-element boundaries and simple, fixed, or free boundary edges to provide a variety of directions and positions for potential yield lines. The slab deformations due to external loadings are defined in terms of the displacement of element centroids and the geometric compatibility between adjacent elements is considered.

This approach differs from the method put forward by Munro and Da Fonseca in the way that constraints impose geometrical compatibility criteria between elements. Thus in the proposed method, relative translational displacement variables are added to constraint equations which govern the movement between elements at the interfaces (such translational displacement variables correspond in a virtual work sense to the inter-element shear forces referred to previously). This provides greater freedom of relative movement between adjacent elements. In this way, yield lines are not restricted to be only developed along element boundaries. This is important as it should reduce the mesh dependency of the results.

Having developed compatibility (or equilibrium) conditions between elements, the next stage is to apply the principle of virtual work. Based on this, a mathematical model can be developed and posed in linear programming form.

4.4.4 Problem formulation

The problem of finding the minimum load factor which will lead to global collapse of a slab at the ultimate limit state can be formulated by adopting an approach based on kinematic admissibility or static equilibrium. Although duality principles mean that there is actually no need to physically incorporate both formulations into a computer program, the intention here is to present both formulations to facilitate a better understanding of the overall problem.

4.4.5 The kinematic approach

As previously mentioned, if the rotations and displacements correspond to a possible collapse mechanism that satisfies the conditions of geometric compatibility, then the virtual work done at all sections in the structure will be positive. In the case of RC slabs, the value of the moment along an axis of rotation will equal the fully plastic moment of resistance. According to the upper-bound theorem of limit analysis, the load factor is obtained by minimizing the kinematically admissible load multiplier. This can be posed as a linear programming problem. Thus, the kinematic formulation in general terms for a slab discretized to n elements with m interfaces between these elements may be presented as follows:

$$\text{Minimize} \quad \lambda \mathbf{f}_L^{\mathrm{T}} \mathbf{d} = \mathbf{m}_p^{\mathrm{T}} \boldsymbol{\Theta} \tag{4.7}$$

where λ is the collapse load factor and where the whole slab live load, elements displacement rates, interfaces plastic moments and rotations are denoted respectively $\mathbf{f}_L^{\mathrm{T}}=[f_{L_{x_1}}, m_{L_{x_1}}, m_{L_{y_1}}, f_{L_{x_2}}, m_{L_{x_2}}, m_{L_{y_2}}, ..., f_{L_{x_n}}, m_{L_{x_n}}, m_{L_{y_n}}]$, $\mathbf{d}^{\mathrm{T}} = [\delta_{z_1}, \phi_{x_1}, \phi_{y_1}, \delta_{z_2}, \phi_{x_2}, \phi_{y_2}, ..., \delta_{z_n}, \phi_{x_n}, \phi_{y_n}]$, $\mathbf{m}_p^{\mathrm{T}} = [m_{p_1}^+, m_{p_1}^-, m_{p_2}^+, m_{p_2}^-, ..., m_{p_m}^+, m_{p_m}^-]$ and $\boldsymbol{\Theta}^{\mathrm{T}}= [\theta_1^+, \theta_1^-, \theta_2^+, \theta_2^-, ..., \theta_m^+, \theta_m^-]$.

Subject to constraints which:

1. Stipulate geometric compatibility between elements i.e.

$$\mathbf{A}_{i_{j,k}}\mathbf{d}_{i_{j,k}} - \mathbf{C}_i\mathbf{r}_i = 0 \ \} \text{ for } i = 1,...,m \text{ between } j \text{ and } k \qquad (4.8)$$

where $\mathbf{A}_{i_{j,k}}$ and $\mathbf{C}_i$ are suitable (6×3) transformation matrices derived from the geometry of the structure; and where $\mathbf{d}^{\mathrm{T}}_{i_{j,k}}=[\delta_{z_j}, \phi_{x_j}, \phi_{y_j}, \delta_{z_k}, \phi_{x_k}, \phi_{y_k}]$ represent elements j,k rotations about the x and y axes and the translational displacement of the element centroid and where $\mathbf{r}^{\mathrm{T}}_i=[\delta^+_{i_1}, \delta^-_{i_1}, \delta^+_{i_2}, \delta^-_{i_2}, \theta^+_i, \theta^-_i]$ represent the translational displacements between these elements at interface i and the rotation of interface i.

The above constraint is established by considering the relative displacement between the centroids of adjacent elements which share interface i through node 1 and node 2 on this interface and the final rotation of this interface as shown in Fig. 4.8(a).

To derive these matrices, consider the two adjacent elements in a certain discretization of a slab with n elements and m interfaces shown in Fig. 4.8(a) with the dimensions shown in 4.8(b). Suppose that the centroid of each element is defined as the local origin of each element. When the slab is subjected to a small (virtual) displacement, these elements will rotate about the x and y axes as well as about element boundaries.

Using basic trigonometry, it can be shown that the relative displacement between the centroids of element j and element k, as shown in Fig.4.8(b), through node 1 and node 2 on interface i and the final rotation at this interface can be written as:

$$\begin{bmatrix} -1 & -x_{i_{j_1}} & -y_{i_{j_1}} & 1 & x_{i_{k_1}} & y_{i_{k_1}} \\ -1 & -x_{ij_2} & -y_{i_{j_2}} & 1 & x_{i_{k_2}} & y_{i_{k_2}} \\ 0 & -dn_{i_j}\sin\alpha_i & dn_{i_j}\cos\alpha_i & 0 & -dn_{i_k}\sin\alpha_i & -dn_{i_k}\cos\alpha_i \end{bmatrix} \begin{bmatrix} \delta_{z_j} \\ \phi_{x_j} \\ \phi_{y_j} \\ \delta_{z_k} \\ \phi_{x_k} \\ \phi_{y_k} \end{bmatrix} -$$

$$\begin{bmatrix} 1 & -1 & 0 & 0 & 0 & 0 \\ 0 & 0 & 1 & -1 & 0 & 0 \\ 0 & 0 & 0 & 0 & -1 & 1 \end{bmatrix} \begin{bmatrix} \delta_{i_1}^+ \\ \delta_{i_1}^- \\ \delta_{i_2}^+ \\ \delta_{i_2}^- \\ \theta_i^+ \\ \theta_i^- \end{bmatrix} = \begin{bmatrix} 0 \\ 0 \\ 0 \end{bmatrix} \quad (4.9)$$

Where dn_{i_j} and dn_{i_k} are the normal distances, respectively, from the centroids of element j and element k to interface i.

Thus it follows from equation 4.9 that the transformation matrices $\mathbf{A}_{i_{j,k}}$ and $\mathbf{C}_i$ will be of the form:

$$\mathbf{A}_{i_{j,k}} = \begin{bmatrix} -1 & -x_{i_{j_1}} & -y_{i_{j_1}} & 1 & x_{i_{k_1}} & y_{i_{k_1}} \\ -1 & -x_{ij_2} & -y_{i_{j_2}} & 1 & x_{i_{k_2}} & y_{i_{k_2}} \\ 0 & -dn_{i_j}\sin\alpha_i & dn_{i_j}\cos\alpha_i & 0 & -dn_{i_k}\sin\alpha_i & -dn_{i_k}\cos\alpha_i \end{bmatrix}$$

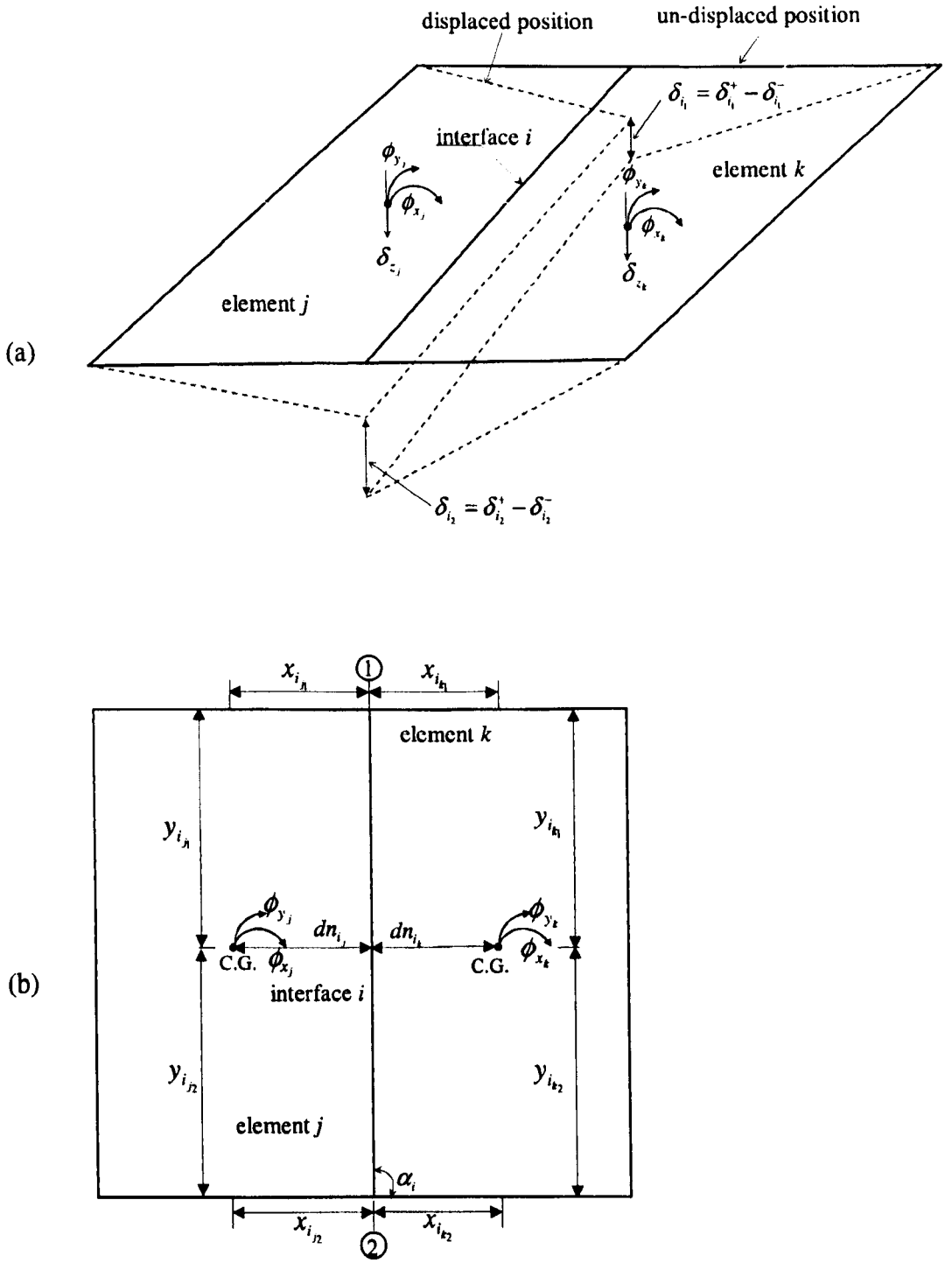

Figure 4.8: Two adjacent elements in a discretization: (a) rotations and displacements; (b) dimensions

and

$$\mathbf{C}_i = \begin{bmatrix} 1 & -1 & 0 & 0 & 0 & 0 \\ 0 & 0 & 1 & -1 & 0 & 0 \\ 0 & 0 & 0 & 0 & -1 & 1 \end{bmatrix}$$

2. Limit translational displacements

To prevent interface translational displacements from being relatively large and leading to zero load factors being obtained, an additional constraint is needed. Basically with this constraint, no translational displacements at any interface can take place unless there is a relative rotation between the two elements shared by this interface. This can be done intuitively by linking the translational displacements at each node on interface i to the actual rotation (θ_i) at this interface through a function which accounts for the worst case for a yield line position encountered in a given mesh whilst considering the geometrical properties of the mesh i.e.:

$$d_{i_j}\theta_i^+ + d_{i_k}\theta_i^- - 0.5(\delta_{i_1}^+ + \delta_{i_1}^- + \delta_{i_2}^+ + \delta_{i_2}^-) \geq 0\} \text{for } i = 1,...,m \text{ between } j \text{ and } k \tag{4.10}$$

where $d_{i_j} = sf_{i_j}dn_{i_j}$ and $d_{i_k} = sf_{i_k}dn_{i_k}$ and where sf_{i_j} and sf_{i_k} are referred to as shear factors. d_{i_j} and d_{i_k} are similar to d in 4.6. For the derivation of these factors, the reader is referred to Appendix I.

3. Apply a unit work

Displace the slab according to the live load such that:

$$\mathbf{f}_L^T\mathbf{d} = 1 \tag{4.11}$$

4.4.6 The static (equilibrium) approach

In the static (equilibrium) approach the aim is to identify the internal forces corresponding to the maximum possible external load intensity. All equilibrium equations must be fulfilled and yield condition must not be violated at interfaces. Thus, the static formulation for a slab with n elements and m interfaces between these elements can be expressed as:

$$\text{Maximize} \quad \lambda \tag{4.12}$$

Subject to constraints which impose:

1. Equilibrium:

$$\lambda \mathbf{f}_L = \mathbf{B}\mathbf{q} \tag{4.13}$$

where λ is the collapse load factor and where the whole slab live load and resulting forces at interfaces are denoted respectively $\mathbf{f}_L^{\mathrm{T}}=[f_{L_{x_1}}, m_{L_{x_1}}, m_{L_{y_1}}, f_{L_{x_2}}, m_{L_{x_2}}, m_{L_{y_2}}, ..., f_{L_{x_n}}, m_{L_{x_n}}, m_{L_{y_n}}]$ and $\mathbf{q}^{\mathrm{T}}=[m_1, s_1, t_1, m_2, s_2, t_2, ..., m_m, s_m, t_m]$ where m_1, s_1 and t_1 are respectively the bending moment, shear force and torque at interface 1. $\mathbf{B}$ is a suitable $(3n \times 3m)$ equilibrium matrix.

2. Yield condition:

Equivalent to translational displacements at interfaces in the kinematic formulation, shear forces at interfaces are assumed to exist. Accordingly the modified yield condition will be:

$$-m_{p_i}^- + s_i d_{i_j} \leq m_i \leq m_{p_i}^+ - s_i d_{i_k} \quad \text{for} \quad i = 1, ..., m \tag{4.14}$$

Where m_i and s_i are respectively the bending moment and shear at interface i.

4.4.7 Status of solutions

To understand better the proposed method, consider the following:

1. If inter-element translational displacements (shear forces in the static formulation) are all zero, then the obtained solution must be a genuine upper-bound solution (as the collapse mechanism then becomes kinematically admissible). Hence as these displacements tend towards zero (e.g. as element size is reduced) it can be expected that the solution will tend towards an upper-bound solution.

2. However, as the element size is reduced, it might be expected that the solution will tend towards a lower-bound solution. This is because by increasing the number of elements (and hence decreasing the element size) a better representation for the stress distribution will be achieved.

3. If (2) is true then it implies that as the element size becomes infinitely small, the solution tends towards the exact value.

4. Choosing different values for the shear factor, will alter the relative importance of (1) and (2). Thus if reducing the mesh size increases the load factor, the indication is that (2) dominates and the solution will be a lower-bound. Conversely if reducing the mesh size reduces the load factor, the indication is that (1) dominates and the solution will be an upper-bound.

Thus with $shearfactor = 0$ the Munro and da Fonseca solution will be obtained; with $shearfactor = \infty$ the solution obtained will be 0. There must therefore be some value of $shearfactor$ at which the load factor will be the exact solution.

4.5 Examples

Based on the approach described above and by adopting an object-oriented approach, a C++ program called SLAB has been developed by the author to evaluate the collapse load factor for RC slabs and bridge decks. To demonstrate the effectiveness and the versatility of the approach described in the previous section, and to test the program's capabilities, a variety of example problems have been attempted. A number of these problems have a known exact solution. Other problems studied were case study problems presented by various authors. The load factor λ quoted in all examples has been obtained by taking the slab plastic moment m_p as unity per unit length and pL^2 as a unity, where p is the uniformly distributed load per unit area and L is the characteristic length. The definition for the number of divisions in the x and y directions is shown in Fig. 4.9. In any given mesh, the number of elements is a function in the number of divisions in the x and y directions. Both terms (i.e. the number of divisions and the number of elements) will be used to describe the mesh size.

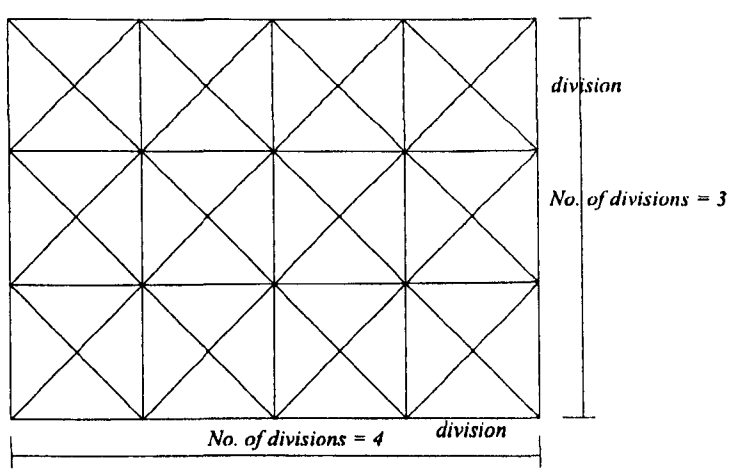

Figure 4.9: Number of divisions

A brief description for the program is presented in Appendix C.

4.5.1 Benchmark problems with known exact solutions

4.5.1.1 Simply supported square slabs with uniformly distributed load

The first example is possibly the simplest slab which can be analysed: a simply supported square slab with uniformly distributed loading. Suppose the slab is isotropically reinforced, thus giving equal moment of resistance in every direction. This example has been widely studied in the past and a load factor of $\lambda = 24$ obtained with the square yield criterion is the exact solution.

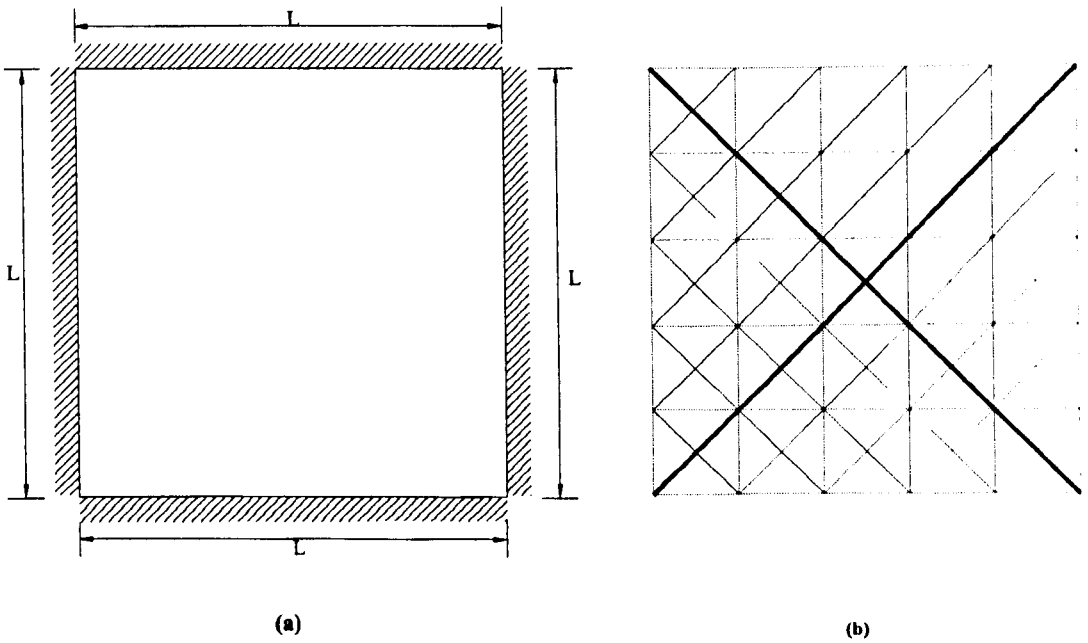

Figure 4.10: (a) A simply supported square slab subject to uniformly distributed load; (b) yield line pattern

Using triangular elements, the exact solution (Fig. 4.10(b)) is obtained with any number of divisions provided that the finite element mesh contains elements with 45° angles to the horizontal as in Fig. 4.10(b). It is easy to see that the collapse pattern is easily mapped by the mesh as the diagonal yield lines of the first element to the last element map exactly on the actual collapse yield lines.

With quadrilateral elements, the real advantage of the method becomes obvious. No actual mapping or matching-up of any sort between the mesh and the actual yield line pattern, which corresponds to the known exact solution, is possible; yet the program manages to home in on the exact solution and to successfully identify the correct fracture pattern at failure, as shown on Fig. 4.11. With the number of divisions per side increased, the load factor converged towards the exact solution. Once the exact solution has been attained, refining the mesh further does not affect the resulting load factor, which remains constant at 24, as in Fig. 4.12. This has only been tried with square elements.

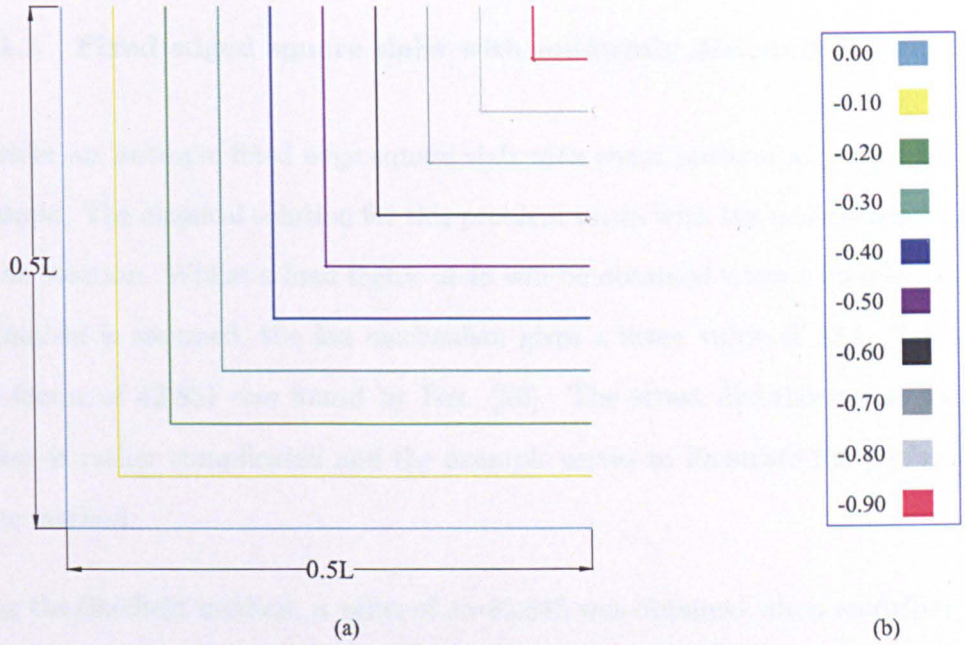

Figure 4.11: (a) Displacement contours for one quarter of a simply supported square slab using quadrilateral elements; (b) legend

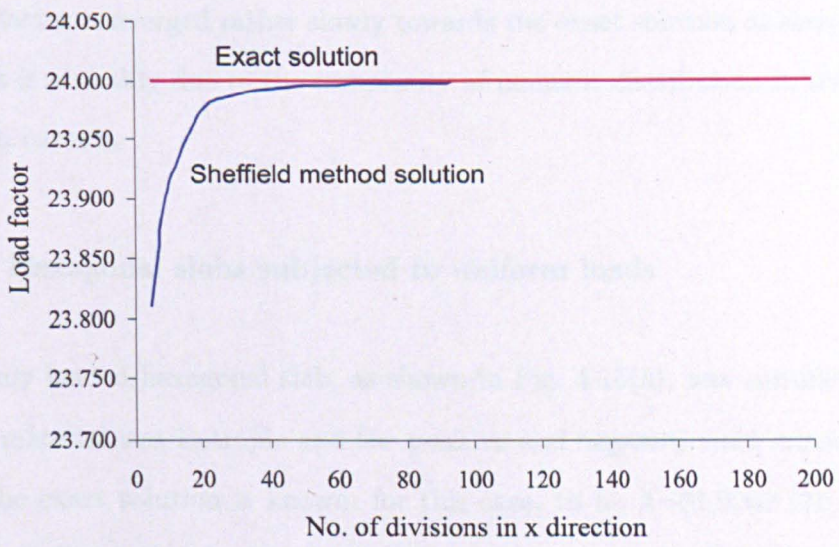

Figure 4.12: Variation of load factor with number of divisions for a simply supported square slab using quadrilateral elements

4.5.1.2 Fixed edged square slabs with uniformly distributed load

Consider an isotropic fixed edge square slab with equal positive and negative yield moments. The classical solution for this problem varies with the mechanism adopted for the solution. Whilst a load factor of 48 will be obtained when a simple diagonal mechanism is assumed, the fan mechanism gives a lower value of 43.5. The exact load factor of 42.851 was found by Fox [20]. The stress distribution in the slab corners is rather complicated and the example serves to illustrate the performance of the method.

Using the Sheffield method; a value of λ=42.845 was obtained when modelling only 1/8 of the slab (utilizing symmetry) and discretizing this part of the slab using a mesh of 400 by 400 divisions. The program identified the failure mechanism in terms of displacement contours shown on Fig. 4.13. Although only 1/8 of the slab was modelled, the displacement contours for the whole slab are shown for clarity.

The load factor converged rather slowly towards the exact solution as shown in Fig. 4.14. This is probably due to the complexity of moment distribution in the vicinity of the slab corners.

4.5.1.3 Hexagonal slabs subjected to uniform loads

A uniformly loaded hexagonal slab, as shown in Fig. 4.15(a), was considered next. The slab material was isotropic and the positive and negative yield moments were equal. The exact solution is known, for this case, to be λ=21.9962 [21]. As can be seen from Fig. 4.15 (b), the actual yield line form an angle of 65° to the x-axis, making it unlikely that the exact solution would be obtained using the traditional Munro and Da Fonseca approach, unless the geometry of the critical yield line pattern was known in advance. With the Sheffield method, a load factor of λ= 21.9953 was obtained using only one quarter of the slab due to symmetry and a

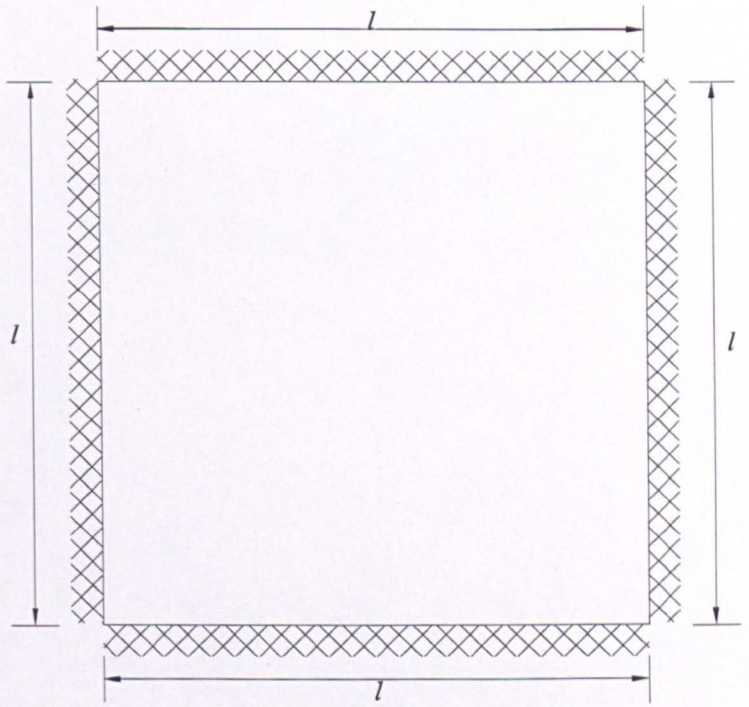

(a)

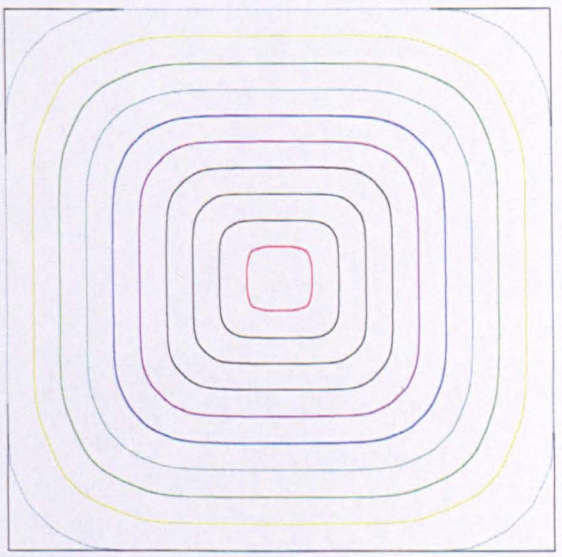

(b)

Figure 4.13: (a) A fixed edged square slab with uniformly distributed load; (b) displacements contours

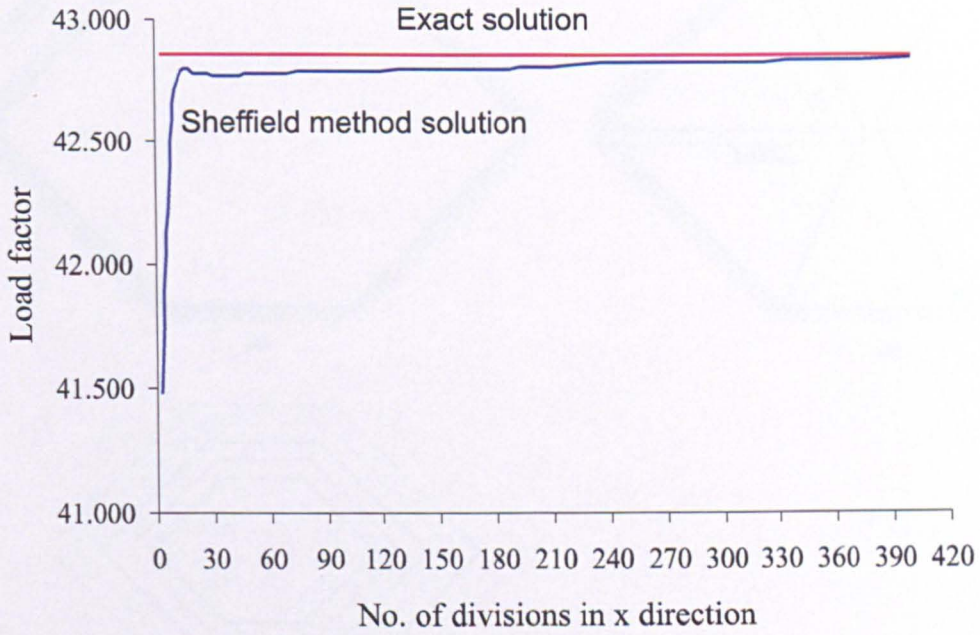

Figure 4.14: Variation of load factor with number of divisions for a fixed edged square slab

discretization of 140×140 divisions. All elements in the discretization had an aspect ratio of 1.

4.5.2 Other benchmark problems

In this section a number of slabs previously analysed by other researchers will be studied.

4.5.2.1 Fixed edged irregular slab

Figure 4.17(a) shows the geometry of a slab studied in the past firstly by Regan [22] and subsequently by Johnson [15]. They both suggested the yield line pattern

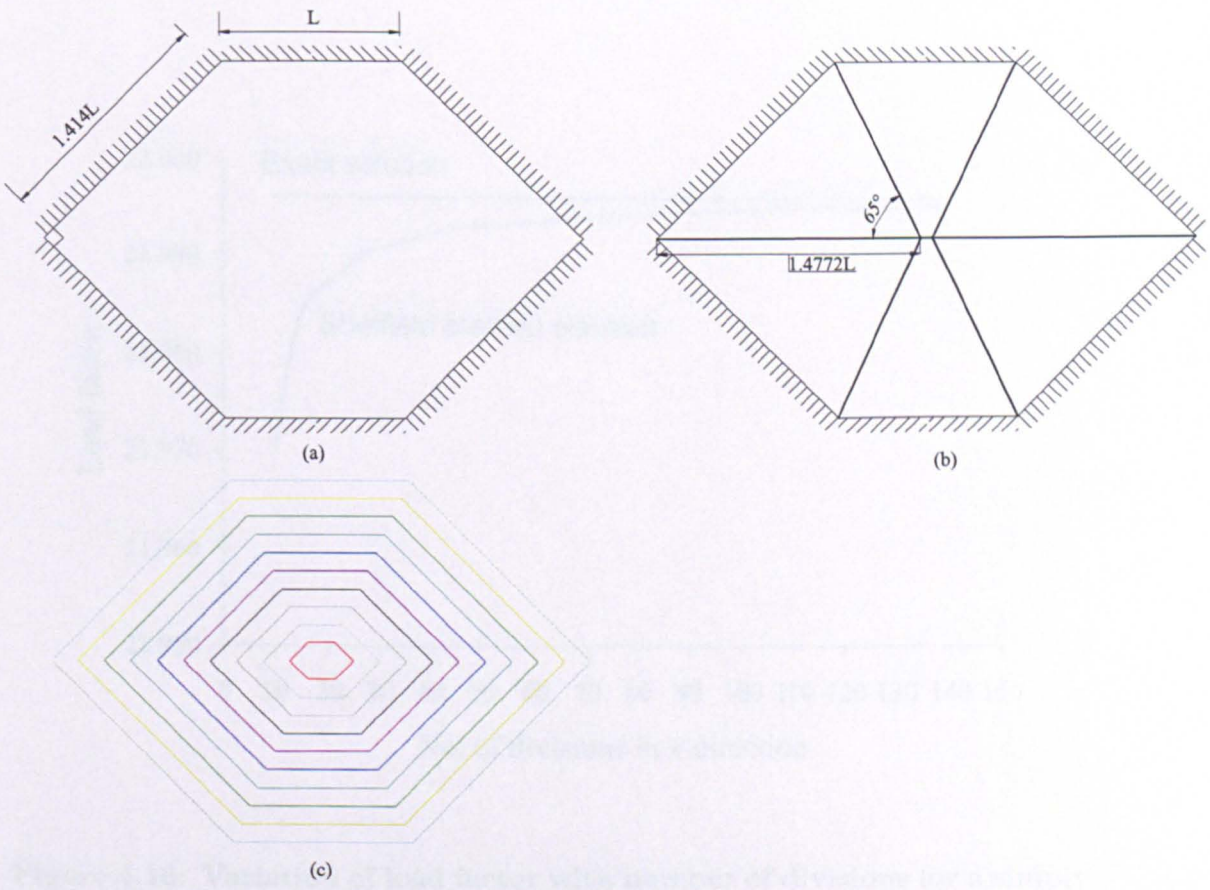

Figure 4.15: (a) A simply supported hexagonal slab subject to uniform loads; (b) the critical yield line pattern; (c) displacement contours

shown in Fig. 4.17(a) with a load factor of 37.0. The traditional Munro and Da Fonseca finite element approach indicated a load factor of 38.4 for the yield line pattern shown in Fig. 4.17(b) with the displacement contours shown in Fig. 4.18(a). Using the Sheffield method, the load factor converged to a value of 35.0 as shown in Fig. 4.19. The corresponding yield line pattern is represented by displacement contours in Fig. 4.18(b).

4.5.2.2 Irregular slab with simple and fixed edges

Figure 4.20(a) shows the geometry of a slab considered by Johnson in his 1994 paper [15]. Based on Regan's assumed yield line pattern, he founded a load factor of 32.5.

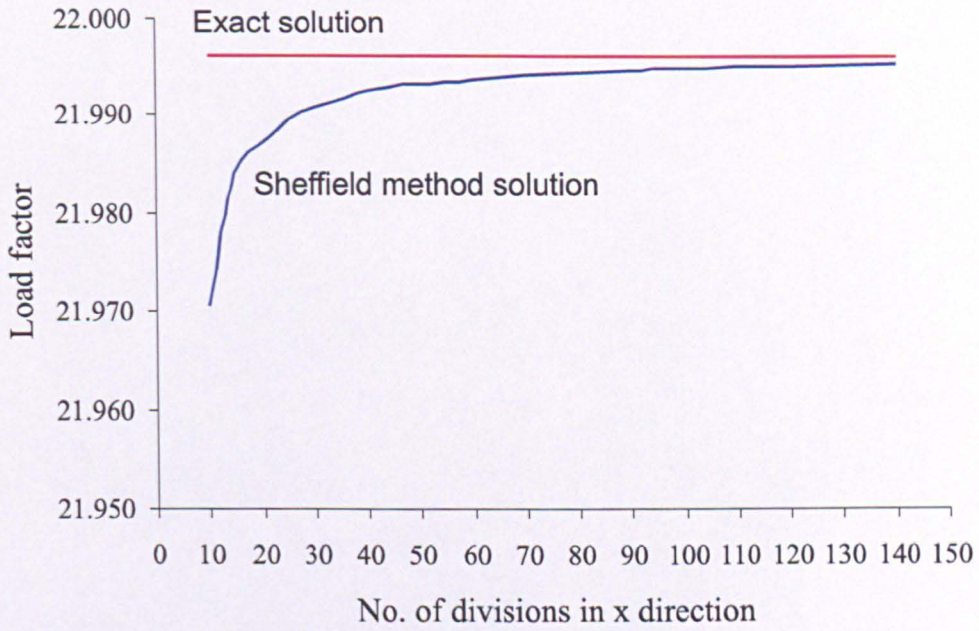

Figure 4.16: Variation of load factor with number of divisions for a simply supported hexagonal slab

The traditional Munro and Da Fonseca finite element approach indicated a load factor of 33.1 and the yield line pattern shown in Fig. 4.20(b) with the displacement contours shown in Fig.4.21(a). More recently, Jennings *et al.* [18] predicted a load factor of 29.20 based on a geometry optimization approach. Using the Sheffield method, the load factor also converged to a value of 29.2 as shown in Fig. 4.22. The corresponding yield line pattern which is represented by displacement contours is shown in Fig. 4.21(b).

4.5.2.3 Uniformly loaded floor-slab

The uniformly loaded floor-slab shown in Fig. 4.23(a) contains much of the complexity of a real design problem. The cut-out area is for stairs. The boundary

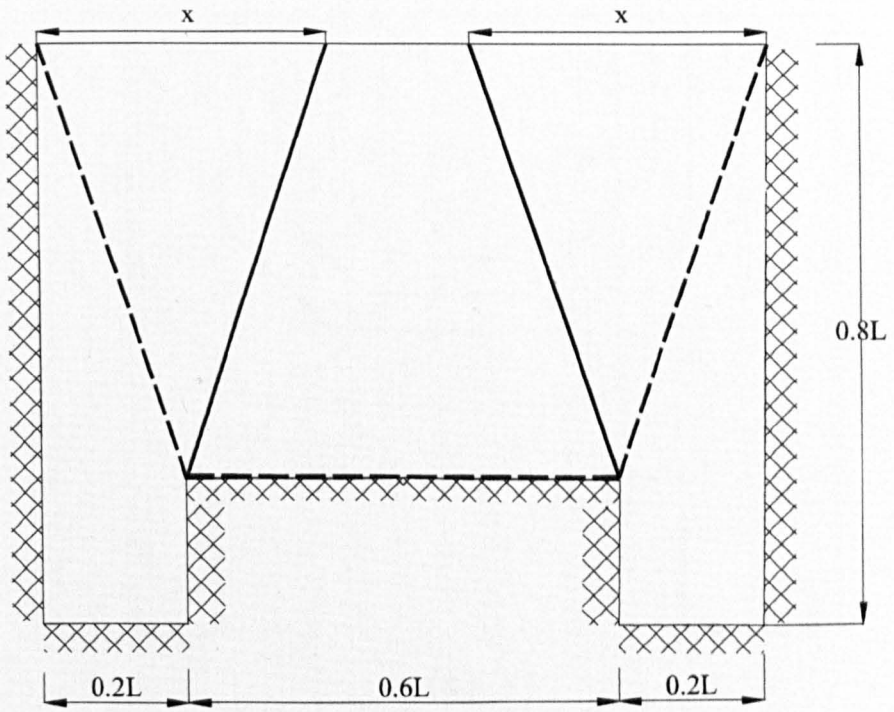

(a)

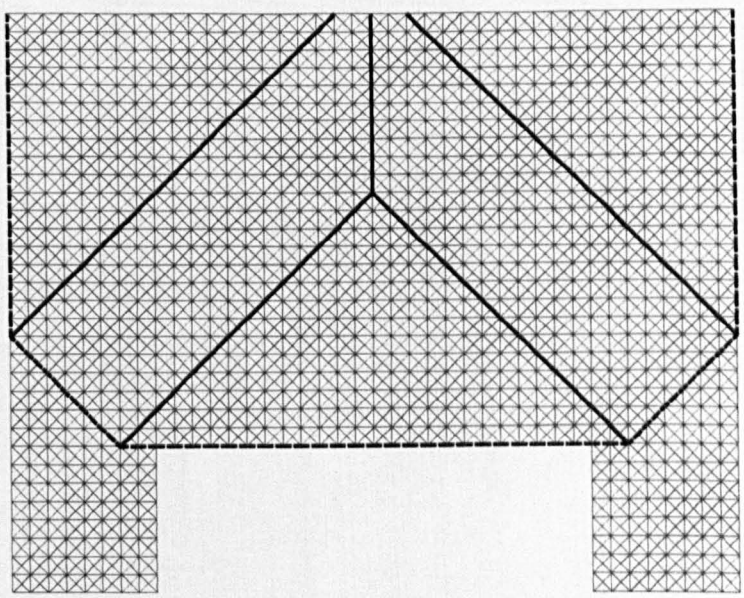

(b)

Figure 4.17: Fixed edged irregular slab: (a) yield line pattern suggested by Regan [22]; (b) Munro and Da Fonseca solution

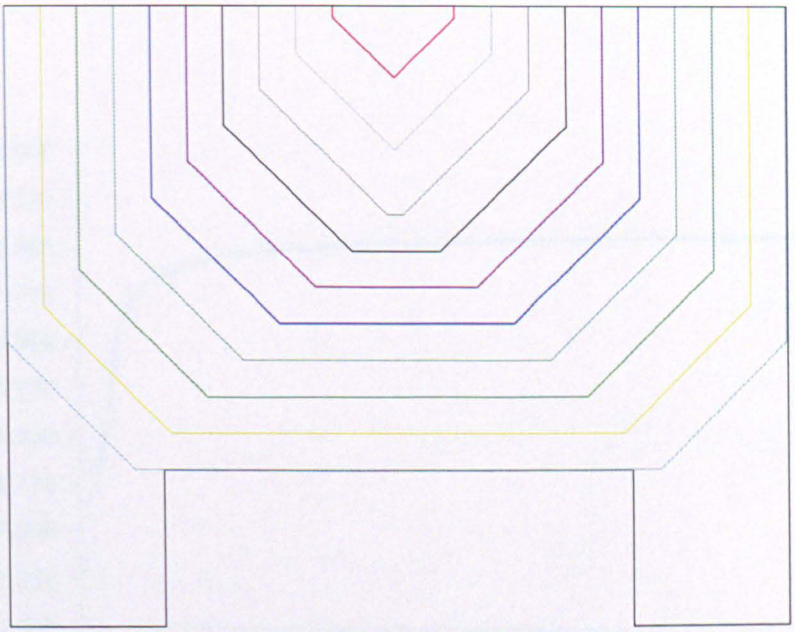

(a)

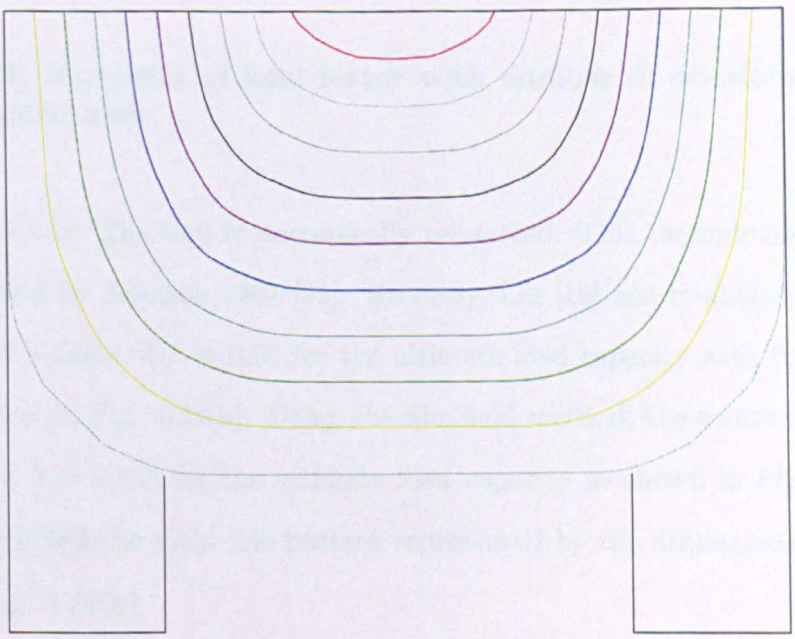

(b)

Figure 4.18: Fixed edged irregular slab: (a) Munro and Da Fonseca method: displacement contours; (a) Sheffield method: displacement contours

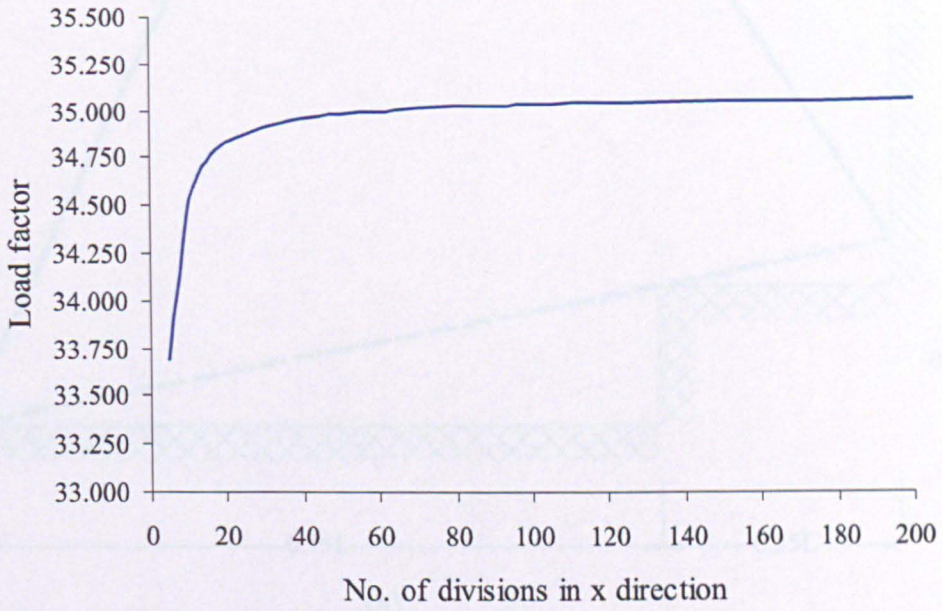

Figure 4.19: Variation of load factor with number of divisions for fixed edged irregular slab

edges are built in. The slab is isotropically reinforced. This example has been previously studied by Johnson 1967 [23]. Recently, Liu [19] has re-analysed the slab. He predicted a value of $\lambda = 0.95$ for the ultimate load capacity with the yield line pattern shown on Fig. 4.23(a). Using the Sheffield method, the solution converged to a value of $\lambda = 0.845$ for the ultimate load capacity as shown in Fig. 4.25. The program identified the yield line pattern represented by the displacement contours shown on Fig. 4.24(b)

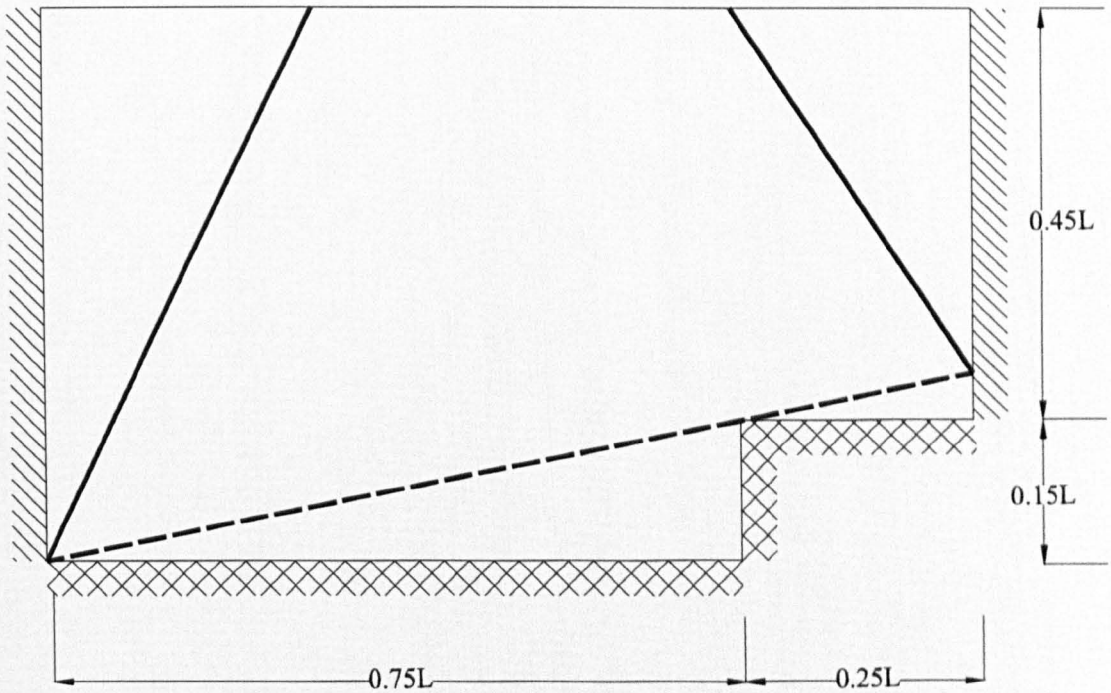

(a)

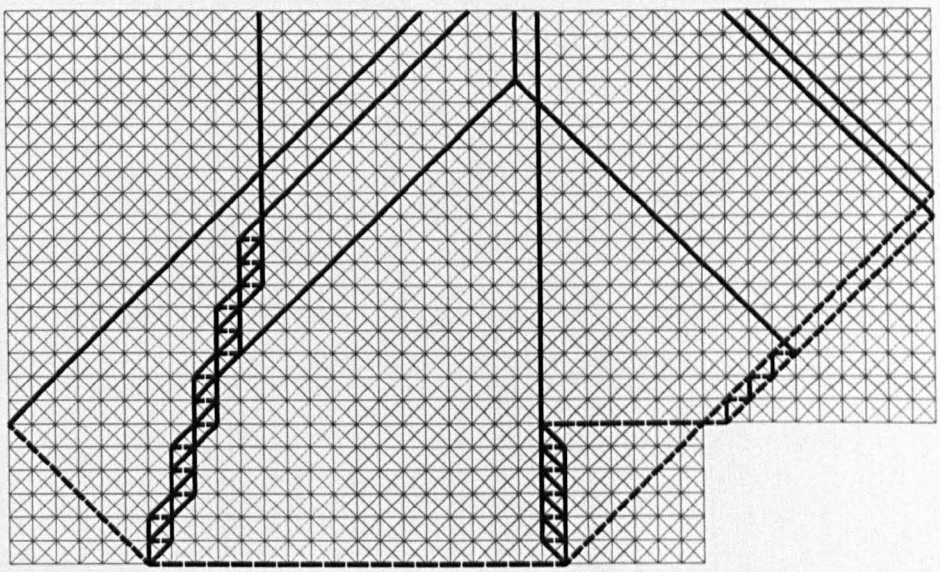

(b)

Figure 4.20: Irregular slab with simple and fixed edges: (a) yield line pattern suggested by Regan and Johnson [15]; (b) Munro and Da Fonseca solution

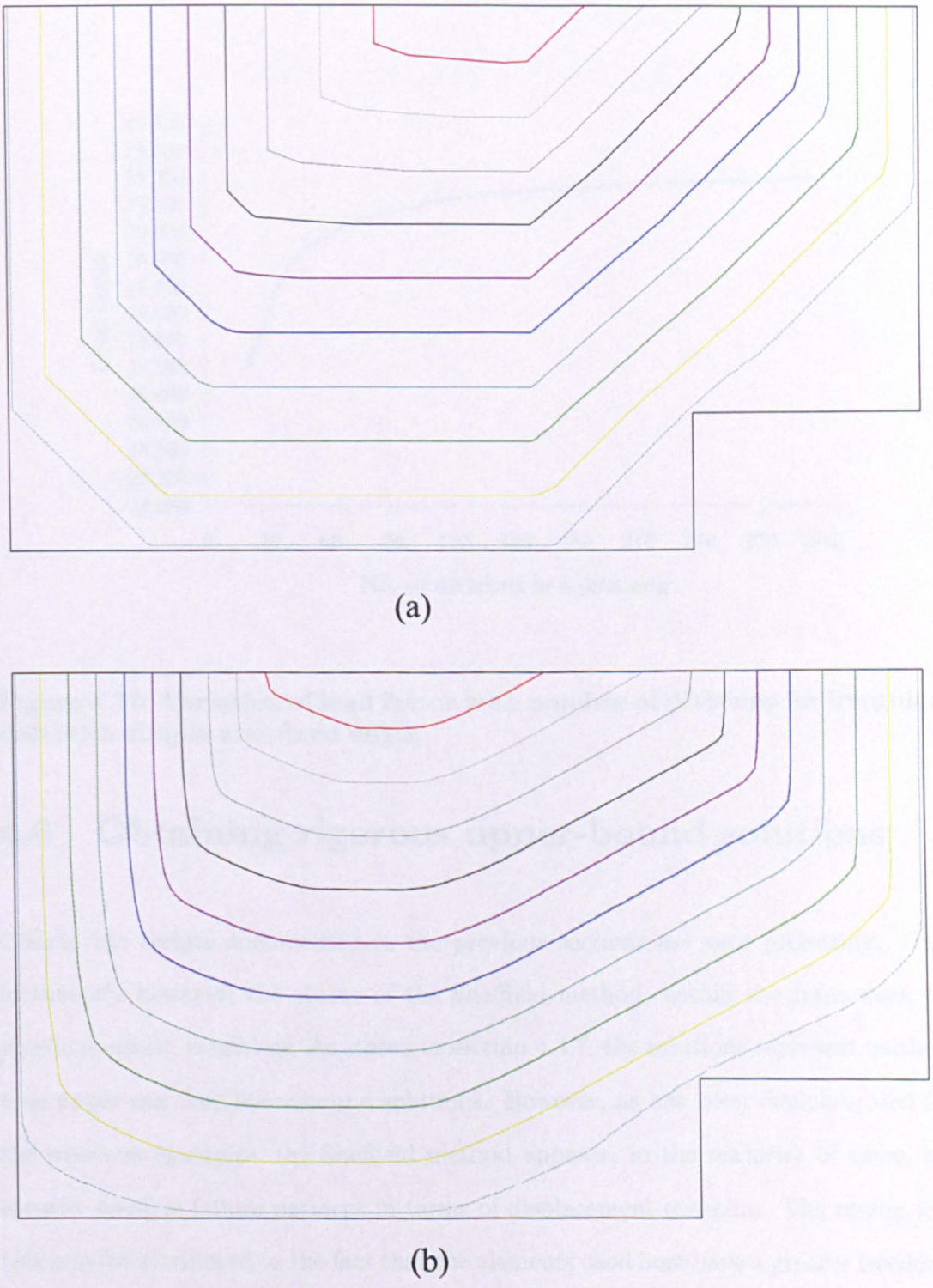

Figure 4.21: Irregular slab with simple and fixed edges: (a) Munro and Da Fonseca method: displacement contours; (b) Sheffield method: displacement contours

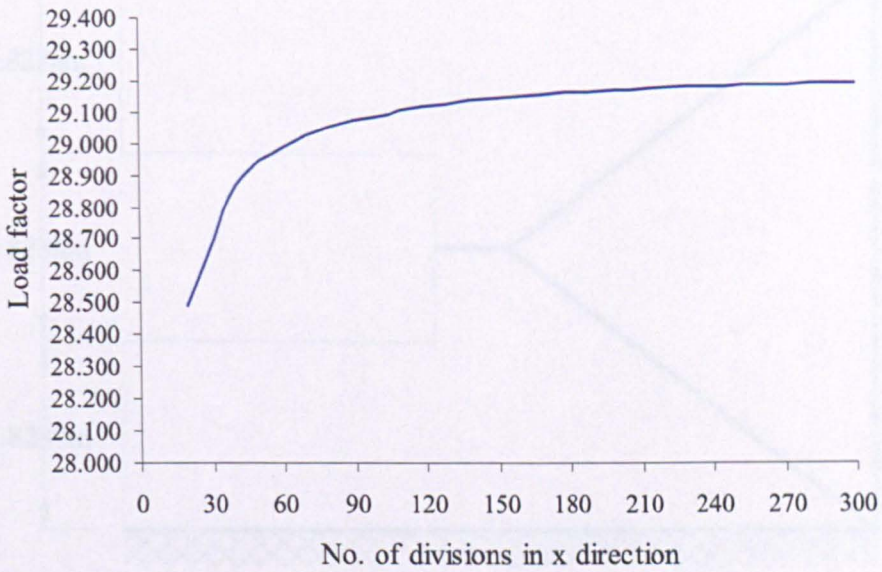

Figure 4.22: Variation of load factor with number of divisions for irregular slab with simple and fixed edges

4.6 Obtaining rigorous upper-bound solutions

Clearly the results documented in the previous sections are very promising. Unfortunately however, the status of the Sheffield method, within the framework of plastic analysis, is unclear. As stated in section 4.4.7, the solutions represent neither true upper nor true lower-bound solutions. However, as has been demonstrated in the previous examples, the Sheffield method appears, in the majority of cases, to identify sensible failure patterns in terms of displacement contours. The reason for this may be attributed to the fact that the elements used here have a greater freedom to deform. Linear programming solvers will always try to find the solution (or in other words, the failure pattern) which gives the lowest load factor. In the majority of these cases, the predicted failure pattern closely matches that corresponding to the exact solution.

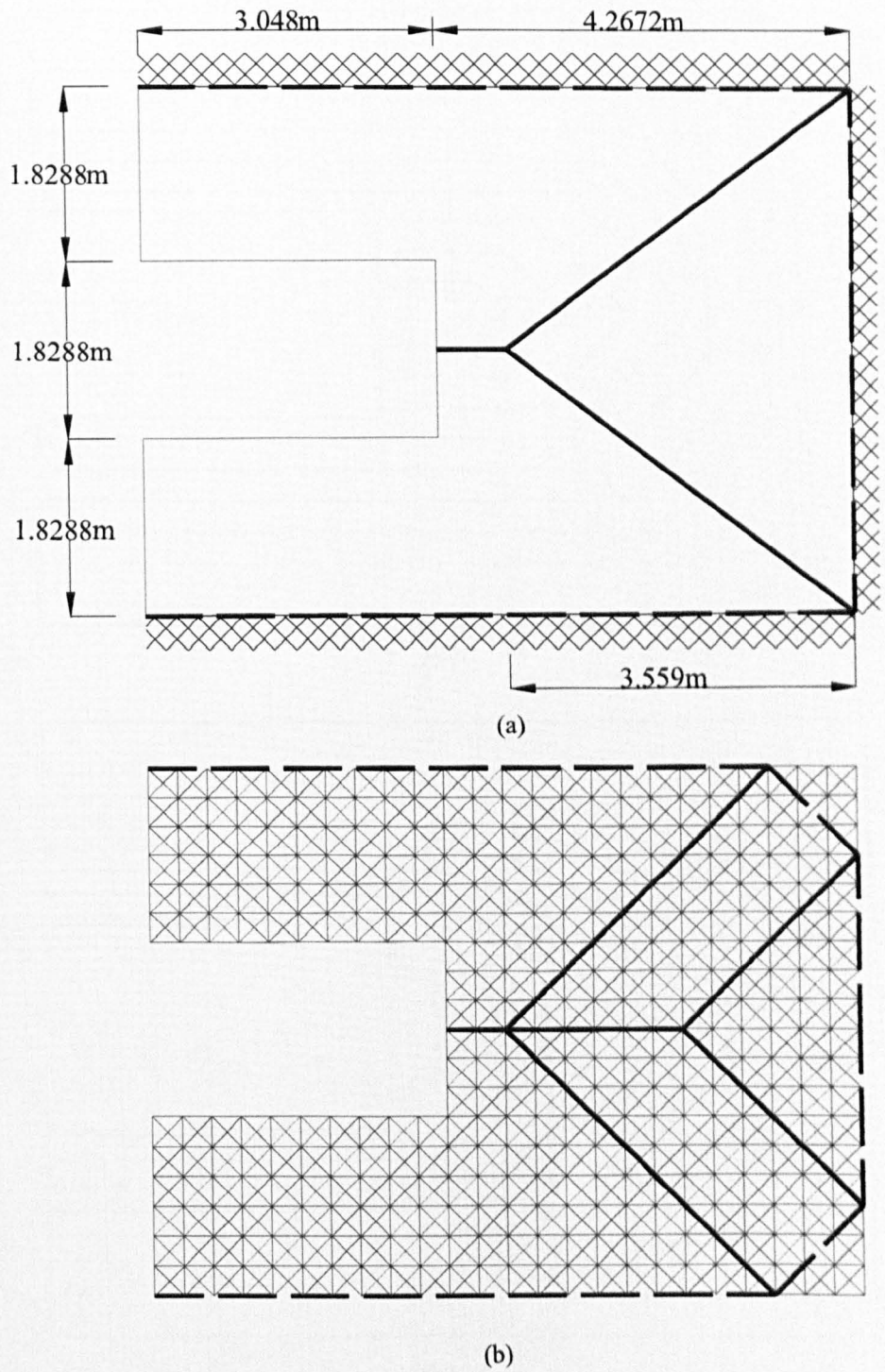

Figure 4.23: Typical RC floor: (a) yield line pattern proposed by Liu [19]; (b) predicted yield line pattern and FE mesh based on the Munro and Da Fonseca approach

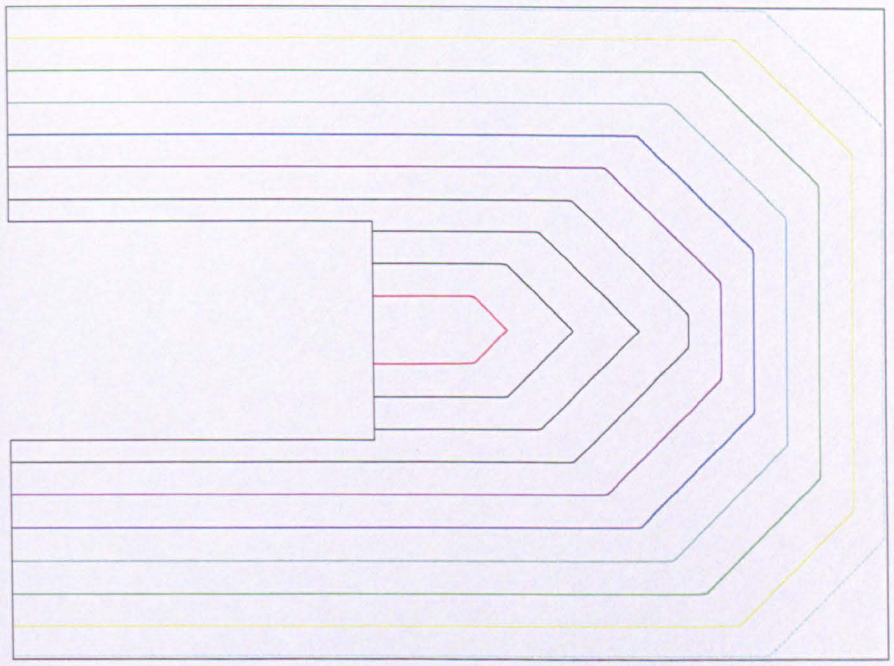

(a)

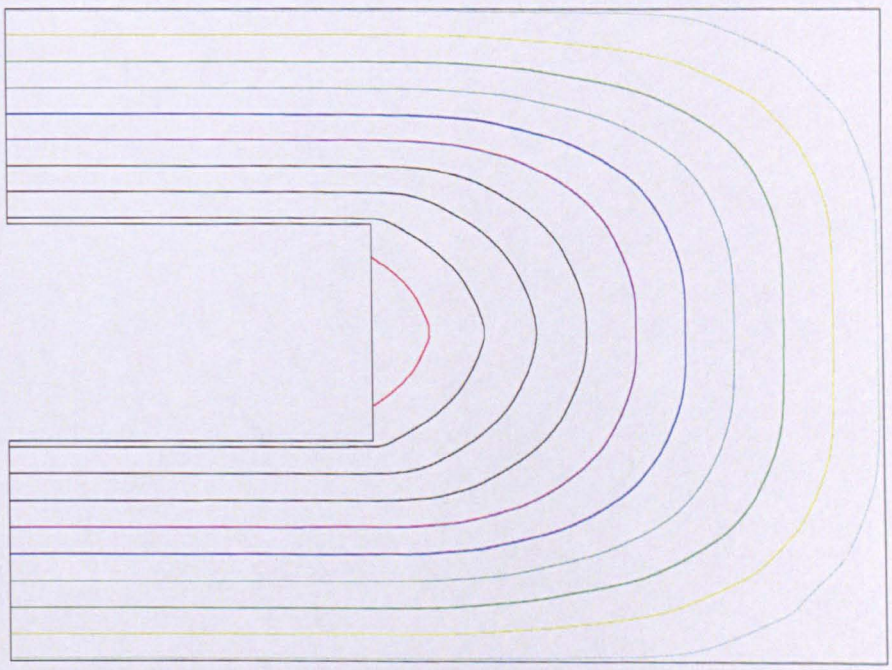

(b)

Figure 4.24: Typical RC floor-slab: (a) Munro and Da Fonseca method: displacement contours (b) Sheffield method: displacement contours

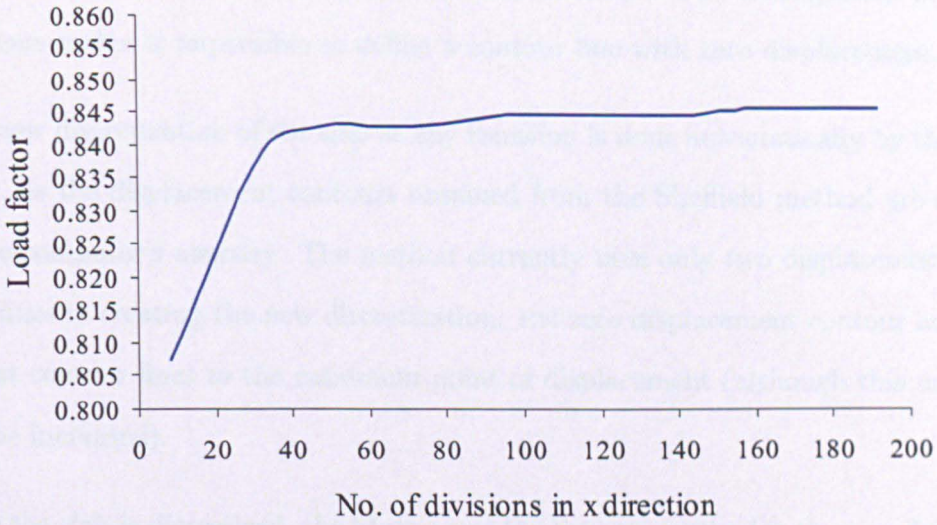

Figure 4.25: Variation of load factor with number of divisions for floor slab

A new method or 'the two-phase Sheffield method' comprises two phases. In phase 1, the problem is set-up and solved using the Sheffield method. Once a viable solution has been obtained, then phase 2 is executed. In phase 2, the deformed shape of the slab at failure is analysed and the slab is re-meshed in such a way that the boundaries of elements are selected so as to permit the observed deflected shape. This is simply done by finding the locations of the points in the slab with the maximum displacements and then discretizing the slab into a number of segments starting radially from these points. A 2D mesh of triangular elements is created by the intersection of these radial segments and the displacement contours.

There are number of issues to consider. For example, a tolerance for zero displacement contours (tol_0) is introduced. A typical value for this tolerance is 10^{-4}. This means that a contour with a displacement which is less than $10^{-4}\times$ the maximum displacement is considered to be a zero displacement contour. This is introduced

because in some situations, such as the case of fixed edged square slabs, a number of elements near a corner will have zero displacement. The arrangement of these elements makes it impossible to define a contour line with zero displacement.

The new discretization of the slab at any iteration is done automatically by the program, as the displacement contours obtained from the Sheffield method are stored in the computer's memory. The method currently uses only two displacement contour lines in creating the new discretization: the zero displacement contour and the closest contour lines to the maximum point of displacement (although this number can be increased).

Once the slab is discretized, the Munro and Da Fonseca method is then used to find the failure load for the slab under consideration. If required, the program may be run several times until the arrangement of elements that gives the lowest load factor is found. The key thing is that the lowest load factor obtained will still be a genuine upper-bound on the true load factor.

4.6.1 Creating a new mesh using a Sheffield method solution

Crucial to this method is the development of a means to automatically generate a new mesh from a Sheffield method solution. Simplified intuitive rules may be developed to generate the mesh to be used in phase 2 of the Sheffield method. These rules are explained with the help of Fig. 4.26 and Fig. 4.27 which shows the different construction stages of the new mesh from the Sheffield method solution for the two cases which will be investigated in this section.

Figure 4.26(a) shows the first case, where there is only one point with the maximum displacement. Also the last contour line is symmetric around this point. Therefore, this point is used as the origin of the radial segments to be used in the new discretization. Points of intersection between these segments and the contour lines are

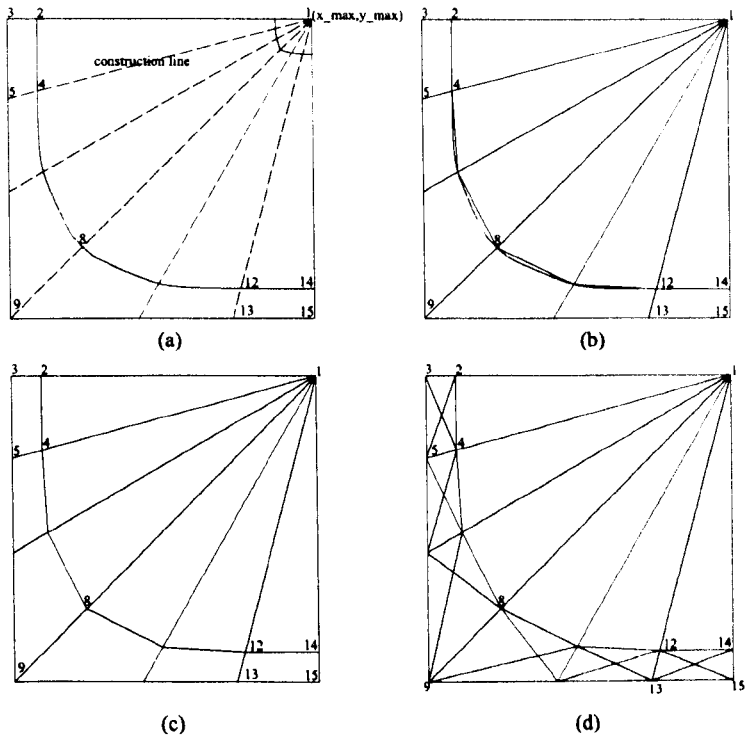

Figure 4.26: Construction stages of the new mesh for case 1 (a) discretizing the slab into a number of segments; (b) creating points; (c) connecting points to create quadrilateral elements; (d) dividing quadrilateral elements into triangular elements

established and then connected to create quadrilateral and triangular elements as shown in Fig. 4.26(b) and Fig. 4.26(c), respectively.

In the slab shown in case 2 (Fig. 4.27) the last contour line is asymmetric around the point with the maximum displacement therefore a simple intuitive rule is used to establish the new mesh. The point with the maximum displacement is used as the origin of the radial segments. However, because the closest contour line to this point (shown in red) is in a shape of ellipse with the major axis in the x-direction, the x coordinates of the origin of the radial segments are replaced by the x coordinates of the point of the intersection between the radial segments and the contour lines as shown in Fig. 4.27(a). Points of intersection between these segments and the contour lines are established and then connected to create quadrilateral elements as shown in Fig. 4.27(b) and Fig. 4.27(c). These quadrilateral elements are then

divided into triangular elements as shown in Fig. 4.27(d).

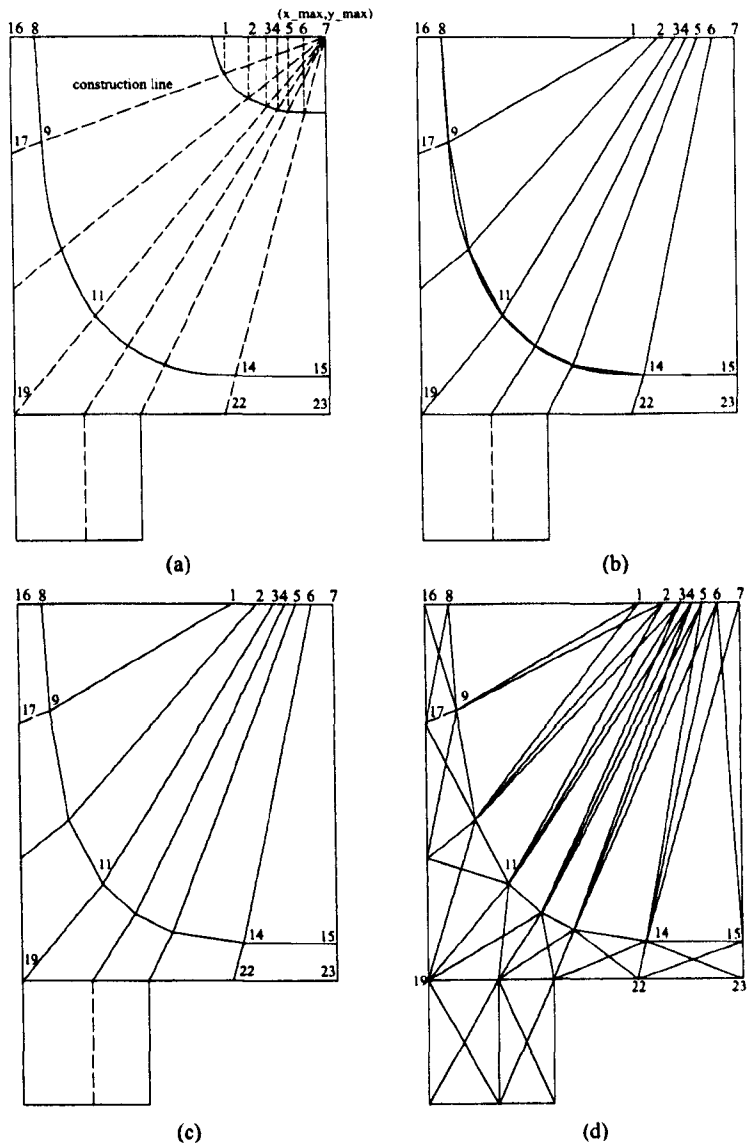

Figure 4.27: Construction stages of the new mesh for case 2 (a) discretizing the slab into a number of segments; (b) creating points; (c) connecting points to create quadrilateral elements; (d) dividing quadrilateral elements into triangular elements

It has to be stressed here that this rule is based on the authors experience and the slab geometry. Broadly speaking, the pattern suggested is likely to take place as the horizontal side is greater than vertical side in the case of the slab shown in Fig. 4.30 and the slab shown in Fig. 4.31. Also the asymmetry of the last contour line

indicates that the construction lines are likely to meet at a point outside the slab. Accordingly, these lines will intersect the free edge at a number of points which can be determined intuitively by projecting points from the inner contour. This will potentially provide possible locations for yield lines which are likely to result in a lower load factor being obtained.

4.6.2 Algorithm for the two-phase Sheffield method

The suggested procedure for the two-phase Sheffield method involves carrying out an initial analysis using the original Sheffield method and then performing a number of analyses using the Munro and Da Fonseca method. A step-by-step description for the procedure is as follows:

1. Set iteration count $k = 1$. Set-up a standard LP problem using the Sheffield method.
2. Solve LP problem.
3. Find the maximum displacement and the points with the maximum displacement. Store the displacement contours and the coordinates of the points with the maximum displacement.
4. Delete the old discretization from the computer memory.
5. Use the iteration number (k) to decide the number of segments and the zero displacement contour tolerance (tol_0) to be used in the new discretization of the slab and discretize the slab accordingly.
6. Set-up a standard LP problem using the Sheffield method with translational displacements at all interfaces being set to zero.

7. Solve the LP problem. If k=2, set the current load factor as the minimum and store it in the computer memory along with the iteration number. If k >2, compare the current load factor with the minimum load factor. If the current load factor is less than the minimum load factor, then set this as the minimum load factor and store it in the computer memory along with the iteration number.

8. $k = k + 1$; if $k <$ the maximum number of iterations; repeat from step 4, else output the minimum load factor and plot the corresponding mesh.

It is worth mentioning here that, the Munro and Da Fonseca method can also be used in phase 1 to set-up the problem.

4.6.3 Examples

To demonstrate the capability of the two-phase Sheffield method, a number of previously examined examples are re-visited.

4.6.3.1 Simply supported square slabs with uniformly distributed load

The simply supported square slab dealt with in 4.5.1.1 was re-analysed. Quadrilateral elements were initially used and a discretization of 20×20 divisions was used to set-up the problem in phase 1. A new mesh consisting of triangular elements was created and the exact load factor was obtained after one iteration. The program also identified the correct yield line pattern, as shown in Fig. 4.28.

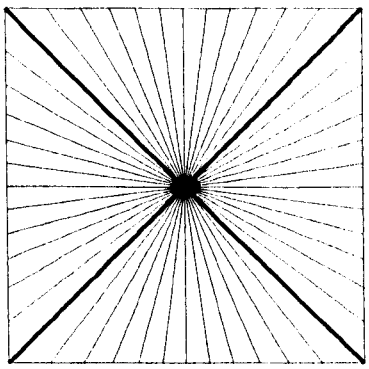

Figure 4.28: The critical yield line pattern for a simply supported square slab with UDL

4.6.3.2 Fixed edged square slabs with uniformly distributed load

The problem of a uniformly loaded, isotropic fixed edged square slab is more complicated. Sobotka [24] proposed various kinematic upper-bound solutions with yield line fans at the corners. Symmetry may be used so that only one eighth of the slab needs to be analysed. Using a mesh of 20×20, a load factor of 42.9827 was obtained compared with 43.8375 when the Munro and Da Fonseca method was used

to initially set-up the problem by identifying the initial failure pattern instead of the Sheffield method. The displacement contours shown on Fig. 4.29 are very similar to those corresponding to the exact solution derived by Fox [20].

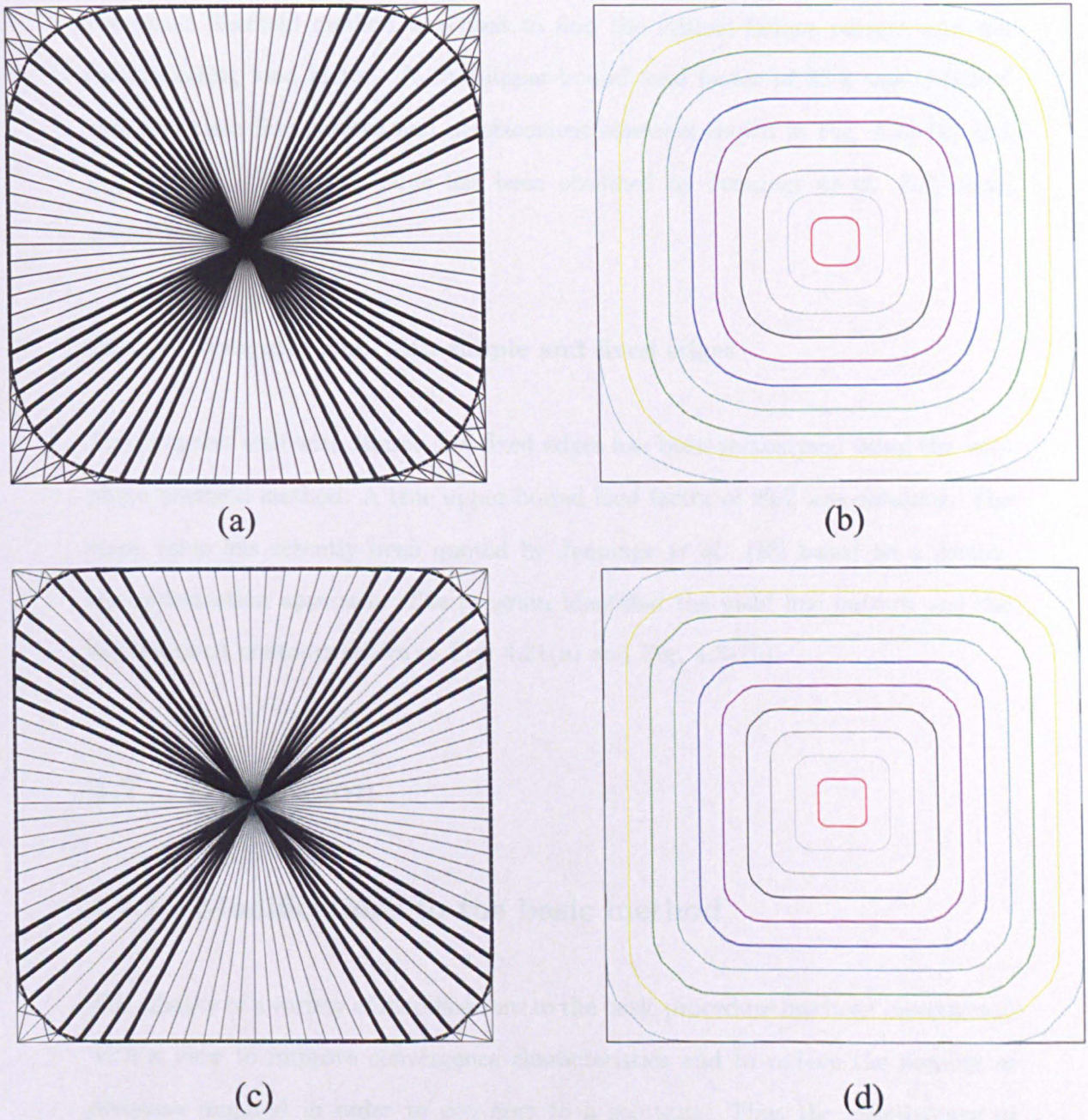

Figure 4.29: Fixed edged square slab with UDL: (a) yield line pattern: the Sheffield method; (b) displacement contours: the Sheffield method; (c) yield line pattern: the Munro and Da Fonseca method; (d) displacement contours: the Munro and Da Fonseca method

4.6.3.3 Fixed edged irregular slab

This example problem has been studied previously in section 4.5.2.1. Here the two-phase Sheffield method was used to find the critical failure pattern and the corresponding load factor. A true upper-bound load factor of 35.8 was obtained with the yield line pattern and displacement contours shown in Fig. 4.30 (a) and Fig. 4.30(b). The same value has been obtained by Jennings *et al.* [18] using geometry optimization.

4.6.3.4 Irregular slab with simple and fixed edges

The irregular slab with simple and fixed edges has been re-analysed using the two-phase Sheffield method. A true upper-bound load factor of 29.2 was obtained. The same value has recently been quoted by Jennings *et al.* [18] based on a geometry optimization approach. The program identified the yield line pattern and the displacement contours shown in Fig. 4.31(a) and Fig. 4.31(b).

4.7 Discussion

4.7.1 Modifications to the basic method

The efficacy of a variety of modifications to the basic procedure has been investigated with a view to improve convergence characteristics and to reduce the number of divisions required in order to converge to a solution. Thus the effectiveness of introducing adaptive discretization was investigated initially. However, apart from the case of the simply supported slab modelled with square elements, this was found not to perform well in the majority of the cases which have been studied. There was no clear trend showing how the load factor converges towards the exact solution.

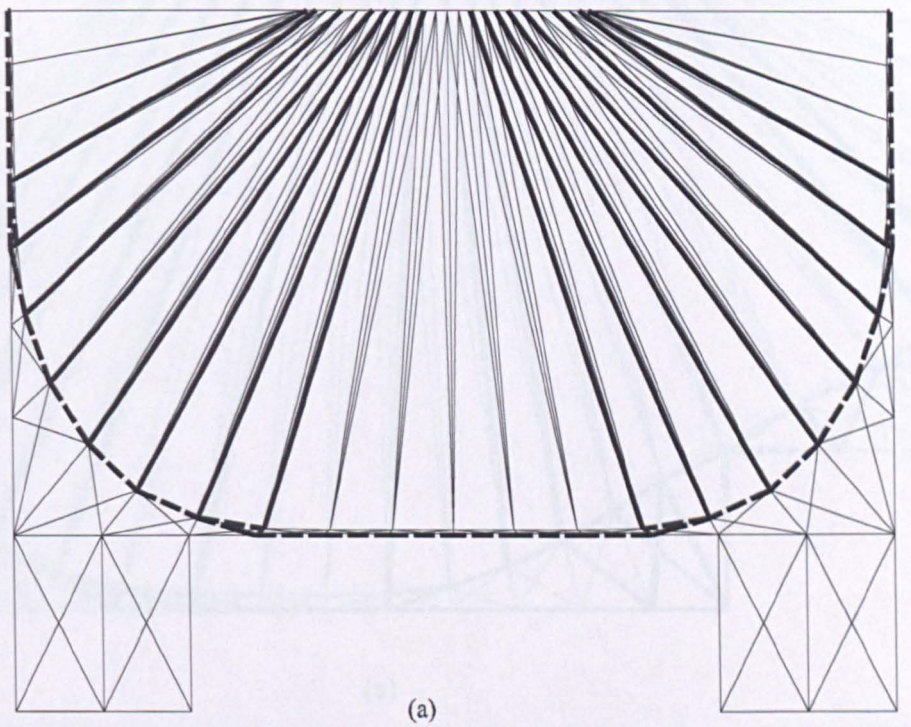

(a)

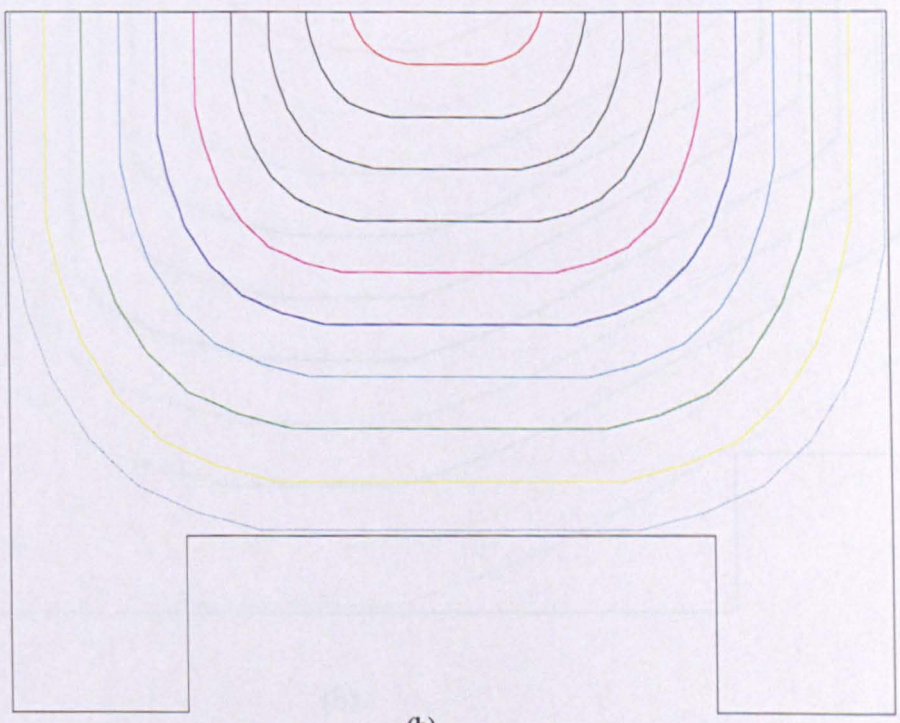

(b)

Figure 4.30: Fixed edged irregular slab: (a) FE mesh and yield line pattern; (b) displacement contours

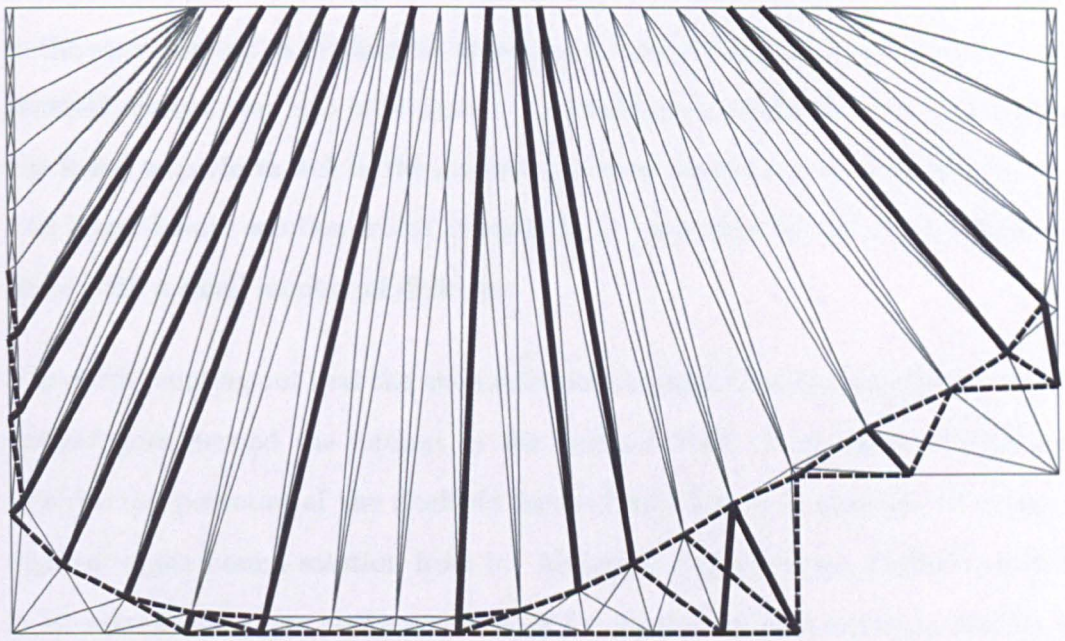

(a)

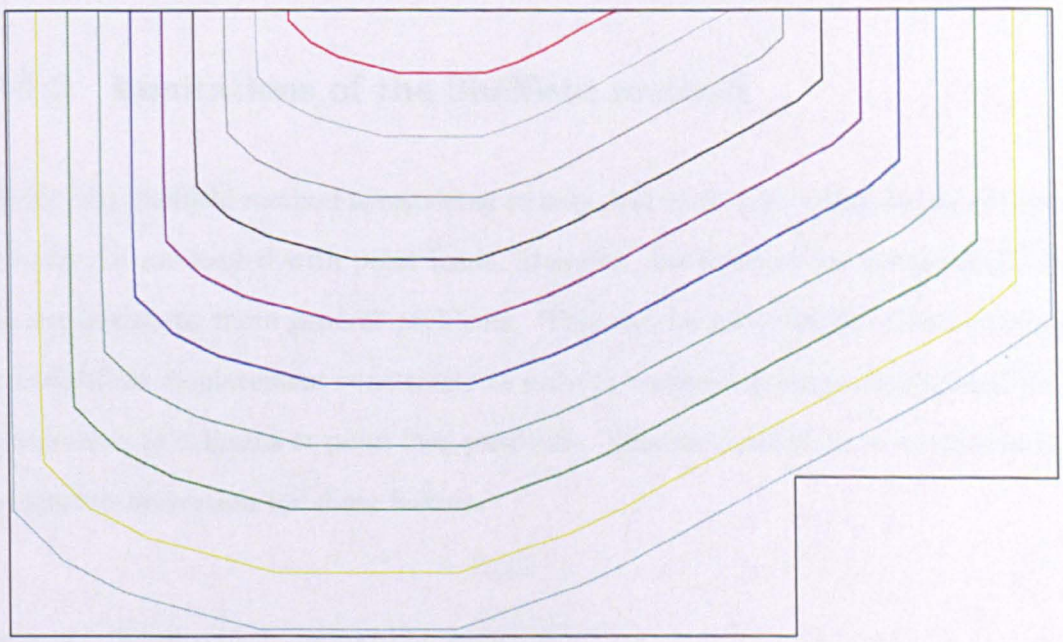

(b)

Figure 4.31: Irregular slab with simple and fixed edges: (a) yield line pattern; (b) displacement contours

In the same context, a method for obtaining a true upper-bound solution using the Sheffield method was also investigated. The two-phase Sheffield method developed was found to perform well in the majority of cases which have been investigated. A true upper-bound solution which is equal to or very close to the exact solution is found with a small number of divisions.

It is worth pointing out that the main intention in presenting the two-phase Sheffield method goes beyond the interest in the method itself. It is intended primarily to show the potential of the Sheffield method and how it is possible to obtain a rigorous upper-bound solution from it. Although the two-phase Sheffield method in its current form has performed well so far, further work is certainly needed to improve the method.

4.7.2 Limitations of the Sheffield method

So far, the Sheffield method is restricted to only deal with slabs which do not contain columns or are loaded with point loads. However, the method has the potential to be applicable to more general problems. This can be achieved by re-establishing translational displacement constraints to prevent excessively large translational displacements at columns or point load positions. This also should be accompanied by a rigorous derivation for shear factors.

4.7.3 Influence of shear factor

Central to the concepts behind the Sheffield method is the idea of allowing shear forces to exist at interfaces. The yield condition is modified with these forces multiplied by the normal distance from element centroid to the interface under consideration and the shear factor. As stated in section 4.4.7, the Sheffield method rests

largely on the correct choice of shear factor. However, when the 'right' shear factor is chosen the method seemed to perform well. The derivation of the shear factor has been performed only for elements with aspect ratio of 1. Therefore, it is crucial to a develop a general expression for the shear factor so that elements with aspect ratios different from 1.0 can be considered.

4.8 Conclusions

A computerized yield line analysis method for slabs has been presented. A kinematic analysis approach is adopted for the problem formulation. Translational displacements at interfaces between elements are allowed in order to account for the fact that critical yield lines may reside inside elements rather than on elements edges.

The Sheffield method appears, in the majority of cases, to be capable of:

- Producing a satisfactory solution using a variety of different element geometries, unlike other methods such as the Munro and Da Fonseca method. For example, there will no feasible solution if the Munro and Da Fonseca method is used to find the critical yield line pattern for simply or fixed edged square slabs if quadrilateral elements are used instead of triangular elements.
- Converging to the exact solution regardless to the element type, provided that a sensible value for the shear factor is used.

It was also found that it is possible to obtain true upper-bound solutions using a two-phase version of the method.

References

[1] Hodge, P. G. and Belytschko, T. Numerical methods for the limit analysis of plates. *Journal of Applied Mechanics*, 35:796–802, 1968.

[2] Anderheggen, A. and Knopfel, H. Finite element limit analysis using linear programming. *International Journal of Solids and Structures*, 8:1413–1431, 1972.

[3] Krenk, S., Damkilde, L. and Hoyer, O. Limit analysis and optimal-design of plates with equilibrium elements. *Journal of Engineering Mechanics-ASCE*, 120(6):1237–1254, 1994.

[4] Vanderbei, R. J. *Linear Programming: Foundations and Extensions.* Kluwer Academic Publishers, London, UK, 1998.

[5] Krabbenhoft, K. and Damkilde, L. Lower bound limit analysis of slabs with non-linear yield criteria. *Computers & Structures*, 80:2043–2057, 2002.

[6] Da Fonseca, A. M. A. *Plastic analysis and synthesis of plates and shells by mathematical programming.* PhD Thesis, Imperial College London, Department of Civil Engineering, 1979.

[7] Balasubramanyam, K. V. and Kalyanaraman, V. Yeild line analysis by linear programming. *ASCE Journal of Structural Engineering*, 114:1431–1437, 1988.

[8] Cohn, M. Z., Ghosh, S. K. and Parimi, S. R. Unified approach to theory of plastic structures. *Journal of Engineering Mechanics Division, ASCE*, 98:1133–1158, 1972.

[9] Bauer, D. and Redwood, R. G. Numerical yield line analysis. *Computers & Structures*, 26(4):587-596, 1987.

[10] Dickens, J. and Jones, L. A general computer program for the yield line solution of edge supported slabs. *Computers & Structures*, 30(3):465–476, 1988.

[11] Shoemaker, W. Computerized yield line analysis of rectangular slabs. *Computers & Structures*, 20:62–65, 1989.

[12] Hillerbog, A. Yield Line analysis. *Concrete International*, 13:9–10, 1991.

[13] Islam, N., Abbas, H. and Jain, P. A computer-oriented procedure for the yield line analysis of slabs. *Computers & Structures*, 52:419–430, 1993.

[14] Johnson, D. Yield line analysis by sequential linear-programming. *International Journal of Solids and Structures*, 32(10):1395–1404, 1995.

[15] Johnson, D. Mechanism determination by automated yield-line analysis. *The Structural Engineer*, 72:323-327, 1994.

[16] Ramsay, A. C. A. and Johnson, D. Analysis of practical slab configurations using automated yield-line analysis and geometric optimization of fracture patterns. *Engineering Structures*, 20(8):647–654, 1998.

[17] Thavalingam, A., Jennings, A., McKeown, J. J. and Sloan, D. A computerised method for rigid-plastic yield-line analysis of slabs. *Computers & Structures*, 68(6):601–612, 1998.

[18] Thavalingam, A., Jennings, A., McKeown, J. J. and Sloan, D. Computer-assisted generation of yield-line patterns for uniformly loaded isotropic slabs using an optimisation strategy. *Engineering Structures*, 21(6):488–496, 1999.

[19] Liu, T. Automatic computational method for yield line analysis. *Structural Engineering and Mechanics*, 8:311–324, 1999.

[20] Fox, E. N. Limit analysis for plates: The exact solution for a clamped square plate of isotropic homogeneous material obeying the square yield criterion and loaded by uniform pressure. *Philosophical Transactions of The Royal Society of London, Series A, Mathematical and Physical Sciences*, 227:121–155, 1975.

[21] Save, M.A. and Massonnet, C.E. *Plastic analysis and design of plates, shells and disks.* North-Holland publishing company, Amsterdam-London, 1974.

[22] Regan, P. E. and Yu, C. W. *Limit State Design of Structural Concrete.* Chatto and Windus, London, UK, 1973.

[23] Johnson, R. P. *Structural Concrete.* McGraw-Hill, London UK, 1967.

[24] Sobotka, Z. *Theory of plasticity and limit design of plates.* Academia, Prague, Czech Republic, 1989.

Appendix I

Derivation of shear factors

To prevent uncontrolled interface translational displacements an additional constraint is needed. This constraint can be established by linking the translational displacements at each node on any interface to the actual rotation (θ_i) at this interface via a function which accounts for the worst case for a yield line position encountered in a given mesh and considers at the same time the geometrical properties of the mesh i.e.

$$d_{i_j}\theta_i^+ + d_{i_k}\theta_i^- - 0.5(\delta_{i_1}^+ + \delta_{i_1}^- + \delta_{i_2}^+ + \delta_{i_2}^-) \geq 0\} \text{for } i = 1,...,m \text{ between } j \text{ and } k \quad (4.15)$$

where d_{i_j} and d_{i_k} are the normal distances from the actual yield line indicated by a dashed line, and the closest possible yield line which can represent this yield line as shown in Fig. 4.33 for triangular elements. $d_{i_j} = sf_{i_j} dn_{i_j}$ and $d_{i_k} = sf_{i_k} dn_{i_k}$, where sf_{i_j} and sf_{i_k} are the shear factors.

To derive this relationship, consider the two adjacent elements shown in Fig. 4.32.

The total displacement of element j (at the mid point on the interface i) with respect to the location of the yield line in its worst position, considering the location of the true yield line in a certain mesh, is equal to $0.5(\delta_{i_1}^+ + \delta_{i_2}^+)$-$\theta_i^+ d_{i_j}$.

Similarly, the total displacement of element k at the same node is equal to $\theta_i^- d_{i_k}$-$0.5(\delta_{i_1}^- + \delta_{i_2}^-)$. As translational displacements at any interface can only occur if

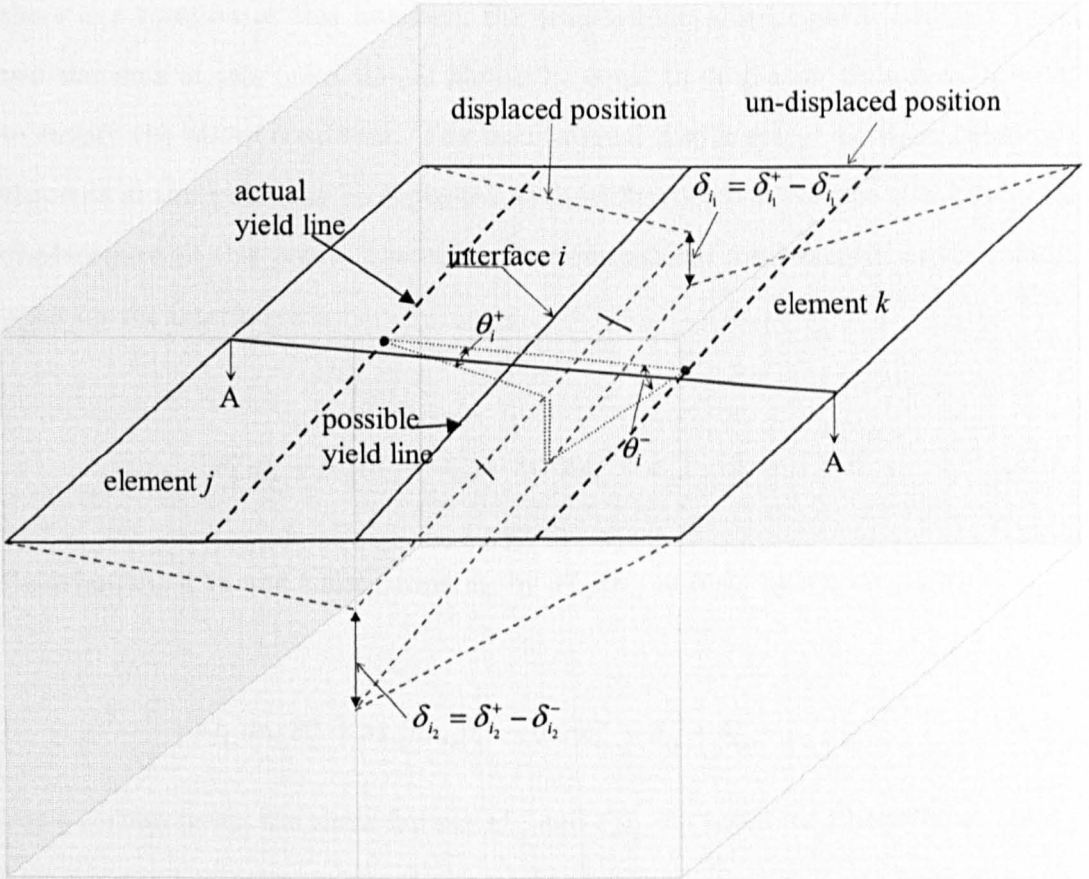

(a)

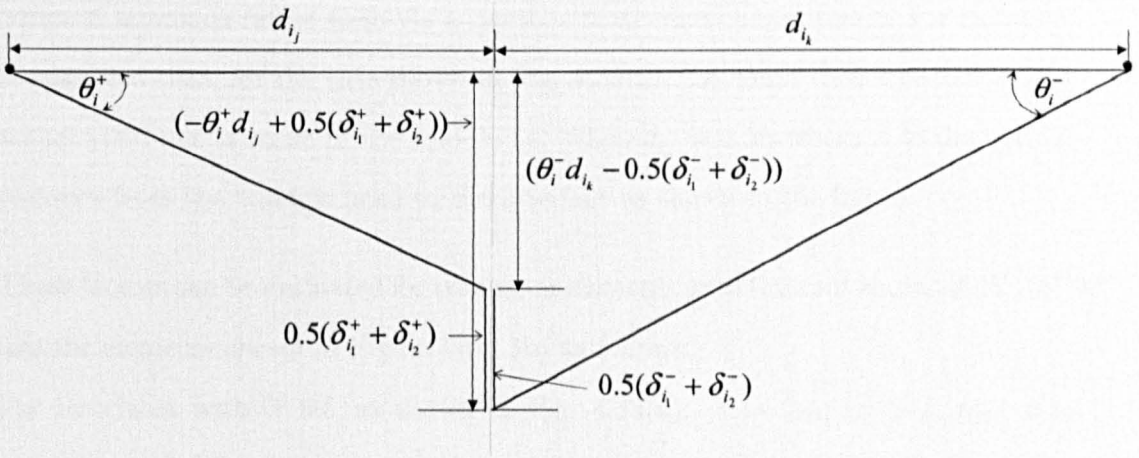

(b)

Figure 4.32: Translational displacements at the mid-point in a certain interface (a) 3D view; (b) section A-A

there is a rotation at this interface, the translational displacement between these two elements at this point should always be equal to or greater than zero in order to satisfy the above condition. The translational displacement between these two elements at this point can be expressed as the difference between the elements' total displacement at this point. Therefore, the translational displacement at the middle point on the interface i is :

$$\theta_i^- d_{i_k} - 0.5(\delta_{i_1}^- + \delta_{i_2}^-) - (0.5(\delta_{i_1}^+ + \delta_{i_2}^+) - \theta_i^+ d_{i_j}) \geq 0 \tag{4.16}$$

Re-arranging 4.16 and substituting d_{i_j} by $sf_{i_j} dn_{i_j}$ and d_{i_k} by $sf_{i_k} dn_{i_k}$ gives:

$$sf_{i_j} dn_{i_j} \theta_i^+ + sf_{i_k} dn_{i_k} \theta_i^- - 0.5(\delta_{i_1}^+ + \delta_{i_1}^- + \delta_{i_2}^+ + \delta_{i_2}^-) \geq 0 \tag{4.17}$$

For a certain mesh, the shear factors sf_{i_j} and sf_{i_k}, for interface i between element j and element k, can be evaluated using basic trigonometry. It has to be mentioned, that the derivation of these factors is based on an intuition and learning from experience approach rather than via a rigorous mathematical approach. For example, It appeared that, for the case shown in Fig. 4.33(a), the worst case scenario for the actual yield line is to lie in the middle i.e. when $d_{i_j} = 0.5h$ where h is the normal distance from the triangle head to the interface as shown in the figure.

These factors can be evaluated for triangular elements with internal angles of 45°,45°,90° like the elements shown in Fig. 4.33(a),(b) as follows:

For interfaces with 0°,90° as shown in Fig. 4.33(a): $h = 2d_{i_j} = 2sf_{i_j} dn_{i_j}$, also $h = 3dn_{i_j} \Rightarrow sf_{i_j}$=1.5

Similarly, for interfaces with 45° as shown in Fig. 4.33(b)

sf_{i_j}= d_{i_j}/dn_{i_j}= $0.5h/(2/3h) \Rightarrow sf_{i_j}$= 0.75

Furthermore, d_{i_j} and d_{i_k} can also be evaluated for quadrilateral elements. It has

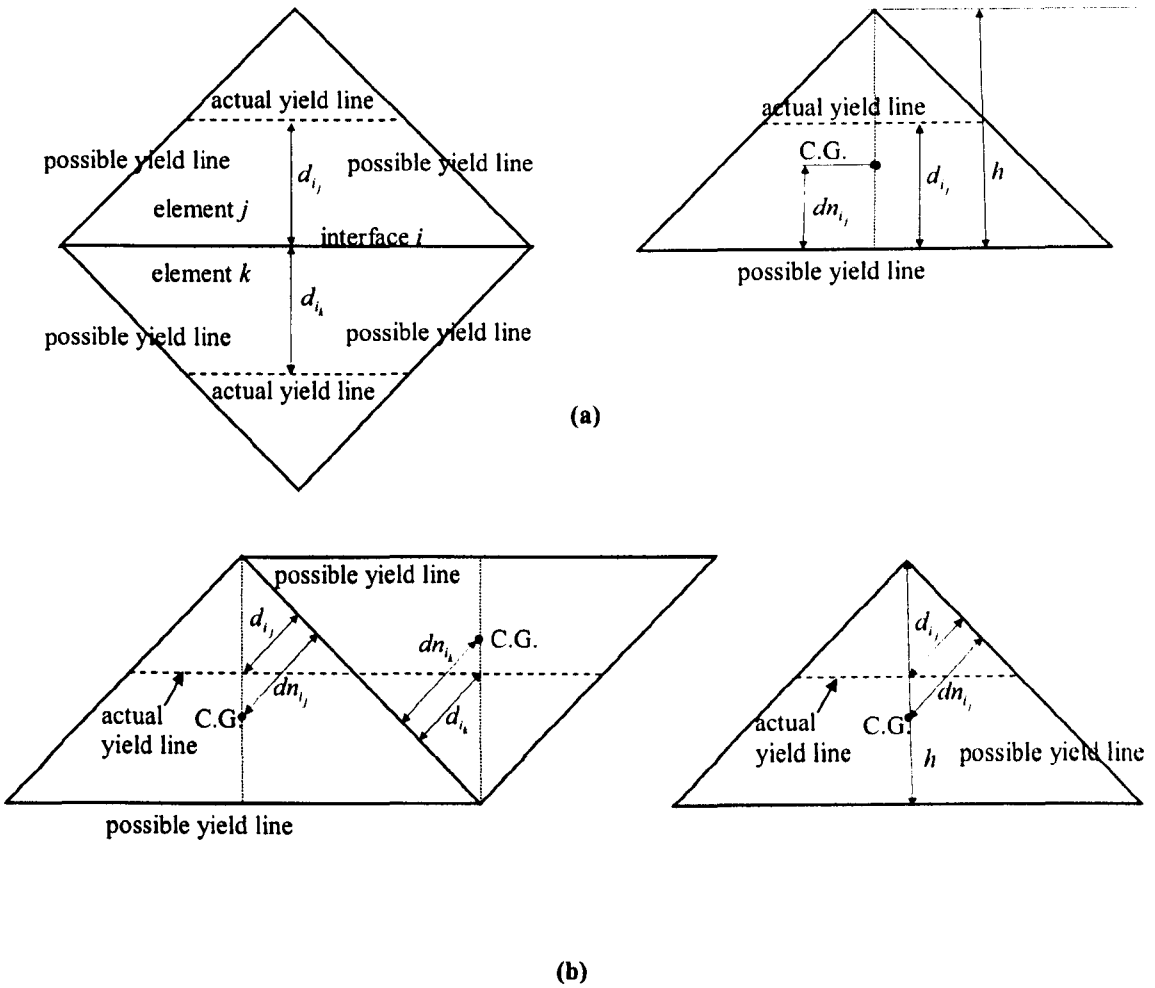

Figure 4.33: Actual yield lines and possible yield lines in a certain discretization: (a) geometry of two adjacent elements: a horizontal interface; (b) geometry of two adjacent elements: an inclined interface

been shown in section 4.4.3 that if these distances have been taken as half the normal distance from the element center to the interface under consideration, the correct load factor will be obtained, as shown in Fig. 4.34. However, this valid only for one-way spanning slabs. In the case of one-way slabs, for each element in the mesh, there are only 2 sides which are active (as the sides on the free edges are not involved). Generally, for an interface between two quadrilateral elements, sf_{i_j} and sf_{i_k} can be evaluated as follows:

$sf_{i_j} = sf_{i_k} = (n \times 0.5/2) = (n/4)$

where n is the number of active sides.

For example, for the case where the four sides are active, sf_{i_j}= (4×0.5/2) ⇒ sf_{i_j} = 1.0 or d_{i_j}=dn_{i_j}. This agrees with the fact that the distance from the yield line position at the worst case scenario is equal to the normal distance between the interface under consideration and the centre of gravity of the quadrilateral element as shown in Fig. 4.35(a),(b) where the yield line at the worst case scenario has equally-possible two locations.

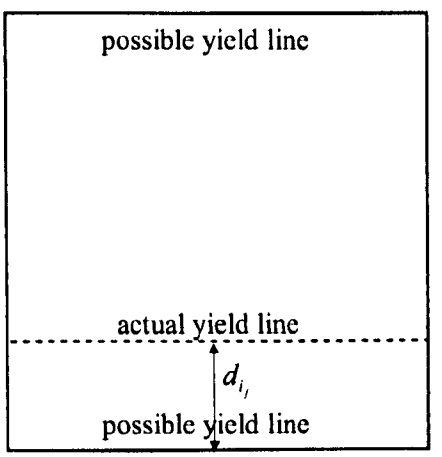

Figure 4.34: A quadrilateral element with possible yield lines at two edges

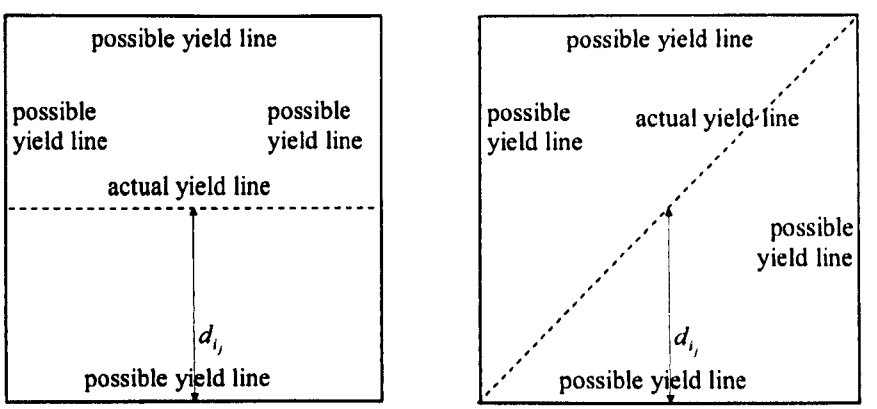

Figure 4.35: A quadrilateral element with possible yield lines at all edges (a) a horizontal yield line; (b) an inclined yield line

Chapter 5

Limit Analysis of Masonry Block Structures with Non-Associative Frictional Joints Using Linear Programming

5.1 Abstract

† Although limit analysis has been found to be a valuable tool for analysing the stability of masonry gravity structures, modelling non-associative Coulomb sliding friction can be problematic. A simple iterative procedure which involves the successive solution of simple linear programming sub-problems is presented in the paper. The procedure involves the use at each contact interface of a specially modified Mohr-Coulomb failure surface, which is modified at each iteration until a converged solution is obtained. The procedure is applied to problems from the literature and

† This chapter forms the basis of a journal paper manuscript co-authored with M. Gilbert (University of Sheffield) and C. Casapulla (University of Naples).

also to new, considerably larger, benchmark problems.

Keywords: Masonry structures; Limit analysis; Non-associative friction; Flow rule; Coulomb friction; Linear programming

5.2 Introduction

Kooharian and Heyman [1, 2] were amongst the first to consider (vaulted) block structures in the context of the plastic limit analysis theorems which emerged during the last century. Initially the assumptions were simple: constituent blocks possess infinite compressive strength, joints have zero tensile strength and sliding failures are not permitted. Whilst such a simple idealization is undeniably attractive in that it simplifies a hand or computer-based analysis, it is also problematic. For example in the case of flat arches, failure simply cannot occur without some sliding and/or crushing of the material.

Ignoring crushing at present, it is clearly necessary to study the mechanics of masonry structures assuming that sliding failures can occur. However, it is well-known that the bounding theorems of plastic limit analysis do not in general provide unique solutions for the collapse load factor if a non-associative flow rule is specified. Unfortunately the standard Coulomb sliding friction model is clearly non-associative since it does not require that sliding at frictional interfaces is accompanied by movement normal to the interface (i.e. dilatancy). A practical consequence is that satisfying equilibrium and yield conditions alone is not sufficient to guarantee that a structure is safe (because the dilation implied by the limit analysis theorems may not be present in reality).

Drucker [3] was amongst the first to identify the difficulty of treating Coulomb sliding friction. He stated modified upper-bound conditions assuming either complete

attachment or dilatancy and a lower-bound condition assuming a zero coefficient of friction.

With reference to a generic non-standard material, other authors [4, 5, 6, 7] provided lower and upper-bounds on the exact solution by using Radenkovic's theorems. However, such bounds will often be too wide to be of use in practice. For example, if a zero coefficient of friction is used the collapse load factor for a simple masonry arch rib (a particular, but extremely common, assemblage of blocks) will typically be bounded from below by a load factor of zero.

More recently Livesley [8, 9], using a lower-bound approach, developed a formal linear programming (LP) procedure to compute the load factor for two and three-dimensional structures formed from rigid blocks, assuming initially an associative friction model. Since Charnes and Greenberg [10] had shown many years previously that when "mechanism" and "equilibrium" limit analysis formulations are linearized they give rise to dual LP problems, Livesley was also able to plot a collapse mechanism directly after performing a lower-bound analysis. In doing so, he identified apparently anomalous failure mechanisms, and also demonstrated cases when the associative friction load factor over-estimated the Coulomb sliding friction load factor. Consequentially he proposed a post-optimality analysis to test the validity of the solutions obtained (applicable to simple masonry vault problems), although no remedy was proposed in cases of load factor overestimation.

It should perhaps be mentioned that for certain classes of problems the assumption of associative friction has been found to provide numerical predictions which are in broad agreement with experimentally observed results. For example, in a study of the behaviour of multi-ring arches Gilbert [11] established the importance of failure modes involving sliding for this structural form but also observed that associative friction solutions appeared to agree reasonably well with experimental results.

Nevertheless, Livesley's pioneering initial study of non-associative friction stimulated a line of research [12, 13, 14, 15, 16] concerned with developing numerical procedures for such problems. One of these was given by Lo Bianco and Mazzarella [12], followed by Baggio *et al.* [13, 14]. Here the non-associative problem was solved using procedures which involved identifying load factors simultaneously satisfying the kinematic and static conditions. However the procedures were found to be rather onerous in terms of time and memory requirements, because of the non-linear and non-convex optimization procedures required.

Others have identified particular non-associative problems which are amenable to simplification and which will hence furnish solutions in favour of safety which are both statically admissible and which satisfy the normality rule [17, 18]. Then Casapulla [19, 20, 21] identified important problem types, depending on loading and geometry conditions, for which unique solutions can be found. For certain other problems, procedures have been suggested to get closer to the exact solution moving from the bounds given by two associative kinematic models [22]. However, such different lines of research are still far from a general method of analysis for non-associative problems of arbitrary geometry.

Most recently the problem has been posed as a mixed complementarity problem (MCP) and a mathematical programming with equilibrium constraints (MPEC) formulation has been proposed for masonry limit analysis problems involving non-associative frictional sliding [23, 24, 25, 26]. Unfortunately relatively specialised non-linear programming solution methods must be employed and it also seems that solving the MPEC formulation in the way proposed may for practically large problems be prohibitively computationally expensive.

The inherently non-linear problem of analysing the stability of structures composed of rigid blocks in the presence of material crushing has been tackled with some success by using an approximate procedure which involves the solution of a series of suc-

cessively modified LP problems [27]. A key aim of the present study is to determine whether a similar approach can be applied to problems involving non-associative friction (which are both non-linear and non-convex). Breaking the problem down to the solution of a series of successively modified LP problems is attractive since modern interior-point based LP solvers are efficient, robust and now very widely available. Additionally such a solver is already used in the RING rigid block analysis software for masonry arch bridges, originated by Gilbert (www.shef.ac.uk/ring) and significantly improved by the author.

5.3 Discrete block model with frictional constraints

Since the specific bonding pattern of masonry structures often influences the failure mode and load factor, there is some justification for modelling masonry structures as assemblages of discrete blocks. This is assumed here, along with the following assumptions: constituent blocks are rigid and infinitely strong; no tension may be transmitted across joints and blocks may slide and/or rock relative to each other.

In order to develop the governing equations for this model we consider, as in [9], the block interfaces as elements and the blocks as extended nodes connecting the elements. Here three degrees of freedom are associated with the centroid of each block and three stress resultants (i.e. normal force n, shear force s and bending moment m) act at each contact interface, as shown in Fig. 5.1 for a typical block j. Assuming there are b blocks and c contact surfaces then equilibrium of the whole structure can be expressed as:

$$\mathbf{Bq} - \lambda \mathbf{f}_L = \mathbf{f}_D \tag{5.1}$$

where $\mathbf{B}$ is a suitable ($3b \times 3c$) equilibrium matrix and $\mathbf{q}$ and $\mathbf{f}$ are respectively $3c$ and $3b$ vectors of contact forces and block loads. Thus $\mathbf{q}^T = [n_1, s_1, m_1, n_2, s_2, m_2, ..., n_c, s_c, m_c]$;

$\mathbf{f} = \mathbf{f}_D + \lambda \mathbf{f}_L$ where $\mathbf{f}_D$ and $\mathbf{f}_L$ are respectively vectors of dead and live loads; λ is the load factor.

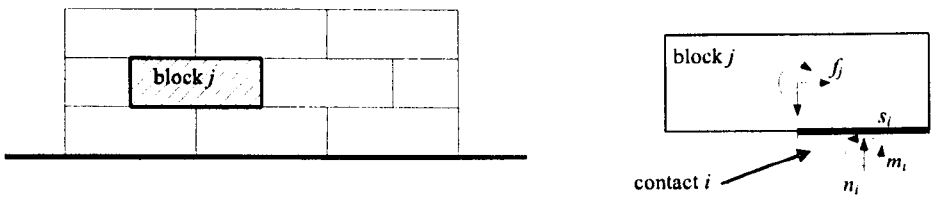

Figure 5.1: Block j and contact forces for interface i

Alternatively considering the failure mechanism, geometric compatibility requires that:

$$\mathbf{u} = \mathbf{B}^{\mathrm{T}}\mathbf{d} \tag{5.2}$$

where $\mathbf{u}$ is a $3c$-vector of all such contact displacement rates describing joint separation, sliding and rotation (ε,γ,κ) (related to $\mathbf{q}$ in a virtual work sense) and $\mathbf{d}$ is a $3b$-vector of nodal unconstrained displacement rates corresponding to the nodal loads $\mathbf{f}$.

Furthermore, for each contact interface yield conditions in the $n-s-m$ domain are required to define the failure criteria governed both by sliding and rocking. Although there is no interaction between the generalized shear force s and bending moment m it appears meaningful to represent the overall yield domain as shown in Fig. 5.2 together with the relevant flow rules to enable detailed consideration of the model.

In this figure, since the resultant displacement rates v_i and r_i are normal to the corresponding limit surfaces an associative flow law is indicated for both (b) sliding, and (c) rocking. Thus in the associative sliding model $\varphi_i^0 = \varphi_i$. However, when a Coulomb friction model is instead adopted, $\varphi_i^0 = 0$. The figure also indicates a possible cohesion intercept, c_i. Associative flow is however maintained for rocking, as indicated by the equality of angles η_i.

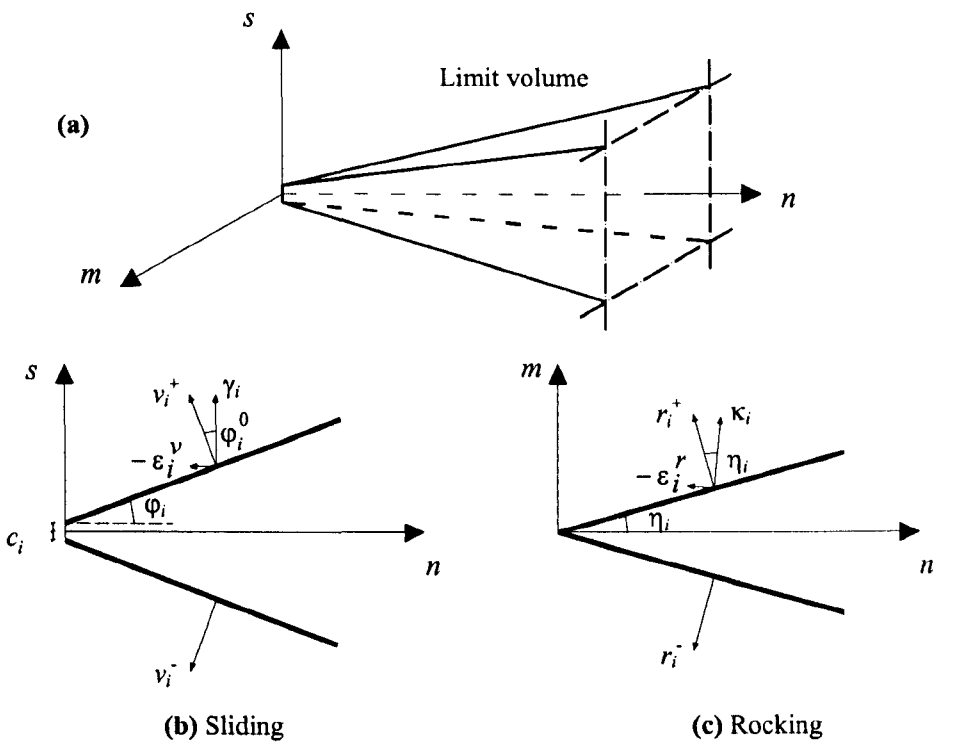

Figure 5.2: Yield domain for contact interface i

Hence, the yield domain for a generic contact interface i can be expressed compactly as:

$$\mathbf{z}_i = \mathbf{C}_i^{\mathrm{T}}[\mathbf{q}_i - \mathbf{c}_i] \leq 0 \tag{5.3}$$

or in explicit form, with s_i and m_i now each represented by two LP style non-negative variables:

$$\begin{bmatrix} z_i^{s+} \\ z_i^{s-} \\ z_i^{r+} \\ z_i^{r-} \end{bmatrix} = \begin{bmatrix} -\sin\varphi_i^0 & \cos\varphi_i^0 & 0 & 0 & 0 \\ -\sin\varphi_i^0 & 0 & \cos\varphi_i^0 & 0 & 0 \\ -\sin\eta_i & 0 & 0 & \cos\eta_i & 0 \\ -\sin\eta_i & 0 & 0 & 0 & \cos\eta_i \end{bmatrix} \left[\begin{bmatrix} n_i \\ s_i^+ \\ s_i^- \\ m_i^+ \\ m_i^- \end{bmatrix} - \begin{bmatrix} 0 \\ c_i \\ c_i \\ 0 \\ 0 \end{bmatrix} \right] \leq \begin{bmatrix} 0 \\ 0 \\ 0 \\ 0 \end{bmatrix} \tag{5.4}$$

Furthermore, for the same contact interface, the displacement rates contained in $\mathbf{u}_i$ are related to the respective non-negative resultant displacement rates in $\mathbf{p}_i$ as follows:

$$\mathbf{u}_i = \mathbf{D}_i \mathbf{p}_i, \quad \mathbf{p}_i \geq 0 \tag{5.5}$$

or in explicit form, with γ_i and κ_i now each represented by two LP style non-negative variables:

$$\begin{bmatrix} \varepsilon_i \\ \gamma_i^+ \\ \gamma_i^- \\ \kappa_i^+ \\ \kappa_i^- \end{bmatrix} = \begin{bmatrix} -\sin\varphi_i & -\sin\varphi_i & -\sin\eta_i & -\sin\eta_i \\ \cos\varphi_i & 0 & 0 & 0 \\ 0 & \cos\varphi_i & 0 & 0 \\ 0 & 0 & \cos\eta_i & 0 \\ 0 & 0 & 0 & \cos\eta_i \end{bmatrix} \begin{bmatrix} v_i^+ \\ v_i^- \\ r_i^+ \\ r_i^- \end{bmatrix}, \begin{bmatrix} v_i^+ \\ v_i^- \\ r_i^+ \\ r_i^- \end{bmatrix} \geq 0 \tag{5.6}$$

The normality rule is satisfied when $\mathbf{C}_i = \mathbf{D}_i$, i.e. when $\varphi_i^0 = \varphi_i$.

The system of governing equations is completed by the following two conditions:

$$\mathbf{f}_L^{\mathrm{T}} \mathbf{d} > 0 \tag{5.7}$$

$$\mathbf{z}_i^{\mathrm{T}} \mathbf{p}_i = 0 \tag{5.8}$$

that represent respectively the positive work of live loads and the complementarity condition (in this problem the complementarity condition basically stipulates that flow cannot occur unless the contact forces are located on the failure surface). It is the complementarity condition which makes this problem inherently difficult when $\varphi_i^0 \neq \varphi_i$.

The contact interface level relations (5.3-5.6 and 5.8) can easily be extended to the whole structure.

5.4 Associative friction problem formulation

On the basis of the above assumptions, the static (equilibrium) LP problem may be stated as follows:

$$\text{Maximize } \lambda$$

subject to:

$$\left.\begin{aligned} \mathbf{Bq} - \lambda \mathbf{f}_L &= \mathbf{f}_D \\ \mathbf{C}^{\mathrm{T}}[\mathbf{q} - \mathbf{c}] &\leq 0 \end{aligned}\right\} \tag{5.9}$$

Using this formulation the problem variables are clearly the contact forces: n_i, s_i, m_i (where, using LP style non-negative variables: $s_i = s_i^+ - s_i^-$, $m_i = m_i^+ - m_i^-$, and where $n_i, s_i^+, s_i^-, m_i^+, m_i^- \geq 0$).

The kinematic LP problem formulation may be expressed as:

$$\text{Minimize } \lambda \mathbf{f}_L^{\mathrm{T}}\mathbf{d} = \mathbf{f}_D^{\mathrm{T}}\mathbf{d} + \mathbf{u}^{\mathrm{T}}\mathbf{c}$$

subject to:

$$\left.\begin{aligned} &\mathbf{f}_L^{\mathrm{T}}\mathbf{d} = 1 \\ &\mathbf{B}^{\mathrm{T}}\mathbf{d} - \mathbf{C}\mathbf{p} = 0 \\ &\mathbf{p} \geq 0 \end{aligned}\right\} \tag{5.10}$$

Using this formulation the linear programming problem variables are the nodal absolute and contact relative displacement rates.

Duality theory means that whichever formulation is solved, the other is automatically solved too. Additionally conditions 5.7 and 5.8 are automatically satisfied.

5.5 Treating the non-associative friction problem

As indicated previously, the standard LP formulation will not necessarily lead to good estimates of the collapse load factor for problems which involve non-associative frictional sliding. What is required is a procedure which is both capable of identifying safer non-associative friction solutions (should they exist) and is also numerically tractable for reasonably large problems. Hence what follows is a description of a conceptually simple heuristic method which involves merely the solution of a succession of simple LP sub-problems.

The difficulty with the standard LP formulation is that flow is by default normal to the yield surface (i.e. because the so-called 'normality rule' holds). It is however possible to modify the yield surface for each interface in a sub-problem so as to ensure that the required flow when the problem is solved again is parallel to the shear force axis, as indicated on Fig. 5.2(b) when $\varphi_i = \varphi_i^0 = 0$ (this was actually

first proposed by Livesley [8] to correct his anomalous failure mechanisms). In other words, behaviour of a contact becomes governed by a Mohr-Coulomb failure surface, with an effective cohesion intercept but a zero angle of friction. However, this transformation then leads to a loss of dependency of the limiting shear force on the normal force, as indicated on Fig.5.3(a). This dependency can however be re-imposed if an iterative analysis is performed, with the normal forces computed in the current iteration being used to define the failure criteria for the next iteration. The starting values for the normal forces in the iterative procedure may be obtained in a number of ways, but it will often be convenient to start with the values from an initial associative friction solution.

Thus, denoting the computed normal force during this iteration (k=1) at interface i as n_i^k, the limit surface for sliding may be rotated about a point $(n_i^k, n_i^k \tan\varphi_i)$ so as to become horizontal, with this newly modified LP problem then being solved at the next iteration. If for each interface $n_i^k = n_i^{k+1}$ then this implies that the problem being considered is not influenced by the particular flow rule selected. Alternatively, if $n_i^k \neq n_i^{k+1}$ for one or more interfaces then the flow rule may be influencing the solution. In this case the current solution, which may well be highly inaccurate because of the transformed failure surface, should be improved by revising the failure surface again such that the limiting shear force at the next iteration is correct for the current normal force. This process can continue until any inaccuracy becomes acceptably small.

However, the aforementioned procedure appears to work much more effectively in practice if behaviour of a contact in a sub-problem is instead governed by a Mohr-Coulomb failure surface with an effective cohesion intercept *and a negative angle of friction* (Fig. 5.3 (b)). The normality rule then indicates that contraction at each failing interfaces will occur and a lower load factor will generally result, for reasons which will be explained. To subsequently remove this unwanted, kinematically in-

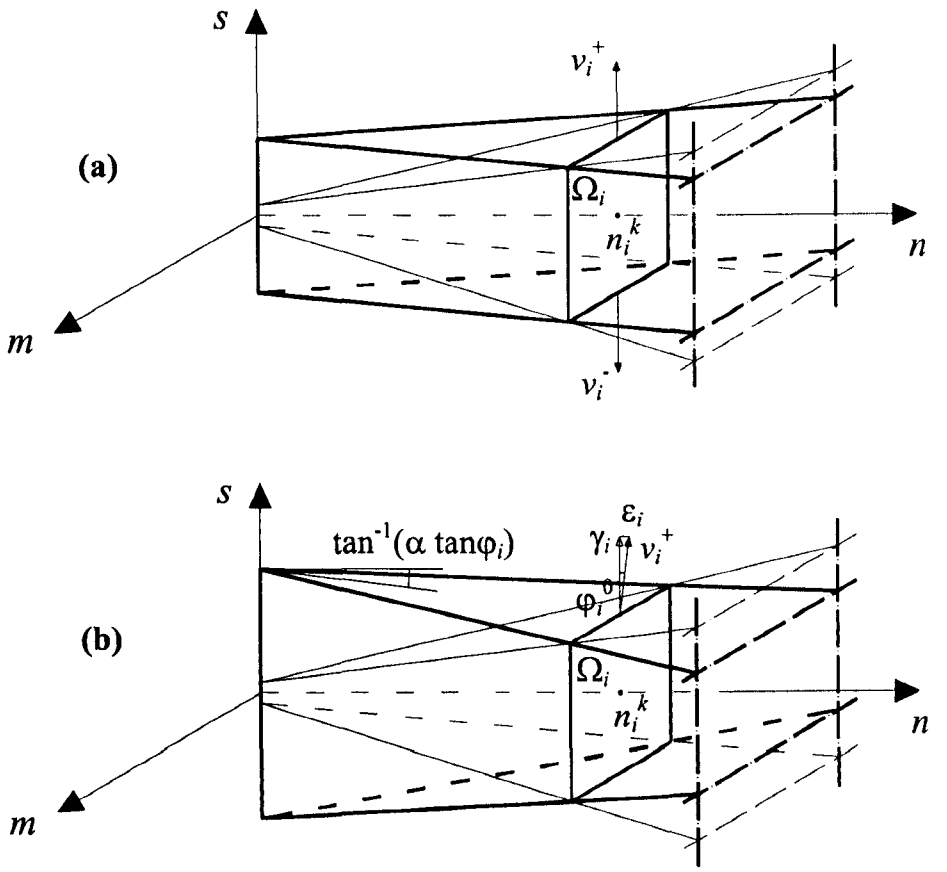

Figure 5.3: Modified yield domains for a typical contact interface i

admissible, response, the angle of friction may be successively relaxed towards zero as the iterative procedure progresses.

In fact, the rationale behind the method is to identify low values of the normal forces at contact interfaces, noting that these are more likely to be identified if there is contraction at active sliding interfaces, rather than expansion (as there is in the associative friction solution).

As described in [19], let it now be supposed that at every contact interface in a masonry structure the absolute minimum value that the normal force can take on (among all the statically admissible solutions) has been successfully identified. Then, assuming Coulomb friction, it can be assumed that at each interface the masonry

behaves essentially as a standard rigid-plastic material, taking the cohesion to be the identified minimum normal force multiplied by the friction coefficient. This would mean that the internal virtual work done cannot be greater than the internal work done by the true shear forces. As a consequence, the load factor cannot be greater than the true collapse factor and hence the solution must be safer than the exact one.

Of course the assumption of a negative angle of friction by no means guarantees that the forces at all contact interfaces will necessarily take on absolute minimum values, but it does mean that the solution so obtained is likely to bound from below the majority of the many solutions which are both statically and kinematically admissible when non-associative friction is present (Fig. 5.4(b)).

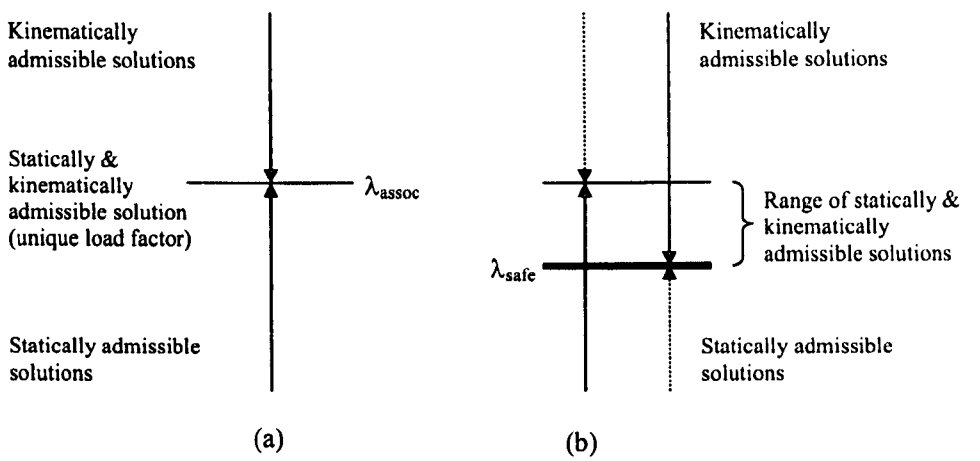

Figure 5.4: Static and kinematic admissibility of (a) associative, and (b) non-associative solutions

Note that when a problem is being idealized as a linear program, duality principles ensure that it is immaterial whether the static (maximization) or kinematic (minimization) problem is formulated and solved; both will lead to the same solution.

The likely correspondence between the minimum normal force at interfaces and the assumption of negative angle of friction (contraction) in early iterations can be demonstrated practically by studying the kinematics of a simple two-block problem.

5.5.1 Simple two-block problem

Consider the simple two block assemblage shown in Fig. 5.5(a). Each block is of the same size (3×1 units) and weight (1 unit). One of the blocks, A, is also subject to a horizontal load. Suppose also that the interfaces underneath and at the top of block A possess a relatively low angle of friction φ but that the contact between block B and its support is sufficiently rough to prevent sliding. Hence failure will involve sliding along the interfaces lying at the base and top of block A.

Now if dilatancy at the interfaces is present (i.e. as it will be when the normal LP formulation is used) then block A effectively expands, ensuring that block B has to rock, as indicated on Fig. 5.5(b). Here the normal force at the interface between blocks is clearly determinate and hence the load factor may easily be determined by considering the equilibrium at (1) and (3) as in Fig. 5.6:

Equilibrium of moments about (3) implies:

$$2n_2 - 1 \times 1.5 = 0 \Rightarrow n_2 = 0.75,\ s_2 = 0.75 \tan\varphi$$

Vertical equilibrium at (1) requires:

$$n_1 = n_2 + 1.0 \Rightarrow n_1 = 1.75 \text{ and } s_1 = 1.75 \tan\varphi$$

Horizontal equilibrium of the structure yields:

$$\lambda_1 = 0.75 \tan\varphi + 1.75 \tan\varphi = 2.5 \tan\varphi.$$

If there is zero dilatancy it becomes more difficult to determine the load factor since the force transmitted from block B onto block A becomes indeterminate. However, alternatively suppose that block A contracts slightly, as indicated in Fig. 5.5(c). In this case the normal force transmitted between blocks clearly becomes determinate again, and a considerably lower computed load factor results ($\lambda_2 = 1.5 \tan\varphi$). It

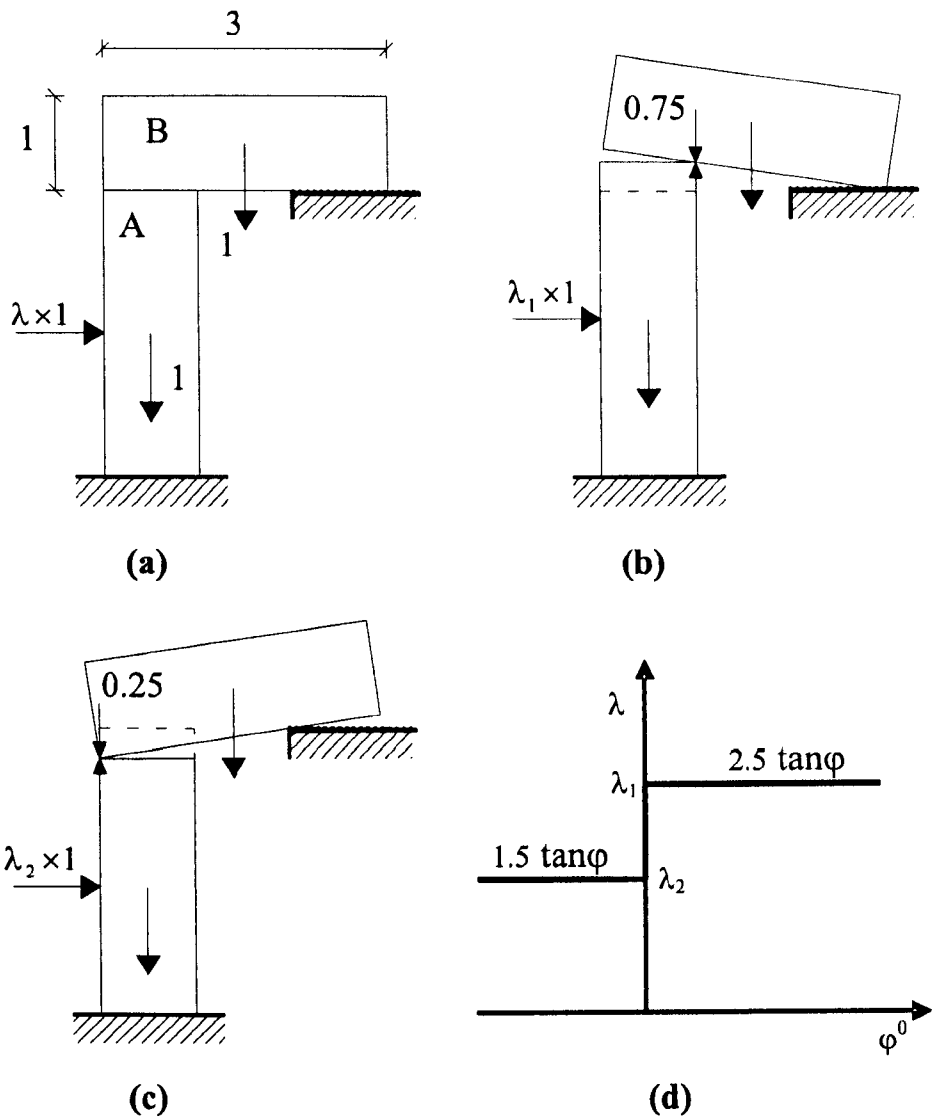

Figure 5.5: (a) Two-block example: (b) expansion; (c) contraction. (d) relationship between load factor and angle of dilatancy φ^0

will typically be the case that stipulation of negative dilatancy (i.e. contraction) will lead to lower load factors.

Now consider this problem in the context of the proposed LP based iterative solution procedure. First consider the case when the modified limit domain is of the form shown in Fig. 5.3(a), i.e. no expansion or contraction is implied. Thus Fig. 5.7(a) shows a plot of the normal and shear forces present at the interface between blocks

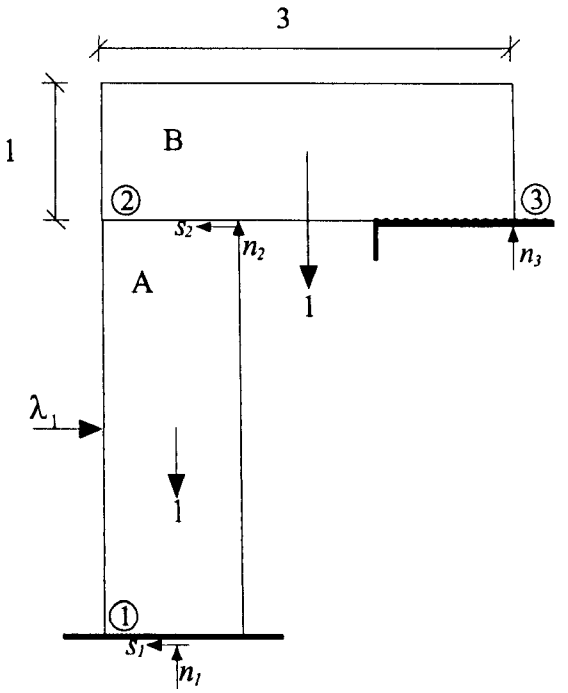

Figure 5.6: Two-block example

A and B when $\tan\varphi = 0.1$, at iterations 1,2 and 3. The load factors at each iteration are also indicated, together with the active failure surfaces (the starting sub-problem is the standard associative friction problem). At the first iteration, the standard LP problem is solved based on the associative friction model (failure surface 1 in Fig. 5.7(a) and Fig. 5.7(b)) and the normal force n_1 is determined and used to establish failure surface 2. The problem is then reformulated based on this failure surface and solved and the normal force n_2 is computed and is used to determine failure surface 3. Again, the problem is re-formulated and solved.

It is clear that the procedure identifies a normal force somewhere between the upper and lower limits[†]. Consequentially the load factor obtained using the procedure lies somewhere between λ_1 and λ_2 ($\lambda = 1.9535\tan\varphi$).

Figure 5.7(b) shows the comparable situation when the modified limit domain is

[†] This is actually a natural consequence of using an *interior-point* based LP solver, which will, in cases where there are multiple optimal solutions, provide a solution comprising parts of all these.

of the form shown in Fig. 5.3(b), i.e. contraction is initially present. In this case it is evident that the procedure correctly identifies the minimum possible value of the normal force at the interface, and consequentially also the lowest load factor ($\lambda = 1.5 \tan \varphi$). Note that the amount of contraction is successively reduced as the iterative procedure proceeds, as indicated on the figure.

Thus this example illustrates the likely promise of a modified procedure which involves the use of a negative angle of friction in early iterations (i.e. imposition of net contraction at sliding interfaces).

It is also evident that there is an abrupt discontinuity in the relationship between the computed load factor and the dilatancy angle φ^0 when the latter changes from just below to just above zero, as indicated on Fig. 5.5(d). However this is in fact a problem-specific feature and if the interface between blocks A and B were inclined at some angle ϕ to the horizontal, so that block A effectively forms a wedge (but all other details remain the same), then the discontinuity would occur at $\pm\phi/2$[†].

5.5.2 New algorithm for non-associative friction problems

The proposed algorithm to enable non-associative friction problems to be tackled can be described in terms of kinematic or static (equilibrium) problem formulations; here a static formulation will be used. Using this formulation the objective function and equilibrium constraints of (5.9) are maintained, as are the limits on the moment variables. However, the limits on the shear variables are modified as outlined previously following the first iteration. The algorithm developed is as follows:

[†] In such cases it is the wedge geometry which instead often governs whether net dilation or contraction occurs. Here the abrupt change in load factor occurs when $\varphi^0 = -\phi/2$ if movement of the wedge causes expansion, or $\varphi^0 = \phi/2$ if this leads to contraction (of the space originally occupied by block A). This might explain why many arch forms containing wedge shaped blocks, and which cause expansion when pressed in, are often insensitive to the particular flow rule specified, provided $\varphi^0 \geq 0$.

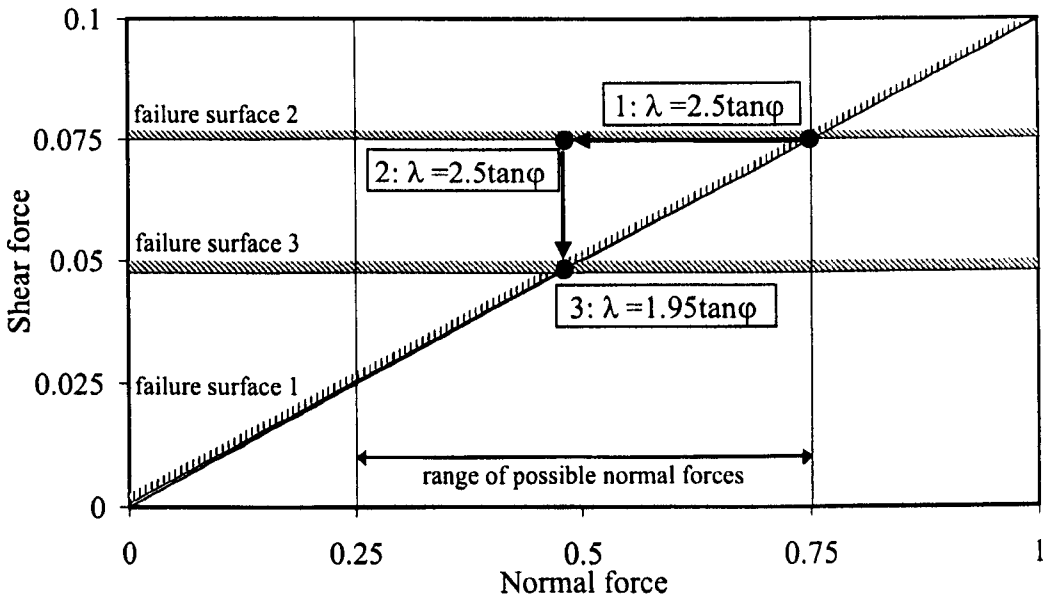

(a)

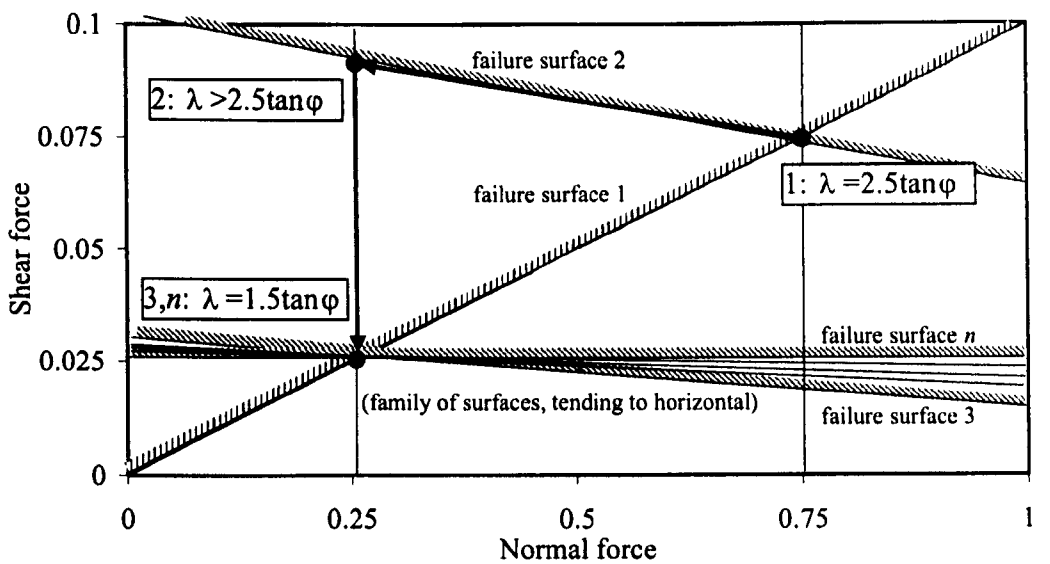

(b)

Figure 5.7: Forces and failure surfaces at interface between blocks A and B, (a) using modified limit domain Fig.5.3(a); (b) using modified limit domain Fig. 5.3(b)

1. Set iteration count $k = 1$ and set up a standard initial LP problem, e.g. the limiting sliding resistance in this problem could be given (as failure surface 1 Fig. 5.7(a) and Fig. 5.7 (b)) by:

$$|s_{k,i}| \leq n_{k,i} \tan \varphi_i$$

or alternatively, to provide an initial solution without dilatancy, the initial shear resistance could simply be specified to be:

$$|s_{k,i}| \leq c_i^{trial}$$

where c_i^{trial} is some (arbitrary) trial initial cohesion intercept.

2. Solve the LP problem. At each interface i the computed normal force at collapse is denoted $n_{k,i}$.

3. If $k > 1$ and $|\lambda_k - \lambda_{k-1}|/\lambda_k <$ tol, the prescribed convergence tolerance, then the algorithm stops.

4. Formulate new sliding friction failure criteria for the next LP iteration (as failure surfaces 1,2 in Fig. 5.7(a) and Fig. 5.7(b)), so that at each interface the new limiting sliding resistance is given by

$$|s_{k+1,i}| \leq c_{k+1,i} - \alpha n_{k+1,i} \tan \varphi_i$$

where:

$$c_{k+1,i} = c_i^0 + (1 + \alpha)\, n_{k,i} \tan \varphi_i$$

and where α is an algorithm parameter which, together with the angle of friction, determines the slope of the $n - s$ surfaces (see Fig. 5.3(b)), taken as some small value, say initially 0.3, and where c_i^0 is a very small interface cohesion value.

5. $k = k + 1$; if $\alpha > \alpha_{min}$ then $\alpha = \alpha$ / 2 else $\alpha = \alpha_{min}$; repeat from step 2.

6. Correct λ_k by subtracting the total energy dissipated by the presence of the small cohesion: $\sum_{i=1}^{c} c_i^0 |\gamma_i|$

Additionally, to reduce the tendency for oscillating about a value without convergence, an additional algorithm parameter β may be introduced so that $n_{k,i}$ in step 4 is replaced with:

$$\beta(n_{k,i}) + (1\text{-}\beta)n_{k-1,i}$$

where β may typically be taken from 0.1 to 0.9 (a smaller value generally leads to more likelihood of convergence, but to more iterations being required). This approach was previously applied to problems involving masonry crushing [25].

The small cohesion value c_i^0 is required to avoid uncontrollable penetration potentially resulting when the normal force at a contact is zero (this could occur since otherwise the two $n - s$ failure surfaces would be simultaneously active, with the normality rule then permitting uncontrollable contraction).

5.6 Numerical examples

A variety of different problems have been run using the proposed procedure. Unless stated otherwise the associative friction problem was specified as the starting problem and the algorithm parameters were set as follows: α=0.3 (α_{min}=10^{-3}); β=0.6; convergence tolerance tol = 10^{-5}; small cohesion c_i^0=$10^{-5} n_{max}$, where n_{max} is the largest normal force in a given problem.

The Mosek (version 2.5) interior-point LP solver which uses a homogeneous and self-dual algorithm (www.mosek.com) was used for the numerical studies. The problem

was passed to the solver in memory using the supplied subroutine library. Problems were run on an Intel Pentium-M 'Centrino' based PC (running at 1.4GHz) with 768Mb of RAM, running under Microsoft Windows XP Professional. The CPU time identified later in this paper is the cumulative time required to solve all the LP sub-problems.

5.6.1 Livesley's classic two block problem

Livesley [9] presented a problem involving two wedge shaped blocks to illustrate when an associative friction model is unrepresentative of Coulomb sliding friction. Each block is of the same size and weight (N_0). The left hand block is subject to vertical load as shown in Fig. 5.8.

Physical intuition indicates that the correct failure mechanism is shown in Fig. 5.9(b) with the free body diagram shown in Fig. 5.8(b). The corresponding value can be evaluated by considering, respectively, horizontal and vertical equilibrium for the loaded block and the right hand block as follows :

$$\left.\begin{aligned} -n_1 \cos 10 \; - s_1 \sin 10 \; + n_2 &= 0 \\ \lambda N_0 - s_2 + n_1 \sin 10 - s_1 \cos 10 &= N_0 \\ n_3 \cos 10 \; - s_3 \sin 10 \; - n_2 &= 0 \\ s_2 + n_3 \sin 10 + s_3 \cos 10 &= N_0 \end{aligned}\right\} \tag{5.11}$$

Also

$$\left.\begin{aligned} s_1 &= n_1 \tan 9 = 0.15838 n_1 \\ s_2 &= n_2 \tan 9 = 0.15838 n_2 \\ s_3 &= n_3 \tan 9 = 0.15838 n_3 \end{aligned}\right\} \tag{5.12}$$

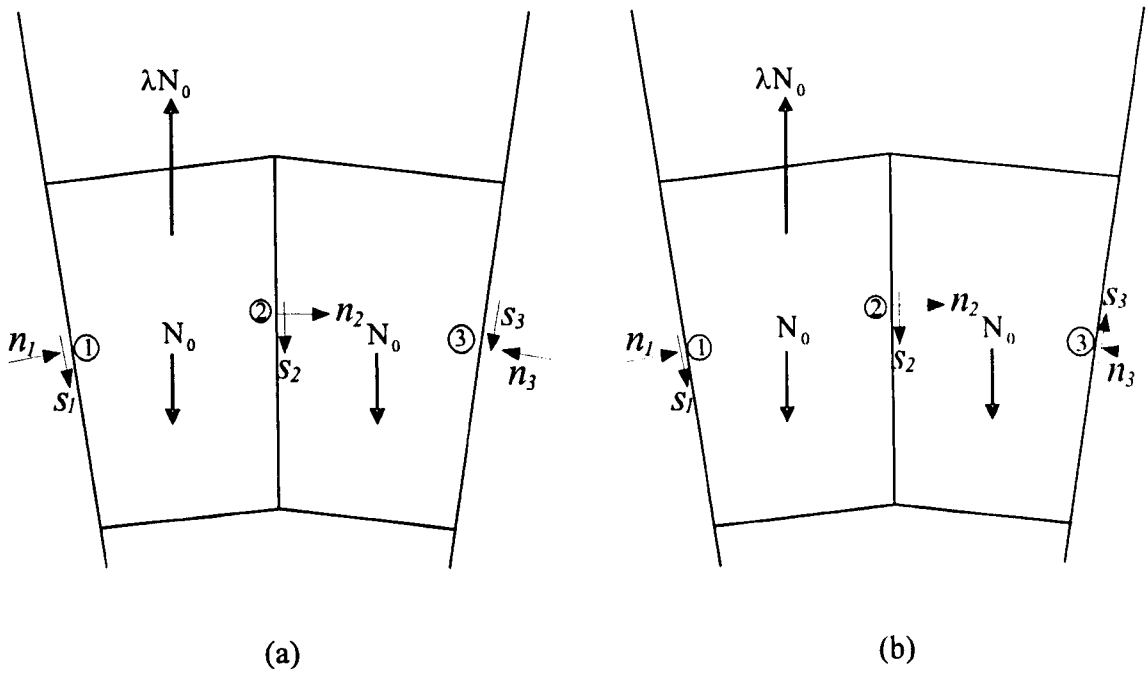

Figure 5.8: Free body diagrams for two-block wedge problem: (a) associative friction; (b) non-associative friction

Substituting 5.12 in 5.11 gives:

$$\left.\begin{aligned} &-1.01230n_1 + n_2 = 0 \\ &\lambda N_0 - 0.15838n_2 + 0.01762n_1 = N_0 \\ &-n_2 + 0.9573n_3 = 0 \\ &0.15838n_2 + 0.32957n_3 = N_0 \end{aligned}\right\} \qquad (5.13)$$

Solving the equations in 5.13 gives:

$\lambda N_0 = 1.28N_0 \Rightarrow \lambda = 1.28$

If associative friction is assumed as in Fig. 5.8(a), s_3 in 5.11 will have an opposite

sign, accordingly 5.13 becomes:

$$\left.\begin{aligned} &-1.01230n_1 + n_2 = 0 \\ &\lambda N_0 - 0.15838n_2 + 0.01762n_1 = N_0 \\ &-n_2 + 1.0123n_3 = 0 \\ &0.15838n_2 + 0.017669n_3 = N_0 \end{aligned}\right\} \tag{5.14}$$

Solving the equations in 5.14 gives:

$\lambda N_0 = 1.8N_0 \Rightarrow \lambda = 1.8$

Figure 5.9(a) shows the associative friction solution, which is clearly implausible if Coulomb friction were present. Furthermore, a relatively high upward force is predicted to be required in order to free the left hand block and the unloaded right hand block also unexpectedly moves upwards.

Figure 5.9(b) indicates the reduced predicted uplift force required and also the more realistic failure mechanism when the new procedure is employed. The solution obtained ($1.28N_0$) is identical to that computed by Fishwick [25] and to what has been computed here.

5.6.2 Arch rib problems

Casapulla and Lauro [20] have identified a special class of non-associative friction problems for which provably unique solutions exist. The class comprises arches with symmetrical loading and geometry. The proposed procedure was applied to arches of this sort to both verify that the numerical and analytical solutions coincide and to investigate the convergence characteristics of the method.

Figure 5.10 shows the relationship between the predicted minimum arch thickness required for stability and the coefficient of friction in the case of a semicircular arch

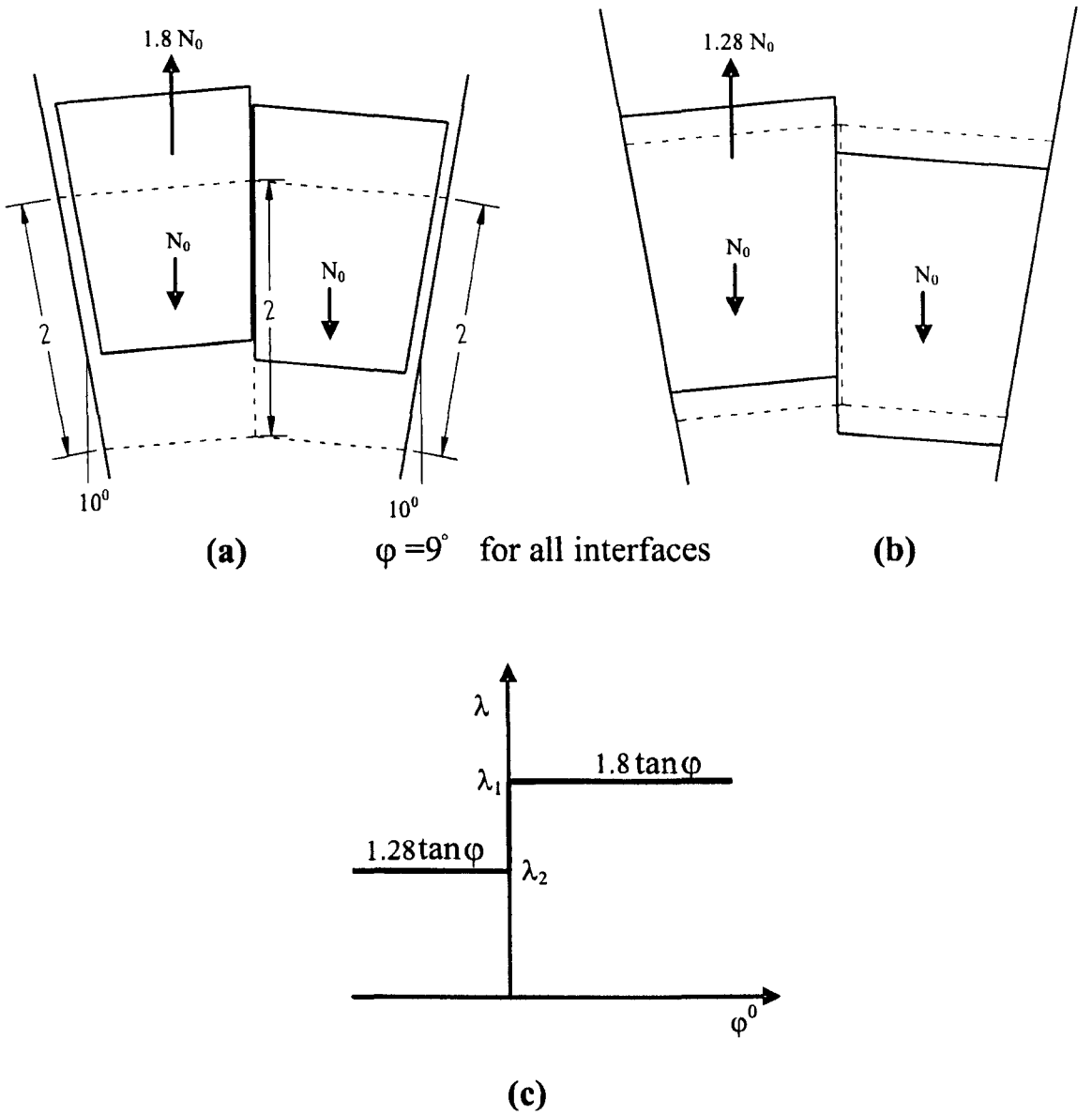

Figure 5.9: Solutions for a two-block wedge problem: (a) associative solution; (b) non-associative (zero dilatancy) solution; (c) relationship between load factor and angle of dilatancy φ^0

of 10m centreline radius, containing 27 discrete blocks. It was found that Heyman's theoretical minimum thickness assuming hinging only of 10.7% of the centreline radius was approximately reproduced with this discretization (10.68%) and that this held providing $\tan\varphi \geq 0.396$. When $\tan\varphi < 0.31$ it was found that the required minimum thickness rose rapidly. These results coincide with those in [20] in terms

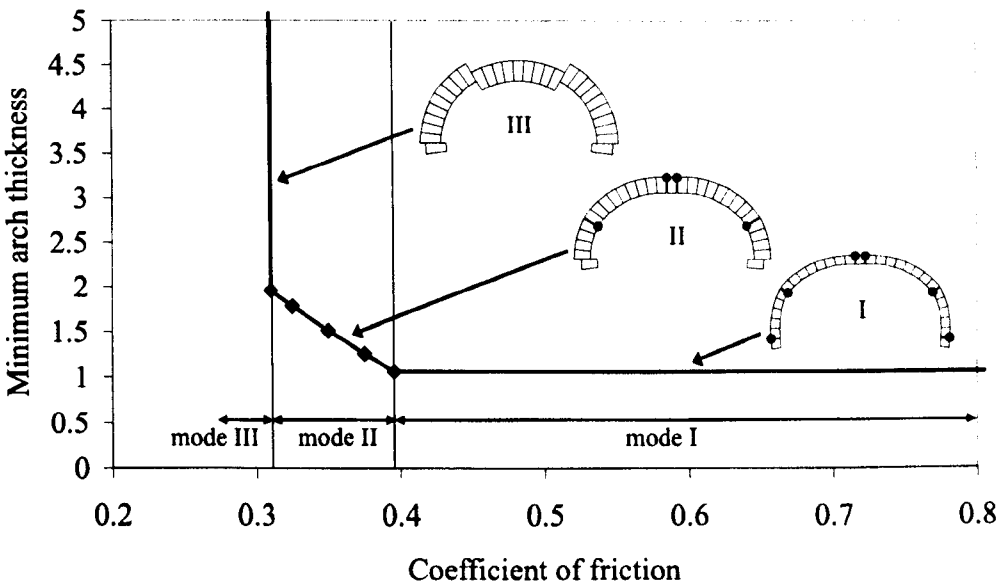

Figure 5.10: Symmetrical arch problem: influence of friction coefficient on minimum arch thickness

of kinematic mechanisms, while there a little discrepancy is about the limiting value of the friction coefficient between the mode I and mode II. There was found to be no difference between the associative and non-associative results in the case of this example.

Considering next arch ribs which are not symmetrically loaded. Those originally tested by Pippard and Ashby [28] were subsequently modelled numerically by Gilbert and Melbourne [29] using an associative friction model. A numerical study of the predicted influence of the coefficient of friction on the computed collapse load of the arch ribs was also performed. This study has now been repeated using the proposed procedure, adopting a non-associative friction model. It was found that provided $\tan\varphi$ was greater than approximately -0.11, then the non-associative and associative friction load factors coincided.

These limited studies appear to suggest that for many single ring arch problems, the flow rule will have no influence on the computed load factor.

5.6.3 Walls subject to in-plane horizontal loading

Ferris and Tin-Loi [23] provided sufficient details of 6 benchmark wall problems to allow these to be re-run using the proposed procedure. Each example problem comprises a freestanding wall supported on a base and subject to in-plane horizontal forces applied to the centroid of each block (to represent earthquake-type loading). Thus each full block had a weight of 1 unit, face area of 4 x 1.75 units, and was subject to a unit horizontal live load (for half blocks these quantities were reduced by half); $\tan\varphi$ was taken as 0.65. Results are shown in Table 5.1 and on Fig. 5.11.

The associative friction solutions obtained in the present study were identical to those obtained in [23] with one exception: a completely different solution was obtained for example 3. This different solution was also obtained independently using different software and it thus seems likely that the results quoted in the table in [23] actually related to a different wall configuration (or coefficient of friction) to that published in the paper. From Table 5.1 it is clear that in all cases the computed load factors are less than or equal to published MCP values and within a few percent of published MPEC values. Additionally all failure mechanisms (Fig. 5.11) were visibly identical to those obtained by Ferris and Tin-Loi. In some cases the computed non-associative friction load factors are more than 20 percent lower than the corresponding associative friction load factors.

The influence of changing the starting conditions and the algorithm parameters α and β on the convergence characteristics was also investigated. Figure 5.12 shows the results from such a study in the case of example problem 6. It was found that for this problem the computed load factor was remarkably insensitive to both the choice of starting condition and to the choice of algorithm parameters. Converged solutions equal or very close to the solution of 0.29649 given in Table 5.1 were always obtained, even when $\alpha = 0$. However, when β was set to 1.0, oscillating about a value during repeated iterations prevented a solution from being obtained (the plot

Table 5.1: Computational results for Ferris and Tin-Loi examples

Example no. [23]	Size	Associative friction λ	Ferris & Tin Loi [23]			Proposed method		Diff: λ proposed vs. assoc. friction	Diff: λ proposed vs. MPEC	Time ratio, proposed: MPEC
			MCP λ	MPEC λ	MPEC time (sec)*	λ	time (sec)			
1	33 × 83	0.64286	0.64285	0.63898	1.2	0.63982	0.7	0.5%	0.1%	0.58
2	55 × 141	0.58000	0.56368	0.55742	2.2	0.56262	0.9	3.1%	0.9%	0.41
3	46 × 102	0.40369	-	-	-	0.35582	1.0	13.5%	-	-
4	55 × 116	0.33195	0.26374	0.26374	1.3	0.26374	0.6	25.9%	0.0%	0.46
5	61 × 120	0.23964	0.21584	0.20863	1.5	0.21455	1.1	11.7%	2.8%	0.73
6	146 × 345	0.34782	0.29725	0.29577	55.1	0.29649	4.3	17.3%	0.2%	0.08

*normalized to a 1400MHz PC (multiplied by 333/1400)

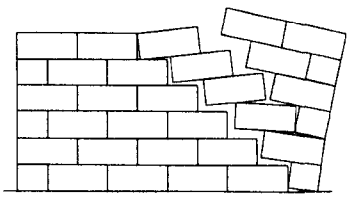

(a) example 1

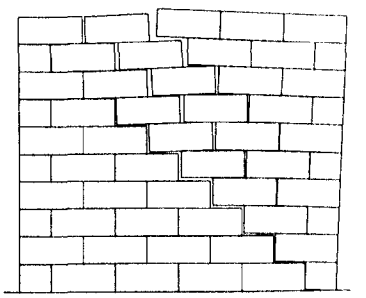

(b) example 2

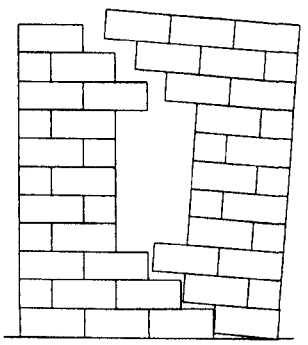

(c) example 3

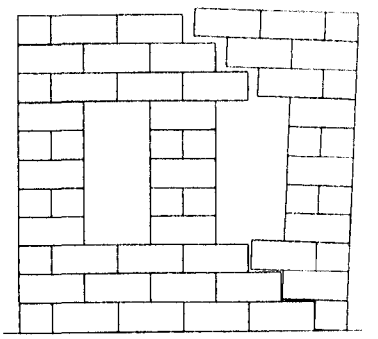

(d) example 4

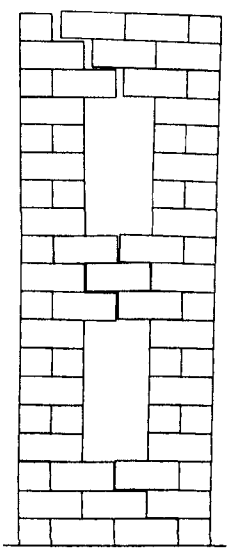

(e) example 5

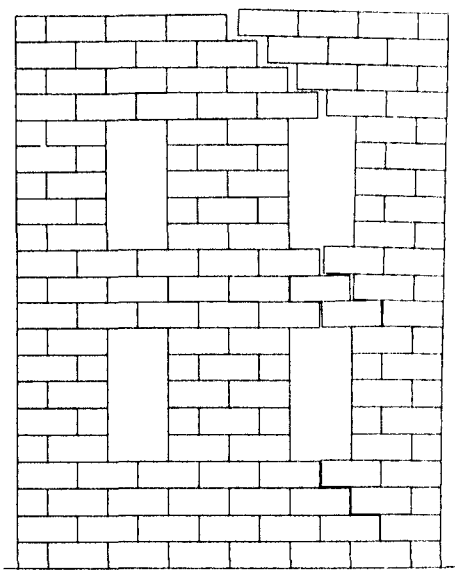

(f) example 6

Figure 5.11: Ferris and Tin Loi example wall problems: failure modes using the proposed procedure.

for this case is omitted from Fig. 5.12 for clarity). When β was set to 0.2 a solution was eventually obtained but many (a total of 85) iterations were required.

For these problems the proportion of the total energy (virtual work) dissipated in Coulomb sliding friction during the analysis was also studied. For example, Fig. 5.13 shows the situation for example problem 6.

Figure 5.13 indicates that in the initial associative friction solution the presence of dilatant friction means that all energy is recorded simply as an increase in potential energy. At subsequent iterations the increase in potential energy reduces, with some sliding friction energy being dissipated at sliding interfaces[†].

When developing the method it was found to be impractical to prescribe that strictly zero violation of the actual Mohr-Coulomb yield surface occurred in the final solution. Instead a somewhat less rigorous, energy based, check was used: the actual and corrected sliding interface energies were computed and compared, with the corrected energy being obtained by multiplying the sliding displacement (taken from the dual problem solution) by the normal force multiplied by the friction coefficient (over all contact interfaces). In all cases tried it was found that the difference between these energies was suitably small (e.g. when expressed as a proportion of the total energy dissipated, always $< 0.1\%$).

It is also apparent from Table 5.1 that for the smaller problems (examples 1 to 5) the CPU times for the proposed method are of the same order as those presented in [23]. In the case of example 6, which is slightly larger, the difference is greater, with the implication that the proposed procedure may be increasingly efficient compared with other methods as the problem size increases. Thus it is of interest to also study a much larger problem recently presented by Orduna and Lourenco [24], solved using the same method as that proposed by [23]. The wall chosen for study was subjected

[†] In the case of examples 3 and 4, the algorithm both converged to rocking only solutions, with zero Coulomb friction energy dissipation. This also explains why in the case of example 4 all solution procedures converged to the same value.

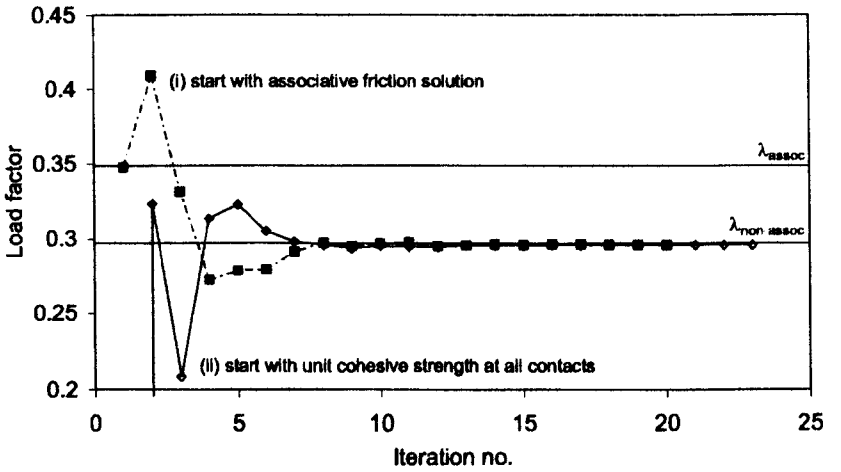

(a)

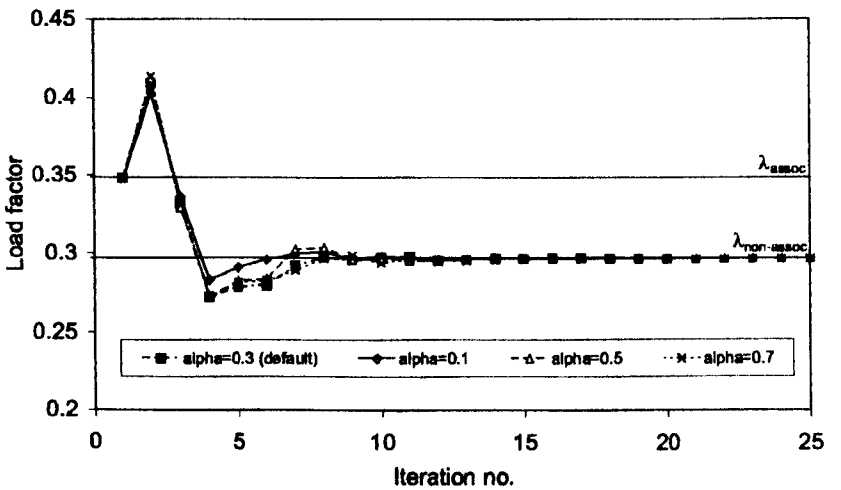

(b)

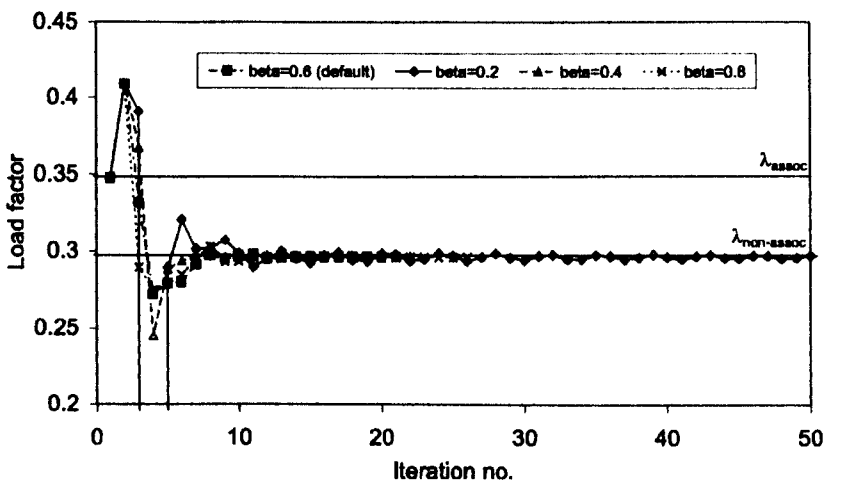

(c)

Figure 5.12: Characteristics for example 6, showing influence of modifying: (a) starting conditions; (b) algorithm parameter α; (c) algorithm parameter β

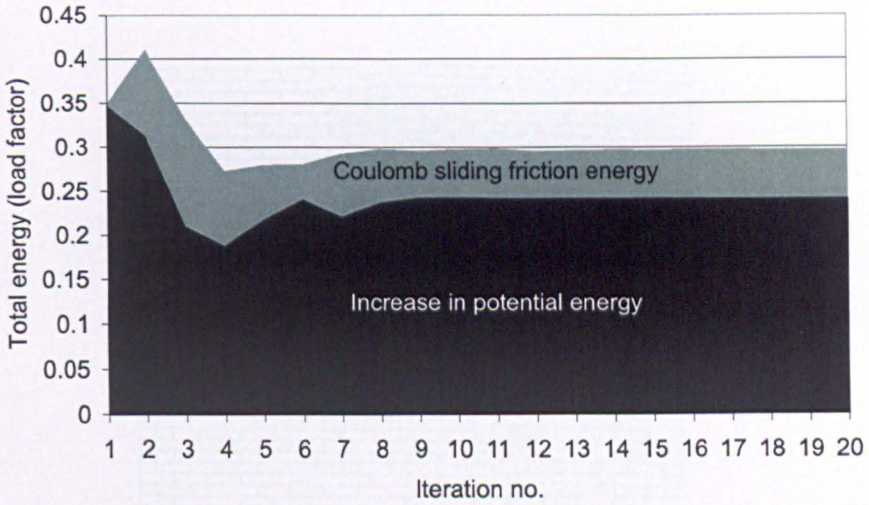

Figure 5.13: Breakdown of total energy vs. iteration no. (example 6 with default parameters)

to the same horizontal live loading as in the previous examples, but the length:height ratio of the constituent blocks was 3:1 and $\tan\varphi$ was taken as 0.75.

Assuming the masonry possesses infinite compressive strength, for this problem Orduna and Lourenco obtained a non-associative solution of 0.539 in 15 hours and 46 minutes when using a 551MHz PC [30]. Using the proposed method for the same problem, a solution of 0.53886 was obtained in 122 seconds on a 1.4GHz PC. i.e. a near identical solution was obtained more than two orders of magnitude more quickly, even taking into account the differences in CPU speed. Figure 5.14 shows the predicted collapse mechanism of the wall using the proposed method (note that the computed associative friction load factor for this problem was 0.545034).

To investigate increasingly large (and potentially increasingly realistic) problems, a pattern of blocks around a representative opening was created and this was then repeated to create a notional facade comprising n_x openings horizontally and n_y openings vertically. The same block aspect ratio, loading conditions and coefficient of friction as adopted in Orduna and Lourenco's example were used. For simplicity the lintels were also assumed to weigh 1 unit, and were also subject to unit hori-

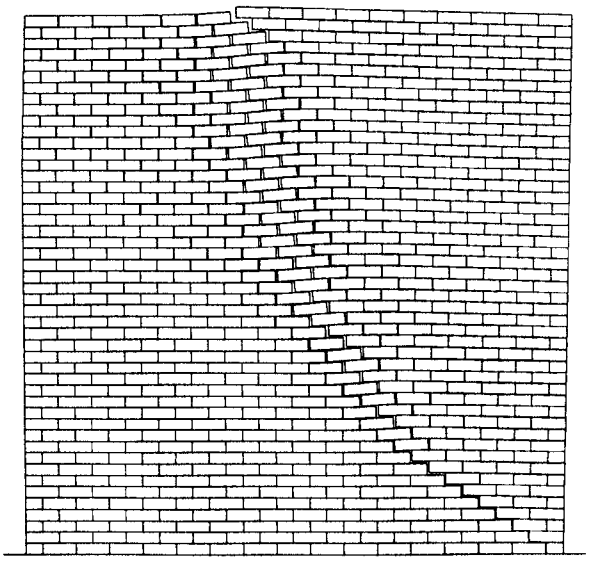

Figure 5.14: Solution to Orduna and Lourenco's wall problem

zontal live load. Also note that the uppermost block on the left-hand side of the facade was always omitted, as this could be locally unstable under dead load alone. Additionally, to ensure a solution was obtained even in the largest problems tried the convergence tolerance was relaxed slightly, to 2×10^{-5} .

Figure 5.15 shows the predicted collapse mechanism for the case when n_x=2 and n_y=6. The non-associative friction analysis was completed in 203 seconds and the computed load factor was 0.20550. In comparison, the computed load factor for the equivalent associative friction problem was 0.21306, obtained in just 5.6 seconds.

Figure 5.16 shows the predicted collapse mechanism for the case when n_x=4 and n_y=12. This may be considered to be a real life scale problem, albeit one modelled only in 2D. The non-associative friction analysis was completed in 694 seconds and the computed load factor was 0.21161. In comparison, the computed load factor for the equivalent associative friction problem was 0.21870, obtained in 55 seconds.

Figure 5.17 shows the CPU times for increasingly large problems of the same aspect ratio (i.e. containing 1×3, 2×6, 3×9 and 4×12 openings).

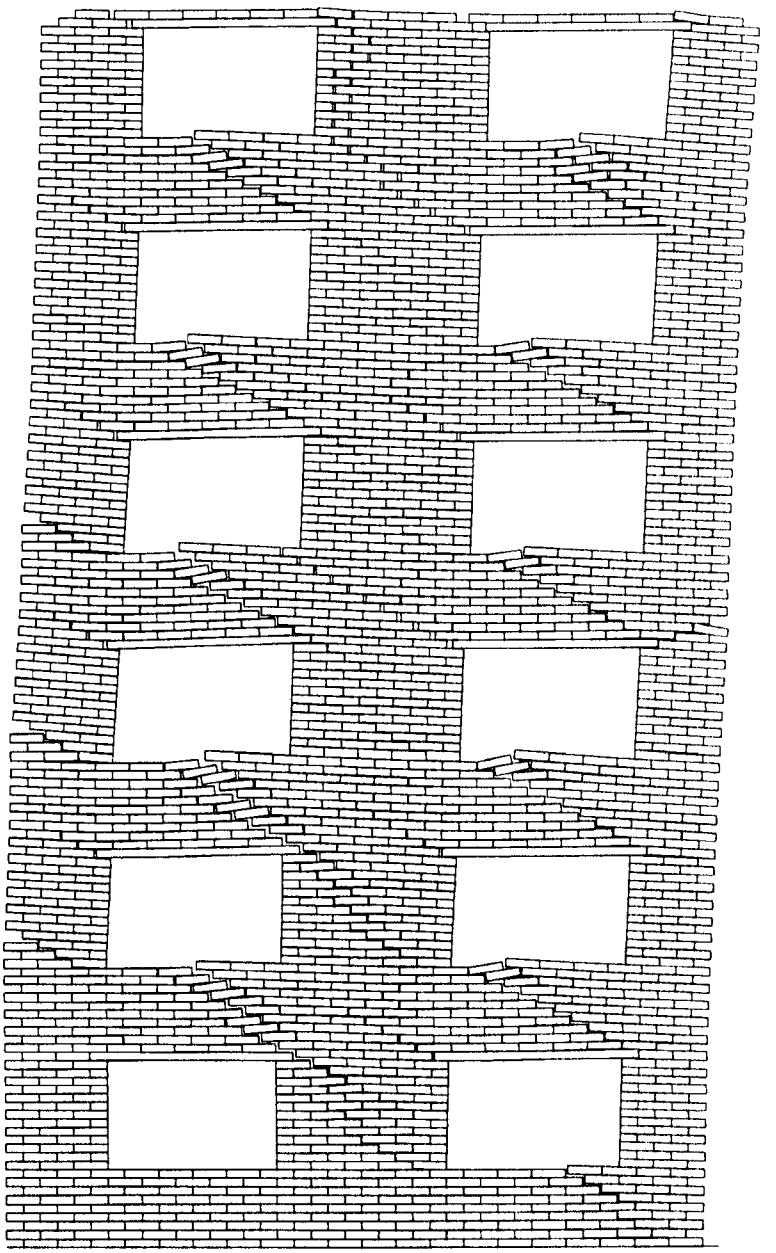

Figure 5.15: Example problem comprising 2 × 6 openings

The indication from Fig. 5.17 is that the proposed method can be applied to reasonably large problems (significantly larger than have hitherto been described in the literature), with the CPU time being between one and two orders of magnitude greater than that required for an associative friction solution (i.e. between 10 and 100 LP iterations required to obtain a solution).

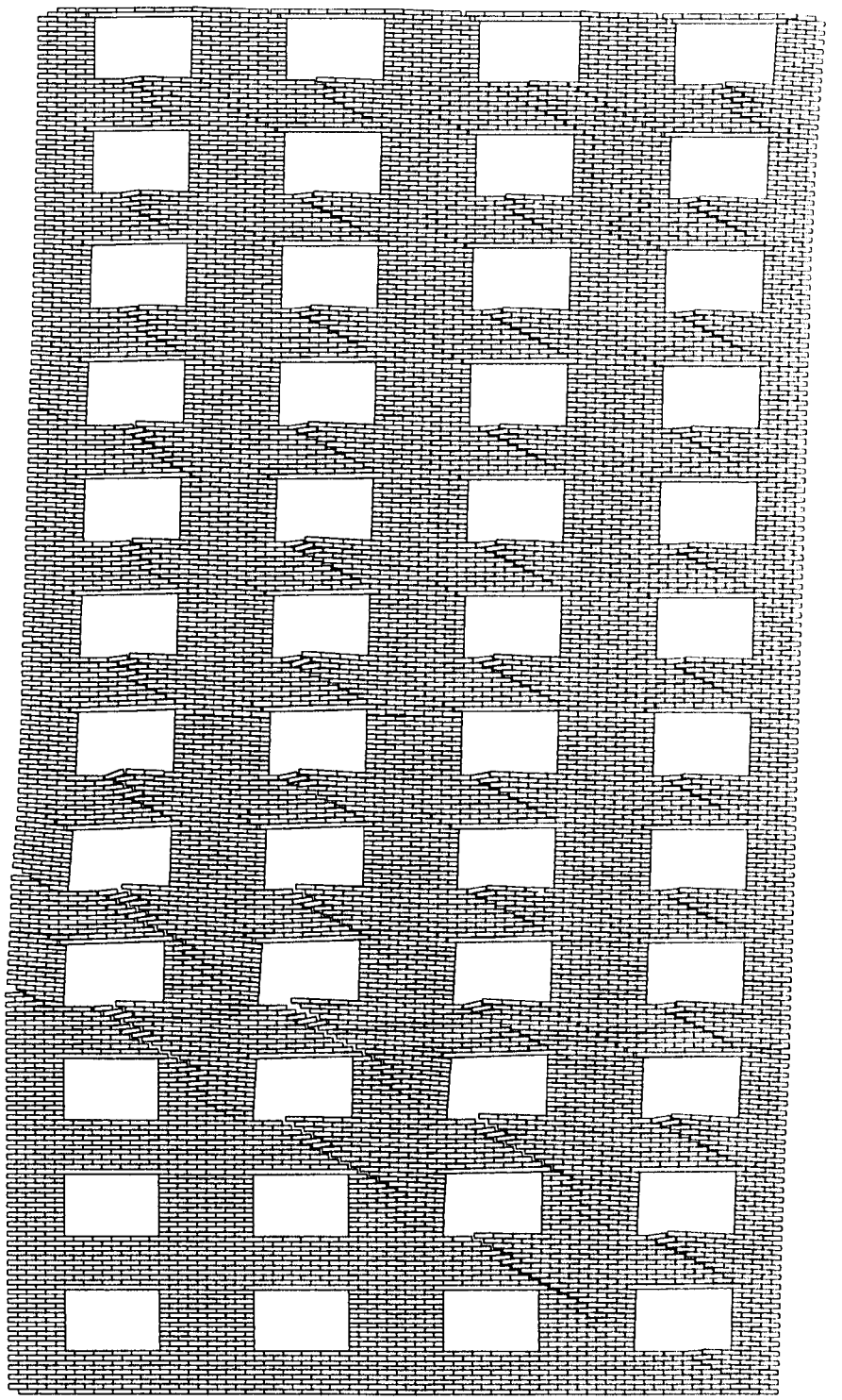

Figure 5.16: Example problem comprising 4 × 12 openings

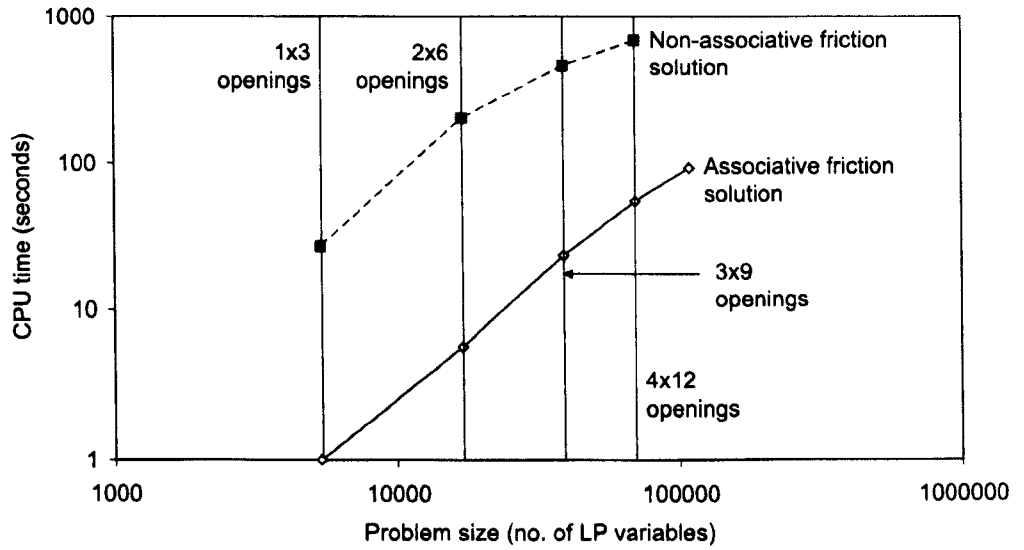

Figure 5.17: Influence of problem size on CPU time

5.7 Discussion

5.7.1 Comparison with other numerical methods

It appears to be generally accepted that the full non-associative friction problem is difficult to solve using direct methods. Thus although Fishwick [25] was able to solve small problems using direct enumeration, other workers have chosen to temporarily relax one or more of the problem constraints, before then iteratively solving a series of simpler sub-problems.

For example Ferris and Tin-Loi [23] temporarily relax the complementarity term† and then solve a series of non-linear programming sub-problems with the complementarity condition gradually imposed. The same technique was used by Orduna and Lourenco[24] , although more recently Orduna [26] has proposed an alternative 'load path following procedure' in which MCP problems with successively increasing limiting compressive stresses are solved. This has been found to sometimes lead to

† The scalar product of yield functions vector and flow multipliers vector.

lower load factors (though sometimes higher too), and also appears to permit some understanding of structural behaviour prior to collapse to be gained.

In that a simpler sub-problem is identified and then solved as part of an iterative process, the proposed method is similar to the methods mentioned above. The main difference is that the sub-problem chosen to be solved here is simply a standard LP problem, which can be solved rapidly using well developed and widely available LP solvers.

5.7.2 Status of solutions

Most workers in this field indicate that their ultimate goal is to obtain the lowest possible failure load factor for non-associative friction masonry block problems. However, practically speaking, it is of course very difficult to obtain a load factor which provably represents the true, global minimum, since the non-associative friction problem becomes essentially a combinatorial one, with considerable computational expense required to identify minimum load factors for real-world problems.

However recent studies by Orduna [26] have indicated that even the locally minimum load factors obtained using recently developed methods may in fact sometimes significantly underestimate the true load factor of a loaded structure. In reaching this finding he also performed parallel non-linear finite element studies to obtain load factors. Thus there may be a paradox: although, except in trivial cases, computed load factors cannot be guaranteed to represent true lower-bounds on the actual load factor, at the same time, there is a danger that they may in fact grossly underestimate the capacity of a real structure which, to use a suitable anthropomorphism, is not necessarily 'clever enough' to identify the worst case load path identified numerically.

Thus, from a practical engineering perspective, the computed globally minimal load

factor may effectively be unreachable (or perhaps only observed once when, say, a billion structures are tested, with most other structures failing at much higher loads). In other words, although having a rigorous lower-bound certainly has some value, the high associated computational effort coupled with the likelihood that the globally minimum solution is unrepresentative, means that the latter is likely to be of academic rather than practical interest.

In optimization terms, the present method involves use of a problem specific heuristic† to identify a 'good' solution to the MCP problem (there being no attempt to tackle the more difficult underlying combinatorial problem). The heuristic, which involves prescribing a negative angle of friction and thereby contraction at all failing interfaces at the early stages of an iterative procedure appears to work remarkably effectively and seems to permit much larger problems to be solved than has hitherto been the case.

5.7.3 Starting conditions and convergence characteristics

As indicated on Fig. 5.12, the procedure appears relatively insensitive to the starting conditions used. However, one advantage of specifying joints as purely cohesive rather than frictional in the starting problem is that it overcomes the problem of an initial solution potentially not being obtainable because of volumetric locking due to (erroneous) dilatancy at interfaces.

Several problems which are larger than those documented in this paper have also been tested. However, it has been found for very large problems that convergence is often difficult to achieve, with cycling occurring. This seems to be most common when there are several alternative load paths which correspond to solutions with very similar load factors. This issue requires further study.

† Heuristic relates to exploratory problem-solving methods that utilize self-educating techniques to improve performance. It has come to emphasize techniques for searching a space of possibilities quickly–not necessarily finding the optimum possibility but finding one that is "good enough".

5.7.4 Modifications to the basic method

The efficacy of a variety of modifications to the basic procedure has been investigated with a view to reducing the number of iterations required in order to obtain a solution. Thus the effectiveness of introducing move limits was investigated initially, with limits set on the percentage and/or absolute change in the magnitude of the normal contact force permitted. However, this was found not to work well: the required computational effort was not reduced and also the risk of converging to an artificially high load factor appeared to be increased.

Additionally the effectiveness of only modifying the failure surface for a contact interface with forces lying on the failure surface was investigated (rather than automatically modifying the failure surface for all contacts, which is the default). In fact it was found that this modification made very little difference to the convergence characteristics of the procedure.

5.7.5 Including dilatancy as a function of normal stress

Attention has so far focussed on removing unwanted dilatancy, so as to model classical Coulomb sliding friction. However it has been observed in practice that some dilatancy does occur (e.g. [31]), and that this is particularly pronounced when normal stresses are low. Using the proposed numerical procedure it is in principle perfectly possible to take account of this, and, as well as being arguably more realistic, it may even be advantageous computationally to do so. This feature will therefore be implemented in the future.

5.8 Conclusions

A new computational limit analysis procedure for rigid block assemblages comprising non-associative frictional interfaces has been presented. The procedure involves solving a series of LP problems with successively modified failure surfaces (rather than working directly with the full Mixed Complementarity Problem (MCP) as others have done). In the procedure the behaviour of a contact is governed by a Mohr-Coulomb failure surface with an effective cohesion intercept and, in early iterations, a negative angle of friction. Both these parameters are updated at each iteration by referring to the real problem, with the angle of friction also normally being successively relaxed towards zero (thereby implying zero dilatancy).

The proposed method appears to be capable of identifying reasonable estimates of the load factor for a wide range of problems. In all the cases tried, the computed load factors were less than or equal to published MCP values and within a few percent of published MPEC values. The method appears to be particularly suited to comparatively large problems. For one such problem contained in the literature, it was found that the load factor computed using the proposed procedure was virtually identical to that computed previously but was obtained two orders of magnitude more quickly.

References

[1] Kooharian, A. Limit analysis of voussoir (segmental) and concrete arches. *Journal of American Concrete Institute*, 24(4):317–328, 1952.

[2] Heyman, J. The stone skeleton. *International Journal of Solids and Structures*,, 2:249–279, 1966.

[3] Drucker, D. C. Coulomb friction, plasticity, and limit loads. *Journ. Appl. Mech. Trans. ASME*, 21(4):71–74, 1954.

[4] Michalowski, R. and Mroz, Z. Associated and non-associated sliding rules in contact friction problems. *Arch. of Mech.*, 30(3):259–276, 1978.

[5] Sacchi Landriani, G. and Save, M. A note on the limit loads of non-standard materials. *Meccanica*, 3:43–45, 1968.

[6] Palmer, A. C. A limit theorem for materials with non-associated flow laws. *Journ. Mcanique*, 5,:217–222, 1966.

[7] De Josselin de Jong G. Lower bound collapse theorem and lack of normality of strain rate to yield surface for soils. *Proc. I.U.T.A.M. symp., Grenoble*, Rheology and soil mech., 69–78, 1964.

[8] Livesley, R. K. A. Limit analysis of structures formed from rigid blocks. *International Journal for Numerical Methods in Engineering*, 12:1853–1871, 1978.

[9] Livesley, R. K. A. A computational model for the limit analysis of three-dimensional masonary structures. *Meccanica*, 27(1):61–72, 1992.

[10] Charnes, A. and Greenberg, H. J. Plastic collapse and linear programming. *Bulletin American Mathematical Society*, 57:480–490, 1951.

[11] Gilbert, M. and Melbourne, C. Collapse behaviour of multiring brickwork arch bridges. *The Structural Engineer*, 73:39–47, 1995.

[12] Lo Bianco, M. and Mazzarella, C. Limit load of masonry structures. *Final Report of the IABSE Symp., Venice*, 187–194, 1983.

[13] Baggio, C., Masiani, R. and Trovalusci, P. Modelli discreti per lo studio della muratura a blocchi. *Proceeding of the 5th National Conference on LIngegneria Sismica in Italia, Palermo*, volume II, 1205–1218, 1991.

[14] Baggio, C. and Trovalusci, P. Collapse behaviour of three-dimensional brick-block systems using non-linear programming. *Struct. Eng. (&) Mech*, 10(2):2000, 181-195.

[15] Boothby, T. E. and Brown, C. B. Stability of masonry piers and arches. *Journal of Engineering Mechanics, ASCE*, 83:118–367, 1992.

[16] Begg, D. W. and Fishwick, R. J. Numerical analysis of rigid block structures including sliding. *Comp. Meth. Struct. Masonry*, 3:177–183, 1995.

[17] Casapulla, C., De Riggi, T., and Jossa, P. Il ruolo dellattrito nella resistenza di pareti murarie. *Ing. Sism*, 3:32–40, 1996.

[18] Casapulla, C. and Jossa, P. A safety method in static analysis of block masonry. *Proceedings of the III International Seminar on Structural Analysis of Historical Constructions, Guimaraes, Portugal*, 2001.

[19] Casapulla, C. Dry rigid block masonry: unique solutions in presence of Coulomb friction. *Proceedings of the 7th International Conference on Structural Studies,*

Repairs and Maintenance of Historical Buildings (STREMAH), Bologna, 251–261, 2001.

[20] Casapulla, C. and Lauro, F. A simple computation tool for the limit-state analysis of masonry arches. *Proceedings of the 5th International Congress on Restoration of Architectural Heritage, Firenze*, 2000.

[21] Casapulla, C. and Ayala, D. Lower bound approach to the limit analysis of 3D vaulted block masonry structures. *Proceedings of the 5th International Symposium on Computer Methods in Structural Masonry (STRUMAS V), Rome*, 28–36, 2001.

[22] Casapulla,C. Resistenze attritive in una parete muraria soggetta ad azioni normali al suo piano medio. *Proceedings of the 9th National Conference on Ingegneria Sismica in Italia, Torino*, 1999.

[23] Ferris, M. C. and Tin-Loi, F. Limit analysis of frictional block assemblies as a mathematical program with complementarity constraints. *International Journal of Mechanical Sciences*, 43(1):209–224, 2001.

[24] Orduna, A. and Lourenco, P. B. Cap model for limit analysis and strengthening of masonry structures. *J. Struct. Eng., ASCE*, 129(10):1367–1375, 2003.

[25] Fishwick, R. J. *Limit analysis of rigid block structures.* PhD Thesis, University of Portsmouth, Department of Civil Engineering, 1996.

[26] Orduna, A. *Seismic assessment of ancient masonry structures by rigid blocks limit analysis.* PhD Thesis, Universidade do Minho, Escola de Engenharia, Portugal, 2003.

[27] Gilbert, M. On the analysis of multi-ring brickwork arch bridges. *Proceedings of the 2nd International Arch Bridges Conference, Venice*, 109–118, 1998.

[28] Pippard, A. J. S. and Ashby, R. J. An experimental study of the voussoir arch. *Proceedings of The Institution of Civil Engineers*, 10:383–404, 1939.

[29] Gilbert, M. and Melbourne, C. Rigid-block analysis of masonry structures. *The Structural Engineer*, 72:356–360, 1994.

[30] Orduna, A. Personal communication, 2004.

[31] Rots, J. *Structural Masonry-An Experimental/Numerical Basis for Practical Design Rules.* Balkema, Rotterdam, 1997.

Chapter 6

Practical Application of Computational Limit Analysis: Masonry Arch Bridges

6.1 Abstract

Although the rigid block analysis formulation for masonry arches was first put forward by Livesley [1] more than two decades ago, few researchers or practitioners have had access to software based on the rigid block analysis formulation despite the apparent advantages of the method.

Since 2001 the RING [2] limit analysis software for masonry arch bridges has been publicly available via an internet site. The author has been responsible for re-writing the kernel.

This paper describes recent developments to the software which is currently being completely revised again, including: order of magnitude improvements in its computational efficiency; a non-associative constitutive model for sliding friction and a

gross displacement analysis facility. A number of example local authority bridges are re-assessed in the light of the new features. The recent increase in the execution speed of the program enables the use of a larger number of blocks per ring than previously. This means more possibilities for collapse mechanisms and hence potentially lower load factors.

Keywords: Limit analysis; Masonry arch bridges; Rigid block; Linear programming

6.2 Background

Despite the fact that the widespread building of masonry arches ceased around hundred years ago in the UK, masonry arch bridges still represent a crucial part of the transport system.

During the 18^{th} and 19^{th} centuries, engineers were required to provide bridges for firstly the canal network and later the rail network. These bridges represent a large proportion of the bridges in use today. Due to the extensive programme of building bridges for the rail network over a short period of time, there existed an acute shortage of skilled stonemasons in the construction industry. This led to an increase in the popularity of brickwork in the fabrication of bridges.

Today there are more than 40,000 masonry arch bridge spans in the UK alone, which represent approximately 40 percent of the UK's bridge stock. The majority of these bridges were built during the 19^{th} century. The current levels of loading are beyond those envisaged by their designers. In some cases a small increase in loading on a given bridge leads to rapid deterioration in condition, and so a high level of maintenance is needed.

It was estimated in 1986 that the cost of replacing all of the masonry arches carrying Britain's roads with modern equivalents would be approximately £7 billion [3].

Almost two decades latter, the cost will have significantly increased. Taking this into consideration, an improved and rational assessment procedure to extend the useful life of these structures is of paramount importance.

Historically, the analysis and design of masonry arch bridges has been conducted according to empirical rules. Generally, not much attention was paid to material properties; instead rules were based on observation of traditional bridges which had proved to be safe through the years. Although this approach may be effective in designing new bridges, it is not of great use for assessing existing ones.

The established method of assessment as recommended by the UK Highways Agency is the modified Military Engineering Experimental Establishment (MEXE) method [4]. The method evolved from an early elastic method proposed by Pippard [5]. The maximum load which can be supported is calculated based on the geometry of the arch. Modification factors are then applied to account for the fill depth, the type of material used, the condition of the arch and other characteristics.

Although the method is easy to use, it cannot be relied upon. It has been noted that in many cases the method underestimates the bearing capacity of bridges [3]. Conversely, the method can sometimes lead to unsafe assessments of bridges capacity. Research carried out at Bolton Institute by Gilbert and Melbourne [6, 7], commissioned by British Rail, concluded that the MEXE method greatly overestimated the load bearing capacity of bridges with the defect of ring separation.

In recent years, very active research aimed at developing and applying advanced computational models to masonry gravity structures has been conducted. One particularly important practical application has been the determination of the ultimate carrying capacity of masonry arch bridges. Here the objective of most limit analysis procedures is to determine the magnitude of the load which just transforms the structure into a mechanism.

The mechanism analysis procedure utilizes the concept of plastic hinges. The basic method assumes that a masonry arch ultimately fails by forming at least four hinges. Assuming that the masonry possesses infinite compressive strength and with the applied load being increased, the thrust line (i.e. the line through the resultants of the compressive stresses in successive cross sections) approaches the edges of the cross-section. Eventually, this line alternately touches the extrados and the intrados. Since at the hinge points bending moments are zero, it is then possible to use statics to determine the magnitude of the applied load which will cause the arch to collapse.

This was demonstrated by Pippard [5] and the approach was later placed securely within the framework of plastic limit analysis by Heyman [8]. Thus, a 'mechanism' (or 'upper- bound') limit analysis involves an assumed hinge configuration with the lowest upper-bound solution being the correct one since in this case the thrust line between hinges will lie entirely within the arch. Thus, in this case, the 'safe' (or 'lower-bound') theorem is also satisfied (the latter states that if a thrust line can be found for the complete arch which is in equilibrium with the external self weight and which lies every where within the masonry of the arch ring, then the arch is 'safe').

However, because of the complexity of arch bridge geometry coupled with the complex loading patterns typically found in practice, hand-based limit analysis is not generally practicable. Additionally, some of Heyman's original assumptions are no longer considered generally acceptable (e.g. infinite masonry crushing strength; no sliding failures). Hence various computer-based methods have been proposed [1, 6, 9, 10]. These methods use either rigorous or 'ad-hoc' optimization techniques to identify the critical failure mode. Among these methods, the rigid block method of analysis [1, 6] is the most generally applicable and may, for example, easily be applied to arch problems involving multiple arch rings and/or spans.

Currently the only widely available software based on the rigid block computational

limit analysis method is the RING software which was originated by Gilbert [11, 12]. It was created originally as a research tool. The first publicly available version of RING was released in January 2001 (version 1.1). The software has proved remarkably popular and now is widely used by practitioners worldwide to analyse masonry arch bridges.

However, parts of RING version 1.1 dated back more than a decade and it became difficult to enhance and extend the existing software without expending effort disproportionate to the benefit gained. Hence, the decision was taken to rewrite the software from scratch. This has also stimulated a review of all parts of the existing software. Thus there were two main issues which were identified as priorities for the current and forthcoming releases of RING:

1. Improved speed of execution (particularly for multi-ring arch problems). This has already been achieved in RING 1.5.

2. Enhanced realism of the computational model (e.g. better modelling of friction, soil-structure interaction etc). This will be incorporated in RING 2.0.

After briefly describing the key elements of the rigid block analysis formulation, some of the practical requirements that a bridge analysis program has to fulfil in order to be useful to practitioners and the position of the current version of RING (version 1.5) with respect to these requirements are discussed. Problems associated with fulfilling these practical requirements are also identified.

6.3 The rigid block analysis method

6.3.1 Basic method

The problem in hand concerns an assemblage of rigid blocks comprising c contacts separating b blocks. The constituent blocks may initially be assumed to be both rigid and infinitely strong. The block interfaces are considered as elements and the blocks as extended nodes connecting the elements. Here three degrees of freedom are associated with the centroid of each block and three stress resultants (i.e. bending moment m, normal force n and shear force s) act at each contact interface, as shown in Fig. 6.1 for a typical block j.

The objective here is to find the maximum load factor, which when applied to live loading, will lead to collapse. Thus, the problem formulation may be concisely stated as follows:

$$\text{Maximize} \quad \lambda$$

subject to:

$$\mathbf{f} = \mathbf{B}\mathbf{q} \tag{6.1}$$

$$\left.\begin{aligned} m_i &\le 0.5 n_i l_i \\ m_i &\ge -0.5 n_i l_i \\ s_i &\le \mu_i n_i \\ s_i &\ge -\mu_i n_i \end{aligned}\right\} \text{for each contact, } i = 1,...,c \tag{6.2}$$

where λ is the load factor, $\mathbf{B}$ is a suitable $(3b \times 3c)$ equilibrium matrix derived from the geometry of the structure and $\mathbf{q}$ and $\mathbf{f}$ are respectively vectors of contact forces and block loads. Thus $\mathbf{q}^{\mathrm{T}} = [n_1, s_1, m_1, n_2, s_2, m_2, ..., n_c, s_c, m_c]$; $\mathbf{f} = \mathbf{f}_D + \lambda \mathbf{f}_L$ where

$\mathbf{f}_D$ and $\mathbf{f}_L$ are respectively vectors of dead and live loads. Using this formulation the linear programming problem dependant variables are clearly the contact forces: n_i, s_i, m_i (where $n_i \geq 0$; s_i, m_i are free variables).

It should be noted that implicit in the above formulation is an associative, or 'saw-tooth' type friction model (i.e. stipulating that dilatancy accompanies sliding). This issue will be returned to in section 6.5.2. Additionally, in order for masonry crushing to be accommodated, an iterative analysis in which the effective contact length is modified at successive iterations is required (as discussed in [12]).

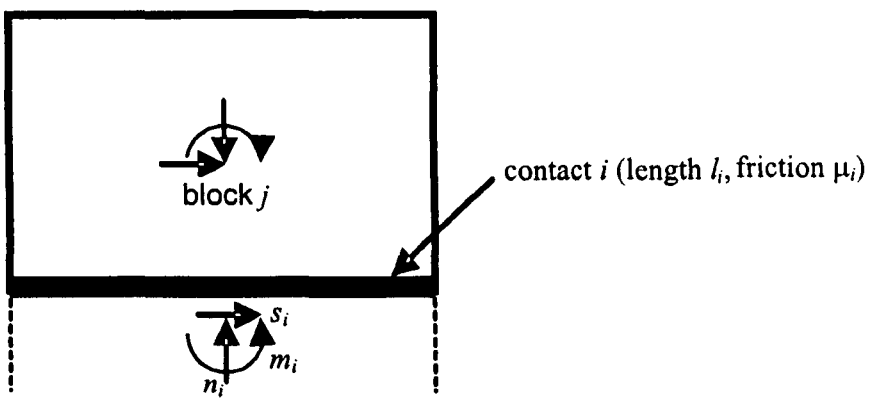

Figure 6.1: Block j and contact forces for interface i

6.4 Practical issues:

6.4.1 Execution speed

RING 1.1 used a redundant forces limit analysis problem formulation [13]. This produces a very compact but potentially very densely populated linear programming (LP) constraint matrix. Although most simple single and multi-span problems could be solved almost instantaneously, as far as the user was concerned, on a modern PC, it was noticed that execution times for more demanding multi-ring problems were often undesirably long, even when a state-of-the-art PC was employed.

The problem partly stemmed from the fact that the original formulation developed by Gilbert *et al.* [6, 7] was intended to be used in conjunction with the Simplex LP algorithms [14] dominant in the early 1990s, yet RING 1.1 was necessarily distributed with a freely available interior-point LP solver, more suited to solving large, sparse, problems.

In recent investigations by the author [15] it has been found that although the conventional joint equilibrium formulation [13] presented in section 6.3.1 produces a large number of constraints and variables, the proportion of non-zero elements is generally extremely small, which means that it can be solved very efficiently using modern interior-point based LP algorithms.

The significant improvements in computational efficiency attributable to the use of a joint equilibrium formulation when used in conjunction with an interior point LP solver has meant that this has now been implemented in a new RING release, version 1.5.

In order to demonstrate the comparative computational efficiency of RING 1.5, the 3m and 5m span single-span arch ribs and bridges, previously tested by Melbourne and Gilbert [16], were modelled numerically. The bridges of interest here contained detached spandrel walls and the defect of ring separation, this being achieved in the laboratory by using dampened sand in place of mortar between the rings.

Table 6.1 shows sample RING analysis results for these bridges. To obtain the RING results, a standard coefficient of lateral earth pressure was specified (rather than the back-substituted experimentally recorded pressures, as used in the original publications [16]). A lateral earth pressure coefficient value of 4.5 was used (approximately equal to $K_p/3$ when K_p is calculated using classical vertical wall passive pressure theory with the measured backfill internal angle of friction of 60 °). Additionally, a Boussinesq type model was used to simulate dispersion of the applied load through the fill.

Table 6.1 contains the run times obtained using a 1.4GHz Pentium 'M' (Centrino) PC. In all cases the PCx [17] interior point linear programming solver distributed with RING was used, rather than a commercial solver as used in the original publications. In general, commercial solvers are more efficient, particularly in the case of redundant forces formulation problems.

Bolton arch rib/ bridge ref.	Expt. Failure load (kN)	RING 1.1 (redundant forces formulation)		RING 1.5 (joint equilibrium formulation)		Difference: RING 1.5 vs. 1.1	
		Failure load (kN)	CPU time (s)	Failure load (kN)	CPU time (s)	Failure load increase	CPU speedup factor
Arch 2	1.5	1.44	6.1	1.45	0.16	0.7%	38×
Bridge 3-2	360	252	7.9	253	0.25	0.3%	31×
Bridge 5-2	500	482	236	486	0.98	0.8%	241×

Table 6.1: Multi-ring arches: experimental and infinite crushing strength analysis results with redundant forces and joint equilibrium formulations

From Table 6.1 it is evident that when using PCx, the speedups associated with the use of a joint equilibrium formulation are very significant, more than 200 × in the case of Bridge 5-2. It is also notable that the computed failure loads are slightly greater when using the joint equilibrium formulation. This is because whereas previously a joint between adjacent rings was idealized using a series of point contacts, in the joint equilibrium formulation all contacts in the problem are treated identically, whether these lie in radial or circumferential joints (i.e. these are all treated as surfaces). In all cases the computed capacities are lower than the experimentally recorded values. This is likely to (at least partly) result from the simplified soil model employed. Apart from the case of bridge 3-2, experimentally recorded collapse loads were a few percent higher than RING predictions. According to Gilbert [16] there are no clear reasons why the experimentally recorded collapse load in the case of bridge 3-2 is very high, given that a nominally identical bridge tested with attached, rather than detached, spandrel walls failed at a much lower load (320kN).

For problems involving finite masonry crushing strengths, the reduced solution times have also meant that in RING 1.5 finite masonry crushing strength calculations can now be performed for all load cases in multiple load case problems in a reasonable time. Previously a crushing analysis was just performed for the load case found to be critical following initial, infinite crushing strength, analyses for all load cases. This sometimes led to a non-conservative load factor being computed. Fig. 6.2 shows an example recently encountered in practice.

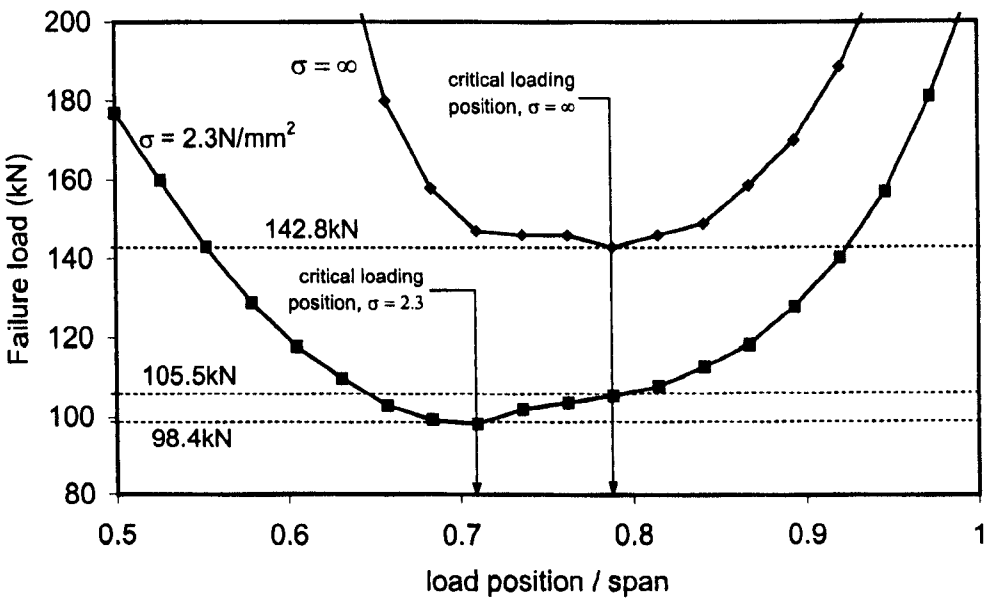

Figure 6.2: Computed axle load at collapse vs. position

Examining Fig. 6.2 reveals that here the critical load positions for the $\sigma = \infty$ and $\sigma = 2.3\text{N/mm}^2$ cases do not coincide. Taking the critical load position for the $\sigma = \infty$ case and performing crushing calculations only for this load case leads to a predicted capacity of 105.5kN, overestimating the actual carrying capacity of 98.4kN by 8.5 percent.

6.5 Realism of computational model

In terms of complexity, computational limit analysis models are positioned midway between traditional (hand-based) methods and (non-linear) elastic analysis tools. Computational limit analysis has the advantage of simplicity, as relatively modest operator expertise is required, and certain classes of problems regarded as 'difficult' (e.g. uniaxial contact problems) can be solved very simply and quickly using LP solvers, which are widely available and improving in efficiency year-on-year.

However, computational limit analysis models are not always linear. For example, when finite material strength is involved, the problem formulation becomes non-linear and hence, if LP solvers are still to be used, an iterative analysis procedure must be used. Additionally, whilst RING versions 1.1 & 1.5 are capable of modelling sliding failures, it is inherently assumed that associative (or 'saw tooth') friction exists between the constituent blocks. This is not entirely realistic. If the problem is re-formulated to obey the non-associative rule it becomes non-linear. Again, an iterative analysis procedure is required.

In the next section, material crushing analysis, non-associative friction analysis and gross displacement analysis are discussed. The very important but rather neglected issue of soil-structure interaction is also briefly considered.

6.5.1 Material crushing analysis

Real materials have finite compressive strength. The effect of material crushing on the load carrying capacity for masonry arches can be studied by performing an iterative analysis. Gilbert [12] proposed an iterative procedure to determine the influence of crushing. The procedure starts by performing an initial analysis without material crushing being considered to provide an estimate of the force in the arch at

failure. The magnitude of the force of a given section is then used, in conjunction with the crushing strength and the width of arch, to determine the required depth of material to transmit the force. A number of iterations are generally required before a converged solution is obtained.

6.5.2 Modelling sliding failures

Drucker [18] pointed out that assuming associative (or 'saw tooth') friction between smooth blocks will, in general, lead to upper-bound (unsafe) load factors. Despite this, it was previously found by Gilbert [16] that when modelling multi-ring brickwork arch bridges, reasonably good agreement between experimental and numerical results could be obtained when associative friction was assumed (in fact it was found that the numerical multi-ring model always under-estimated the experimentally observed carrying capacity).

Since then, a number of workers have proposed algorithms to model non-associative friction (e.g. refer to reference [19] for details). Unfortunately the non-associative problem becomes essentially a combinatorial one, with considerable computational expense required to identify minimum load factors for real-world problems. Furthermore, except in trivial cases, these load factors cannot be guaranteed to represent true lower-bounds on the actual load factor yet, at the same time, may in fact grossly underestimate the capacity of a real structure.

In spite of these difficulties, the author, jointly with other researchers, have recently developed a conceptually simple and comparatively computationally inexpensive procedure for treating non-associative friction problems [20, 21], with a view to offering this as an option in RING 2.0. What follows is a brief description of the method and its application to multi-ring arch problems.

6.5.3 A simple procedure for non-associative friction

In the proposed procedure, rather than make use of highly complex and specialized mathematical programming algorithms as others have done, only a standard LP solver is required. Central to the thinking behind the method is the fact that, when using linear programming to solve limit analysis problems, flow will always occur normal to the specified failure surface (i.e. according to the so-called 'normality rule'). The proposed procedure starts with an initial associative friction analysis. Then, to avoid unwanted dilatancy, a subsequent analysis is performed using a new failure surface, formed by rotating the original failure surface about point $(n, \mu n)$ until it is orientated horizontally (where n is the normal force from the previous iteration; refer to Fig. 6.3). The procedure continues, using successively modified failure surfaces, until a converged solution is obtained. Details of a number of minor modifications to this basic procedure in order to improve convergence are provided elsewhere [20].

6.5.3.1 Non-associative friction examples

The benchmark in-plane block wall problems used by Ferris and Tin-Loi [19] were initially investigated using the procedure [20]. For these problems it was found that when using a non-associative (and zero dilatancy) friction model, predicted load factors were up to approximately 25 percent lower than their associative friction counterparts. Whilst the load factors obtained using the proposed method were never as low as the published MPEC results [19], they were always within 2 or 3 percent of these.

The proposed method is here applied to multi-ring arch problems for the first time. Thus the arches considered in section 6.4.1 are now re-analysed assuming non-associative friction (and zero dilatancy). Table 6.2 presents the main results whilst

obvious visible differences in the failure modes are highlighted in the case of bridge 5-2 on Fig. 6.4.

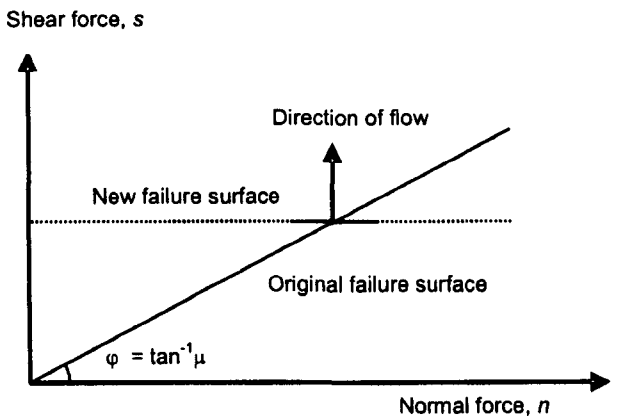

Figure 6.3: Non-associative (zero dilatancy) sliding friction: original and modified failure surfaces

For the cases detailed in Table 6.2 it is evident that modest reductions in the computed collapse load result from the use of the non-associative friction model (up to 6%). It is also evident that considerable extra computational effort is required in order to obtain the results (up to 25× more CPU time required).

6.5.4 Gross displacement analysis

Field and laboratory tests carried out over the last two decades in the UK have shown that the presence of the backfill pressures significantly enhance the ultimate bridge strength. Mechanism analysis programs generally assume that backfill pressures are mobilized by infinitesimal structural displacements although in practice, peak horizontal backfill pressures can only be mobilized by relatively large displacements. The assumption of infinitesimal displacements will therefore lead to non-conservative

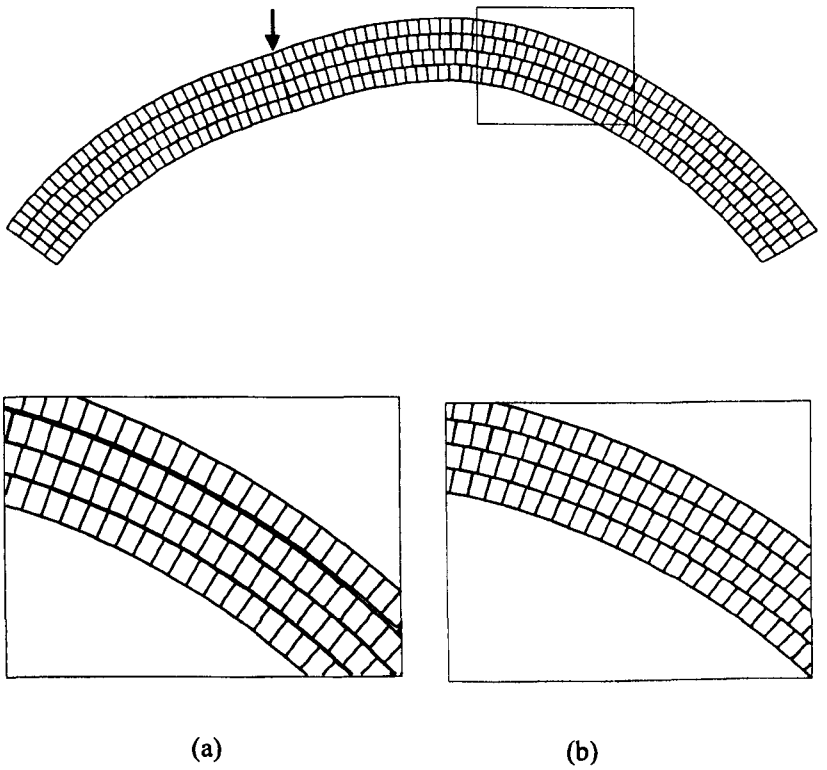

Figure 6.4: Bridge 5-2 predicted failure modes: (a) associative friction; (b) non-associative friction

results. Indeed, the UK Department of Transport bridge assessment memorandum BA16/93 [22] states that:

'the mechanism method ..may not be appropriate where soil resistance is important, which found to be the case even for relatively flat arches ..these (mechanism) programs may therefore produce arbitrary results'

The assumption that peak horizontal pressures are mobilized by infinitesimal structural displacements can also lead to erroneous failure mechanism being identified when the mechanism method is applied to multi-span arch bridges. Though this problem can be overcome by manually adjusting the fill pressures until a correct mechanism is obtained, a more elegant way to deal with this problem is to use an

Bolton arch rib/bridge ref.	Expt. Failure load (kN)	RING 1.5 (associative friction formulation)		RING: output from non-associative friction procedure		Difference: non-associative vs. associative	
		Failure load (kN)	CPU time (s)	Failure load (kN)	CPU time (s)	Reduction in failure load	CPU slow-down factor
Arch 2	1.5	1.45	0.16	1.44	1.6	0.7%	10×
Bridge 3-2	360	253	0.25	248	1.3	2%	5.2×
Bridge 5-2	500	486	0.98	457	24.1	6%	25×

Table 6.2: Multi-ring arches: experimental and infinite crushing strength analysis results with associative and non-associative friction models

iterative gross displacement analysis, as proposed by Gilbert [23].

For a gross displacement analysis, it may be assumed that the build-up in soil resistance pressures occurs gradually. In a study performed by Gilbert [23], it was found that the recorded build up in pressure, in the case of 3m single and multi-span bridges tested at Bolton Institute, was non-linear but could approximately be described by the empirical relationship $p = p_{peak}(1 - (1 - 2R)^5)$, where R is net barrel rotation in degrees. The suggested procedure for gross displacement analysis involves carrying out 'standard' mechanism analyses sequentially. A step-by-step description for the procedure is as follows:

1. Perform 'standard' mechanism analysis of structure.
2. Perform material crushing analysis to determine the effect of material crushing at hinges.
3. Magnify infinitesimal displacements to determine new positions for the blocks.
4. Modify soil-structure pressures as necessary.
5. Repeat from step 1.

The success of the above procedure relies on the use of relatively small displacement increments in step 2.

6.5.5 Soil-structure interaction

In addition to the issue of the amount of displacement required in order to mobilize soil restraining pressures, there are other problems: the backfill acts both to disperse the applied loading and to restrain sway of the barrel into the fill. However, conventional limit analysis (and many other) models often suffer from the fact that unless the backfill is modelled explicitly, backfill pressures restraining the masonry generally need to be stipulated in advance of an analysis (yet in reality these will be a function of the failure mode, which is not known in advance).

To illustrate this point it is worthwhile to consider some sample problems using RING. This software, in common with other masonry arch bridge analysis programs, has been calibrated against results from full-scale bridges which, for various reasons, have tended to fail in 4 hinge mechanisms. In RING the presence of uniaxial backfill elements [12] means that although it is unnecessary to specify in advance the sense of the pressures, the *magnitudes* of the pressures do need to be specified in advance. Thus, in order to approximately reproduce the results from full-scale tests, horizontal passive zone restraining pressures might commonly be entered as $K_p/3$ where K_p= $(1 + \sin\phi)/(1 - \sin\phi)$, and where ϕ is the internal angle of friction of the backfill material. However, RING chooses the critical failure mechanism from a multitude of possible ones and a 4 hinge failure mechanism is by no means always identified as being critical. For example, Fig. 6.5 shows two failure modes encountered when recently assessing a number of local authority-owned field bridges.

Both the predicted failure modes shown in the figure involve sliding failures (non-associative failure modes are shown, but in these cases the predicted non-associative

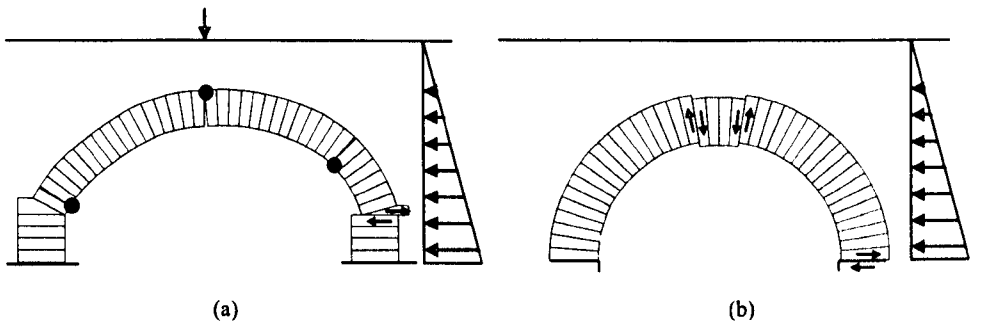

Figure 6.5: Standard predicted failure modes: (a) 3 hinges and abutment sliding; (b) sliding only mechanism

failure loads were identical to their associative friction counterparts). In the case of the bridge shown in Fig. 6.5(a), despite the fact that horizontal restraining pressures were in this case applied to the back of the skewback†, the latter was predicted to slide. However, the magnitudes of the pressures specified were calculated using modified classical vertical retaining wall theory as outlined above, whereas in reality such a failure mode would almost certainly mobilize significantly larger soil pressures. The same is also true for the mechanism indicated in Fig. 6.5(b). Thus in both cases the RING strength predictions are likely to be quite conservative.

One way to address this issue properly is to move away from an indirect modelling strategy for the soil towards, instead, modelling the soil explicitly (i.e. using solid elements to represent the soil). Though this is, in principle, relatively straightforward since RING is designed to be a rapid analysis tool, an important challenge is to implement the capability in a computationally efficient manner. Whilst it is unlikely that sufficient validation will have been performed to enable explicit modelling of the soil to be implemented in RING 2.0, it is anticipated this will be incorporated in a subsequent release. Further discussion of the important issue of soil-structure interaction is provided in [24].

† The inclined support at each end of a segmental arch.

6.6 Practical application of computational limit analysis to masonry arch bridges

Three local authority bridges (A, B and C) have been selected in order to test the capability of RING. The following section identifies why the particular bridges were chosen.

Firstly, in the case of many bridges studied here, the depth of the fill above crown[†] is greater than the barrel thickness. Hence, according to BD21/01, an alternative method of analysis to the modified MEXE must be applied. All these bridges have a relatively short span. In short span bridges, stresses will generally be comparatively low and the effect of second order elastic shortening is negligible, consequently such bridges will likely to fail in mechanisms involving predominantly rigid body rotations and/or translations. Other modes of failure are less likely to take place. Additionally, the self weights of these bridges, are relatively small compared with potential live loads. In these circumstances RING is an ideal tool.

Secondly, all the example bridges comprise a number of rings of brickwork. The inter-ring mortar joints in these bridges are potential surfaces of weakness and may conservatively be modelled as friction-only joints. Previous assessments of these bridges have been conducted using RING 1.1, which inherently assumes associative friction. A research version of RING 1.5 has the capability to perform a non-associative friction analysis and hence it is of interest to see the effect of the flow rule on the predicted load capacity and the corresponding failure mechanism.

Thirdly, all these bridges incorporated backfill material to fill the spandrel void areas. The research version of RING 1.5 also has the capability of performing a gross displacement analysis, which allows the influence of the build up in restraining soil pressures to be investigated.

[†] The highest point along the external surface of the arch rib.

6.6.1 Parameters used in the RING analyses for the present study

Unless stated otherwise, the following values have been used in the re-assessments:

Parameter	Value	Note
Characteristic brickwork strength (N/mm^2)	2.3	From BD21/01, assuming London Stocks
Coefficient of friction between units	0.6	Value used in BS5628 pt 1
Brickwork unit weight (kN/m^3)	20	
Fill unit weight (kN/m^3)	18	
Loaded length (m)	0.3	BD21/01 value used for trough decks (see BD21 para. 6/11)
Limiting load dispersion angle (degrees)	30	For use with Boussinesq type distribution
Coefficient of passive pressure, K_p	1	Equivalent to one third of the classical value when $\phi = 30°$
Number of blocks per arch ring	40	
Load dispersion type	Boussinesq	

Table 6.3: Parameters used in the RING analyses for the present study

Fill depth refers to the distance between the arch supports level and the road level.

6.6.2 Bridge A

Bridge A comprises two brickwork arch spans supported on brickwork abutments as shown in Fig 6.6. Geometrical and material properties are given in Table 6.4. A number of different analyses were performed using RING 1.1 and the research version of RING 1.5. Results are presented in Table 6.7 and in Fig. 6.8.

As expected, modelling the arch using two rings rather than a single ring had a large impact on the predicted carrying capacity. It is also evident that when non-associative friction is assumed, the predicted carrying capacity reduces by almost 25% (from 24.7 to 18.63kN/m). Failure mechanisms are shown in Fig. 6.7.

Figure 6.6: Bridge A

Parameter	Value
Number of spans	2
Span	3.5m, 2.5m
Rise	1.090m, 0.6m
Number of rings	2
Ring thickness	0.1175m, 0.1175m, 0.345m
Fill depth	1.56m, 2.15m

Table 6.4: Bridge A: geometrical and material properties

6.6.3 Bridge B

Bridge B, which is shown in Fig. 6.9, is a very short (1.8m) span, three-ring thick, brick arch bridge which has an approximately semicircular profile. Geometrical and material properties are given in Table 6.5. Unlike most of the other bridges in the current study, this bridge does not have a depth of fill above crown greater than the barrel thickness. RING predictions for this bridge are shown in Table 6.7 and Fig. 6.11.

In the case of this bridge, the influence of the choice of friction model on carrying capacity was less pronounced, though the associative and non-associative failure

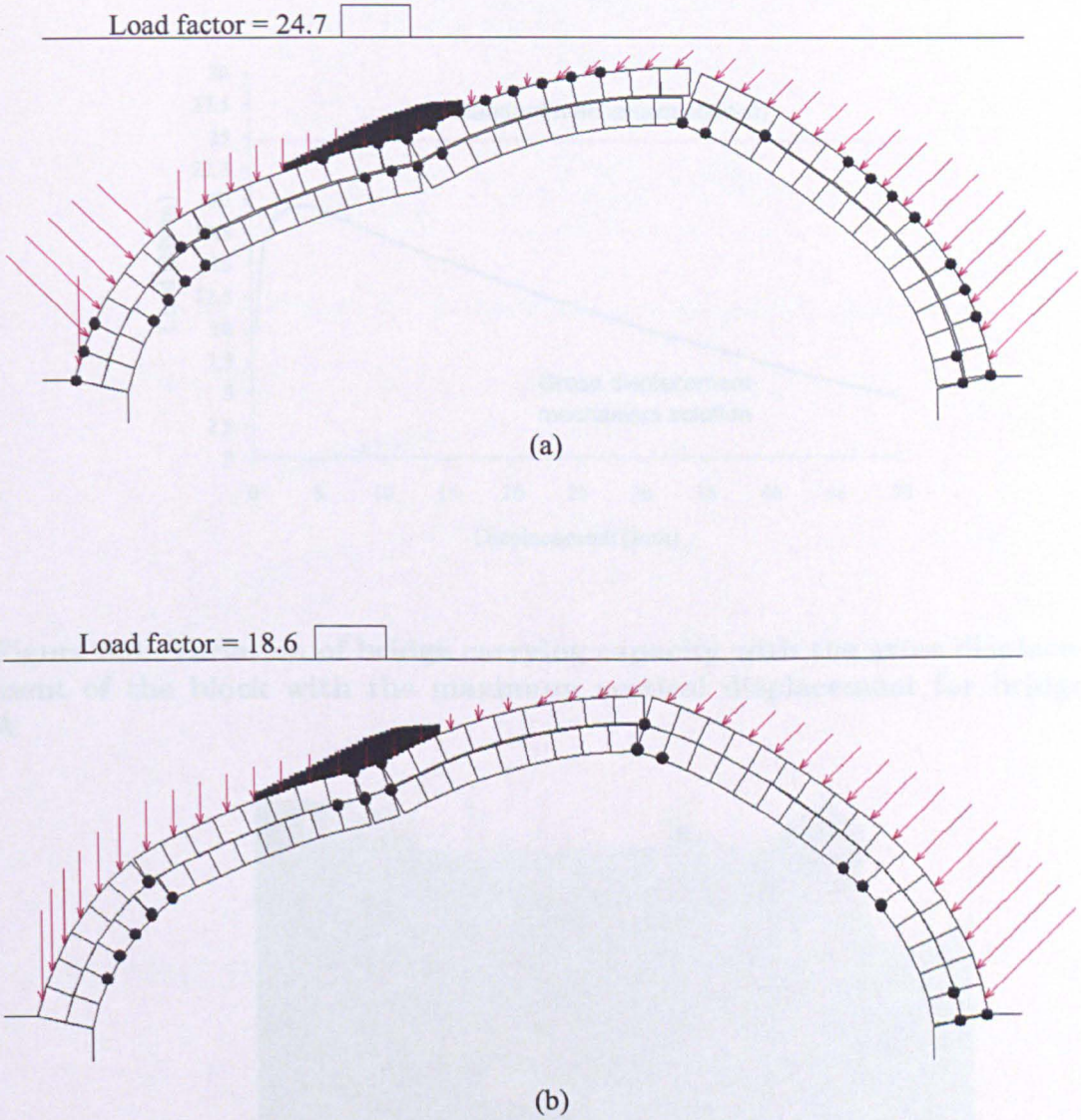

Figure 6.7: Bridge A failure mechanisms: (a) associative friction analysis; (b) non-associative friction analysis

mechanisms were visibly different (Fig. 6.10).

Very significant difference in failure modes were also in evidence when this bridge was modelled as a single ring (Fig. 6.12) though in this case the associative and non-associative friction load factors were identical.

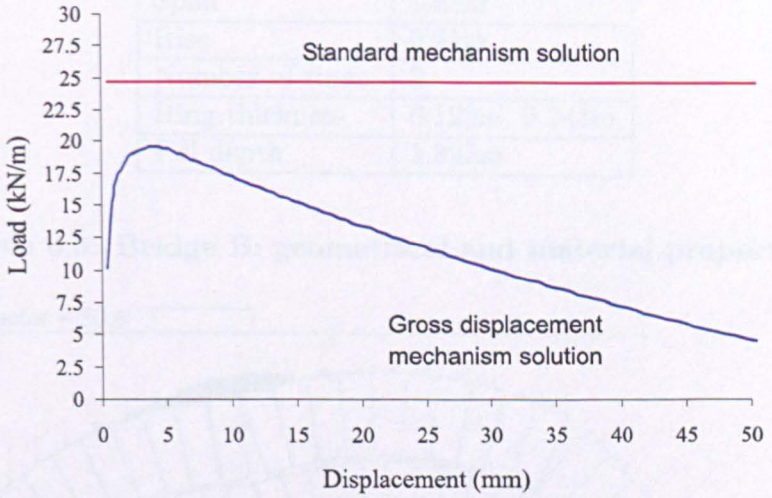

Figure 6.8: Variation of bridge carrying capacity with the gross displacement of the block with the maximum vertical displacement for bridge A

Figure 6.9: Bridge B

Parameter	Value
Number of spans	1
Span	1.81m
Rise	0.91m
Number of rings	2
Ring thickness	0.122m, 0.243m
Fill depth	1.395m

Table 6.5: Bridge B: geometrical and material properties

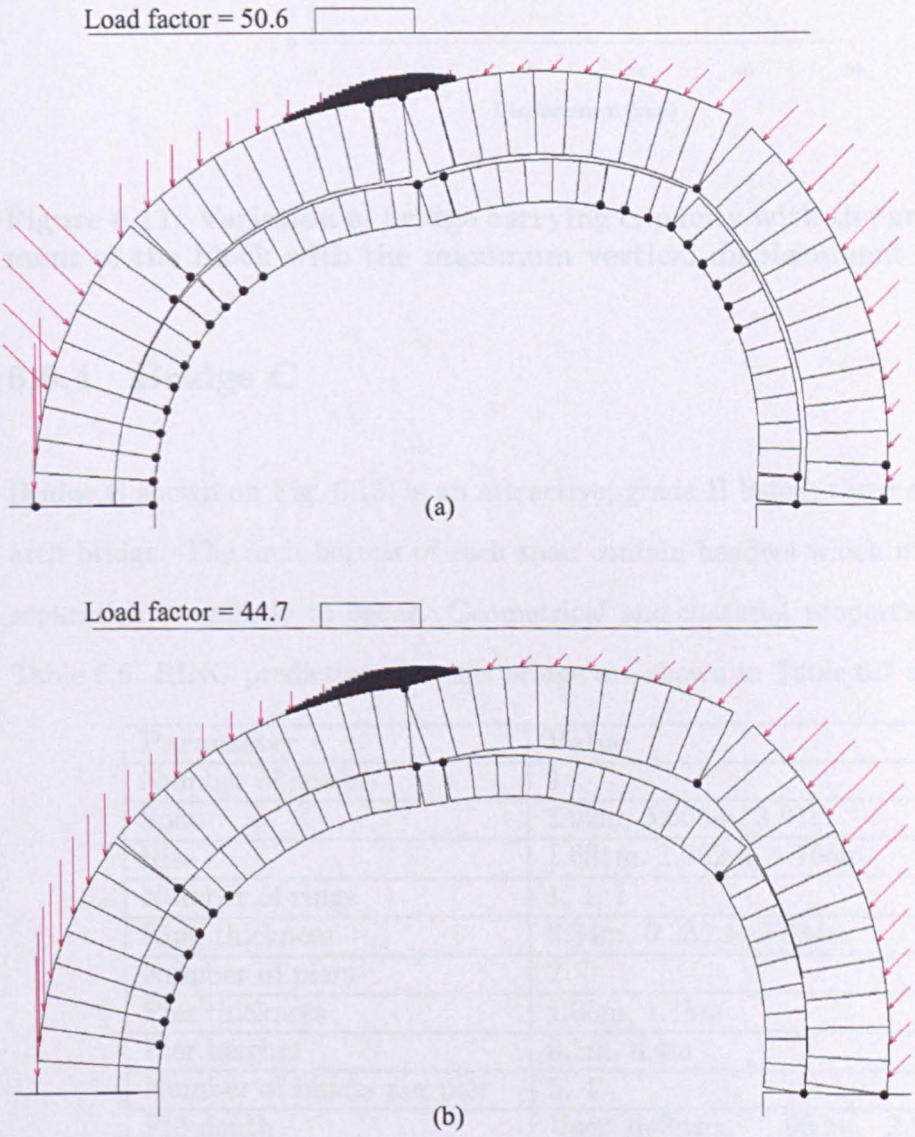

Figure 6.10: Bridge B: (a) associative friction analysis; (b) non-associative friction analysis

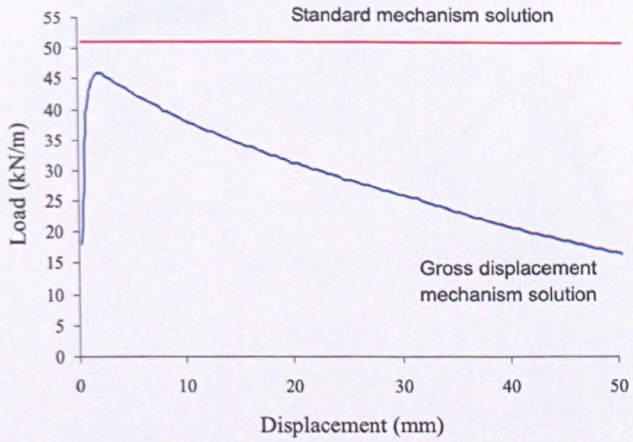

Figure 6.11: Variation of bridge carrying capacity with the gross displacement of the block with the maximum vertical displacement for bridge B

6.6.4 Bridge C

Bridge C shown on Fig. 6.13, is an attractive, grade II listed, three span brickwork arch bridge. The arch barrels of each span contain headers which means that ring separation is unlikely to occur. Geometrical and material properties are given in Table 6.6. RING predictions for this bridge are shown in Table 6.7 and Fig. 6.15.

Parameter	Value
Number of spans	3
Span	3.92m, 5.565m, 3.91m
Rise	1.681m, 1.962m, 1.765m
Number of rings	1, 1, 1
Ring thickness	0.34m, 0.335m, 0.334m
Number of piers	2
Pier thickness	1.05m, 1.15m
Pier heights	0.5m, 0.4m
Number of blocks per pier	5, 4
Fill depth	User defined: 1.960m, 2.556m, 7.753m, 2.695m, 1.3640m, 2.545m

Table 6.6: Bridge C: geometrical and material properties

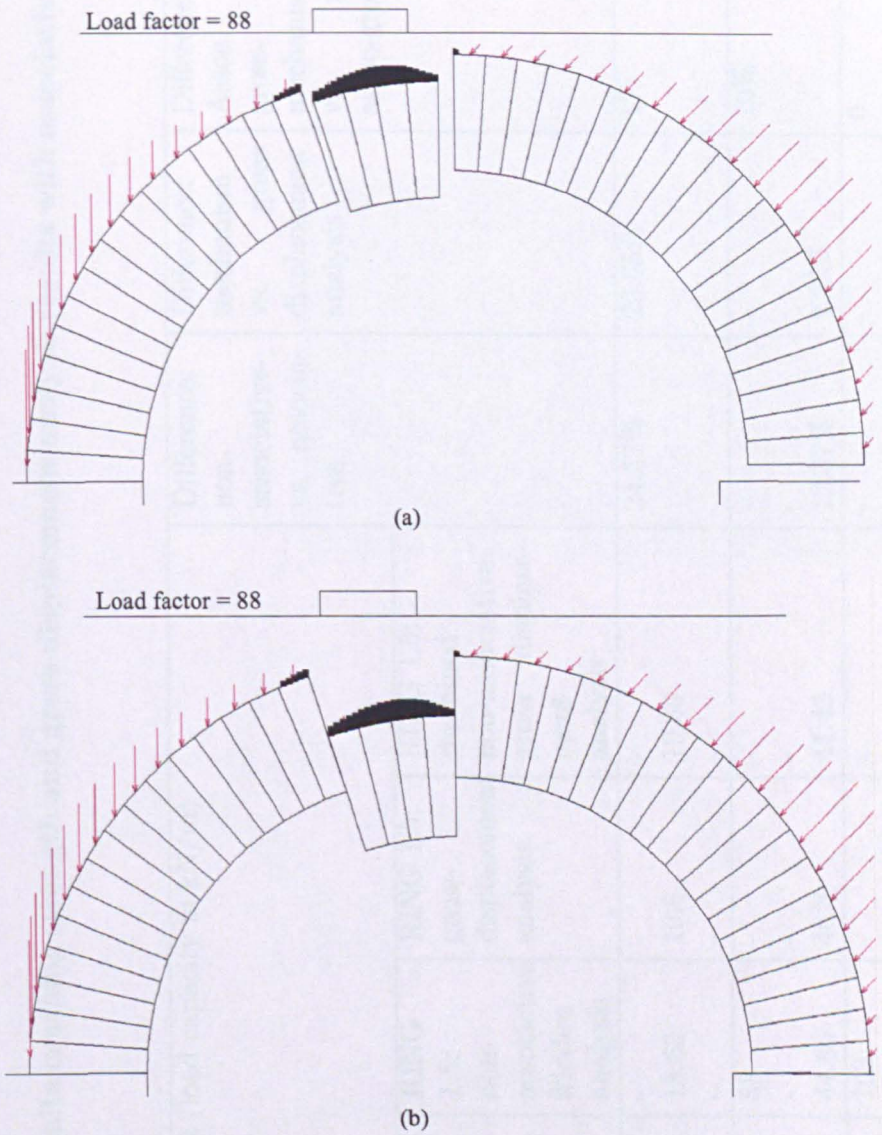

Figure 6.12: Sliding failure mode for bridge B: (a) associative friction model; (b) non-associative friction model

This bridge was found not to be exceptionally sensitive to gross displacements or to the particular friction model used. However, an interesting finding was that when backing was included in the model this led to two spans being involved in the failure mechanism, despite the stocky piers (Fig. 6.14).

To facilitate the subsequent discussion and to enable comparisons to be made, the analysis results are presented in Table 6.7.

Table 6.7: A local authority bridges: finite crushing strength and gross displacement analysis results with associative and non-associative friction models

Bridge	No. of rings	No. of blocks per ring	RING assessment (load capacity in kN/m)					Difference: non-associative- vs. associa-tive	Difference: mechanism vs. gross displacement analysis	Difference: Assoc. gross-mechanism vs. non-assoc-gross
			RING 1.1	RING 1.5	RING 1.5: non-associative friction analysis	RING 1.5: gross-displacement analysis	RING 1.5: combined non-associative gross displace-ment analysis			
A	1 2 2	40 40 140	43.3 24.2 -	43.3 24.7 24.1	- 18.63 -	- 19.6 -	- 19.39 -	24.57%	20.65%	1%
B	1 1 2	40 140 40	88 - 51	88 87 51	88 - 44.69	- - 46.3	- - 41.43	- - 12.37%	- - 9.22%	10%
C With backing Without-backing	1 1 1 1	40 140 40 140	103.5 - 88.3 -	103 105 87.45 87.43	103 - 87.45 -	- - 85 -	- - 85 -	- - 0 -	- - 2% -	0

Figure 6.13: Bridge C

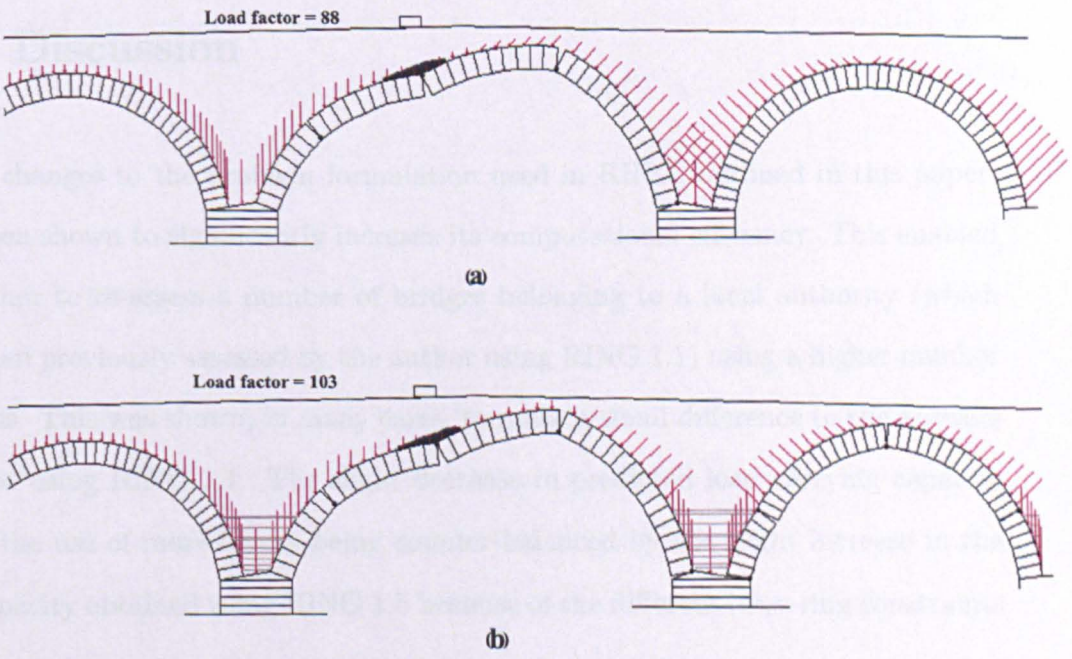

Figure 6.14: View of failure mechanisms for bridge C: (a) without backing; (b) backing included

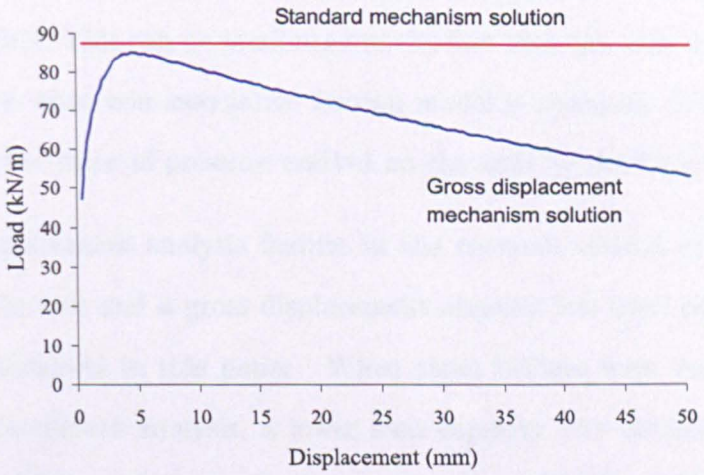

Figure 6.15: Variation of bridge carrying capacity with the gross displacement of the block with the maximum vertical displacement for bridge C

6.7 Discussion

Recent changes to the problem formulation used in RING, outlined in this paper, have been shown to significantly increase its computational efficiency. This enabled the author to re-assess a number of bridges belonging to a local authority (which have been previously assessed by the author using RING 1.1) using a higher number of blocks. This was shown, in many cases, to make a small difference to the answers obtained using RING 1.1. The slight decrease in predicted load carrying capacity due to the use of more blocks being counter-balanced by the slight increase in the load capacity obtained using RING 1.5 because of the different inter-ring constraints used.

When a research version of RING 1.5 was used to re-assess these bridges with the assumption of a non-associative model for friction it was found that reductions from 0-25% in the predicted capacity resulted. Additionally, in many cases, different failure mechanisms, which looked visibly more sensible, were obtained. It was also

observed that there was a local distinct change in soil pressure direction (Fig.6.7(b) and Fig.6.10 (b)). This can be attributed to the fact that the arch moves less to the fill in the cases when non-associative friction model is assumed. Consequently, the direction and the value of pressure exerted on the arch by the fill will change.

The gross displacement analysis feature in the research version of RING 1.5 has been put to the test and a gross displacement analysis has been performed for all the bridges presented in this paper. When these bridges were re-analysed using the gross displacement analysis, a lower load capacity was obtained in all cases. The difference between the gross displacement analysis and the ordinary mechanism method analysis predictions varied between 9-20%. This compares well with the 8-12% reductions previously found by Gilbert [23].

The current method which uses rotation of the arch barrel(s) to determine the magnitude of passive resistance pressures is not general. In the future it would be preferable to model the soil explicitly in a coupled analysis.

6.8 Conclusions

Recent developments to the RING masonry arch bridge analysis software are described in this paper. Additional features such as a non-associative constitutive model for sliding friction and a gross displacement analysis capability have been discussed. The software was applied to a number of typical local authority bridges. The significant improvements of the computational efficiency of RING 1.5 with its predecessor RING 1.1 have been demonstrated.

The rigid block analysis method was found to provide a conceptually simple, yet powerful and efficient means of determining the critical collapse mechanism and associated load factor, whether the bridge contained single or multiple spans and/or arch rings.

Although arguably more realistic, it was found that non-associative friction and gross displacement analysis were computationally expensive. It will remain up to the judgment of the assessment engineer as to whether this additional expense is justified. It was also found that the gross displacement analysis predicted a lower load capacity.

6.9 Acknowledgements

Network Rail (formerly Railtrack) have supported the development of RING versions 1.1 and 1.5. RING 2.0 is being developed in collaboration with the International Union of Railways (UIC), as part of their 'Improving Assessment, Optimization of Maintenance, and Development of Database for Masonry Arch Bridges' project.

References

[1] Livesley, R. K. A. Limit analysis of structures formed from rigid blocks. *International Journal for Numerical Methods in Engineering*, 12:1853–1871, 1978.

[2] http://www.shef.ac.uk/ring

[3] Harvey, W. J. Testing times for arches. *New Scientist*, 54–59, 15 May 1986.

[4] Military Engineering Experimental Establishment. Classification (of civil bridges) by the reconnaissance and correlation. Christchurch, UK, May 1963.

[5] Pippard, A. J. S. and Baker, J. F. *The analysis of engineering structures.* Arnold, London, UK, 1943.

[6] Gilbert, M. and Melbourne, C. Rigid-block analysis of masonry structures. *The Structural Engineer*, 72:356–360, 1994.

[7] Gilbert, M. and Melbourne, C. The behaviour of multiring brickwork arch bridges. *The Structural Engineer*, 73:39–47, 1995.

[8] Heyman, J. *The masonry arch.* Ellis Horwood, Chichester, UK, 1982.

[9] Harvey, W. J. The application of the mechanism method to masonry arch bridges. *The Structural Engineer*, 66(5):77–84, 1988.

[10] Crisfield, M. A. and Packham, A. A mechanism program for computing the strength of masonry arch bridges. TRL research report 124, DoT, UK, December 1987.

[11] Gilbert, M. RING: a 2D rigid-block analysis program for masonry arch bridges. *Proceedings of the 3rd International Arch Bridges Conference*, Paris, 2001.

[12] Gilbert, M. On the analysis of multi-ring brickwork arch bridges. *Proceedings of the 2nd International Arch Bridges Conference*, 109-118, Venice, 1998.

[13] Tam, T. and Jenning, A. Classification and comparison of LP formulations for the plastic design of frames. *Engineering Structures*, 11:1197-1216, 1989.

[14] Dantzig, G. B. Computational algorithm of the revised Simplex method, 1953. Rand Corporation reprint RM-1266.

[15] Ahmed, H. M. and Gilbert, M. The computational efficiency of two rigid block analysis formulations for application to masonry structures. *Proceedings of The Ninth International Conference on Civil and Structural Engineering Computing*, Egmond-aan-Zee; The Netherlands, 2003.

[16] Gilbert, M. *The behaviour of masonry arch bridges containing defects*. PhD Thesis, University of Manchester, 1993.

[17] Czyzyk, J. PCx user guide (version 1.1), technical report oct 96/01. Argonne National Laboratory, U.S.A., October 1996.

[18] Drucker, D. C. Coulomb friction, plasticity, and limit loads. *Journ. Appl. Mec. Trans. ASME*, 21(4):71–74, 1954.

[19] Ferris, M. C. and Tin-Loi, F. Limit analysis of frictional block assemblies as a mathematical program with complementarity constraints. *International Journal of Mechanical Sciences*, 43(1):209–224, 2001.

[20] Gilbert, M., Ahmed, H. M. and Casapulla, C. Computational limit analysis of masonry structures in the presence of non-associative friction. *Proceedings of the VI STRUMAS Conference*, Rome, 2003.

[21] Gilbert, M., Casapulla, C. and Ahmed, H. M. Limit analysis of masonry block structures with non-associative frictional joints using linear programming. *Submitted to Computers & Structures.*

[22] Highways Agency. BA16/97: The assessment of highway bridges and structures, part of design manual for roads and bridges. HMSO, London, UK, 1997.

[23] Gilbert, M. Gross displacement mechanism analysis of masonry bridges and tunnels. *Proceedings of the 11th International Brick/Block masonry conference*, Shanghai, 1997.

[24] Smith, C. C., Gilbert, M. and Callaway, P. A. Geotechnical issues in the analysis of masonry arch bridges. *Proceedings of the 4th International Arch Bridges Conference*, Barcelona, 2004.

Chapter 7

Discussion

7.1 Introduction

The overall objective of the research leading to this thesis was to develop a general model for limit analysis of RC slabs and masonry structures and to apply this to a variety of practical problems within the context of reinforced concrete and masonry structures. As an assessment or design tool, the developed model should be suitable to be used in practical engineering projects, oriented to assess the load capacity of RC slabs/masonry structures.

Structural engineers are presently assessing more structures than designing new ones. With many assessment indications suggesting that current bridges have insufficient load carrying capacity, bridge owners are faced with a problem. The resources needed for strengthening/or reconstruction, or the economic impact of imposing weight restrictions, have prompted the search for more efficient and accurate methods for assessment. This has stimulated a line of research focusing on developing efficient and practically useable analysis tools. The current research presented in this thesis can be considered to follow this line. Furthermore, the continued advances in

computing power has enabled treatment of problems which have been only few years earlier would have been considered to be intractable, or only solvable by researchers rather than practicing engineers.

The particular applications that have been considered in the thesis are reinstated below.

7.2 Automated yield line analysis of RC slabs

As second order effects for short span slabs are negligible, the appropriateness of using non-linear analysis methods for the determination of load carrying capacity of RC slabs becomes questionable. Hence, there is need to develop techniques which are more suitable for the assessment of RC slabs, whether these form floors slabs or bridge decks. To be practically useable, the developed techniques should be easy to use, conceptually simple and applicable to a large number of structures.

In the UK, the assessment code provides scope for engineers to use a variety of methods to assess the load carrying capacity of structures. Although the main emphasis in the code is on the elastic analysis methods, engineers are free to use other methods such as plastic analysis methods, non-linear finite element methods or load testing in appropriate circumstances [1, 2].

Elastic methods found favour for many reasons: they are well established and supported by many computer software packages. Engineers also feel they can trust these methods as they are effectively lower-bound methods which produce conservative results. This may be acceptable for design purposes, however, it may be less justifiable for assessment purposes.

A typical approach for assessing RC slabs is to use a linear elastic analysis. This can be carried out by using the finite element method or the grillage method. Using

these techniques, locations of maximum moment and shear forces are identified. In fact, in RC slabs, cracks would form at these locations which would result in moment distribution since these slabs are usually under-reinforced. A linear elastic analysis is incapable of accurately modelling moment distribution. Accordingly, elastic methods are very conservative as the failure of one part of the structure is taken as the failure for the whole slab.

There is a large body of evidence from model and full scale tests that RC slabs are able to carry loads well beyond their predicted capacity using elastic methods [3]. This means engineers should consider other methods which are efficient and economical. Three options can be considered: performing a more sophisticated analysis using non-linear finite element methods, conducting load tests on the structure itself to verify its load capacity or performing a plastic collapse analysis.

Non-linear finite element modelling is more suited to in-depth, specialized assessments of major structures or for laboratory research and is not presently considered to be a practical option for use in assessing large numbers of existing structures. Load testing can be carried out on individual cases, but it is not a practical option for the volume of structures expected to be involved.

Plastic collapse analysis in the form of a yield line analysis [4] can be used to assess the strength of RC slabs/bridge decks. Yield line analysis, in common with other plastic analysis methods, considers the failure of the whole slab rather than failure of a part. This fully utilizes the distributed strength capacity of a structure. Consequently, the method is less conservative than elastic methods.

Traditional "hand" yield line methods are somewhat cumbersome to apply to all but the simplest structural geometries, reinforcement arrangements and loadings. Hence, the complex nature of most real world structures has limited its use. The implementation of plastic collapse methods in computer software allows design/assessment

engineers to analyse more complicated structures in seconds and the optimization of a collapse pattern under many different loading configuration becomes possible.

In this context, the Highways Agency in the UK commissioned the Department of Engineering at Cambridge University to develop a yield line analysis program for RC bridges. The resulting program is called COBRAS [3, 5]. The COBRAS program contains a library of pre-defined failure patterns for RC bridges. The program iterates through these to find the one which gives the lowest load. Although the program has been successfully applied in many cases, it cannot be considered general enough as it is restricted to a range of geometrical configurations.

The goal of the present work has been to formulate a more generally applicable approach. The 'Sheffield method' developed is promising but one issue of concern with the new formulation is the derivation of the shear factor used to modify yield condition constraints. Values used here were derived geometrically based on intuition rather than mathematically; it cannot be claimed that they are rigorous but it seemed the method is working with them and appeared to give sensible results.

For example, one problem which has been extensively studied in the past is the case of a fixed edged square slab. The exact solution for this case consists of complicated field moments near the slab corners and therefore serves well to test the program capability and the method performance. A value which is less than 0.2% from the exact solution was obtained with fairly small number of divisions. A solution with a higher number of divisions per side was sought, however the limitations of the available computer power/hardware made it impossible to run such big problems on a 32 bit desktop computer running Windows XP and therefore a move to 64 bit UNIX system was necessary. This enabled modelling of the slab problem using a higher number of divisions per side. Fully utilizing the symmetry of the slab in hand, only 1/8 of the slab may be modelled. Using a discretization of 400×400, a load factor of 42.845 was obtained, which is within 0.01% of the exact solution (42.851).

The problem could not be solved when the number of divisions exceeded 400 per side due to an unforseen problem with the optimizer (Mosek 2.5) [6]. It appeared that the load factor was converging towards the exact solution and, if it becomes possible to use the same or an alternative optimizer to model this slab with a finer mesh, the exact solution may eventually be obtained using identical hardware.

For all cases presented in the thesis, the load factor was found to converge towards the exact solution from below when the number of divisions per side was increased. For many of the examples considered, a fairly small number of elements is needed in order to obtain the exact solution. However in a few cases, for example the case of fixed edged square slabs, a large number of elements are needed to achieve close approximations of exact solutions. However, as previously explained, the computing resources available then became the limiting factor. Therefore an adaptive discretization strategy may be useful.

Although it is not documented in the thesis, the author experimented with adaptive meshing, and found that (apart from the case of simply supported slab modelled with square elements) this did not perform as well as expected in the majority of cases tried. The simple idea was to examine the translational displacements at interfaces: as it is known in advance that the solution will converge towards the exact solution when these displacements tend to zero, so, elements which share interfaces with a given translational displacement were refined. This should minimize the translational displacements and consequently allow the load factor to converge towards the exact solution. Although preliminary results for the case of a simply supported slab modelled with square elements were encouraging, as in Fig. 7.1, this approach could not be fully utilized without rigorously deriving shear factors, as the element aspect ratios are constantly changing. Shear factors need to be derived in a way that fully considers all types of elements.

Another approach, which can be followed to predict load factors at a higher number

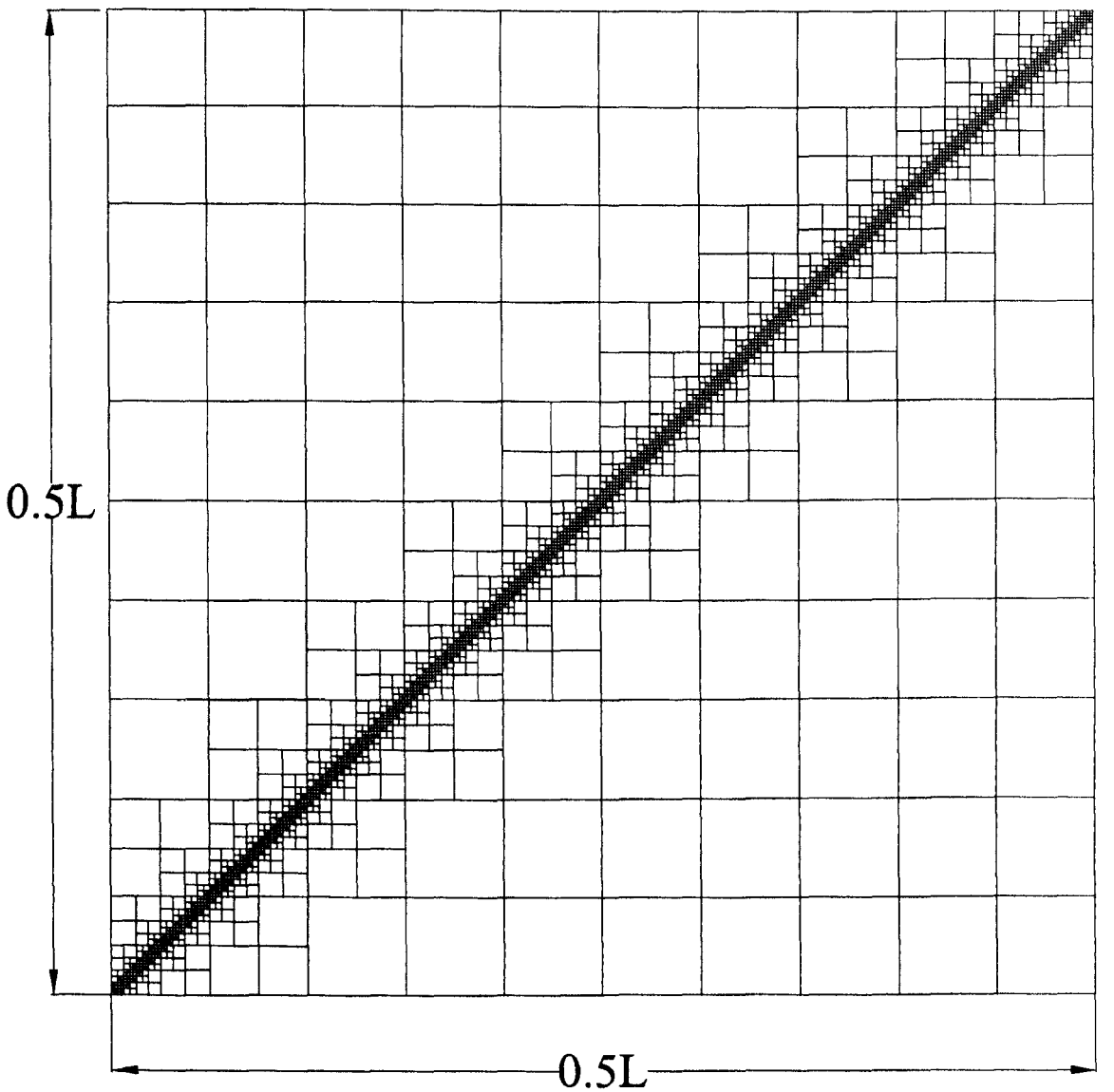

Figure 7.1: Adaptive meshing for a simply supported square slab modelled with square elements

of elements without actually performing the analysis with this number of elements, is to extrapolate results at the required mesh size. This can be carried out using Richardson's extrapolation. Other researchers have tried this approach [7, 8] to confirm that their solution is converging to the exact solution.

So far, the method has performed well for the problems that have been investigated. However, one important issue remains to be resolved: the method developed has

no formal status within the framework of plastic analysis. In other words, before performing initial analyses with different number of elements, one cannot define the status of the solution obtained (i.e. whether it is an upper-bound or lower-bound solution). In order to establish the status of the method, an attempt has been made to obtain kinematically admissible solutions and thus rigorous upper-bound solutions using the method.

The 'two-phase Sheffield method' relies on the fact that previous examples have demonstrated that the original Sheffield method appears, in the majority of cases, to identify sensible failure patterns in terms of displacement contours. The method appeared to perform well and has promise; however the time available did not allow the method to be fully investigated. It can be considered as a minor step towards obtaining genuine upper-bound solutions from the Sheffield method.

Finally, it is worth mentioning here that analogous techniques (i.e. using finite elements with discontinuities) have been used in formulating problems of limit analysis in the geotechnical field [9, 10, 11]. Here the technique has been found to perform reasonably well e.g. overcoming the disadvantage of traditional finite element formulations. The main differences between the Sheffield method and these methods is that, unlike in the case of the Sheffield method, in-plane rather than out-of-plane problems have been considered.

7.3 Limit analysis of masonry block structures with non-associative frictional joints using linear programming

Environmental changes and increasing axle loads accelerate the rate of deterioration of masonry arch bridges. This resulted in an acute demand for reliable assessment

methods for bridges. Elastic methods here are widely used for the same aforementioned reasons.

In recent years, non-linear finite element analysis has been applied to masonry problems. However, in the case of masonry arch bridges there are many uncertainties regarding the properties, constructional details and initial stress states. This means that the wisdom of using sophisticated, computationally expensive and highly sensitive finite element packages becomes questionable.

It is also well known that masonry structures do not deform elastically. Collapse of masonry structure usually occurs without significant prior elastic deformations which means that there are few warning signs that failure will take place. Such characteristic behaviour is more like a rigid block behaviour.

Well established methods for masonry arch bridge analysis such as the 'mechanism' method and the 'thrust-line' method inherently assume that frictional failures do not happen. This is ,perhaps, justifiable in the case of voussoir arches, as failure mechanisms mainly involve rotations at hinges. However, for other masonry assemblages such as masonry walls, the friction plays an important role and therefore such an assumption is not valid.

Modelling Coulomb sliding friction mathematically can be problematic and hence the role of the friction in the assessment of rigid block structures has been largely neglected until recently, when sophisticated new mathematical programming methods have been applied to the problem. Whilst undoubtedly promising, specialized non-linear programming solvers have had to be employed to obtain solutions. There is also a concern that the methods proposed may be prohibitively computationally expensive when applied to even moderately large problems.

For these reasons, a much simpler iterative procedure, which involves the successive solution of simple LP sub-problems, has been considered in the fifth chapter.

The method has generally been found to perform well, although some improvements are needed, particularly the convergence performance for very large problems.

A number of issues related to the proposed method, such as the solution status and the influence of the choice of starting problem, have already been discussed in this chapter. The next section is devoted to application of computational limit analysis to real-world problems.

7.4 Practical application of computational limit analysis: masonry arch bridges

So far, it has been shown that it is possible to develop relatively computationally inexpensive limit analysis computer programs for RC slabs and masonry structures. To fulfil the aim of applying limit analysis to practical applications, the sixth chapter in the thesis was devoted to masonry arch bridge case study problems. It was initially intended to use the automated yield line method, developed in the fourth chapter, in the assessment of real RC bridges. However, time constraints meant this was not possible.

The bridges which have been considered in the re-assessment exercise were primarily chosen to illustrate the newly developed features of RING. Another important consideration was that these bridges should have relatively short spans so that they will likely to fail in a mechanism involving predominantly rigid body rotations and/or translations.

The implementation of the non-associative friction analysis feature in RING 1.5 shown to affect the computed load factor by between 0-25% with the largest differences being found when multi-ring brickwork arches were considered.

When a gross displacement analysis was conducted, a lower load capacity was obtained in all cases. However, gross displacement analysis will only be useful if the user has an appropriate knowledge of the behaviour of the backfill when the arch sways into this.

RING 1.5 does have some limitations. For example, although the program can be used to assess the load capacity of multi-ring arch bridges with the defects of ring separation, it cannot detect the ring separation which may take place during the loading process. The program is also limited to short and medium span bridges, where second order effects are negligible.

The purpose of RING, as any software, is to remove the burden carrying out computations manually. It is intended to be user friendly and efficient; accordingly, the software has been programmed so that only simple data is required in order to give a solution. With RING, assessments are automatically obtained once the geometry, material properties and the nature of loading are identified, removing the need for tedious manual calculations. Although the RING software is fully automated, engineering judgement or intuition in some situations is needed in order to fully utilize the software. For example, the issue of ring separation: RING cannot detect whether ring separation is likely to occur. The user has to specify in advance in the input section, based on engineering judgment, whether the arch under consideration should be modelled as a multi-ring or single ring arch. Similarly, an appropriate knowledge of the likely behaviour of the backfill is required to ensure reliable results are obtained. Also a judgement needs to be made as to whether the rigid block method of analysis can be applied to the problem in hand at all. The decisions made by the individual, extending from the analytical description of the structure, the judgement on the correctness of the numerical analysis and through to the interpretation of the results, are not acquiescent to computerization. One must understand the principles of the analysis and use own's judgements. Comput-

erization has relieved the burdens of the rote operations in structural analysis, but it cannot relieve the responsibility of using such results.

7.5 The future of mathematical programming applications to limit analysis

For all methods presented in the thesis, a unifying element has been the use of mathematical programming, in the form of linear programming, to find the optimum solution for the structural analysis models developed. For any structural analysis model the main components are structural model and material constitutive model. The structural model adopted here consists of assemblages of finite elements. These may be assemblage of finite elements interacting through interfaces with translational displacements, in the case of RC slabs, or rigid blocks interacting through non-tensional interfaces in the case of masonry structures. The constitutive models considered have included the square yield criterion and Mohr-Columb model.

The importance of mathematical programming has been recognized for some time, However, despite this importance, mathematical programming is seldom used in structural analysis. This is partly attributed to the computer power and the relatively primitive algorithms available when computer based methods were first developed in 1960s and 1970s. However there are signs that mathematical programming will be used in limit analysis problems more in the future. Interior point optimization algorithms are now robust, powerful and scale well to large problems.

References

[1] The Highways Agency. The assessment of concrete highway bridges and structures, 1995. BD44/95.

[2] British Standards. Steel, concrete and composite bridges: general statement, 1988. BS5400: Part 1: 1988.

[3] Middleton, C. R. Concrete Bridge Assessment. *Bridge Surveyor Conference*, London, UK, 1998.

[4] Johansen, K. W. *Yield Line Theory.* Cement and Concrete Association, London, UK, 1962.

[5] http://www.cobras.co.uk

[6] http://www.mosek.com

[7] Andersen, K. D., Christiansen, E. and Overton, M. L. Computing limit loads by minimizing a sum of norms. *SIAM Journal on Scientific Computing*, 19(3):1046–1062, 1998.

[8] Christiansen, E. and Pedersen, O. Automatic mesh refinement in limit analysis. *International Journal for Numerical Methods in Engineering*, 50(6):1331 – 346, 2001.

[9] Van Rij, H. M. and Hodge, P. G. A slip model for finite element plasticity. *Transactions of the ASME, Journal of Applied Mechanics*, 45:527-532, 1978.

[10] Sloan, S. W. and Kleeman, P. W. Upper bound limit analysis using discontinuous velocity fields. *Computer Methods in Applied Mechanics and Engineering*, 127:293-314, 1995.

[11] Alwis, W. A. M. Discrete element slip model of plastity. *Engineering Structures*, 23:1494–1504, 2000.

Chapter 8

Conclusions and Recommendations for Further Work

8.1 Introduction

The work described in this thesis can be divided into three sections: limit analysis of RC slabs, limit analysis of masonry structures and application of computational limit analysis to masonry structures. Conclusions related to each section will be grouped together.

8.2 Limit analysis of RC structures

1. A novel limit analysis method for RC slabs has been developed (the 'Sheffield method'), and implemented in a computer program. The method uses a discrete description of the slab as an assemblage of elements. A kinematic approach is adopted in the problem formulation. Translational displacements at

interfaces between elements are permitted in order to account for the fact that critical yield lines may reside inside elements rather than on elements edges.

2. In order to evaluate the merits of permitting translational displacements (or non-zero shear forces in the static (equilibrium) formulation), results from the program have been compared with existing solutions from the literature for a number of cases. The results obtained agree quite well with known exact solution for different slab configurations and boundary conditions.

3. The fixed edged square slab case demonstrated how regular meshes can capture complicated displacement contours near to the slab corners.

4. The Sheffield method appeared, in the majority of cases, to be capable of producing a solution using a variety of different element geometries, unlike other methods such as that proposed by Munro and Da Fonseca. For example, no feasible solution will be found if the Munro and Da Fonseca method is used to find the critical yield line pattern for simply or fixed edged square slabs if quadrilateral elements are used instead of triangular elements.

5. Using the Sheffield method a close estimate of the exact solution can normally be obtained.

6. In most cases the solution converged to the exact solution regardless to the element type, provided that a sensible value for the shear factor is used.

7. In the cases where the exact solution for the load factor is obtained, refining the mesh further does not lead to any change in the load factor.

8. The Sheffield method was found, in the majority of cases, to identify sensible failure patterns in terms of displacement contours.

9. It was found that it is possible to obtain true upper-bound solutions using a two-phase version of the method.

10. It was also found that solutions obtained, when the Sheffield method was initially used to set-up the problem for phase 2, gave lower load factors compared to solutions obtained when the Munro and Da Fonseca method was initially used to set-up the problem for phase 2.

8.3 Limit analysis of masonry structures

1. A new computational limit analysis procedure for rigid block assemblages comprising non-associative frictional interfaces has been presented. The proposed method involves solving a series of LP problems with successively modified failure surfaces.

2. The proposed method appears to be capable of quickly ascertaining whether associative and non-associative solutions differ.

3. The method was also found to identify 'good' estimates of the load factor for a wide range of problems (in all cases tried the computed load factors were less than or equal to published MCP values and within a few percent of published MPEC values).

4. The method appears to be particularly suited to comparatively large problems. For one such problem contained in the literature it was found that the computed load factor was virtually identical, but this was obtained two orders of magnitude more quickly.

8.4 Practical application of computational limit analysis: masonry arch bridges

1. Recent developments to the RING masonry arch bridge analysis software have been described. Additional features such as a non-associative constitutive model for sliding friction and a gross displacement analysis capability have been discussed.

2. The software has been applied to a number of typical local authority bridges. Significant improvements of the computational efficiency of RING 1.5 compared with its predecessor RING 1.1 have been demonstrated.

3. The rigid block analysis method has been found to provide a conceptually simple, yet powerful and efficient means of determining the critical collapse mechanism and associated load factor for arch bridges, whether the latter contain single or multiple spans and/or arch rings.

4. Although arguably more realistic, it was found that non-associative friction and gross displacement analysis were computationally expensive. It will remain up to the judgment of the assessment engineer as to whether this additional expense is justified.

5. It was found that the gross displacement analysis procedure will always predict lower load capacities than the normal (infinitesimal displacement) analysis procedure.

8.5 Overall conclusions

1. The numerical procedures for limit analysis methods presented here are conceptually simple, computationally efficient, yet describable.

2. The computer programs which have been developed based on these methods have shown that the limit analysis approach has the potential for becoming a powerful and a widely used numerical analysis tool for RC slabs and masonry structures. The approach can be used by non-specialists as the results of the analyses do not require the kind of interpretation normally required when post processing finite element program results. Limit analysis should certainly be considered in situations where the use of more complex analysis tools is not justified.

8.6 Recommendations for further work

Numerical procedures developed based on the concepts of limit analysis can be extended and modified. Particular suggestions and amendments are as follows:

8.6.1 Limit analysis of RC structures

A rigorous derivation of the shear factor used in the Sheffield method is an obvious initial step to be taken. This will facilitate other amendments to the method. In detail these are:

8.6.1.1 Investigating methods to reduce computer time

In the majority of the cases which have been investigated using the Sheffield method, the load factor which has been obtained when using a moderate number of divisions per side was usually between 0-10% different to the exact load factor. There is a belief that the exact load factor will be obtained when the size of the elements tends to zero. This is however clearly not a practical option. Therefore, adaptive

discretization strategies to reduce computer time can be useful. Adaptive mesh refinement in limit analysis has been investigated by Christiansen and Pedersen [1] and it has been found to generally perform well. Another approach is to use Richardson's extrapolation to extrapolate the load factor at very small element sizes. It can also be used to estimate errors [2].

8.6.1.2 Investigating other techniques to improve the overall performance of the Sheffield method

Including allowances for the enhancement to the ultimate load capacity of laterally restrained slab strips offered by the membrane action in the Sheffield method will make the predictions obtained by the method more reliable. Ideas developed in the limit analysis of masonry structure can be utilized to develop a method which combines membrane analysis and yield line analysis in one formulation.

8.6.1.3 Applying a similar technique to in-plane analysis of slabs

The idea of allowing discontinuity in the velocity fields between elements at interfaces can be applied to in-plane slab analysis problems. For instance, work carried out by Poulsen and Damkilde [3] could provide the basis for such a method.

8.6.1.4 Material optimization

As mentioned in the third chapter, one of the outcomes from the European Concrete Building Project at Cardington was that the yield line design of concrete flat slabs was found to be '*easily the best opportunity identifiable to the concrete frame industry*'. Therefore, an automated method for an optimum of design of RC slabs will be practically useful.

A computer program for an optimum design of RC slabs based on the yield line method can be developed by extending the formulation of the Sheffield method to consider material optimization. Material optimization using limit analysis has been considered by Borkowski [4], Da Fonseca *et al.* [5], Krenk *et al.* [6] and has been shown that considerable material savings can be achieved.

8.6.2 Limit analysis of masonry structures

8.6.2.1 3D analysis of masonry structures

Extending the rigid block method of analysis capability to three dimensions is an obvious next step. A 3D model will enable the computer program to tackle problems involving asymmetric loading on an arch barrel, and could also be adapted to model skew bridges, presently difficult to analyse accurately in 2D. It will also enable the assessment of masonry domes and vaulted structures.

8.6.2.2 Improving soil-structure interaction model

Gross displacement analysis has been found to provide a way of improving the modelling of soil-structure interaction. However, in common with similar simplified elastic models, a problem is that the method requires that pressure distribution are known in advance of an analysis. This is unsatisfactory and a more detailed model in which the arch and the soil are both modelled explicitly is really required.

References

[1] Christiansen, E. and Pedersen, O. Automatic mesh refinement in limit analysis. *International Journal for Numerical Methods in Engineering*, 50(6):1331 - 346, 2001.

[2] Andersen, K. D., Christiansen, E. and Overton, M. L. Computing limit loads by minimizing a sum of norms. *SIAM Journal on Scientific Computing*, 19(3):1046–1062, 1998.

[3] Poulsen, P. N. and Damkilde, L. Limit state analysis of reinforced concrete plates subjected to in-plane forces. *International Journal of Solids and Structures*, 37(42):6011–6029, 2000.

[4] Borkowski, A. Optimisation of slab reinforcement by linear programming. *Institue of Fundamental Technological Research , Polish Academy of Sciences, Varsaw, Poland*, 1976.

[5] Figueiredo, A. J. M., Da Fonseca, A. and Azevedo, A. F. M. Analysis and optimization of reinforced concrete slabs. In Hernandez S., Kassab A. J., and Brebbia C. A., editors, *Computer Aided Optimum Design of Structures VI*, 237–246, Southampton, UK, 1999.

[6] Krenk, S., Damkilde, L. and Hoyer, O. Limit analysis and optimal-design of plates with equilibrium elements. *Journal of Engineering Mechanics-ASCE*, 120(6):1237–1254, 1994.

Appendix A

The computational efficiency of two rigid block analysis formulations for application to masonry structures

H. M. Ahmed and M. Gilbert

Department of Civil & Structural Engineering

University of Sheffield, Sheffield, United Kingdom

A.1 Abstract

† Rigid block analysis is a computational limit analysis method which is now widely applied to the analysis of masonry gravity structures such as arch bridges. Various

† Paper presented at "The Ninth International Conference on Civil and Structural Engineering Computing", Egmond-aan-Zee, the Netherlands, September 2003.

formulations of the rigid block analysis method have been proposed, with linear programming (LP) generally being used in the solution process. However, there appears to be little information in the literature on the relative computational efficiencies of the various formulations (when used either with traditional Simplex or newer interior point LP solvers). Thus a 'redundant forces' formulation put forward previously by the second author is here compared with an alternative 'joint equilibrium' formulation. It is found that the joint equilibrium formulation is the most computationally efficient formulation when applied to complex geometrical arrangements of blocks, such as those found in multi-ring arches.

Keywords: limit analysis, masonry arch bridges, rigid block, linear programming, joint equilibrium, redundant forces.

A.2 Introduction

In recent years limit state analysis methods for masonry gravity structures have been extensively studied. One particularly important practical application has been the determination of the ultimate carrying capacity of masonry arch bridges. This is also the main application considered in this paper. In the case of masonry arch bridges the objective of most limit analysis procedures is to determine the magnitude of the load which just transforms the structure into a mechanism. Thus the simplest limit analysis methods for single-span arches typically assume that ultimate failure occurs when four hinges form. Assuming the masonry possesses infinite compressive strength, these hinges can be assumed to form on the extrados (outer surface) and the intrados (inner surface) of an arch, with, at failure, the thrust line (i.e. the line through the resultants of the compressive stresses in successive cross sections) passing through the hinges which form alternately on the extrados and intrados. Since at the hinge points bending moments are zero, it is then possible to use

statics to determine the magnitude of the applied load which will cause collapse. This was demonstrated by Pippard [1] and the approach was later placed securely within the framework of plastic limit analysis by Heyman [2]. Thus, a 'mechanism' (or 'upper-bound') limit analysis involves an assumed hinge configuration with the lowest upper-bound solution being the correct one since in this case the thrust line between hinges will lie entirely within the arch. Thus in this case the 'safe' (or 'lower-bound') theorem is also satisfied (the latter states that if a thrust line can be found for the complete arch which is in equilibrium with the external self weight and which lies every where within the masonry of the arch ring, then the arch is 'safe'). However, because of the complexity of arch bridge geometry coupled with the complex loading patterns typically found in practice, hand-based limit analysis is not generally practicable. Additionally, some of Heyman's original assumptions are no longer considered generally acceptable (e.g. infinite masonry crushing strength; no sliding failures). Hence various computer-based methods have been proposed [3, 4, 5, 6]. These methods use either rigorous or ad-hoc optimization techniques to identify the critical failure mode. Among these methods, the rigid block method of analysis [5, 6] is the most generally applicable and may for example easily be applied to arch problems involving multiple arch rings and/or spans. The simple rigid block analysis software 'RING', which was originated by the second author [7, 8], is now widely used by practitioners worldwide to analyse masonry bridges. However, although the RING software can solve most simple single and multi-span problems almost instantaneously as far as the user is concerned on a modern PC, it has been found that execution times for more demanding multi-ring problems are often undesirably long, even when a state-of-the-art PC is employed (e.g. see Fig. A.1 for sample multi-span and multi-ring analysis screen displays). Exploring ways of reducing execution times has been the main stimulus for the present study of alternative rigid block analysis problem formulations.

A.3 Rigid block analysis: alternative problem formulations

Most researchers working on rigid block analysis have presented lower-bound 'equilibrium' formulations, as first proposed by Livesley [5]. Conversely, Gilbert and Melbourne presented a 'mechanism' formulation [6, 9]. However, the choice as to whether an 'equilibrium' or 'mechanism' formulation is used is essentially merely a matter of preference since when these formulations are linearized they give rise to dual linear programming problems (and modern linear programming solvers can easily switch between these, or solve both simultaneously). More important is the particular choice of problem variables and constraints. According to the classification of LP formulations presented by Tam and Jennings for plastic frame design [10], Livesley's original equilibrium formulation may be classified as a 'joint equilibrium' approach. In this approach the problem variables comprise both the interface forces and the resultant forces acting on each and every block. Conversely, Gilbert and Melbourne's formulation for single and multi-span arch bridges may be classified as a 'redundant forces' approach (though the dual form of this was actually presented). In this approach the problem variables are both the interface forces and (only) the redundant forces.

In general the redundant forces method will produce LP tableaux containing fewer variables and constraints than the joint equilibrium method, a feature which made it attractive to the second author when developing a rigid block method for masonry arches some years ago [6]. However, in the case of multi-ring arch problems, a problem with the redundant forces method is that the presence of inter-ring contacts leads to numerous redundant forces (i.e. additional forces at every contact point on the interface between rings). Hence the resulting tableaux, although compact, will be very heavily populated with non-zero elements; this can be quite computa-

tionally expensive to solve. A recent reappraisal of the situation has also indicated that modern LP methods (i.e. interior-point based LP methods) may in fact be well suited to the solving the type of large sparse tableaux produced by the joint equilibrium method; this will be investigated in this paper.

A.4 Rigid block analysis: two dual LP formulations

This section identifies similarities and differences between joint equilibrium and redundant forces formulations. However, maintaining the authors' previous preference for mechanism (or 'kinematic') formulations, the dual of these will be presented.

The problem in hand concerns an assemblage of rigid blocks comprising m interfaces separating n blocks (this includes notional boundary support blocks in the case of the joint equilibrium formulation and [only] redundant support blocks in the case of the redundant forces formulation).

The constituent blocks may initially be assumed to be both rigid and infinitely strong. Suppose also that the assemblage is subjected to both dead load $\mathbf{p}$ and live loading $\mathbf{q}$. The dual problem is to find the minimum load factor λ which when applied to live loading will lead to collapse. This problem can be formulated using an approach based on virtual work, as:

$$\text{Minimize } \lambda\,|\mathbf{q}|\,[1] = \mathbf{p}^{\mathrm{T}}\mathbf{d} \tag{A.1}$$

where the whole structure live load, dead load and displacement vectors are denoted respectively $\mathbf{q}^{\mathrm{T}}=\{q_1,q_2,\ldots,q_n\}$, $\mathbf{p}^{\mathrm{T}}=\{p_1,p_2,\ldots,p_n\}$, and $\mathbf{d}^{\mathrm{T}}=\{d_1,d_2,\ldots,d_n\}$. And

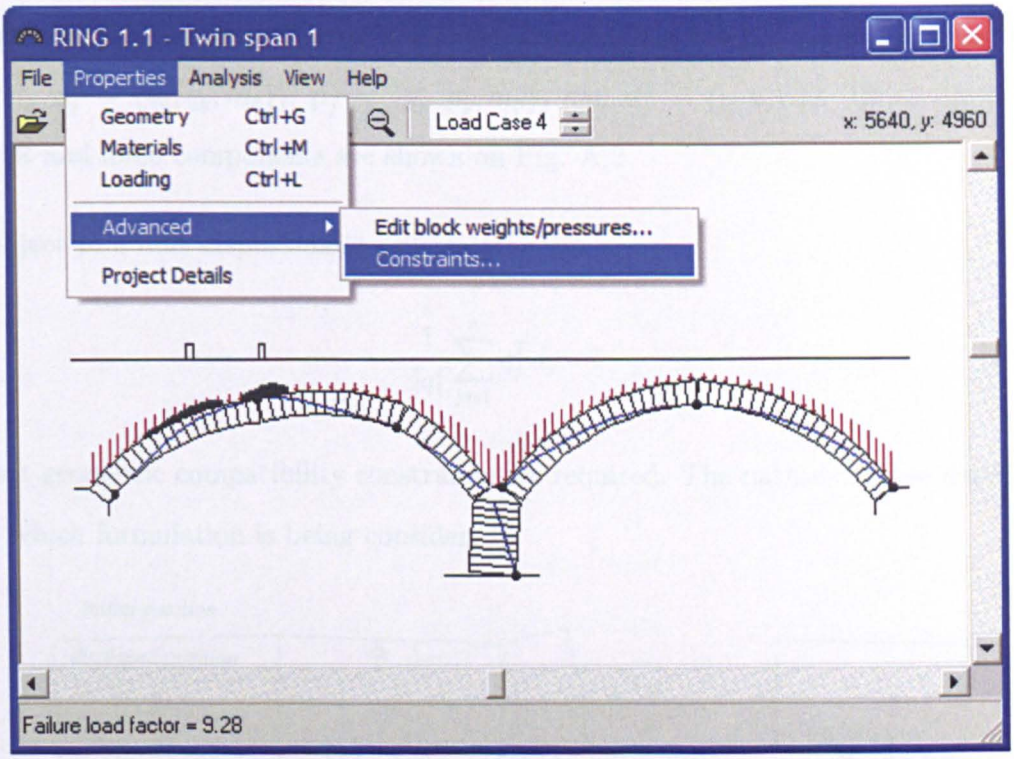

(a)

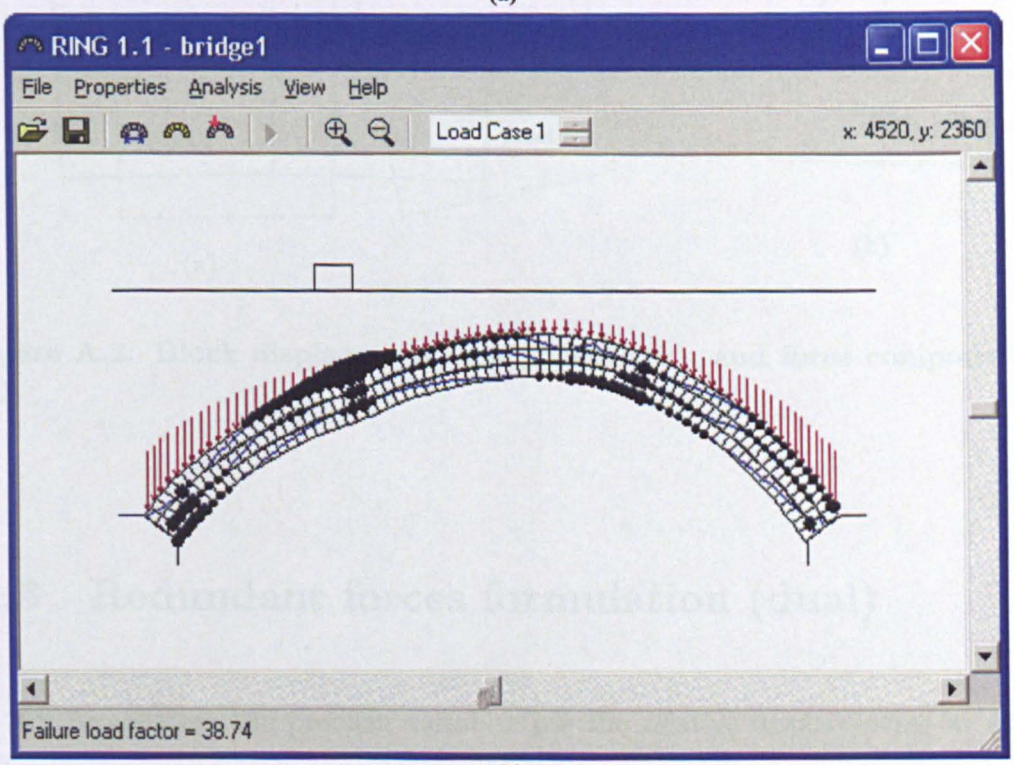

(b)

Figure A.1: Sample RING output: (a) Multi-span; (b) Multi-ring arch analysis

where the block live load, dead load and displacement vectors are denoted respectively $\mathbf{q}_j^{\mathrm{T}} = \{q_x, q_y, m_q\}_j$, $\mathbf{p}_j^{\mathrm{T}} = \{p_x, p_y, m_p\}_j$ and $\mathbf{d}_j^{\mathrm{T}} = \{u, v, \phi\}_j$. Block displacement and force components are shown on Fig. A.2.

Subject to a unit displacement constraint:

$$\frac{1}{|q|}\sum_{j=1}^{n} q_j^T d_j = 1 \tag{A.2}$$

Next geometric compatibility constraints are required. The nature of these depends on which formulation is being considered.

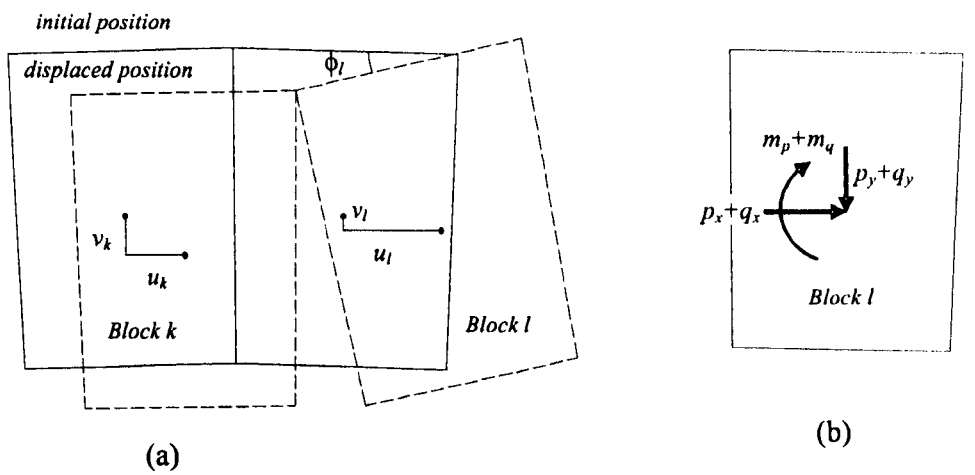

Figure A.2: Block displacement components (a), and force components (b)

A.5 Redundant forces formulation (dual)

In this formulation the problem variables are the relative displacements at each interface i. The absolute displacement components of block j are in this formulation not defined as problem variables. However, the displacement of block j can be expressed as a function of the relative rotations between adjacent units lying between

the block and a datum fixed support. i.e as:

$$\boldsymbol{d}_j = \mathbf{A}_j\mathbf{r} + \mathbf{B}_j\mathbf{s} \tag{A.3}$$

where $\mathbf{A}_j$ and $\mathbf{B}_j$ are suitable transformation matrices derived from the geometry of the structure (see reference [9] for further details); $\mathbf{r}^{\mathrm{T}}=\{\mathbf{r}_1, \mathbf{r}_2, ..., \mathbf{r}_m\}$, where $\mathbf{r}_i^{\mathrm{T}}=\{\theta_i^A, \theta_i^B\}$ and where θ_i^A, θ_i^B respectively represent rotations about endpoints A and B of interface i ($\theta_i^A, \theta_i^B \geq 0$). And where $\mathbf{s}^{\mathrm{T}}=\{\mathbf{s}_1, \mathbf{s}_2, ..., \mathbf{s}_m\}$,where $\mathbf{s}_i^{\mathrm{T}}=\{y_i^+, y_i^-\}$ and where y_i^+, y_i^- are the positive and negative sliding displacements on interface i ($y_i^+, y_i^- \geq 0$). Note also that $\mathbf{B}_j$ is formed using the usual LP limit analysis assumption that the normality rule holds when sliding occurs. i.e. normal displacements of magnitude $s_b(y_i^+ + y_i^-)$ occur, where s_b is the coefficient of dilatant friction between blocks.

With the dual redundant forces formulation the number of geometrical compatibility constraints required equals to the number of redundant forces. e.g. for a single span arch the requisite compatibility constraint is:

$$d_n = \begin{bmatrix} u_n \\ v_n \\ \phi_n \end{bmatrix} = \begin{bmatrix} 0 \\ 0 \\ 0 \end{bmatrix} \tag{A.4}$$

(where block n is a fixed abutment block remote from the datum fixed support).

A.6 Joint equilibrium formulation (dual)

In this formulation the problem variables comprise both the relative displacements at each interface and the absolute displacements of each block. Thus for an interface i between two blocks k and l(e.g. see Fig. A.2), the requisite joint compatibility

constraint may be defined as follows:

$$\boldsymbol{d}_i - \boldsymbol{d}_k = \mathbf{C}_i\mathbf{r}_i + \mathbf{D}_i\mathbf{s}_i \tag{A.5}$$

where $\mathbf{C}_i$ and $\mathbf{D}_i$ are suitable compatibility matrices. Note that $\mathbf{D}_i$ is formed using the usual LP limit analysis assumption that the normality rule holds when sliding occurs. Finally, boundary conditions may readily be prescribed using this formulation. e.g. if block n is to be fixed in space then constraint (A.4) should be imposed.

A.7 Solution

Once the objective function, variables and constraints have been defined, any standard linear programming technique can then be used to obtain a solution for λ. Note though that if it is found that there is 'no feasible solution' to the problem this is likely to be because the structure is geometrically locked. Alternatively the solution may be found to be 'unbounded' which indicates that the structure is unstable under dead loads alone

A.8 Case study problems

A.8.1 Multi-ring brickwork arch rib problem

A fictitious multi-ring arch problem containing a reasonably large number of rings and units per ring was set up in order to test the efficiency of both the redundant forces and joint equilibrium formulations. The problem specification is given in Fig. A.3. To solve the problem three different LP solvers were used. These were: the commercial Xpress MP Simplex based solver (version 12); the publicly available

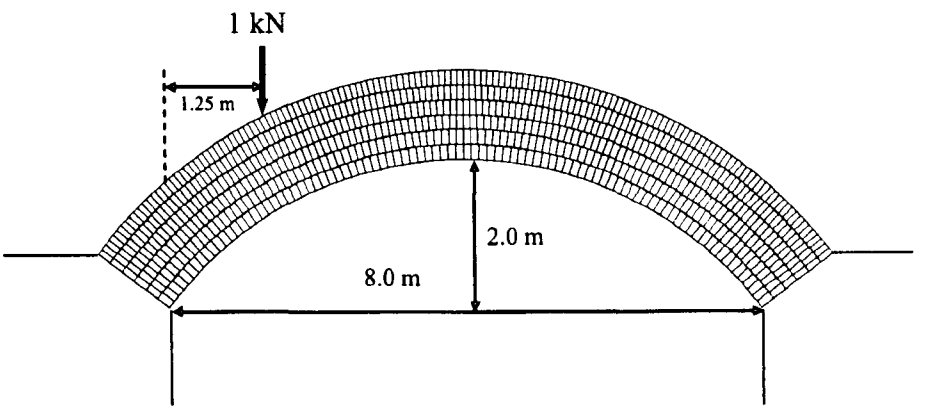

Figure A.3: Case study problem: multi ring arch subject to a concentrated load

PCx interior point solver (version 1.1) used currently by RING and the commercial Mosek interior-point solver (version 2.0). Figure A.4 shows the predicted collapse mechanism for this problem. Note that the load factor and associated mechanism were essentially identical irrespective of problem formulation or solver used (load factor = 47.7). Finally, Fig. A.5 shows the execution times for both the joint equilibrium and the redundant forces formulations (all problems were run on a 800MHz Pentium III PC running Microsoft Windows NT).

It is evident from Fig. A.5 is that a very substantial saving in CPU time is realisable when the joint equilibrium formulation is used. This is because although a much greater number of variables and constraints are present in this case, the proportion of non-zero elements in the LP tableau is much reduced compared with that in the redundant forces formulation. This greatly speeds the solution process when using most modern linear programming solvers, particularly those based on interior point methods.

It is also evident that for this type of problem that whilst the Simplex solver solves

Parameter	Value
Number of rings	6
Number of blocks	90/100/110/120/130/140
Ring thickness	0.2m
Arch width	1.0m
Friction coefficient	0.6 (radial), 0.0 (tangential)
Unit weight	18.0kN/m^3

Table A.1: Multi-ring brickwork arch rib: geometrical and material properties

the redundant forces problem approximately 8× more quickly than the two interior-point solvers tried, conversely the interior-point solvers solve the joint equilibrium problem up to 8× more quickly than the simplex solver.

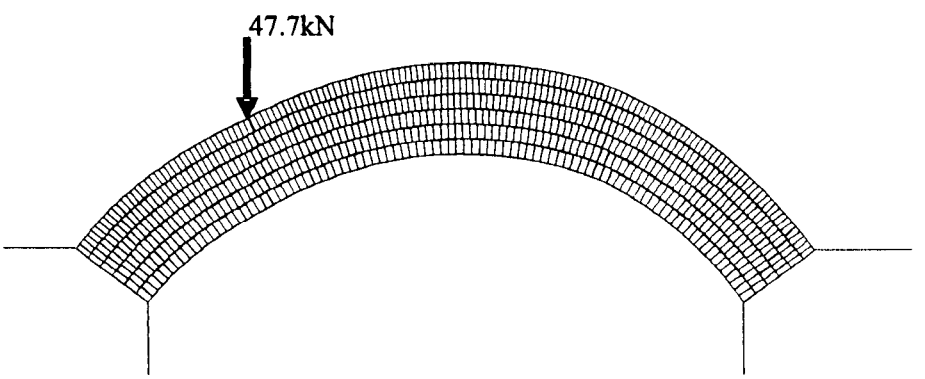

Figure A.4: Benchmark problem: predicted collapse mechanism and load

A.8.2 Multi-span arch rib problem

As mentioned previously, it is known that the redundant forces method works well with simple 2D single and multi-span arch problems. However, a case study problem was set up to check the performance of the joint equilibrium formulation for such problems. A fictitious problem containing several hundred blocks was selected so as to represent the upper end of the size of problem likely to routinely tackled by assessment engineers. The problem specification is given in Fig. A.6. In this

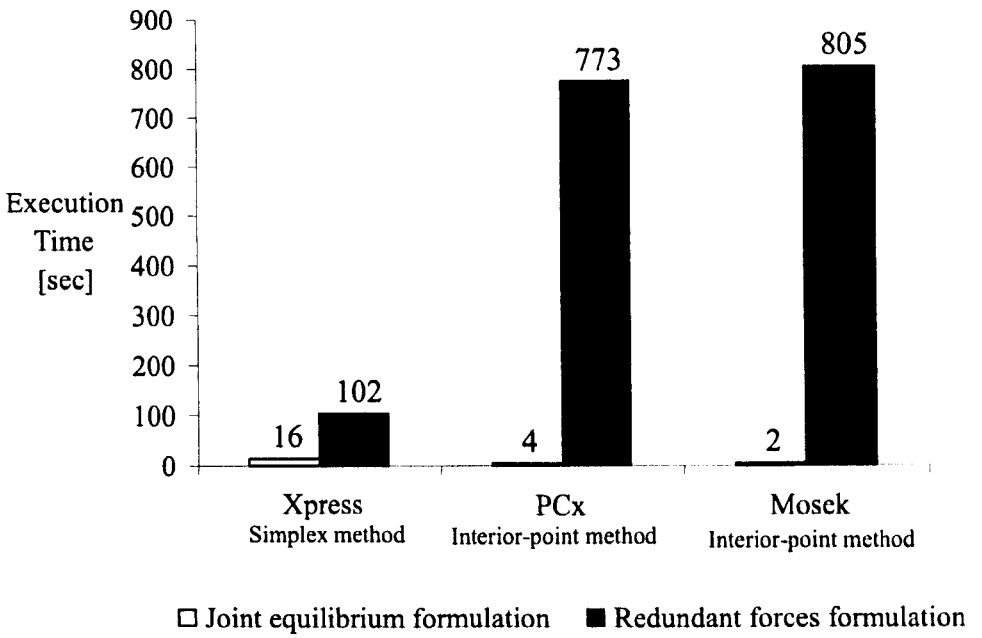

Figure A.5: Case study problem: execution times for different problem formulations & LP solvers

case the problem was solved quite quickly whichever formulation was used. The redundant forces formulation was solved in 0.05 and 0.1 seconds using the PCx and Mosek solvers respectively. When the joint equilibrium formulation was used run times were somewhat longer, being 0.22 and 0.20 seconds using the PCx and Mosek solvers respectively (these problems were solved using a 1.6GHz Athlon PC running Windows XP Professional). The computed failure load for this structure was 91.3kN.

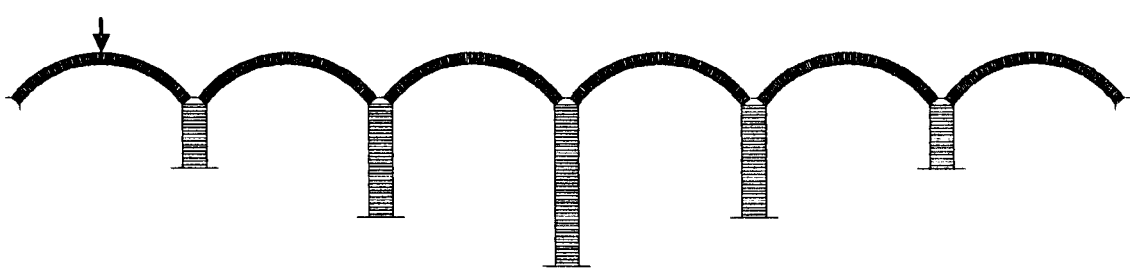

Figure A.6: Case study problem: multi span arch rib subject to a concentrated load (at midspan of span 1)

Parameter	Value
Number of spans	6
Span	5m
Rise	1.25m
Number of rings	1
Number of blocks per ring	100
Ring thickness	0.33m
Number of piers	5
Pier thickness	0.75m
Pier heights	2.5m/3.5m/5m/3.5m/2.5m
Number of blocks per pier	25/35/50/35/25
Arch width	1.0m
Coefficient of friction	0.65
Unit weight	18.0kN/m^3

Table A.2: Multi-span arch rib: geometrical and material properties

A.9 Discussion

The greater efficiency of the joint equilibrium formulation in solving 'difficult' multi-ring problems means that this has now been incorporated into a new version of the masonry arch bridge analysis software RING [7]; this will be made publicly available via the website [8] shortly. Using the joint equilibrium formulation it is also much easier to automatically set up and solve general two and three dimensional rigid block problems. However, there is an important proviso: the formulation described here assumes the principle of normality holds true when blocks slide relative to each other [i.e. an associated flow rule is assumed]. Drucker [11] has shown that results from an analytical model in which frictional interfaces are modelled in this way will be upper-bounds on the 'exact' values whilst Livesley [5] discussed this issue in the context of rigid block analysis. In many cases the difference between computed load factors obtained when an associated flow rule is, or is not, assumed to hold true will be small. Unfortunately though, this cannot be guaranteed and the magnitude of the difference will generally be highly problem dependent. Thus in the case of multi-ring brickwork arch bridges it has been found that a rigid block analysis which

incorporated associative friction produced computed results which agreed quite well with experimental results [12] (in fact the analysis typically slightly underestimated actual bridge strength). However, when some other geometrical configurations of blocks are considered the importance of modelling friction as non-associative is likely to be greater. For example, consider the block wall problem shown in Fig. A.7. Here the computed (associative) load factor was 0.33195, yet Ferris and Tin Loi [13] have obtained a non-associative load factor for this problem of 0.26374. This lower load factor is some 20 percent lower; it is also possible that an even lower non-associative load factor will be found for this problem in the future. In fact this is very much an active research area at present, with useful work being carried out recently by workers such as Baggio and Trovalusci [14] and Ferris and Tin-Loi [13]. Unfortunately the methods proposed to date have tended to rely on the use of rather specialised solution algorithms (not LP). It is also generally observed that when using such algorithms, problems quickly become intractable as their size increases. However, a new method for treating non-associative friction is currently under development by the authors. The method involves successively solving a series of modified LP problems. Initial results are extremely promising and details will be published soon. Finally, a note about the assumption of infinite material strength made in this paper. Though methods of including material crushing have not been discussed here, crushing can readily be included in most formulations, e.g. see reference [15].

Parameter	**Value**
Block dimensions	4×1.75 (2×1.75)
Dead load per block	1 (0.5)
Horizontal ('earthquake') live load per block	1 (0.5)
Coefficient of friction	0.65

Table A.3: Typical masonry wall analysis problem: geometrical and material properties

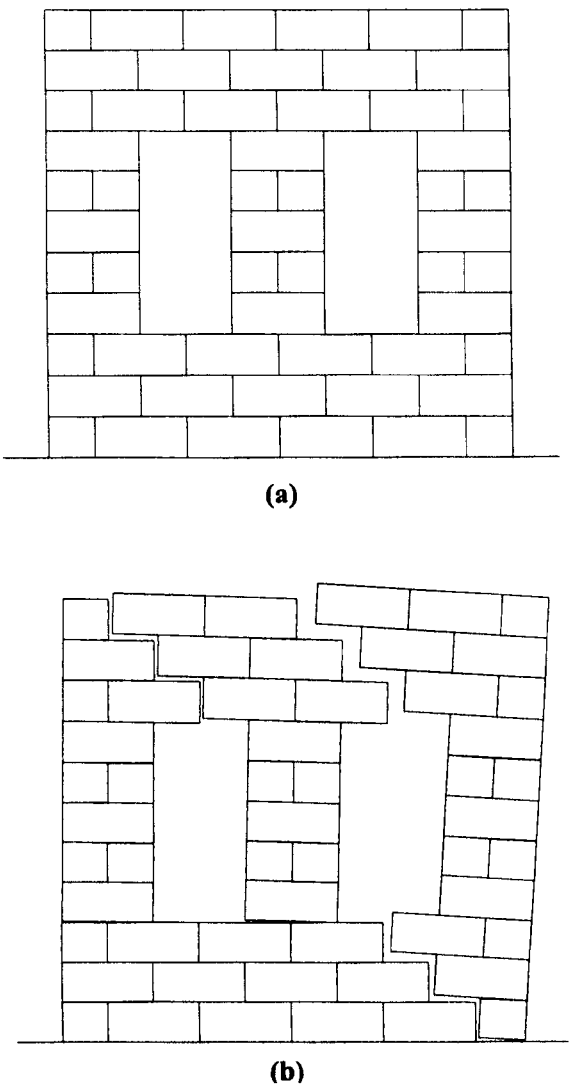

Figure A.7: Typical masonry wall analysis problem: (a) initial geometry, (b) predicted collapse mechanism (assuming normality at frictional interfaces)

A.10 Conclusions

This paper has compared joint equilibrium and redundant forces rigid block analysis formulations. For multi-ring masonry arch problems the joint equilibrium formulation appears to be much more computationally efficient than the redundant forces formulation. Consequently a joint equilibrium formulation is currently being incorporated into the now widely used RING software and a new version of this should

be publicly available later in 2003. The joint equilibrium approach is also much easier to apply to arbitrary assemblages of blocks. However, if frictional interfaces are modelled using an associated flow rule, as is common in LP limit analysis, then results must be treated with some caution. A new iterative LP based method of treating non-associative friction in rigid block analysis is currently being tested by the authors; further details will be published shortly.

A.11 Acknowledgements

The first author holds a studentship sponsored by EPSRC. Additionally the authors acknowledge the financial support provided by Network Rail (formerly Railtrack plc) to permit continued development of the RING masonry arch bridge analysis software.

References

[1] Pippard, A. J. S. and Baker, J. F. *The analysis of engineering structures.* Arnold, London, 1943.

[2] Heyman, J. *The masonry arch.* Ellis Horwood, Chichester, UK, 1982.

[3] Harvey, W. J. The application of the mechanism method to masonry arch bridges. *The Structural Engineer*, 66(5):77–84, 1988.

[4] Crisfield, M. A. and Packham, A. A mechanism program for computing the strength of masonry arch bridges, December 1987. TRL research report 124, DoT, UK.

[5] Livesley, R. K. A. Limit analysis of structures formed from rigid blocks. *International Journal for Numerical Methods in Engineering*, 12:1853–1871, 1978.

[6] Gilbert, M. and Melbourne, C. Rigid-block analysis of masonry structures. *The Structural Engineer*, 72:356–360, 1994.

[7] Gilbert, M. RING: a 2D rigid-block analysis program for masonry arch bridges. *Proceedings of the 3rd International Arch Bridges Conference*, Paris, 2001.

[8] http://www.shef.ac.uk/ring

[9] Melbourne, C. and Gilbert, M. Modelling masonry arch bridges. In Bull J., editor, *Computational Modelling of Masonry, Brickwork and Blockwork Structures*, 197–220, Saxe-Coburg, 2001.

[10] Tam, T. and Jennings, A. Automatic plastic design of frames. *Engineering Structures*, 8(3):139–147, 1988.

[11] Drucker, D. C. Coulomb friction, plasticity, and limit loads. *Journ. Appl. Mec. Trans. ASME*, 21(4):71–74, 1954.

[12] Gilbert, M. and Melbourne, C. Collapse behaviour of multiring brickwork arch bridges. *The Structural Engineer*, 73:39–47, 1995.

[13] Ferris, M. C. and Tin-Loi, F. Limit analysis of frictional block assemblies as a mathematical program with complementarity constraints. *International Journal of Mechanical Sciences*, 43(1):209–224, 2001.

[14] Baggio, C. and Trovalusci, P. Limit analysis for no-tension and frictional three-dimensional discrete systems. *Mechanics of Structures and Machines*, 26:287–304, 1998.

[15] Gilbert, M. On the analysis of multi-ring brickwork arch bridges. *Proceedings of the 2nd International Arch Bridges Conference*, 109–118, Venice, 1998.

Appendix B

Mathematical Programming

B.1 Introduction

Broadly speaking, Mathematical Programming (MP) is a mathematical technique applied to a special class of problems, where the main concern is to minimize or maximize a real function of real or integer variables, subject to certain constraints. The scope of mathematical programming is wider than just the calculation of the minimum or the maximum value for a real function in a certain problem, it also includes the study of these problems; their mathematical properties, the development and implementation of algorithms to solve these problems, and the application of these algorithms to real world problems. It should be noted that "programming" does not specifically refer to computer programming. In fact, the term "mathematical programming" antedates computers and means 'preparing a schedule of activities'. Mathematical programming embraces algorithms and heuristics specifically designed to address certain problems. The main features of MP [1] are shown graphically in Fig. B.1.

The MP model which has been abstracted from a real world (or artificial) problem comprises:

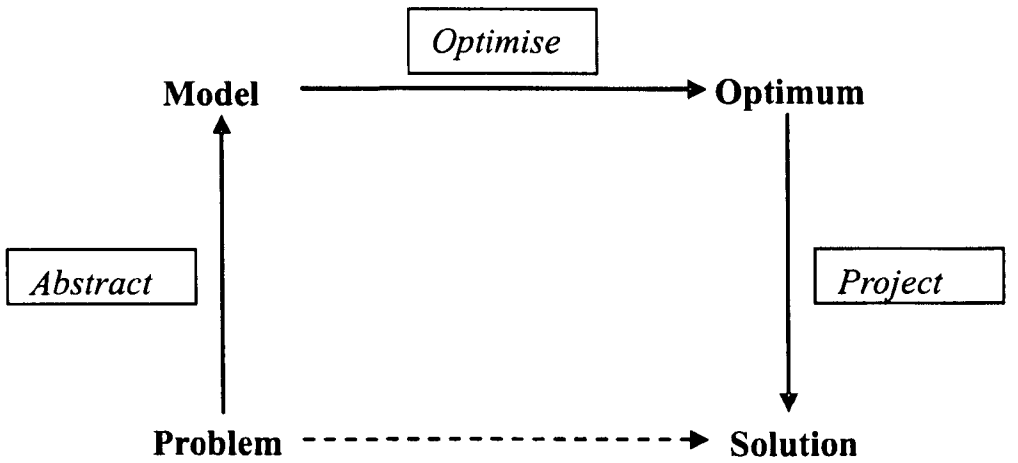

Figure B.1: Mathematical programming features

- a set of **decision variables**, whose values are to be determined;
- the relationships between these variables, known as the **constraints**;
- a means of comparing the quality of solutions which satisfy the constraints, **the objective function**.

Mathematical programming models include linear programming, quadratic programming, and dynamic programming. However the main focus will be on linear programming (LP) as it has been used exclusively in this work.

A full explanation of LP theory can be found in a number of good books, most notably, Dantzig [2], Nash *et al.* [3], Luenberger [4], Garvin [5] and Bazaraa *et al.* [6]. Recently, Vanderbei [7] published a good textbook which covers interior point LP algorithms.

B.2 Linear programming

Linear programming is a mathematical technique, in which a linear function is maximized (or minimized) subject to given a set of linear constraints on these variables

(equalities or inequalities). An LP problem can be expressed as follows (the so-called 'standard form'):

minimize:

$$h(x) = \mathbf{c}^T\mathbf{x} \tag{B.1}$$

subject to

$$\left.\begin{aligned} \mathbf{Ax} &= \mathbf{b} \\ \mathbf{x} &\geq \mathbf{0} \end{aligned}\right\} \tag{B.2}$$

where $\mathbf{x}$ is the vector of variables to be solved for, $\mathbf{A}$ is a matrix of known coefficients, and $\mathbf{c}$ and $\mathbf{b}$ are vectors of known coefficients. The expression h(x) is called the objective function, and the equations $\mathbf{A}$ are called the constraints. All these entities must have consistent dimensions.

The matrix $\mathbf{A}$ is generally not square, hence LP cannot be solved simply by just inverting $\mathbf{A}$. Usually $\mathbf{A}$ has more columns than rows, and $\mathbf{Ax=b}$ is therefore quite likely to be under-determined, offering great latitude in the choice of $\mathbf{x}$ which will minimize h(x).

The importance and the success of linear programming derives in part from its numerous applications. Many real-world phenomena can be approximated reasonably well by linear relationships. There are robust solvers which find the best solution to LP problems rapidly. These solvers are fast and reliable over a substantial range of problem sizes and applications. Unlike non-linear programming, the LP computation time does not increase rapidly as the problem size increases.

B.3 Methods of solution

Two different solution techniques are widely in use nowadays: the Simplex method and interior-point methods. Both methods visit a progressively improving series of

trial solutions, until a solution is reached that satisfies the conditions required of an optimum.

B.3.1 The Simplex method

One of the important properties of linear programmes is that the optimal solution can be found among the extreme points of the convex set of 'basic feasible solutions'. which represents the extreme boundary points of the feasible region defined by $\mathbf{Ax} = \mathbf{b}$, $\mathbf{x} \geq \mathbf{0}$. The Simplex methods, as introduced by Dantzig [2], systematically evaluate "basic" solutions by setting the value of enough variables to their bounding values to convert the constraints $\mathbf{Ax} = \mathbf{b}$ to a square system, which can then be solved for unique values of the remaining variables. The process continues until a terminal status is reached. This occurs when either (i) a finite optimal solution is found (ii) an infinite optimal solution is positively identified, or (iii) conclusive evidence is obtained that the problem has no feasible solution.

B.3.2 Interior-point methods

Although interior-point methods (in some form) have been used by McCormick and Fiacco [8] in solution techniques adopted for non-linear programming, which were developed and popularised in the 1960s, they were not applied to linear programming problems until the 1980s. The first interior-point method was introduced by Karmarkar [9] in 1984. In contrast to the Simplex method, 'barrier', or 'interior-point', methods visit points within the interior of the feasible region defined by $\mathbf{Ax} = \mathbf{b}$, $\mathbf{x} \geq \mathbf{0}$. The method is based on an algorithm which generates iterates that lie in the interior of the feasible region. Interior-point methods are now generally considered competitive with the Simplex method for small problems and superior for large problems.

B.4 The concept of duality

Associated with any standard LP problem is another LP, called the 'dual' problem. The concept of duality is fundamental in connection with linear programming and is of great theoretical and practical importance. Knowledge of duality allows one to develop a better understanding of LP models and their results and an increased insight into LP solution interpretation. Knowing the relation between an LP problem and its dual is vital to understanding advanced topics in linear and non-linear programming and enables a better interpretation/physical meaning of results when, for example, structural analysis/optimization problems are tackled using linear programming. Duality also provides an alternative way of solving LP problems as solving the dual of any problem also simultaneously solves the primal.

B.4.1 The dual of a linear program in standard form

Consider the linear program (in standard form):

$$\left.\begin{array}{ll} \text{minimize:} & \\ & \mathrm{h(x)} = \mathbf{c}^{\mathrm{T}}\mathbf{x} \\ \text{subject to} & \\ & \mathbf{Ax} = \mathbf{b} \\ & \mathbf{x} \geq \mathbf{0} \end{array}\right\} \quad \text{(P)} \qquad \text{(B.3)}$$

With each constraint i (i =1,...,n), a positive, negative or zero variable c_i, is associated (called a 'dual variable'). Consider also the linear program:

$$\left.\begin{array}{ll} \text{maximize:} & \\ & g(y) = \mathbf{d}^T\mathbf{y} \\ \text{subject to} & \\ & \mathbf{Zy} \leq \mathbf{b} \\ & \mathbf{y} \geq \mathbf{0} \end{array}\right\} \quad \text{(D)} \qquad \text{(B.4)}$$

The dual LP (D) is closely related to the primal LP (P). The constraint matrix of (D) (i.e. $\mathbf{Z}$) is the transpose of the constraint matrix of (P) (i.e. $\mathbf{A}$). In this case, both the primal and dual solutions can be obtained by solving either one of the two problems system (D) or (P). This is because the solution of the minimization problem is given by the negative of the 'Simplex multipliers' in the solution to the maximization problem. Conversely, the solution of the maximization problem is given by Simplex multipliers in the solution to the maximization problem.

Generally, the dual for any LP can be found using the following steps:

- If the primal problem is a maximization problem, then the dual problem is a minimization problem and vice versa.
- The coefficients of the objective function of the dual problem are the right-hand side terms of the constraints of the primal problem.
- The right-hand side of the constraints of the dual problem are the coefficients of the objective function of the primal problem.
- The sign constraints of the dual problem as well as the type of each constraint ($\leq$, $\geq$ or $=$) can be deduced from the sign conditions inside the Karush-Kuhn-Tucker conditions of both primal and dual problems.

B.5 The Lagrangian function and Karush-Kuhn-Tucker conditions

The Lagrangian function is an important tool in the analysis and design of algorithms in constrained optimization. It is a linear combination of the objective function and the constraints resulting in an unconstrained function whose optimum coincides with the optimum of the LP problem. Calculus can then be used to find the optimum solution. It also ensures that the imposed constraints are satisfied. Lagrangian function generally takes the following form:

$$L(x, \lambda) = f(x) - \sum_{i=1}^{m} \lambda_i c_i(x) \tag{B.5}$$

The coefficients λ_i are called *Lagrange multipliers.*

More specifically, consider the general LP, with m variables and n constraints:

minimize

$$h = \sum_{i=1}^{i=m} c_i x_i \tag{B.6}$$

subject to:

$$\sum_{i=1}^{i=m} a_{ij} x_j \geq b_j \quad (j = 1, 2, ..., n) \tag{B.7}$$

Or, with slack variables included:

$$\sum_{i=1}^{i=m} a_{ij} x_j - b_j + k_j = 0 \quad (j = 1, 2, ..., n) \tag{B.8}$$

Another way to find the solution for the above LP is to find the solution of:

minimize:

$$L(x,k,\lambda) = \sum_{i=1}^{i=m} c_i x_i + \sum_{j=1}^{j=n} \lambda_j (\sum_{i=1}^{i=m} a_{ij} x_j - b_i + k_j) + \sum_{i=1}^{i=m} v_i(-x_i + t_i) \qquad \text{(B.9)}$$

Which is the Lagrangian function for the problem. Whatever method is used to minimize the above function, the constraints will be satisfied.

The Lagrangian function makes it possible to state the necessary and sufficient optimality conditions for problems which contain inequality constraints and/or sign restricted variables, namely, the Karush-Kuhn-Tucker conditions [10, 11]. The Karush-Kuhn-Tucker conditions can be written as follows:
assign a_{ij}=A, c_i=c, k=u, and b_i=b

$$\begin{bmatrix} \mathbf{0} & -\mathrm{A}^{\mathrm{T}} \\ \mathbf{A} & \mathbf{0} \end{bmatrix} \begin{bmatrix} \mathbf{x} \\ \mathbf{y} \end{bmatrix} - \begin{bmatrix} \mathbf{u} \\ \mathbf{v} \end{bmatrix} = \begin{bmatrix} -\mathbf{c} \\ \mathbf{b} \end{bmatrix} \qquad \text{(B.10)}$$

$$\mathbf{x} \geq 0, \ \mathbf{y} \geq 0, \ \mathbf{v} \geq 0, \ \mathbf{u} \geq 0, \ \mathbf{v}^{\mathrm{T}}\mathbf{x} \geq \mathbf{0}, \ \mathbf{y}^{\mathrm{T}}\mathbf{u} \geq \mathbf{0} \qquad \text{(B.11)}$$

References

[1] http://www.eudoxus.com

[2] Dantzig, G. B. *Linear programming and extensions.* Princeton University Press, New York, USA, 1963.

[3] Garvin, W. *Introduction to linear programmming.* McGraw-Hill, London,UK, 1960.

[4] Luenberger, D. G. *Linear and non-linear programming.* Addison-wesley, London,UK, 1984.

[5] Nash, S. G. and Sofer, A. *Linear and non-linear programming.* McGraw-Hill, London,UK, 1996.

[6] Sherali, H. D., Bazaraa, S. M. and Shetty, C. M. *Nonlinear programming theory and algorithms.* John Wiley & Sons Inc., New York, USA, 1994.

[7] Vanderbei, R. J. *Linear Programming: Foundations and Extensions.* Kluwer Academic Publishers, London, UK, 1998.

[8] Fiacco, A. V. and McCormick, G. P. *Nonlinear Programming: Sequential Unconstrained Minimization Techniques.* John Wiley & Sons, New York, USA, 1968.

[9] Karmarkar, N. A new polynomial-time algorithm for linear-programming. *Combinatorica*, 4:373–3954, 1984.

[10] Karush, W. *Minima of Functions of Several Variables with Inequalities as Side Constraints.* MSc Thesis, Department of Mathematics, University of Chicago, 1939.

[11] Kuhn, H. W. and Tucker, A. W. Nonlinear programming. *Proceedings of the 2nd Berkeley Symposium on Mathematical Statistics and Probability*, 481–492, Brekeley, University of California Press, 1951.

Appendix C

Computer Code

An object oriented programming approach has been adopted for the computer programs developed. In this chapter, a brief review of the basic features of object oriented programming will be made.

C.1 Object-oriented programming

In recent years, object oriented programming languages have been increasingly adopted when developing analysis and design software. Unlike established programming languages (procedural languages) such as Fortran, Pascal and C, object-oriented programming is a completely different way of approaching the idea of encoding a problem within a computer program. In the object-oriented programming approach, the computer program is defined as a collection of objects. The object in itself, it is a powerful structure that contain data and functions, and can communicate with other objects. Thus clearly the program can be described as a collection of interacting objects. In this project, by using an object-oriented language such as C++, a natural way of manipulating objects relevant to structural engineering such as elements, points etc can be developed.

C.2 Classes

Literally, a class is defined as a "*set, collection, group, or configuration containing members regarded as having certain attributes or traits in common; a kind or category*". Within the context of object-oriented programming, an object is an instance of a class. A class in C++ is a very flexible data structure, it associates several data items with each other. The fields of the class are divided into *public* and *private* fields. Access to classes can be restricted, so that only member functions can manipulate the data in it. This enables one to hide information (and protect it). This gives the programmer confidence that other routines not directly associated with the class cannot change the state of the data. Also a field can be a function. This enables one to have special input and output functions to handle the data that are stored in the class.

Two distinct categories of classes are usually encountered in numerical modelling: mathematical classes and geometrical classes. Mathematical classes/objects may be used to represent matrices and vectors permitting high level mathematical operations such as multiplication, divisions ... (usually required in finite element models). Geometrical classes are usually used to describe aspect of a physical problem: its domain, its boundary conditions .... Normally, these classes consist of elements, nodes, members ....

Having reviewed object-oriented programming basic concepts, the next section is devoted to the program code and computer flow chart for the program.

C.3 The program code

The SLAB program used for yield line analysis contains a number of classes these are:

C.3.1 Class 'Element'

The most significant class in the program is the element class. An element contains nodal data, has an area and a centroid. It also stores the element variables used in setting up LP problems whether these are displacements or forces.

C.3.2 Class 'Node'

An element contains nodes, so these are defined as self contained classes. A node class stores a node number, co-ordinates and global functions for distance between nodes, the angle between two nodes ....

C.3.3 Class 'Interface'

An interface class stores the interface type and interface variables used in setting up LP problems. It also stores the shared elements related geometrical functions.

C.3.4 Class 'Contour-line'

It contains lines and nodes and it stores displacement contours.

C.3.5 Class 'Mesh'

The mesh class is a container class for elements, nodes, contour-lines and interfaces.

C.3.6 Class 'Input'

Reads geometrical, material properties and mesh data and discretizes the slab accordingly.

C.3.7 Class 'Output'

Generates Autocad script files for yield line patterns and displacement contours.

C.3.8 Class 'Adapt'

Is only used with the two phase Sheffield method. It generates the new discretization based on the displacement contours obtained using the Sheffield method or the Munro and Da Fonseca method.

C.3.9 Mathematical programming classes

These contain variables and constrains classes and Solve function based on three different LP solvers: (Mosek 2.5, PCx and Xpress 14).

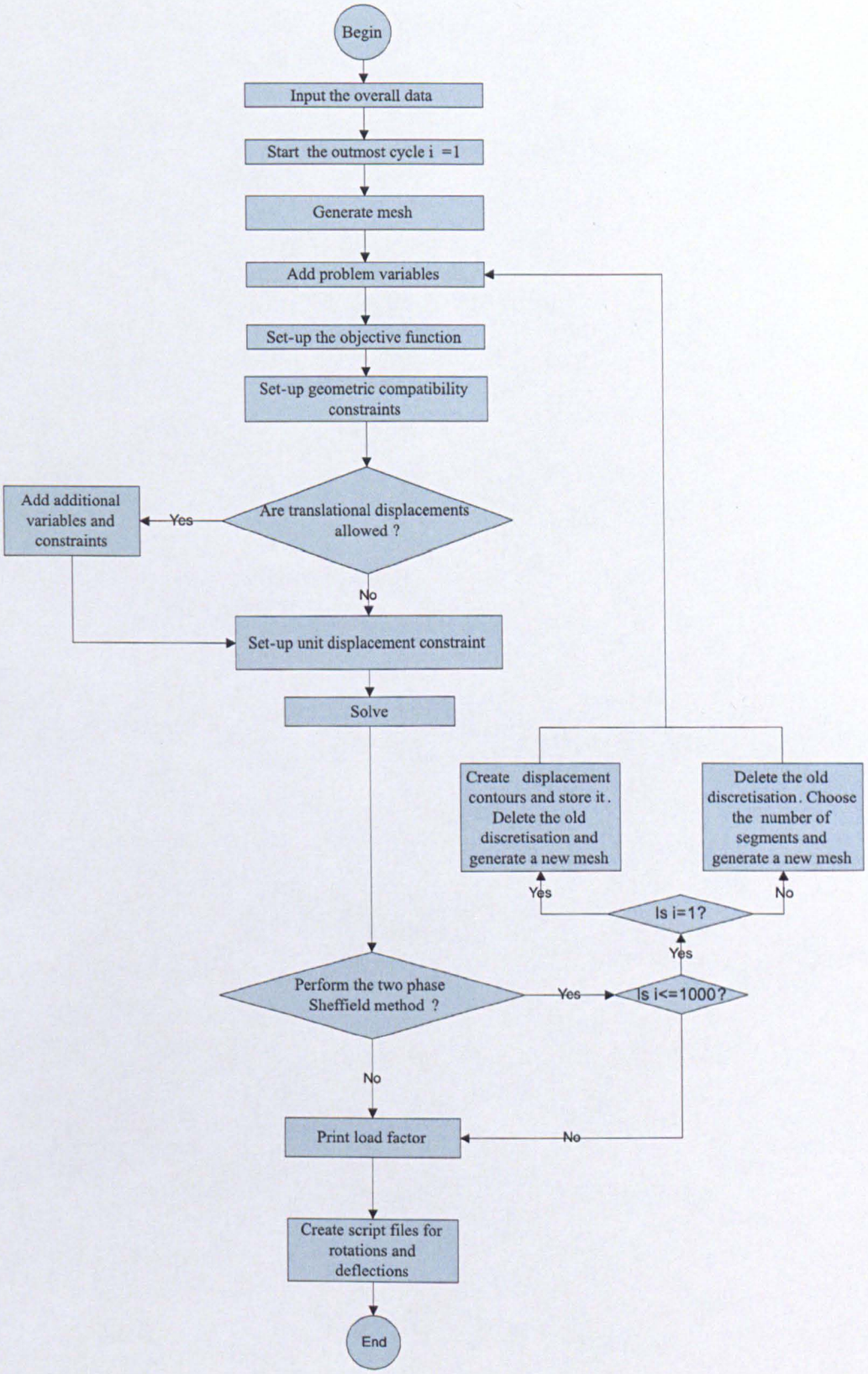

Figure C.1: Computer flow chart for SLAB